Investigating the Metabolic and Molecular Regulators of Diurnal Insulin Secretion

By

Nivedita Seshadri

A thesis submitted to
the Faculty of Graduate Studies
in partial fulfilment of
the requirements for the degree of

DOCTOR OF PHILOSOPHY

Department of Physiology and Pathophysiology
RADY FACULTY OF HEALTH SCIENCES
University of Manitoba
Winnipeg, Manitoba

OCTOBER 2022

Copyright © by Nivedita Seshadri

ABSTRACT

Healthy β-cells secrete insulin in a rhythmic manner to maintain glucose homeostasis; however, the molecular and metabolic players remain unclear. Uncoupling protein 2 (UCP2) expressed in the β-cells negatively impacts insulin secretion; however, its physiological function remain elusive. Increased UCP2 expression was observed during starvation suggesting that UCP2-mediated insulin suppression may prevent hypoglycemia during prolonged fasting. Building on this finding we hypothesize that, in healthy β-cells, UCP2 regulates diurnal cycles of insulin secretion capacity and glucose homeostasis. We also propose that the β-cell circadian clock drives *Ucp2* expression and controls daily cycles of insulin secretion.

Mouse models (*Ucp2*-βKO and wildtype (WT; C57BL6)) and synchronized clonal pancreatic β-cells (MIN6) were used to determine when *Ucp2* is expressed daily and mechanisms controlling glucose-stimulated insulin secretion (GSIS) and glucose tolerance over 24h. Additionally, β-cell-specific *Bmal1* knockout mouse model (*Bmal*1-βKO) and *Bmal1* deficient MIN6 cells were used to address the role of β-cell clock in regulating GSIS capacities via fine tuning *Ucp2* expression (refers to steady state mRNA levels throughout this thesis).

Ucp2 mRNA expression was rhythmic over 24h and inversely correlated with GSIS capacities in synchronized MIN6 cells and islets isolated from WT mice. Using both *Ucp2*-βKO mouse model and a pharmacological inhibitor of UCP2 (Genipin), we show that rhythms in GSIS capacities and glucose tolerance was UCP2 dependant. Rhythms in fuel oxidation capacities, glucose-stimulated Adenosine triphosphate (ATP) production and reactive oxygen species (ROS) production correlated with UCP2 dependant GSIS rhythms. Additionally, diurnal rhythms in *Ldha* mRNA expression suggested existence of additional metabolic regulators aligning GSIS capacities to maintain glucose homeostasis. Loss of *Ucp2* and GSIS rhythms *via* decreased capacity for glucose-stimulated ATP production was observed in both models of circadian dysfunction. These defects were rescued by UCP2 inhibition using Genipin, suggesting that an intact β-cell clock control GSIS capacities via regulating *Ucp2*/UCP2 expression and activity.

The β-cell clock regulates daily cycles of *Ucp2* mRNA expression, which is part of an important metabolic switch needed to align GSIS capacity in a time-of-day dependent manner, defining a novel function for UCP2 in the β-cell. This study highlights the relationship between the circadian timing system and control of insulin secretion over the daily time course.

ACKNOWLEDGMENT

This PhD thesis is made possible by the help and support I received throughout my doctoral studies. I have made the humble effort in thanking all of them in my acknowledgements.

Firstly, I begin by thanking my doctoral thesis supervisor, Dr. Christine Robson Doucette for taking a chance on me and giving me a safe and trustful environment. When I started in the lab, I was unsure of my capabilities and had absolutely no confidence. Thank you for instilling in me confidence and encouraging me as I pursued my PhD degree in your lab. I have learnt a lot from you – not just science. Thank you for being my best and worst critic.

My advisory committee, Dr. Peter Zahradka, Dr. Suresh Mishra, and Dr. Vernon Dolinksy – thank you for your feedback, support and constant encouragement throughout my PhD journey. Special thanks for always having your office doors open for a chat whenever I may have asked for it. Your mentorship is key! Thank you.

My lab members (past and present) – Tianna Flett, Michael Jonasson, Mark Mutawe. Thank you for helping me settle in during my early days. Thank you for showing me most of the techniques that were instrumental in the completion of this work. Thank you, Kris Hunt, for making sure I had everything I needed for my experiments, our coffee sessions and just pure fun conversations. My heartfelt appreciation to all the summer students – Tianna Flett, Youstina Soliman, Yilin Tian, Dianna Prince who spent time and energy on this project. Thank you for your friendship and helping me become a teacher. Thank you, Owen and Krista, for always listening to my project details with equal excitement and encouraging me.

Taylor Morrisseau – I don't even have words to express my gratitude towards you! My colleague, friend, philosopher, and guide. You are someone who inspires me daily. There are some moments which define friendship. I still don't regret "ordering" you to sit next to me in the lab when you joined. A huge Thank you for your help with the project. Thank you for offering to help and not even waiting me to ask! Thank you for showing up at even 10pm to help me. It meant a lot. I can't imagine a better person to share my wins and failures with. You have been my strongest support system away from home. You are the best!

Manuel Sebastian – thank you for all your help with the immunofluorescence staining. We had some frustrating times trying to optimize Bmal1 antibody, but it was worth it, I hope! Thank you for making me laugh all the time and making lab a fun place when times were tough. Thank you.

Bo Xiang and Mario Fonseca – I don't know how to thank the both of you! Thank you for always teaching me and helping me with techniques and mouse work. Bo Xiang – I have not met a more patient teacher than you! Thank you for teaching me Islet perfusion and mouse dissections. Thank you!

I have to mention the DREAM trainees – Matthew Martens, Stepahnie Kereliuk, Matuesz Tomczyk, Gabriel Brawerman, Jared Field and Wajihah Mughal. Thank you all for your friendship and most importantly

support and encouragement during graduate studies. Most of you have been instrumental in me reaching the finish line of my PhD. Started out as mere colleagues but now most of you are my go-to people for advice. Thank you!

I would like to thank everyone at CHRIM. I know the values of a good research environment and CHRIM has been just that. The culture of sharing, teaching and cross mentoring has been very important to me. Thank you, Dr. Joseph Gordon and Dr. Adrian West, for letting me use equipment's in your respective labs. Dr. West – thank you for taking time out and helping me with the circadian experiments and trying to find a way to perform what I envisioned for my study. Thank you, Emily Turner, – for being always welcoming and teaching me how to use equipment at odd hours. A special shoutout to Dr. Grant Hatch and Dr. Laura Cole – thank you for always adjusting to my time restricted experiments, it means a lot when you feel welcome and not as inconvenience. Thank you for Dr. Cole for adjusting your schedule some days just so that I could finish an experiment. Thank you, Debbie and Lana, for always assisting us with anything we wanted!

I would want to thank my home department – Physiology and Pathophysiology for accepting me into the program. Dr. Tooru Mizuno – thank you for showing me how to dissect the hypothalamus for my study. And always being available to answer my queries. Thank you for always welcoming us in your lab after hours no matter how loud we would all be. Dr. Katinka Stecina – you are a role model for many of us. Your kind nature is infectious. Thank you for helping two of my friends when they needed it the most. You have gone out of your way to be helpful to students. Thank you! Gail, Judith, Sharon, and Venessa – your support is invaluable. Thank you!

I would like to thank all my friends at HSC apartments who have made living in Winnipeg fun! I have learnt a lot from each you and have countless memories to cherish. Naming all of you would probably cause me to exceed page limit. Thank you!

Thank you, mom, Savitha Prashant (sister) and Prashanth Venkatraman (brother-in-law). When times get tough, I always had you three to fall back on. Thank you for believing in me! My nephew, Vishisht deserves a special mention. The COVID times were made bearable only because of you. I would end by thanking my best friend, my husband – Jay Narasihman. Your support made the last stages of thesis writing bearable. Thank you! Dr. Krishna Kumar Ramanathan – thank you for inspiring me to study science. I end this section by thanking – Nagarajan Mahadevan for being on my team always.

DEDICATION

"The art is in knowing how to ask."

— Dan Brown.

This thesis is dedicated to my mother – Mrs. Janaki Ramanathan. My first teacher and mentor. You are the strongest human being I know. Thank you for instilling in me hard work and the attitude of never giving up. There have been many moments during my PhD I have needed you and your perspective on things were always a source of positivity and encouragement. The reason I got up on most morning and went to work with a happy smile.

Table of Contents

ABSTRACT ..... **ii**

ACKNOWLEDGMENT ..... **ii**

DEDICATION ..... **v**

Table of Contents vi

LIST OF FIGURES ..... **x**

LIST OF TABLES ..... **xii**

Chapter 1 ..... **1**

General Introduction **1**

1.1 Type 2 Diabetes (T2D) and the Pancreatic ß-cell **2**

1.2 Insulin Secretion: Glucose-Stimulated versus Basal **3**

1.2.1 Glucose-Stimulated Insulin Secretion (GSIS) 3

1.2.2 Basal Insulin Secretion (BIS) 6

1.3 Metabolism-Derived Coupling Factors that Regulate GSIS **7**

1.3.1 ATP/ADP Ratio and the K^{+}_{ATP} Channel 7

1.3.2 Reactive Oxygen Species (ROS) 9

1.4 Regulation of β-Cell Metabolism **11**

1.4.1 Uncoupling Proteins 12

1.4.1.1 The Potential Biochemical Functions of UCP2 ..... **14**

1.4.1.2 Uncoupling Protein 2 and the β-Cell 15

1.4.1.3 UCP2-Mediated Regulation of ROS Production in the β-cell 17

1.4.1.4 UCP2-Mediated Regulation of ATP Production in the β-cell 17

1.4.1.5 UCP2 Upregulation in Response to Starvation: A potential Mechanism to Prevent Hypoglycemia 18

1.4.2 Lactate Dehydrogenase and β-cells 18

1.5 Circadian Control of Insulin Secretion **19**

1.5.1 Organization of the Circadian Clock Timing System 20

1.5.2 Circadian Dysfunction and Metabolic Disease 21

1.5.2.1 Pancreatic Clock **23**

1.5.2.1.1 The Islet and β-Cell Circadian Transcriptomes 24

1.5.2.1.2 Beyond Circadian Transcriptional Regulation of the β-Cell 26

1.5.2.1.3 A Role for the Circadian Clock in Postnatal β-Cell Functional Maturation? 27

1.5.2.1.4 A Role for the Circadian Clock in β-Cell Proliferation and Adaptation to Stress? 28

Chapter 2 ..... **31**

General Hypothesis and Specific Aims **31**

2.1 Specific Aims **32**

Chapter 3 ..... **33**

Materials and Methods ... **33**
3.1 Animal models ... **34**
3.2 Mouse breeding and Establishment of β-cell-specific Knockout Mice ... **35**
3.3 MIN6 cells ... **37**
3.3.1 Entrainment/synchronization of MIN6 cells ... 37
3.3.2 siRNA- mediated Bmal1 knockdown in MIN6 cells ... 39
3.4 Animal colony maintenance ... **40**
3.5 Genotyping ... **40**
3.6 Glucose Tolerance Tests (GTT) and Insulin Tolerance Tests (ITT) ... **42**
3.7 Pancreatic Islet Isolations ... **42**
3.8 Glucose-stimulated Insulin Secretion (GSIS) ... **43**
3.9 Immunohistochemistry ... **43**
3.10 ATP content quantification ... **44**
3.11 ROS measurements ... **45**
3.12 Oxygen consumption and extracellular acidification rate using the XF-Analyzer ... **45**
3.13 Gene expression analyses (RT-qPCR) ... **48**
3.14 Cytosolic lactate quantification ... **49**
3.15 Western Blotting ... **49**
3.16 Mitochondrial membrane potential measurements ... **50**
3.17 Statistical Analyses ... **50**
Chapter 4 ... **51**
Uncoupling protein 2 regulates diurnal rhythms of insulin secretion ... **51**
4.1 Background and Rationale: ... **52**
4.2 Materials and Methods ... **53**
4.3 Results…. ... **53**
4.3.1 *Ucp2* mRNA expression is rhythmic in synchronized MIN6 cells and islets isolated from Ins2-Cre mice. ... 53
4.3.2 Rhythmic *Ucp2* expression inversely regulates insulin secretion capacity ... 54
4.3.3 Diurnal *Ucp2* expression is required for maintaining glucose tolerance over 24 hours. ... 57
4.4 Discussion ... **60**
Chapter 5 ... **63**
Identifying the cellular mechanisms underlying UCP2-mediated diurnal insulin secretion capacities ... **63**
5.1 Introduction ... **64**
5.1.1 Overall Rationale ... 64

5.1.2 UCP2-Mediated Regulation of ATP Production in the β-cell. 64
5.1.3 UCP2-mediated regulation of ROS production in the β-cell 64
5.1.4 UCP2-Mediated Regulation of Mitochondrial Fuel Oxidation 65

5.2 Materials and methods 65

5.3 Results.. 66
5.3.1 Rhythmic *Ucp2* mRNA Expression Translates into Diurnal Changes in Activity Over 24hours. 66
5.3.2 Rhythmic UCP2 Activity Regulates Diurnal Insulin Secretion Capacity Via Fine-tuning ATP Content in a Time-of-Day Manner 67
5.3.3 Rhythmic UCP2 activity regulates dynamic and diurnal changes in ROS production over 24 hours. 69
5.3.4 UCP2-mediated Changes in ROS Signals are Essential for Maintenance of Diurnal Patterns of GSIS 70
5.3.5 Rhythms of *Ucp2* mRNA expression align with fuel oxidation capacities over 24 hours. 72
5.3.6 Rhythmic expression of genes regulating ROS levels in synchronized MIN6 cells.. 74

5.4 Discussion..... 75

Chapter 6 79

The Role of the β-cell Circadian Clock in Regulating Diurnal Rhythms of UCP2 and Insulin Secretion Capacity 79

6.1 Background and Rationale..... 80
6.1.1 Circadian Regulation of *Ucp2*-Mediated Insulin Secretion..... 80
6.1.2 Other Molecular Regulators of Diurnal Rhythms of Insulin Secretion 81

6.2 Material and Methods 81

6.3 Results… 82
6.3.1 *Bmal1* mRNA Expression is Rhythmic in Synchronized MIN6 Cells and Isolated Islets 82
6.3.2 Creation and Validation of β-cell-Specific Circadian-Deficient Models 83
6.3.3 Effects of β-cell-Specific *Bmal1* Deletion on Bodyweight and Fasted Blood Glucose 85
6.3.4 Effect of β-cell-Specific *Bmal1* Deletion on Glucose and Insulin Tolerance..... 87
6.3.5 *Bmal1* Deficiency Impairs GSIS in MIN6 cells and isolated islets. 89
6.3.6 Impaired GSIS in *Bmal1*-Deficient β-cells Is Dependent on Chronic Upregulation of *Ucp2*..... 91
6.3.7 Glucose-Induced ATP Production is Reduced in β-cell *Bmal1* Deficiency. 94
6.3.8 *Bmal1* Deficiency Impairs Rhythms in Glucose Oxidation in MIN6 Cells..... 96
6.3.9 *Bmal1* Knockdown Impairs Rhythmic Expression of Glucose-Sensing and Metabolism Genes 97
6.3.10 *Ldha* mRNA Expression in Synchronized MIN6 Cells and Isolated Islets. 98
6.3.11 LDHA Activity is Rhythmic over 24 hours in synchronized MIN6 cells. 99

6.4 Discussion..... 100

Chapter 7 105

Overall Discussion..... 105

7.1 Overview 106

7.2 Strengths and Limitations..... 110
7.2.1 Strengths 110

7.2.2 Limitations 111
7.3 Impact of COVID-19 pandemic on research and thesis. 112
7.4 Future Directions 112

LIST OF FIGURES

Figure 1.1: Type 2 Diabetes Progression ……..……..3
Figure 1.2: Regulatory Pathways of Glucose-stimulated insulin secretion……6
Figure 1.3: Activation of Uncoupling protein 1……...13
Figure 1.4: Schematic representation of the hierarchical arrangement of the central and peripheral clock…….21
Figure 3.1: Breeding scheme for obtaining β-cell specific *Ucp2* knockout mice (*Ucp2*βKO). ……35
Figure 3.2: Breeding scheme for obtaining β-cell specific *Bmal1* knockout mice (*Bmal1*βKO) …….……....36
Figure 3.3: *In vitro* synchronization using serum shock/stave protocol……..…..37
Figure 3.4: *In vitro* synchronization using Forskolin……38
Figure 4.1: *Ucp2* mRNA expression over 24-36 h in synchronized MIN6 cells and islets isolated from C57BL6 mice……53
Figure 4.2: Glucose stimulated insulin secretion capacity of synchronized MIN6 cells and islets isolated from *Ins2*-Cre……..56
Figure 4.3: UCP2 deficiency impairs glucose tolerance only in the light phase of the daily cycle……..58
Figure 5.1: Assessment of mitochondrial membrane potential at ZT 4 and ZT 16 as a surrogate measure of UCP2 activity……66
Figure 5.2: Daily Rhythms of UCP2 Activity Control the Temporal Capacity of Glucose-induced ATP Content in MIN6 Cells and Isolated Islets……67
Figure 5.3: Daily Rhythms of UCP2 Activity Control Temporal Changes in ROS production in MIN6 cells…68
Figure 5.4: Daily Rhythms of UCP2 Activity Control the Temporal Capacity of Insulin Secretion Via Fine-tuning ROS Signals in MIN6 cells……70
Figure 5.5: Daily rhythms of fuel oxidation capacities is associated temporal capacities in glucose stimulated insulin secretion in MIN6 cells……...73
Figure 5.6: Rhythmic expression of genes regulating ROS levels in synchronized MIN6 cells……..74
Figure 6.1: Circadian expression pattern of *Bmal1* mRNA in MIN6 cells and isolated islets over 24h……81
Figure 6.2: Validation of BMAL1 knockdown after siRNA transfection……82
Figure 6.3: Validation of β-cell specific *Bmal1* deletion in islets isolated from $Bmal1^{F/F}$ (Flox control), $Bmal1^{WT/WT/Cre}$ (Cre Control) and $Bmal1^{F/F/Cre}$ (Bmal1βKO)……84
Figure 6.4: Bodyweight measurements (g) obtained from male and female mice over 13 weeks……85
Figure 6.5: Fasted blood glucose measurements done in male and female mice……..86
Figure 6.6: *Bmal1* deficiency impairs glucose tolerance over 24 hours……87
Figure 6.7: *Bmal1* deficiency has no impact on insulin tolerance in male and female mice……89
Figure 6.8: *Bmal1* deficiency impairs GSIS in synchronized MIN6 cells…….....89
Figure 6.9: *Bmal1* deletion in the β-cell Disrupts Diurnal GSIS Capacity ……90
Figure 6.10: *Bmal1* Knockdown Upregulates *Ucp2 mRNA* Expression at ZT4 and 10pm, Disrupting the Diurnal Rhythms of *Ucp2*Expression……..91
Figure 6.11: Inhibition of UCP2 Activity at ZT4 Recovers Impaired GSIS in *Bmal1*-deficient β-Cells……..92
Figure 6.12: Genipin Restores Impaired GSIS at 10pm in *Bmal1*-Deficient Islets……93
Figure 6.13: *Bmal1* Knockdown in MIN6 Cells Impairs Glucose-Induced ATP accumulation in synchronized MIN6 cells……..94
Figure 6.14: *Bmal1*βKO Islets Display Reduced Glucose-Stimulated ATP Accumulation at 10pm that is Rescued by Genipin. ……95
Figure 6.15: *Bmal1* knockdown impairs glucose oxidation at ZT 4 in synchronized MIN6 cells. …….96

Figure 6.16: *Bmal1* knockdown impairs rhythmic expression of genes known to impact glucose-sensing and metabolism ……...97
Figure 6.17: *Ldha* mRNA expression levels at 4 hour intervals over 36 hours in synchronized MIN6 cells and islets isolated from C57BL6 mice……..98
Figure 6.18: LDHA activity is rhythmic over 36 hours in synchronized MIN6 cells. ……99
Figure 7.1: Pancreatic β-cell clock regulates insulin secretion via UCP2……108

LIST OF TABLES

Table 3.1: Transfection reagents and siRNAs used in *Bmal1* knockdown studies in vitro. 40
Table 3.2: PCR reaction setting for genotyping *Ucp2*βKO mice 41
Table 3.3: PCR reaction settings for genotyping *Bmal1*βKO mice 41
Table 3.4: List of primers used for genotyping 41
Table 3.5: List of primary and secondary antibodies used in Immunofluorescence staining 44
Table 3.6: Formula used to calculate parameters of OCR 46
Table 3.7: Parameters calculations for Glycolysis stress test 48
Table 3.8: List of general primers 48

LIST OF ABBREVIATIONS

Acetyl-CoA	Acetyl coenzyme A
ADP	Adenosine diphosphate
ATF6	Activating transcription factor 6
Atp5fc1	ATP synthase F1 subunit gamma
ATP	Adenosine triphosphate
ATP1A1	ATPase Na^{2+}/K^{+} transporting subunit alpha 1
BIS	Basal insulin secretion
BIP	Binding immunoglobulin protein
Bet1	Blocked early in transport 1
Bcl2	B-Cell CLL/lymphoma 2
BrdU	5-Bromo-2'-deoxyuridine
BSA	Bovine serum albumin
BMAL1	Brain and muscle aryl hydrocarbon receptor nuclear translocator-like protein 1
Cacna1c	Calcium voltage-gated channel subunit alpha 1
Ca^{2+}	Calcium
$CaCl_2$	Calcium chloride
CAT	Catalase
CCCP	Carbonyl cyanide chloromethoxyphenylhydrazone
Ccnb2	Cyclin B2
Cdk6	Cyclin-dependant kinase 6
Cdkn2b,	Cyclin-dependant kinase inhibitor 2b
CADPS	Calcium-dependant secretion activator
Cdc20	Cell division cycle 20
CM-H2-DCFDA	2',7'- dichlorodihydrofluorescein diacetate
CFP	Cyanide fluorescent protein
cAMP	Cyclic adenosine monophosphate
Cl^{-}	Chloride ion
CLOCK	Circadian locomotor output cycle kaput
Cpt-1a	Carnitine palmitoyl transferase-1a
Cox4l1	Cytochrome c oxidase. Subunit 4 lsoform1
Creb1	cAMP responsive element binding
Creb3	cAMP responsive element binding protein 3
Creb3L1	cAMP responsive element binding protein 3 like 1
CRY1	Cryptochrome circadian regulator 1
CRY2	Cryptochrome circadian regulator 2
DAPI	4',6-diaminido-2-phenylindole
DEM	Diethyl-maleate
Dbp	DNA binding domain
DMEM	Dulbecco's minimal essential media
DNA	Deoxy-ribonucleic acid
2-DG	2-Deoxy-glucose

Dsk2	Dominant suppressor of Karyogamy 1
ECAR	Extracellular acidification rate
EDTA	Ethylenediaminetetraacetic acid
Eif2AK3	Eukaryotic translation initiation factor 2 alpha kinase 3
ELISA	Enzyme-linked immunosorbent assay
ER	Endoplasmic reticulum
ERO1β	Endoplasmic reticulum Oxidoreductase 1 β
ES	Embryonic stem cells
$FADH_2$	Flavin adenine dinucleotide
FBS	Fetal bovine serum
FCCP	Carbonyl cyanide p-(tri-fluromethoxy) phenyl-hydrazone
FFA	Free fatty acid
Gadd45a	Growth arrest and DNA damage inducible alpha
GAPGH	Glyceraldehyde 3-phosphate dehydrogenase
GK	Glucokinase
Gcg	Glucagon
GDP	Guanosine diphosphate
Gnaq	G Protein Subunit Alpha Q
GPX	Glutathione peroxidase
Grp94	Glucose-regulated protein 94
GSIS	Glucose-stimulated insulin secretion
GTP	Guanosine triphosphate
GTT	Glucose tolerance test
HCl	Hydrochloric acid
Hus1	Hydroxyurea-sensitive 1
Hsp40	Heat shock protein 40
Hsp70	Heat shock protein 70
H_2O_2	Hydrogen peroxide
HO-	Hydroxide
4-HNE	4-Hydroxynonenal
HIV	Human immunodeficiency virus
HEPES	4-2-hydroxyethyl-1-piperazineethanesulfonic acid
IGT	Impaired glucose tolerance
IAPP	Islet amyloid polypeptide
IRE-1	Inositol-requiring protein 1
ipRGC	Intrinsically photoreceptive retinal ganglion cells
ITT	Insulin tolerance test
Il-1β	Interleukin 1β
K^+	Potassium
K^+_{ATP}	ATP-gated potassium channels
KCl	Potassium chloride

KH_2PO_4	Potassium dihydrogen phosphate
Kir	Inwardly rectifying potassium-selective
KEGG	Kyoto encyclopedia of genes and genomes
KRB	Kreb's ringer solution
Ldha	Lactate dehydrogenase A
LoxP	Locus of X-over P1
MAFA	MAF BZIP transcription factor A
MgADP	Adenosine 5'- (Trihydrogen pyrophosphate), Magnesium salt
$MgSO_4$	Magnesium sulphate
MCF	Metabolic coupling factors
mETC	Mitochondrial electron transport chain
mRNA	Messenger RNA
MIN6	Mouse insulinoma 6 cells
MIP	Mouse insulin promoter
NAC	N-acetyl L- Cysteine
NaCl	Sodium chloride
NAD+	Nicotinamide adenine dinucleotide
NADH	Nicotinamide adenine dinucleotide hydrogen
Na_2HPO_4	Disodium hydrogen phosphate
$NaHCO_3$	Sodium carbonate
Ndufa2	NADH:ubiquinone oxidoreductase subunit 2
NEUROD1	Neuronal differentiation 1
NMRI	Naval medical research Institute
OCT	Optimum cutting temperature
OXPHOS	Oxidate phosphorylation
OCR	Oxygen consumption rate
O_2^-	Superoxide anion
OH^-	Hydroxyl ion
PBA	4-phenylbutyrate
PBS	Phosphate buffer saline
PC	Pyruvate Carboxylase
PCR	Polymerase chain reaction
PDH	Pyruvate dehydrogenase
PDX1	Pancreatic and duodenal homeobox 1
PEP	Phosphoenol pyruvate
PERK	Protein kinase RNA-like ER kinase
PER1	Period 1
PER2	Period 2
PER3	Period 3
PFA	Paraformaldehyde
PFK	Phosphofructokinase
PIP2	Phosphatidylinositol-4, 5-bisphosphate

PK	Pyruvate kinase
PKC	Protein kinase C
PMF	Proton motive force
PVDF	Polyvinylidene fluoride
Rev-Erb α/β also known as NR1D1	Nuclear receptor subfamily 1 group D 1
RIP	Rat insulin promoter
RIPA	Radioimmunoprecipitation assay buffer
ROS	Reactive oxygen species
ROSA	Reverse orientation splice acceptor
ROR α/β	Retinoic Acid Receptor Related orphan receptor α/β
RNA	Ribonucleic Acid
RPMI	Roswell Park Memorial institute
Rbl2	Retinoblastoma transcriptional corepressor-like 2
SCN	Suprachiasmatic nucleus
SDS	Sodium dodecyl sulphate
SGLT2	Sodium glucose transporter 2
Slc2a2	Solute Carrier Family 2 member 2
SLC30A8	Solute Carrier Family 30 member 8
Snap29	Synaptosome associated protein 29
SOD1	Superoxide dismutase 1
SOD2	Superoxide dismutase 2
SOD3	Superoxide dismutase 3
SUR1	Sulfonylurea receptor 1
SYT4	Synaptogamin 4
Stx1a	Syntaxin 1A
STX2	Syntaxin 2
STX6	Syntaxin 6
STZ	Streptozotocin
T1D	Type 1 Diabetes
T2D	Type 2 Diabetes
TAE	Tris-acetate-EDTA
TBST	Tris-buffered saline and polysorbate 20(Tween-20)
TCA	Tricarboxylic acid
TUDCA	Tauroursodeoxycholic Acid
UCP1	Uncoupling protein 1
UCP2	Uncoupling protein 2
UCP3	Uncoupling protein 3
UCP4	Uncoupling protein 4
UCP5	Uncoupling protein 5
Ucn3	Urocortin 3
Vamp3	Vesicle-associated membrane protein 3
Vamp4	Vesicle-associated membrane protein 4
Vamp8	Vesicle-associated membrane protein 8

VDAC	Voltage-dependant anion channels
VGCC	Voltage-gated calcium channels
YFP	Yellow fluorescent protein
WT	Wildtype
ZT	Zeitgeber time

Chapter 1

General Introduction

Sections of this introduction have been published as a review in the journal of *Endocrinology* titled “Circadian regulation of the pancreatic ß-cell”, Nivedita Seshadri and Christine Doucette.2021 Sep 1;162(9)

1.1 Type 2 Diabetes (T2D) and the Pancreatic ß-cell

T2D is a multifactorial metabolic disorder that has a large number of modifiable and non-modifiable risk factors, including, obesity, diet, age, genetics, and circadian disruption, to name a few. According to the International Diabetes Federation, as of 2019, approximately 463 million people are living with T2D worldwide (Federation, 2019). It is expected that by 2043, this number will grow to over 700 million. While the development of insulin resistance is a pathophysiological component of T2D, pancreatic β-cell failure is central to the onset of T2D. While hyperglycemia and T2D themselves are not immediately deadly, many people living with diabetes will develop debilitating and life-threating complications as a result of chronic hyperglycemia, including retinopathy, nephropathy, cardiovascular disease and lower limb amputations, underscoring the burden of this disease and highlighting the need for appropriate prevention and intervention strategies.

T2D onset can be slow and progressive, with metabolic dysfunction occurring years before overt T2D diagnosis. Prior to overt T2D, prediabetes, is characterized by a mildly elevated fasting blood glucose level (5.7 mM – 6.4 mM) and is accompanied by the development of insulin resistance (American Diabetes, 2016). The development of insulin resistance is often coupled to an adaptive β-cell response where insulin output is increased and is often referred to as 'hyperinsulinemia'. In many people, functional compensation is sufficient and glucose homeostasis can be maintained in an insulin-resistant state. In others, functional decline or insufficient functional compensation of β-cells (i.e., not enough insulin is secreted to compensate for insulin resistance) causes blood glucose levels to rise above a diagnostic threshold (>6.4 mM) (American Diabetes, 2016) and overt T2D is diagnosed **[Figure 1.1]**. It is the decline of β-cell function that tips the person into developing overt T2D and is most often considered as the triggering event. Although the mechanisms that cause this decline in β-cell function are not completely understood, targeting β-cells to maintain secretory function is an attractive therapeutic strategy to treat or delay the onset of T2D and its associated comorbidities.

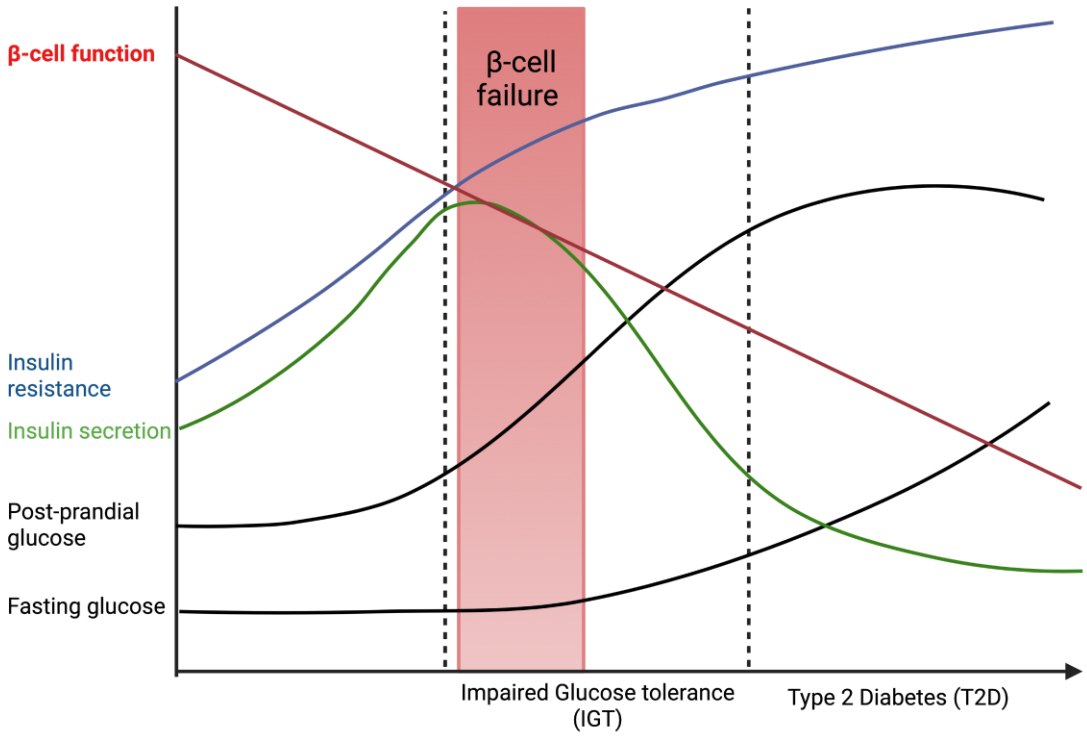


Figure 1.1: Type 2 Diabetes Progression Healthy individuals exposed to modifiable and non-modifiable risk factors develop post-prandial impaired glucose tolerance (when measured after a meal). Insulin resistance in the pre-diabetes or impaired glucose tolerance (IGT) stage is initially counterbalanced by an increased insulin secretion capacity by β-cells maintaining normoglycemia. Pancreatic β-cells failure beyond a certain threshold (indicated by the shaded box) worsens glucose tolerance and results in overt T2D accompanied with an impairment in fasting glucose levels and heightened insulin resistance accompanied with further decline in insulin secretion capacity. Figure adapted from Holman RR. *Diabetes Res Clin Pract*. 1998;40(suppl): S21-S25; Ramlo-Halsted BA, Edelman SV. *Prim Care*. 1999; 26:771-789; UK Prospective Diabetes Study (UKPDS); *Diabetologia*. 1991; 34:877-890.

1.2 Insulin Secretion: Glucose-Stimulated versus Basal

β-cells, located in the Islets of Langerhans, the endocrine portion of the pancreas, play a vital role in maintaining strong control of blood glucose levels across different physiological states; dysfunction of which leads to diabetes development. Depending on the physiological state (i.e., fasting vs. fed), insulin secretion can be sub-divided into two categories: glucose-stimulated and basal.

1.2.1 Glucose-Stimulated Insulin Secretion (GSIS)

In the post-prandial or fed state, glucose and other nutrient secretagogues (with glucose being the strongest secretagogue) (Gembal et al., 1992) trigger a 'burst' of insulin secretion, referred to as glucose-stimulated insulin secretion (GSIS), which is responsible for lowering postprandial blood sugar and directing the storage of metabolic fuels from dietary intake. GSIS rapidly directs glucose uptake into peripheral tissues (muscle, adipose) and controls the oxidation and/or storage of glucose to meet the energy demands of the active phase of the day. Loss of, or insufficient GSIS, manifests as postprandial hyperglycemia and is often an early β-cell defect

contributing to diabetes development. Furthermore, the post-prandial insulin secretory response is bi-phasic in nature (Caumo and Luzi, 2004) with the first phase being fast and robust followed by the second phase, which is slow and prolonged. The first phase response is distinct and lasts for approximately 3-5 mins immediately following a glucose challenge and is comprised mainly of insulin released from the already docked insulin granules at the plasma membrane, referred to as the readily releasable pool (Daniel et al., 1999). Approximately 2% of the insulin granules are released in the first phase. The second phase is an amplified response that lasts for more than 30 mins and is dependent on the remaining 98% of the releasable pool, which are made accessible for release via coupling factors like ATP, cAMP (Dyachok et al., 2008), and NAD^+ (Ivarsson et al., 2005) .

GSIS relies heavily on the metabolism of glucose within the β-cell. Signals generated during glucose metabolism trigger insulin release, effectively coupling elevations in blood glucose to insulin exocytosis. To briefly describe this process, as glucose accumulates in the blood after a meal, glucose passively enters the pancreatic β-cells along its concentration gradient via a constitutively expressed glucose transporter (GLUT-2, encoded by the *Slc2a2* gene in mice; GLUT-1 in humans). Once inside the cell, phosphorylation of the incoming glucose molecule by glucokinase (GK*)* commits glucose to glycolysis and prevents backward flow of glucose out of the cell. In the cytosol, the glycolytic reactions oxidize glucose to pyruvate. Two pyruvate molecules are produced for every molecule of glucose oxidized. Additionally, ATP and nicotinamide adenine dinucleotide hydrogen (NADH) are produced at the end of glycolysis. Pyruvate is then shuttled into the mitochondrion first through the outer mitochondrial membrane via passive diffusion through non-specific voltage dependent anion channels (VDAC) or porins (McCommis and Baines, 2012) and then through the inner mitochondrial membrane via mitochondrial pyruvate carrier 1 and 2 (Bricker et al., 2012, Herzig et al., 2012). Once inside the inner mitochondrial membrane, pyruvate can either be carboxylated by pyruvate carboxylase (PC) to replenish oxaloacetate withdrawn from the TCA cycle or oxidized to acetyl Co-A by an enzyme called pyruvate dehydrogenase (PDH). Acetyl-CoA is a key metabolic intermediate linking glycolysis to the tricarboxylic acid (TCA) cycle. Acetyl-CoA then enters the TCA cycle, where it is fully oxidized to produce CO_2 and reducing equivalents, NADH and Flavin adenine dinucleotide ($FADH_2$), which drive mitochondrial electron transport. Due to differences in electron affinities, NADH and $FADH_2$ donate electrons to oxidized mitochondrial electron transport chain complexes via complex I (NADH:ubiquinone oxidoreductase) and complex II (succinate dehydrogenase), respectively. Electrons are then shuttled along the mitochondrial electron transport chain, which contains 3 large proton pumping complexes (complexes I, III, and IV), two mobile electron carriers (ubiquinone and cytochrome c) and ATP synthase (also known as complex V). At complexes I, III and IV, energy from the redox reactions drive the pumping of protons from the mitochondrial matrix across the inner mitochondrial membrane into the intermembrane space. Accumulation of protons in the intermembrane space creates an electrochemical gradient across the inner mitochondrial membrane, called the proton motive force (PMF). Energy

in the PMF is used by complex V (ATP Synthase) to generate ATP from ADP and P_i in a process called oxidative phosphorylation (OXPHOS). Accumulation of intracellular ATP causes closure of ATP-gated potassium channels (K^+_{ATP}) on the plasma membrane, decreasing the flow of K^+ ions out of the β-cell, resulting in membrane depolarization. The change in plasma membrane potential opens voltage-gated Ca^{2+} channels (VGCC) and voltage gated Na^{2+} channels, which causes an influx of Ca^{2+} into the β-cell; an important signal that drives fusion of docked and primed insulin granules on the plasma membrane leading to insulin exocytosis (Rorsman and Ashcroft, 2018). More specifically, voltage-gated Na^{2+} channels activate ATP-gated potassium channel (K^+_{ATP}) closure, which is critical to cause sustained membrane depolarization thereby enhancing Ca^{2+} influx and insulin secretion (Velasco, 2016) . Additionally, zinc transporters through which zinc ions enter the β-cell play an important role in insulin synthesis, storage, and exocytosis of insulin secretion are activated by membrane depolarization (Lemaire, 2012, Slepchenko, 2012). Besides Na^{2+} ions, an influx of chloride ions has been shown to modulate insulin secretion (Sehlin, 1978) by aiding in membrane depolarization resulting in Ca^{2+} influx (Eberhardson, 2000). This ATP-centric pathway is called the "triggering pathway" or "K^+_{ATP} channel-dependant pathway".

Recently, the canonical model of GSIS being that oxidation of glucose by OXPHOS increases the ATP/ADP ratio which results in insulin exocytosis, also referred to as a one-step model for GSIS, has been challenged. A recent study by Lewandowski et. al., (2020) shows that pyruvate kinase (PK), a cytosolic enzyme that catalyzes the conversion of phosphoenol pyruvate (PEP) to pyruvate and concomitantly generates ATP from ADP in the cytosol, is critically important to the control of GSIS. The study used small molecule activators of PK and observed an increase in ATP and consequential decrease in ADP, Ca^{2+} influx and amplified the insulin secretion response in mouse and human islets, suggesting that PK localized at the plasma membrane and its conversion of ATP from ADP was enough to close K^+_{ATP} channels and induce Ca^{2+} influx (Lewandowski et al., 2020). Previously, the "PEP" cycle was shown to tightly regulate insulin secretion (Jesinkey et al., 2019, Stark et al., 2009). This highlights that the location of PK and its regulation of ATP/ADP ratio in the cytosol is an important regulator of insulin secretion. This study further demonstrates that the regulatory pathways that regulate GSIS are still incompletely understood, and more research is needed to fully understand the regulation of GSIS in the β-cell.

While the triggering pathway is essential for post-prandial GSIS, it should be noted that the triggering pathway alone does not account for the full post-prandial bi-phasic insulin secretory response. Additional metabolic signals that act directly on exocytosis distal to Ca^{2+} influx amplify the exocytotic response. This pathway is referred to as the "amplifying pathway" or K^+_{ATP} channel-independent pathway of GSIS. Several studies have implicated reactive oxygen species (ROS) produced at the level of the electron transport chain as an important insulin secretion amplifying signal.

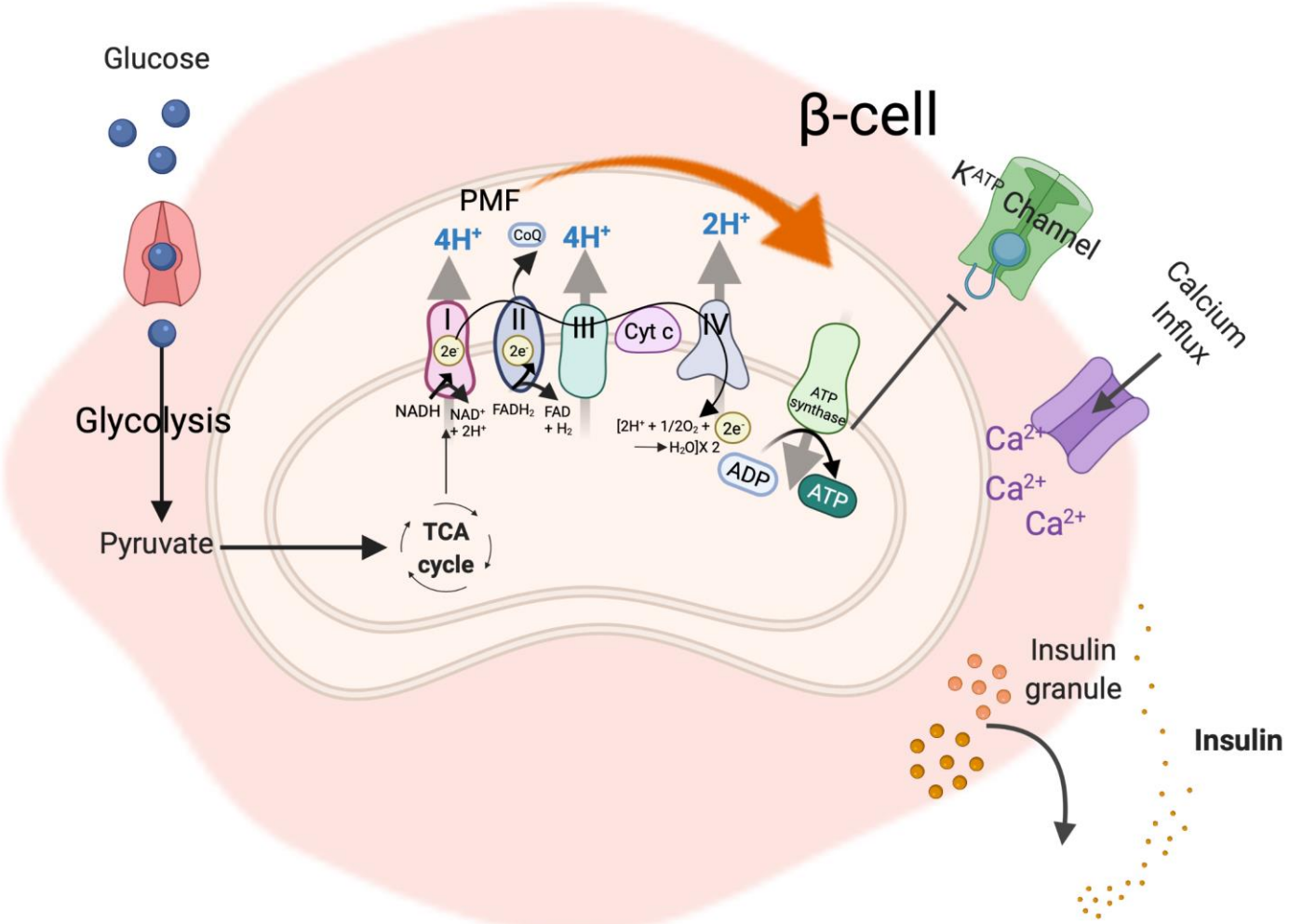


Figure 1.2: Regulatory Pathways of Glucose-stimulated insulin secretion: The Triggering Pathway. Glucose enters the pancreatic β-cell in a concentration dependant manner, via the GLUT-2 transporter. Metabolism of glucose via glycolysis (in the cytosol) and the tricarboxylic acid cycle (TCA cycle in the mitochondria) results in the production of reducing agents such as NADH and $FADH_2$ that donate electrons to the mitochondrial electron transport chain. This results in pumping of protons into the inner mitochondrial membrane spaces, which further creates a proton motive force, driving ATP synthase to produce ATP. As the concentration of ATP within the cell increases, it results in the closure of ATP dependant K^+ channel causing membrane depolarization which leads Ca^{2+} influx. Ca^{2+} is an important co-factor along with other causes exocytosis of insulin from the already docked insulin granules.

1.2.2 Basal Insulin Secretion (BIS)

While GSIS is essential for the regulation of postprandial energy metabolism, in the fasted state (i.e., in between meals, overnight fast), β-cells secrete a constant, lower basal level of insulin that is critical for directing the metabolic response to fasting and maintaining fasted blood glucose levels within a narrow range while ensuring adequate glucose supply to resting insulin-dependent tissues. BIS accounts for about 50% of the total insulin secreted by the β-cell on a daily basis (Ramchandani et al., 2010). A key function of BIS during the fasting

response is to mediate glucagon-directed hepatic glucose production (glycogenolysis and gluconeogenesis), such that insufficient basal insulin results in excessive endogenous glucose production, manifesting as fasting hyperglycemia. Conversely, excessive BIS during fasting has a suppressive effect on hepatic glucose production and can cause hypoglycemia, which can be deadly. BIS further regulates fat metabolism by regulating lipolysis i.e., breakdown of stored triglycerides into free fatty acids (FFA) from the adipose tissue; a source of fuel for glucose-independent tissues during fasting. In addition to fat and glucose metabolism, basal insulin also regulates hepatic ketogenesis. Therefore, it is critical that insulin secretion, both basal and glucose-stimulated, is tightly and dynamically regulated across the cycles of fasting/feeding and activity/rest in a time-of-day-dependent manner to not only ensure that blood glucose levels are maintained within a narrow and appropriate range, but also to ensure that the disparate metabolic needs associated with cycles of fasting/ feeding and activity/rest are met. Despite the essential physiological importance of BIS explained above, the mechanisms that regulate BIS are poorly understood. Note that while BIS is essential for the metabolic regulation in the fasted state, this dissertation will focus on mechanisms that regulate GSIS. As such, unless specified, references to insulin secretion below likely refer to GSIS.

1.3 Metabolism-Derived Coupling Factors that Regulate GSIS

The molecular cascade from glucose-sensing by the pancreatic β-cell to insulin secretion involves numerous critical coupling molecules or co-factors that are generated by metabolism of specific fuels (glucose, amino acids and fatty acids), referred to as metabolic coupling factors, or MCFs. The mechanistic pathway of GSIS outlined in Section 1.2.1 hints at many of these regulatory molecules such as the intermediates of the TCA cycle (citrate, malonyl co-enzyme A etc.) to regulate effector molecules such as ATP, NAD^+ and ROS, which further play an important role in both triggering and amplifying pathways of GSIS. In the upcoming section, I will provide a detailed description of the importance of 1) the ATP/ADP ratio; and 2) mitochondrial ROS signals and their roles in coupling glucose metabolism to GSIS.

1.3.1 ATP/ADP Ratio and the K^+_{ATP} Channel

To understand the regulatory role of ATP/ATP ratio on insulin secretion, it is imperative to first understand the structure and regulation of the K^+_{ATP} channels by ATP/ADP ratio as it is a key event described in Section 1.2.1 that leads to membrane depolarization and ultimately insulin secretion. K^+_{ATP} channels were initially discovered in the heart (Noma, 1983) following which, its existence in all other organs, including the pancreatic β-cell, was confirmed (Ashcroft et al., 1984, Cook and Hales, 1984, Rorsman et al., 1989). The β-cell K^+_{ATP} channel is a hetero-octamer channel located on the plasma membrane consisting of 4 subunits of sulfonylurea receptor (SUR1) and 4 subunits of the potassium channel, Kir6.2 (Miki et al., 1999). SUR1 is an ATP-Binding cassette (ABC) transporter family member and its association with the Kir6.2 subunit renders Kir6.2 sensitive to drugs such as sulfonylureas and increased concentrations of the nucleotide, MgADP (Aguilar-Bryan et al., 1995).

Additionally, the closing and opening of the K^+_{ATP} channels is facilitated by the presence of a phosphatidylinositol-4, 5-bisphosphate (PIP2) subunit required by all Kir family channel proteins (Xie et al., 2008). All 4 subunits of Kir6.2 possess an ATP binding site; however, binding of ATP to any one of the 4 subunits is sufficient to close the channel (Antcliff et al., 2005, Enkvetchakul and Nichols, 2003). The regulatory role of the ATP/ADP ratio on K^+_{ATP} channels and its consequential role in triggering insulin secretion hinges on 1) the closure of K^+_{ATP} channel by binding of ATP to the ligand binding site present on the kir6.2 subunit of the channel; and 2) an activating role of ADP on the SUR1 subunits of the ATP channel. On one hand, a high glucose environment not only generates ATP via OXPHOS, but consequently reduces ADP levels, which closes the K^+ channels and primes the events required for exocytosis of insulin granules. Conversely, the accumulation of ADP in a low glucose environment has no inhibitory effect on K^+ channels. Similar to glucose, hypoglycemic sulfonylureas, such as tolbutamide, bind to the regulatory subunit SUR1 (Aguilar-Bryan and Bryan, 1999, Ashcroft and Gribble, 1999) and result in membrane depolarization, Ca^{2+} influx leading to insulin secretion (Gilon and Henquin, 1992, Panten et al., 1996, Satin, 1996). As mentioned in Section 1.2.1, Ca^{2+} is an important co-factor triggers insulin exocytosis after membrane depolarization that results from closure of K^+_{ATP} channels. Tolbutamide, which binds to the SUR1 subunit triggers a similar rise in intracellular Ca^{2+} as a result of K^+_{ATP} channel closure (Grapengiesser et al., 1990, Herchuelz et al., 1991, Gilon and Henquin, 1992). Stimulation of insulin secretion by sulfonylureas have been effective in cases of diabetes that result from Kir6.2 mutations (Greeley et al., 2010). Alternatively, in cases of congenital hyperinsulinemia, a K^+_{ATP} channel opener, diazoxide, binds to the SUR1 subunit and causes the channel to remain open (Hibino et al., 2010), forcing membrane hyperpolarization and reducing insulin secretion (Arnoux et al., 2010, Kapoor et al., 2009, Ashcroft and Gribble, 2000). Furthermore, mouse models have been used to characterize both loss- (Remedi et al., 2006, Miki et al., 1999) and gain-of function K^+_{ATP} channel activity and have emphasized the physiological importance of K^+_{ATP} channels in insulin secretion.

While the drugs mentioned above to treat diabetes have emphasized the physiological role of K^+_{ATP} channels in regulating insulin secretion, the ATP/ADP ratio is critical for the regulation of the activity of these channels. Evidence from studies as early as 1970s, pointed to a causative relationship between glucose oxidation, ATP/ADP content and insulin secretion in islets isolated from white male mice (Ashcroft et al., 1973, Malaisse et al., 1979, Meglasson et al., 1989, Ohta et al., 1991) and in islets isolated from NMRI mice (Detimary, 1996). ATP content was observed to be increased when islets were incubated in increasing concentration of glucose (3.3mM and 16.7mM) but more importantly ATP content reduced in islets in the absence of glucose (Detimary et al., 1994, Ashcroft et al., 1973). Furthermore, ATP content significantly declined in islets when ATP synthesis was inhibited using an uncoupling agent like carbonyl cyanide p-(tri-fluromethoxy) phenyl-hydrazone (FCCP;0.1µg/ml). Uncoupling of electron transport chain ultimately reduces insulin secretory capacity via

reduced ATP concentrations. The variation of ATP/ADP ratio at stimulatory concentration of glucose have shown to affect several mediatory steps in GSIS pathway such as its association with increases in Ca^{2+} concentration providing further evidence that ATP/ADP ratio plays a central triggering role in the control of insulin secretion.

1.3.2 Reactive Oxygen Species (ROS)

In general, ROS are the inevitable by-products of electron transfer in an oxygen-rich environment. The mitochondrion is the largest source of ROS in the cell (Dan Dunn et al., 2015). The most abundant and common forms of ROS are hydrogen peroxides (H_2O_2), superoxide anions (O_2^-) and hydroxyl ions (HO^-) (Schieber and Chandel, 2014).While ROS can be generated at other sites in the cell under specific physiological conditions (e.g., NADPH oxidase on the plasma membrane)(Brand, 2010), mitochondrial ROS is generally formed as a result of "leak" of electrons at complex I (NADH coenzyme Q reductase) and III (Q-cytochrome c oxidoreductase) of the mitochondrial electron transport chain (mETC) and enzymes that either cause either one or two electron reductions of oxygen (Zorov et al., 2014). Importantly, superoxide radicals (O_2^-) are generated via transfer of single electron from complex I to III of the mETC via the "Q cycle" (Turrens, 2003). When the rate of electron entry into the mETC and the rate of transport of electrons through the mETC are mismatched, superoxide formation increases at complex I and III as the partially reduced ubiquinone radical, Q_2, donates an electron to O_2 resulting in the formation of superoxide radicals (O_2^-). O_2^- is the first produced form of ROS and is the moderately reactive (Dan Dunn et al., 2015). Often, O_2^- is readily converted to a less reactive form of ROS, hydrogen peroxide (H_2O_2) by the antioxidant enzyme family of superoxide dismutases (SOD1, 2 and 3)(Wang et al., 2018). H_2O_2 can then be broken down to O_2 and water by several antioxidant enzymes, including catalase (CAT), glutathione peroxidase (GPX), and peroxiredoxin (Wang et al., 2012). The above mentioned enzymes are all part of the antioxidant system which operate to control ROS levels within a certain threshold in a cell (Wang et al., 2012). If not effectively eliminated, ROS can accumulate above a safe threshold, known as oxidative stress, and can cause sufficient damage, including lipid oxidation, protein oxidation and DNA fragmentation (Schieber and Chandel, 2014). Regulation of these products by the antioxidant system is important for normal biological function. While initially thought of as toxic, in recent years, ROS have been regarded as important signaling molecules that contribute to the control of many physiologically important functions, including cellular proliferation, differentiation, and cellular migration (Rhee, 2006). As the complexities and mechanisms of redox signalling become better understood, it is clear that we need to understand how a cell spatially and temporally directs ROS for different, yet favourable outcomes in a cell.

Importantly, the mitochondrial membrane potential directly controls the degree of mitochondrial ROS formation; even small increases in mitochondrial membrane potential can significantly increase ROS formation. Pancreatic β-cells have a relatively low expression of antioxidant enzymes, which not only makes them more prone to oxidative damage, but also allows for sufficient production of ROS signals that could play important

roles in regulating β-cell function (Lei and Vatamaniuk, 2011). To be more specific, compared to the liver, islets have 1% of catalase, 2% of GPX and 29% of SOD2 activity (Grankvist et al., 1981, Lenzen et al., 1996, Tiedge et al., 1997). As mentioned above, ROS generation which happens at the level of mETC, occurs as a result of metabolism. Despite the mitochondria being the site where the process of GSIS happens, very little importance is given to the potential role ROS and insulin secretion. Conversely, the low ROS scavenging potential in β-cells and the relatively quick turnover of ROS products suggests that ROS may be important signaling molecules that allow for rapid metabolic responses to be translated into altered on-demand insulin secretion capacity. ROS generated as a result of glucose metabolism has been shown to correlate well with insulin secretion (Pi et al., 2007, Robson-Doucette et al., 2011). In line with this hypothesis, several studies have suggested that ROS signals generated as a result of glucose oxidation and metabolism, in isolated rodent islets, enhances the GSIS response (Pi et al., 2007); however, our understanding of the mechanisms behind ROS signaling in the insulin secretory pathway is currently unclear. Many studies have demonstrated that stimulation of β-cells with 20mM glucose increases ROS production, both in *in vitro* (INS1 (832/13) a subclone of INS1 cells originally derived from x-ray induce insulinoma in rats and MIN6 clonal β-cell lines) and *in vivo* mouse models (Llanos et al., 2015, Bindokas et al., 2003, Tanaka et al., 2002) while there are studies that have demonstrated no effect of high glucose exposure on ROS production (Affourtit et al., 2011). Additionally, application of low concentration of exogenous H_2O_2 (1-4μmol/l) or a pro-oxidant, such as diethyl maleate (DEM; 1mM), to both INS1(832/13) which is a derivative of INS1cells and islets isolated from 3- to 4-month-old 129S1/SvImJ mice (Pi et al., 2007) resulted in a robust GSIS response. Conversely, application of an antioxidant or ROS scavenger like N-Acetyl L-Cysteine (NAC) significantly reduced insulin secretion in both models (Pi et al., 2007) (Robson-Doucette et al., 2011). Studies on isolated rat islets revealed a concomitant increase in intracellular Ca^{2+} when incubated with H_2O_2, suggesting that H_2O_2 could be essential for intracellular Ca^{2+} increase in response to glucose metabolism (Llanos et al., 2015). However, the Pi et al (2007) study, showed that H_2O_2-stimulation in islets increased insulin secretion and Ca^{2+} influx suggesting that ROS may be involved in the Ca^{2+} influx machinery which is a key event in GSIS pathway. Interestingly, application of mETC inhibitors (oligomycin, rotenone and antimycin A) that increased mitochondrial ROS production, failed to augment insulin secretion, suggesting that mitochondrial-induced ROS alone is not sufficient to induce insulin secretion, and as the above statement indicates, a concomitant increase in Ca^{2+} concentration may be required. Importantly, it should also be noted that ROS alone cannot stimulate insulin secretion, which emphasizes its dependency on ATP and glucose metabolism-secretion coupling (Pi et al., 2007, Henquin, 2000, Wollheim and Maechler, 2002), suggesting that the amplification and triggering pathways are interdependent and required for an appropriate post-prandial insulin response.

While ROS levels appear to be important for augmentation of GSIS in healthy β-cells, it is not surprising that studies in obese and hyperglycemic environments show significantly increased ROS levels in β-cells, as

excessive ROS production results in oxidative stress (Roma and Jonas, 2020). It has been shown that ROS at high concentrations can dampen GSIS by affecting pathways relating to insulin biosynthesis (i.e., affecting expression of PDX-1 and MafA) (Harmon et al., 2005) and inhibit glycolysis by inactivating key enzymes such glyceraldehyde 3-phosphate dehydrogenase (GAPDH) and phosphofructokinase (PFK)(Mullarky and Cantley, 2015). It has also been well demonstrated that ROS can inhibit TCA cycle enzymes as the TCA cycles consists of 5 enzymes that contain Fe-S clusters, which are highly sensitive to the redox state (Noster et al., 2019).

Elevated endogenous ROS levels have also been shown to correlate with β-cell dysfunction and diabetes development. For example, polymorphisms in *Sod1* and *Sod2* that impede SOD function and increase superoxide formation, were found in some T1D and T2D patients (Flekac et al., 2008). Furthermore, low levels of GPX activity have been observed in rat models of β-cell failure and T2D (Asayama et al., 1986). Mice treated with multiple low doses of streptozotocin (STZ) (to create an animal model of T2D) was characterised by loss in β-cell's secretory function and an increase in H_2O_2 levels (Like and Rossini, 1976, Takasu et al., 1991, Dong et al., 2016) suggesting that increases in ROS is detrimental to β-cell health. Additionally, elevated ROS can trigger apoptosis in β-cells, which has been observed in T2D (Maechler and Wollheim, 2001). Other forms of ROS species, such as HO^-, have found to cause cellular damage in human islets (Crow and Beckman, 1995, Delaney et al., 1996, Gurgul-Convey et al., 2011). Conversely, scavenging ROS has beneficial effects on metabolic health. For example, in the leptin-deficient *ob/ob* mouse model and other models of insulin resistance, treatment with antioxidant agents improved insulin sensitivity (Jacob et al., 1999, Evans et al., 2003, Houstis et al., 2006). Additionally, healthy Wistar rats infused for 48 hours with high glucose to achieve hyperglycemia exhibited oxidative and ER stress markers (Belegri et al., 2017), while co-infusion with superoxide dismutase mimetics, such as tempol, 4-phenylbutyrate (PBA) or tauroursodeoxycholic acid (TUDCA), significantly reduced superoxide levels, reduced ER stress and improved GSIS capacity (Tang et al., 2012). Further, injection of an antioxidant in an STZ-induced rat model of T2D (Robbins et al., 1980) or overexpression of antioxidant enzymes (Xu et al., 1999, Harmon et al., 2009, Mysore et al., 2005, Chen et al., 2001, Kubisch et al., 1994) also abrogated the detrimental effects on pancreatic islets such as the loss of insulin secretion, which ultimately improved glucose tolerance. Conversely, knockout of antioxidant genes such as *Sod1* and *Gpx1* has been shown to worsen β-cell integrity and function leading to T2D (Kikumoto et al., 2010, Loh et al., 2009, Wang et al., 2011).Collectively, the literature suggests that ROS may act as an important signal to regulate GSIS, but beyond a "threshold" can induce oxidative stress in β-cells, leading to dysfunction and diabetes development.

1.4 Regulation of β-Cell Metabolism

While ROS and ATP are important signals generated by metabolism that couple glucose metabolism to insulin secretion, the rate at which these signals are formed is ultimately dependent on the function of a number of metabolic enzymes in the glucose oxidation pathways (glycolysis, TCA cycle and mETC). For example,

glucokinase activity is the rate limiting step of glycolysis and its activity is essential not only for commitment of glucose to glycolysis but also to the rate at which glucose enters this oxidative pathway. While there are several important regulatory proteins in each step of primary metabolism, I will focus on the role of mitochondrial uncoupling protein 2 (UCP2) and cytosolic lactate dehydrogenase (LDH), as these are the focus of my thesis work.

1.4.1 Uncoupling Proteins

Uncoupling proteins (UCPs) are a family of mitochondrial transmembrane proteins that are found in the inner mitochondrial membrane in many tissues. There are currently five known uncoupling proteins in this family (UCP1-5). The first discovered uncoupling protein, named UCP1, was found in brown adipose tissue and has been shown to act as a proton channel in the inner mitochondrial membrane. Activation of UCP1 creates a strong mitochondrial proton leak that completely dissipates the proton motive force formed by mETC electron transfer (Nicholls and Locke, 1984). UCP1 is activated by long chain fatty acids brought on by the breakdown of membrane lipid droplets by adrenergic activation (Cannon and Nedergaard, 2004, Fedorenko et al., 2012). outlined in [**Figure 1.3**] Dissipation of the proton motive force "uncouples" the energy stored in the electrochemical gradient from ATP production and as a result, this energy is dissipated as heat. Accordingly, UCP1 has a thermogenic role in brown adipose tissue (Nicholls and Locke, 1984, Cannon and Nedergaard, 2004, Nedergaard et al., 2005).

Based on sequence homology (not functional homology) to UCP1, several 'novel' uncoupling proteins have been identified (Nedergaard and Cannon, 2003, Nedergaard et al., 2005). UCP2, discovered in 1997, shows 59% amino acid sequence identity to UCP1 and UCP2 shows a high degree of conservation across species (mouse UCP2 shows ~95% homology to human UCP2) (Fleury et al., 1997). Importantly, several regulatory motifs are conserved between UCP1 and UCP2 namely, a mitochondrial carrier protein motif, with possible roles in ion transport in and out of the mitochondrial matrix, and an ATP binding motif. Unlike UCP1, which is expressed only in thermogenic brown adipose tissue, UCP2 is more ubiquitously expressed, with expression observed in non-thermogenic tissues, including skeletal muscle, lung, heart, placenta, kidney, spleen, thymus, leukocytes, macrophage, bone marrow, stomach, and pancreatic islets (Fleury et al., 1997), suggesting a non-thermogenic function for this uncoupling protein. Additionally, expression of UCP2 in immune cells such as leukocytes, macrophages and bone marrow suggest roles for UCP2 in immunity and infections (Vogler et al., 2006, Rousset et al., 2006). The wide expression of UCP2 in non-thermogenic tissues suggests that the biological and physiological function of UCP2 is likely different from the strong uncoupler, UCP1 and UCP2 may have tissue-specific functions.

Around the same time as the discovery of UCP2, Brad Lowell's group at Harvard Medical School discovered a third uncoupling protein homologue by molecular cloning, which was named UCP3. UCP3 is distinct

from UCP1 and UCP2 based on its expression as well as it being most abundant in skeletal muscle in humans, along with skeletal muscle and brown adipose tissue in rodents (Vidal-Puig et al., 1997). UCP3 also shows lower expression in the heart, thyroid, and bone marrow. At the amino acid level human UCP3 is 97% similar to human UCP2 and 57% similar to human UCP1(Vidal-Puig et al., 1997).

In 1999, two years after the discovery of *Ucp2* and *Ucp3*, Mao and group discovered UCP4, which is specifically expressed in the brain. The expression of UCP4 may be involved in thermoregulatory function in the brain as flow cytometry studies show the generation of a proton leak in cells transfected with *Ucp4* over-expressing plasmid (Mao et al., 1999). UCP5, which is also known as brain-specific mitochondrial carrier protein, like UCP4, is regulated by the nutritional and thermo-regulatory requirements in the body (Yu et al., 2000). While several UCPs have been discovered by sequence homology to UCP1, the physiological functions of the 'novel' UCPs (UCP2-5) have not been well-defined, although they are implicated to play vital roles in maintaining metabolic homeostasis.

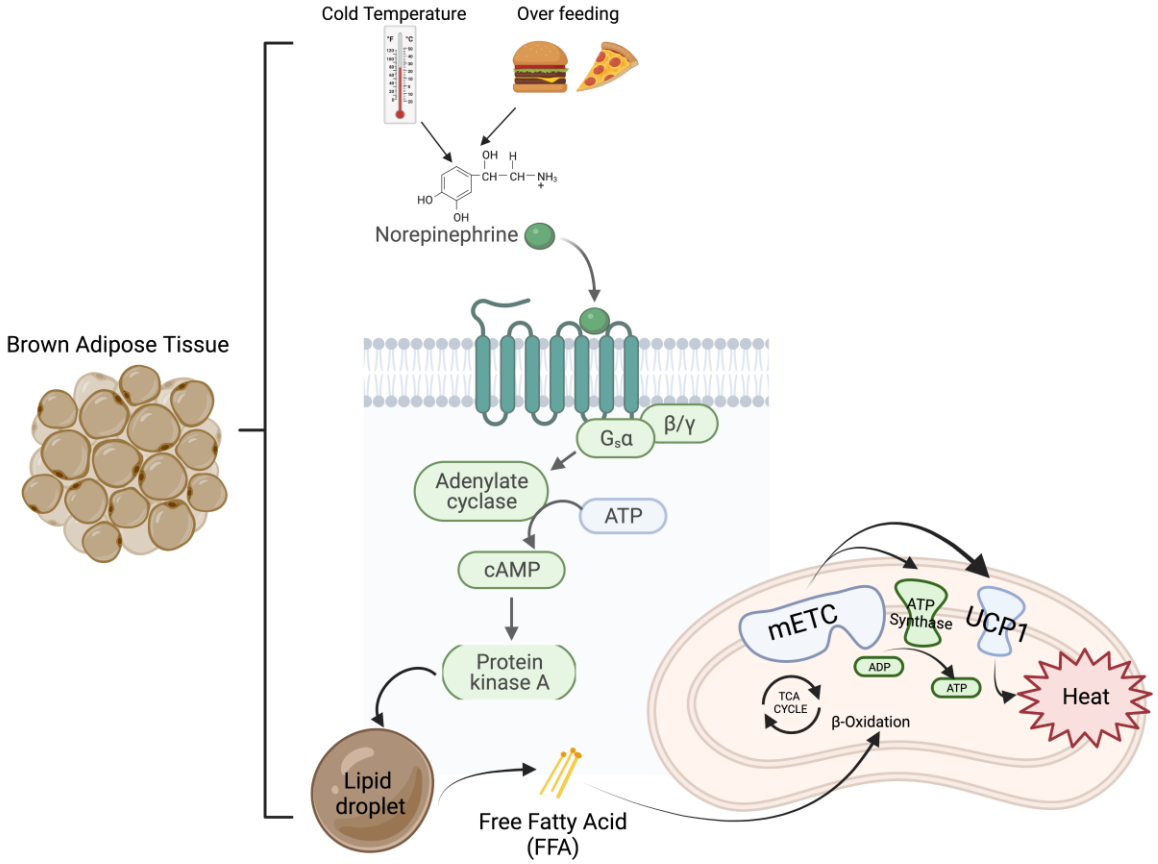


Figure 1.3: Activation of Uncoupling protein 1. Over-nutrition and/or extreme cold temperatures catalyses the binding of norepinephrine to its receptor present on the plasma membrane of lipid droplets present in the brown adipose tissue. The binding activates adenylate cyclase to convert ATP to cyclic AMP. The accumulation of cAMP turns on PKA which helps release free fatty acid (FFA) by phosphorylating an enzyme responsible for converting triglycerides into free fatty acids which via β-oxidation turns on Ucp1 which generates heat.

1.4.1.1 ***The Potential Biochemical Functions of UCP2***

While UCP1 is expressed in the inner mitochondrial membrane and has been shown to completely dissipate the proton motive force (Palou et al., 1998), this has not been clearly demonstrated with the other novel UCPs (2-5). In fact, it is not clear whether the novel UCPs mediate proton transport directly or indirectly. As stated above, UCP2 activity is activated by several pathophysiological states and metabolic by-products, but its precise biochemical function has been widely debated.

In this section, I will discuss the biochemical functions that have been proposed for UCP2. The association of proton leak and UCP2 expression has suggested a possible role for UCP2 as a proton conductor (Affourtit and Brand, 2008b); however, how proton conductance is mediated across the inner mitochondrial membrane (i.e., whether UCP2 directly creates a proton leak via formation of a pore or if the transport of protons occurs secondary to a different function of UCP2) is unclear. It has been suggested that UCP2 catalyzes proton transport across in the inner mitochondrial membrane by the flip-flop model. Firstly, the transport of protons is aided by the negative membrane potential of the inner membrane space. Briefly, protons are picked up by the carboxylic heads of FA anions and transported to the matrix side conferring a positive charge to the inner membrane. Once protons are released onto the matrix side, fatty acids bind to a peripheral site of UCP2 at the matrix site and are displaced back into the outer membrane. The FA mediated proton transport is shown to be inhibited by several purine nucleotides such as ATP, ADP, GDP and GTP as these competitively bind to the peripheral site on UCP2 and prevent the binding of fatty acids. The above model is known as the UCP2 mediated "flipflop" model of transport of protons. Yet another model proposed to explain UCP2's function as protonophore is called the cofactor model. In this model, the carboxy head of the FA anions accept protons from the intermembrane space and transport it to the matrix side through a channel in UCP2 (Krauss, 2005). This model of transport is possible by FA donating protons to amino acid in UCPs. However, it is clear from the above proposed model that UCP2 does not transport the protons but merely binds to the FA anions which do the transport activity.

Yet another postulated biochemical function for UCP2 is in maintaining Ca^{2+} homeostasis by regulating its uptake (Trenker et al., 2007, Madreiter-Sokolowski et al., 2016). The mitochondrion is an organelle well known for its Ca^{2+} handling and the mechanisms by which mitochondria accumulate Ca^{2+} has been extensively investigated for decades (De Stefani et al., 2016). Mitochondrial calcium uniporters have been described in the literature (Patron et al., 2013, Brookes et al., 2008). *Ucp2* overexpression, knockout and mutational studies that resulted in impairment of UCP2 activity have demonstrated its role in mitochondrial Ca^{2+} sequestering in the heart (Waldeck-Weiermair et al., 2010, Turner et al., 2010). Along with UCP2's role in Ca^{2+} transport, its role in dissipating membrane potential and Fatty acid cycling within the mitochondria should be considered. When the proton motive force is dissipated (by *Ucp2* expression) it affects Ca^{2+} uptake and accumulation within the

mitochondria (Waldeck-Weiermair et al., 2010, Turner et al., 2010). These biochemical functions have however not been demonstrated the β-Cell and are not the focus of this thesis.

*1.4.1.2 **Uncoupling Protein 2 and the β-Cell***

Upon its discovery in 1997 and given its potential to uncouple the mitochondrial membrane potential, several diabetes research groups began attempting to decipher a physiological role for UCP2 in the pancreatic β-cell, as mitochondrial uncoupling would have important consequences for insulin secretion. In 2001, Zhang *et. al.* created and characterized the first whole-body *Ucp2* knockout mouse model (*Ucp2*$^{-/-}$), which showed normal body weight gain trajectory compared to its controls and no changes in body temperature upon cold exposure, suggesting that UCP2 does not play a role in regulating body weight and temperature, which would be expected of a "strong" uncoupling protein like UCP1 (Zhang et al., 2001). Additionally, in *ad libitum*-fed *Ucp2*$^{-/-}$ mice, serum insulin levels were higher, which corresponded to lower blood glucose levels compared to control mice. Furthermore, islets isolated from *Ucp2*$^{-/-}$ mice displayed enhanced insulin secretion and significantly higher glucose-stimulated ATP content when compared to wild type (WT) mice, suggesting that UCP2 negatively regulates insulin secretion via regulation of glucose-coupled ATP production (Zhang et al., 2001). Since this initial study, several studies have confirmed this inverse relationship between UCP2 expression and insulin secretion capacity in rodent islets, as well as in β clonal cells (Wang et al., 1999, Chan et al., 2001, Chan and Kashemsant, 2006, Chan et al., 1999, Affourtit and Brand, 2008b).

Increased UCP2 expression is observed in β-cells in several pathophysiological states. Exposure to several pathophysiological agents such as hydrogen peroxide (H_2O_2) at a high concentrations (Li et al., 2001), lipid peroxidation by-products like 4-HNE (Echtay et al., 2003), lipopolysaccharides (Ruzicka et al., 2005), TNFα (Lee et al., 1999), free-fatty acids (Medvedev et al., 2002), as well as a high-fat diet challenge (Surwit et al., 1998), (Parton et al., 2007) have all been shown to increase UCP2 expression in both animal and cell models. *Ob/ob* mice, which experience hyperphagia and excessive weight gain as a result of a mutation in the leptin gene, consequently develop insulin resistance, glucose intolerance, impaired insulin secretion and hyperglycemia, making them a model of obesity-associated T2D. Interestingly, the impaired insulin secretion in the *ob/ob* model was associated with significantly elevated *Ucp2* mRNA and protein expression in isolated in islets (Zhang et al., 2001). Crossing *ob/ob* mice with *Ucp2*$^{-/-}$ mice (i.e., preventing the ability to increase *Ucp2* expression), ameliorated glucose intolerance and restored insulin secretion, demonstrating an important role for UCP2 in β-cell failure in models of obesity and T2D (Zhang et al., 2001).

While these early studies using the whole body UCP2 knockout mouse demonstrate a clear inverse relationship between UCP2 expression/activity level and insulin secretion capacity, these findings are complicated by the fact that UCP2 is expressed in number of metabolic tissues, and whole-body knockout of UCP2 may create signals from other tissues that could impact the β-cell secondary to knockout of *Ucp2* in the β-

cell itself. To circumvent this limitation, a β-cell-specific UCP2 knockout mouse model (*Ucp2*βKO) was established by Robson-Doucette et. al., which showed no impact of β-cell UCP2 deficiency on body weight, fasting glucose or plasma insulin levels (Robson-Doucette et al., 2011), but displayed augmented insulin secretion similar to that seen in the *Ucp2*$^{-/-}$ mice. Unlike whole-body *Ucp2* knockout mice, *Ucp2*βKO mice displayed impaired glucose tolerance despite the improved insulin secretion. Also, unlike *Ucp2*$^{-/-}$ mice, β-cell-specific UCP2 deletion did not increase glucose-induced ATP production, despite a mild increase in glucose-induced mitochondrial membrane potential; however, islets isolated from *Ucp2*βKO showed significantly elevated ROS production. Manipulation of islet ROS levels with anti- and pro-oxidants revealed that UCP2 deficiency in the β-cell enhanced insulin secretion in a ROS-dependent manner. Morphological analyses of pancreata and islets from *Ucp2*βKO mice demonstrated that UCP2 deletion in the β-cell had no impact on β-cell mass, but rather increased α-cell mass, which correlated with altered glucagon biosynthesis and aberrantly high levels of glucagon secretion upon glucose exposure, which was postulated to be the driver behind the impaired glucose tolerance in *Ucp2*βKO mice (i.e., hyperglucagonemia after a glucose stimulus that triggers aberrant endogenous glucose production when it should be suppressed). Collectively, these studies by Robson-Doucette et. al., demonstrate that UCP2 plays a central role in the regulation of insulin secretion by fine tuning β-cell ROS production, which in turn controls insulin secretion capacity. Additionally, this study showed that ROS signals that are regulated by UCP2 in the β-cell can create an intra-islet ROS signal that impacts neighbouring endocrine cell function and overall glucose tolerance.

While a negative relationship between UCP2 expression/activity and insulin secretion has been well-established in rodents, polymorphisms in human *Ucp2* gene have been discovered that demonstrate this relationship in humans. For example, the ~866G/A polymorphism located in the *Ucp2* promotor region results in increased *Ucp2* expression, impaired insulin secretion and susceptibility to the development of T2D (D'Adamo et al., 2004, Sesti et al., 2003, Gable et al., 2006). Other polymorphisms of *Ucp2* also associate with obesity and diabetes, including a missense variation in exon 4, resulting in alanine to valine change (Surniyantoro et al., 2018) and a 45bp insertion in Exon 8 (Li et al., 2019). The missense heterozygous mutation in the *Ucp2* gene, resulting in a loss of UCP2 protein, is observed in patients diagnosed with congenital hyperinsulinemia (Gonzalez-Barroso et al., 2008). These patients experience neonatal hypoglycemia and are sensitive to diazoxide, a well-known K^+_{ATP} channel opener (Gonzalez-Barroso et al., 2008) and suppressor of insulin secretion. Introduction of these mutations into the INS-1E clonal β-cell line showed loss of UCP2 protein activity, which promoted hypersecretion of insulin (Gonzalez-Barroso et al., 2008)

The role of Ucp2 in fatty acid cycling as mentioned above emphasizes that UCP2 functions as fatty acid flippase. Briefly, fatty acids bind to UCP2 facilitating the transport of anions such as FA- which are otherwise unable to cross mitochondrial inner membrane (Skulachev, 1991). Furthermore, FAs also activate UCP2 and

results in its uncoupling activity as demonstrated by studies in insulinoma cells. These FAs arise as a result phospholipid cleavage by ROS by-product H_2O_2 (Jezek et al., 2015) affecting insulin secretion. Evidence from other studies suggests that *Ucp2* expression promotes fatty acid oxidation and results in loss of GSIS (Lameloise et al., 2001). But the impairments in insulin secretion mentioned above are seen specifically in glucolipotoxicity models wherein β-cells or INS1 clonal cells are treated with high concentration of fatty acids such as palmitate and oleate. Disease models do not completely recapitulate physiological conditions. We know fatty acid levels in plasma could increase during an overnight fasting. Can FAs released during an overnight fast potentially activate UCP2? How does it impact insulin secretion in the pancreatic β-cells as cycle between the fed and fasted phase of the day?

1.4.1.3 UCP2-Mediated Regulation of ROS Production in the β-cell

Uncoupling (directly or indirectly) can be perceived as an efficient mechanism to control mitochondrial ROS production as the degree of ROS production is highly influenced by the mitochondrial membrane potential (i.e. the more hyperpolarized the inner mitochondrial membrane, the greater the ROS production). Several studies have shown that UCP2-mediated uncoupling reduces the mitochondrial membrane potential, which also reduces ROS production (Jezek et al., 2014, Robson-Doucette et al., 2011), as such, UCP2 has been touted as having an "antioxidant" role. Inhibition of UCP2 activity using a pharmacological inhibitor (genipin), increases ROS production in islets (Zhang et al., 2006, Robson-Doucette et al., 2011) and INS1-E cells (Zhang et al., 2006, Affourtit et al., 2011) and no changes in mitochondrial membrane potential are observed in islets isolated from *Ucp2*$^{-/-}$ mice when a UCP2 activator is applied (Krause et al., 2011). Additionally, overexpression of UCP2 prevented IL-1β-induced ROS formation in INS-1E cells (Produit-Zengaffinen et al., 2007), demonstrating an antioxidant role for UCP2 during an immune response. In line with above statement, it is important to note that most studies that have examined the role of UCP2 in ROS regulation have done so in loss-of-function or overexpression models or supraphysiological models where UCP2 is chronically upregulated(Lee et al., 2009, Robson-Doucette et al., 2011, Negre-Salvayre et al., 1997). While the above studies demonstrate a plausible role for UCP2 in control of ROS formation, there are studies that show no effect. For example, Galletti et. al., (2009) demonstrated no effect of *Ucp2* overexpression on ROS production following treatment of INS-1E cell with oleate (fatty acid known to activate UCP2 expression)(Galetti et al., 2009). Collectively, these studies emphasize the ambiguity existing around UCP2's in regulation of ROS production.

1.4.1.4 UCP2-Mediated Regulation of ATP Production in the β-cell

In addition to the regulation of ROS, several studies have shown that UCP2 influences glucose-mediated ATP production. Initial studies that explored the role of UCP2 on ATP production, using overexpression of human UCP2 in transgenic mice and INS1-1 cell line showed no effects on GSIS or ATP/ADP ratio (Produit-Zengaffinen, 2007) (Li, 2001). Other groups using adenoviral-mediated overexpression of UCP2 in rat islets

showed impairments on GSIS capacities via impact on ATP/ADP ratio (Chan et al., 1999, Sesti et al., 2003). Whole-body UCP2 knockout mouse models (Zhang et al., 2001, Joseph et al., 2002, Lee et al., 2009) and inhibition of UCP2 using pharmacological agents like Genipin (Zhang et al., 2006) demonstrated suppression of UCP2 improved GSIS via increased ATP production. It is important to note that while some studies show an effect of UCP2 on ATP levels (Joseph et al., 2002, Zhang et al., 2001, Wang et al., 2016, Chan et al., 1999), others do not (Robson-Doucette et al., 2011, Bouillaud, 2009, Couplan et al., 2002). While these discrepant findings could be the result of the models used, the contribution of UCP2 in regulation of insulin-triggering ATP production remains ambiguous and needs to be addressed.

1.4.1.5 UCP2 Upregulation in Response to Starvation: A potential Mechanism to Prevent Hypoglycemia

Given its demonstrated negative impact on insulin secretion, researchers have been trying to understand why the β-cell expresses *Ucp2* (i.e., what is UCP2's physiological function in the β-cell?). Researchers have questioned whether UCP2 has a physiological function in the healthy β-cell or whether it only serves a pathological function in stressed states and in the development of diabetes. Considering the latter, this also raises the question of why would a gene that negatively influences metabolic health not have been eliminated during evolution, which lead researchers, including ourselves, to believe that UCP2 must have an important physiological function in the healthy β-cells. In 2008, a study was published by Sheets et. al., which provided an important clue as to what UCP2's physiological function in the β-cell may be. In this study, Sheets et. al., exposed mice to prolonged fasting/starvation (72hrs) and made the observation that insulin secretion is reduced during prolonged fasting. Importantly, they showed that this reduction in insulin secretion was the result of elevated UCP2 expression (Sheets et al., 2008). Based on this, they postulated that UCP2 may play an important role in the β-cell to inhibit insulin secretion and therefore prevent hypoglycemia during prolonged periods of fasting when blood glucose should be spared for essential tissues (i.e., brain function). Notably, this study only examined UCP2 expression and its impact on insulin secretion in the starvation/prolonged fasted state and did not examine if UCP2 plays a similar function in suppressing insulin secretion in daily cycles of fasting.

1.4.2 Lactate Dehydrogenase and β-cells

Lactate dehydrogenase (LDH) is an enzyme that facilitates the bi-directional conversion of pyruvate to lactate, shuttling glucose away from aerobic respiration and regenerating NAD+ from NADH. Typically, LDH is active when there is a lack of oxygen or hypoxia and was first seen to be beneficial in cancer cell growth and survival, broadly called the Warburg effect. LDH is ubiquitously expressed and as such is often referred to as a 'housekeeping gene'. LDH is active as a homo-dimerization or hetero-dimer of LDH-M and LDH-H encoded by 2 genes namely *Ldha* and *Ldhb*, respectively (Payen et al., 2020, Rani and Kumar, 2016, Granchi et al., 2010). The gene *Ldha* is located on chromosome 11, which is translated into a 332 amino acid protein. High LDH levels in the blood have been indicative of underlying metabolic syndromes like cancer, heart disease, liver disease and

infectious conditions such encephalitis, HIV, meningitis etc (Feng et al., 2018, Mercer et al., 2019, Khan et al., 2020). Studies that examined *Ldha* in models of T2D showed that *Ldha* was also upregulated in islets isolated from rats exposed to hyperglycemia (Bensellam et al., 2012) and in obese-hyperglycemic mice (Hellman and Taljedal, 1967, Prochazka et al., 1970). In 1998, Zhao et. al., demonstrated that overexpression of *Ldha* impairs glucose-stimulated insulin secretion in MIN6 clonal β-cells (Zhao and Rutter, 1998). The above finding has also been previously reported in other glucose-responsive cell lines, including βHC9 (Zhao and Rutter, 1998, Ainscow et al., 2000, Ishihara et al., 1999), collectively suggesting that LDH has a pathological role for in the β-cell.

Despite the wide expression of LDH in the body, healthy pancreatic β-cells express 8-fold lower levels of LDH compared to islet non-β-cells and 122-fold lower levels than the liver. (Sekine et al., 1994, Bricker et al., 2012, Liang et al., 1996, Hellman and Taljedal, 1967). Given the role of LDH in diverting carbon from glucose metabolism away from oxidative phosphorylation and the low levels of LDH in β-cells, it has been suggested that LDH is 'disallowed' from the β-cell. That is, LDH is actively suppressed in healthy β-cells to maintain maximal/optimal capacity to secrete insulin, which could be viewed as an evolutionary adaptation to protect the functionality of insulin secretion (Schuit et al., 2012). More recent studies have shown that *Ldha* is expressed in immature β-cells but is actively silenced by microRNA suppression in the mature β-cells (Thorrez et al., 2011). Notably, immature β-cells are not glucose-responsive and the suppression of *Ldha* in development coincides with the active suppression of LDH (Jacovetti et al., 2017). Given the reliance of mature β-cells on glucose metabolism for insulin secretion, suppression of *Ldha* would only prevent conversion of pyruvate (resulting from the metabolism of incoming glucose by glycolysis) to lactate, diverting pyruvate away from OXPHOS, which would impair insulin secretion (Liu and Hebrok, 2017). While it seems that upregulation of LDH in the β-cell is detrimental to β-cell function and that suppression of LDH activity is required for normal β-cell function, the expression of LDH over 24 hours in the healthy β-cell has not yet been explored and may contribute to the control of insulin secretion as we transition between the fasted and fed phases of the daily cycle.

1.5 Circadian Control of Insulin Secretion

Almost 50 years ago, it was demonstrated that the stimulated insulin secretion capacity (i.e., the amount of insulin that can be secreted when stimulated) is highly regulated in a diurnal manner in humans, which ultimately dictates time-of-day glucose tolerance and whole-body glucose metabolism. In healthy human subjects, the amount of insulin measured in the blood in response to an isocaloric meal or a glucose bolus was found to be greater in the morning at the onset of the fed/active phase compared to the evening, when fasting and inactivity are anticipated (Rigas et al., 1968, Malherbe et al., 1969, Barter et al., 1971). Infusion of tolbutamide, a K^+_{ATP} channel blocker and therefore stimulator of insulin secretion, alongside a glucose challenge in healthy human subjects, caused a greater increase in plasma insulin when infused at 7 am compared to 7 pm, consequently increasing the rate of glucose clearance from the blood in the morning (Carroll and Nestel, 1973). These early

studies elegantly demonstrated that the β-cells is "programmed" to secrete more insulin via GSIS during the active/fed phase of the day and that these pathways are actively suppressed in the inactive/fasted phase.

Since these early in vivo human studies, more direct assessments of the temporal pattern of insulin secretion capacity have been made using isolated islets from rodent models and human cadaveric donors. Rat and mouse islets isolated at various times of the day and immediately assessed for GSIS capacity show greater stimulation of insulin secretion when isolated from animals in the dark/active phase versus animals in the light/inactive phase (Peschke and Peschke, 1998, Delattre et al., 1999, Picinato et al., 2002). Similarly, isolated mouse (Petrenko et al., 2017, Perelis et al., 2015) and human islets (Saini et al., 2016), synchronized *ex vivo* with forskolin, show a similar pattern of rhythmic GSIS capacity, suggesting that the mechanism of rhythmic insulin secretion regulation is conserved across species. In the next sections, I will discuss some of the emerging mechanisms and pathways that control daily rhythms of insulin secretion, including circadian regulated transcriptional programming of the β-cell and metabolic function, as well as discuss some recent evidence that supports a role for the circadian clock in functional β-cell maturation, regeneration, and adaptation to metabolic stress.

1.5.1 Organization of the Circadian Clock Timing System

The circadian timing system is a complex series of cellular circadian oscillators that function in every tissue and cell of the body to translate environmental time into biological time and to align our behavior and physiology with light/dark cycles of our environment. The circadian system is arranged in a hierarchical manner, with the "primary" circadian clock located in the suprachiasmatic nucleus (SCN) within the hypothalamus, which presides over the "secondary" oscillators located in every peripheral tissue of the body (Dibner et al., 2010). Notably, the primary clock in the SCN, a specialized group of about 20,000 neurons, is entrained by light signals via direct input from photosensitive ganglion cells from the retina and directs a number of our circadian behaviors, including the sleep/wake cycle, fasting/feeding behaviors, and cycles of body temperature (Sinturel et al., 2020) (Reppert and Weaver, 2002). There are specialised cells called intrinsically photoreceptive retinal ganglion cells that receive light signals from the retina (Do and Yau, 2010). Unlike the SCN, the peripheral clocks are not entrained by light directly, but rather, are entrained by a number of hormonal, autonomic, and physiological inputs, including critical signals generated by the fasting and feeding cycles (Balsalobre et al., 2000, Hirao et al., 2009). Regardless of body location, the cellular circadian oscillator comprises a highly conserved series of autoregulatory transcriptional and translational feedback loops that drive various clock-controlled output pathways and are also entrained by a series of input pathways that influence the period and amplitude of circadian rhythms. Briefly, CLOCK and BMAL1, two core circadian clock proteins, comprise the main components of the positive arm of the circadian oscillator. Notably, *Bmal1* is the only non-redundant core clock gene (Ko and Takahashi, 2006, Bunger et al., 2000) and as such, is often targeted in transgenic studies to explore the role of the

circadian machinery in cellular and physiological function. Once expressed, CLOCK and BMAL1 heterodimerize in the cytoplasm, translocate to the nucleus and activate the expression of numerous "clock-controlled genes," which include many output genes involved in various biological pathways, and also a set of circadian repressors, Period (*Per1*, *Per2* and *Per3*) and Cryptochrome (*Cry1* and *Cry2*). Accumulation, heterodimerization, and translocation of PER and CRY proteins to the nucleus inhibits CLOCK:BMAL1 binding to target genes, silencing their expression. Turnover and degradation of PER and CRY proteins ultimately dictate the timing of CLOCK:BMAL1 repression and the negative arm of circadian transcriptional cycle, with the entire cycle taking approximately 24 hours to complete. In addition, the CLOCK:BMAL1 dimer also initiates an E-Box mediated activation of orphan nuclear-receptor genes, such as RORα/β and Rev-erbα/β. RORα/β inhibits BMAL1 while Rev-erbα/β initiates BMAL1 transcription by competitive binding to RORE binding sites located within the Bmal1 promoter region, together forming an additional feedback loop, which operates in parallel.

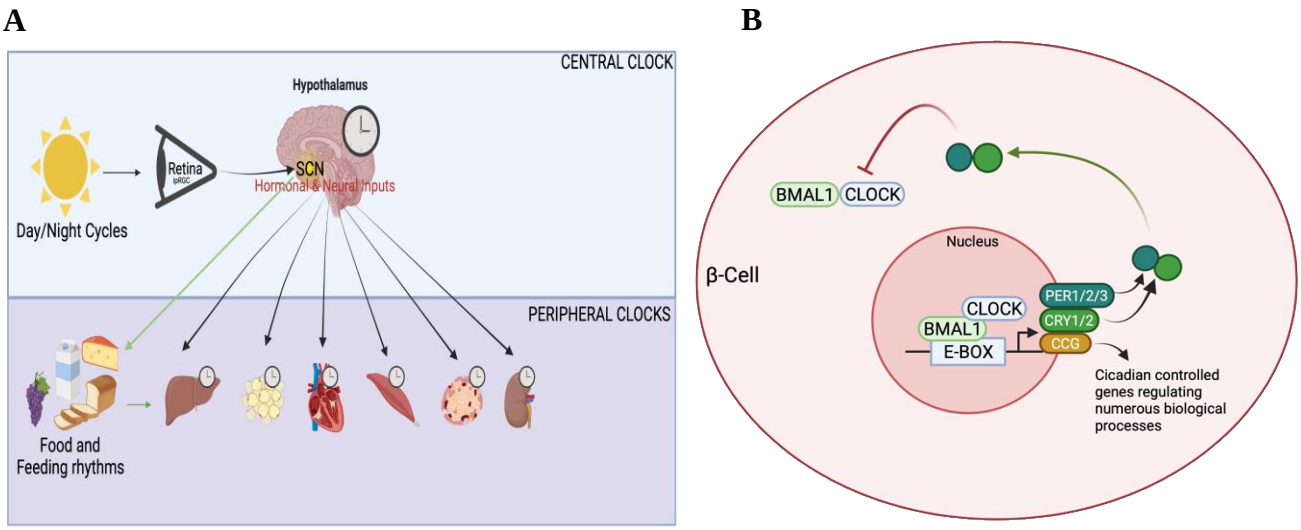


Figure 1.4: Schematic representation of the hierarchical arrangement of the central and peripheral clock. [A] The suprachiasmatic nuclei in the hypothalamus in the brain receives inputs from the sun via intrinsically photosensitive retinal ganglion cells (ipGRC), activating the central clock. The central clock, via hormonal, autonomic, and physiological inputs, entrain the peripheral clocks located in every organ and tissue in the body. Additionally, the peripheral clocks can be independently entrained by fasting and feeding rhythms, uncoupling them from the central clock. **[B]** Simplified diagrammatic representation of the molecular machinery of the β-cell circadian clock. At the core of the 24-hour cycle are two transcription factors namely BMAL1 and CLOCK, which upon heterodimerization are translocated to the nucleus. Once in the nucleus, they bind to E-BOX regulatory elements in the promoter region of many circadian-controlled genes, including PER1/2 an CRY1/2/3, which are repressors of the BMAL1: CLOCK heterodimer by disruption of this complex. Turnover of PER and CRY dictates the length of BMAL1: CLOCK repression, allowing the cycle to begin again.

1.5.2 Circadian Dysfunction and Metabolic Disease

A seminal study by Nagy and Nakagawa in 1987 showed that the SCN is responsible for the control of daily fluctuations in plasma glucose concentrations (Yamamoto et al., 1987) where plasma glucose levels are

highest in the morning at the onset of the active/fed phase. Mice with lesions caused by ablation in the SCN showed no temporal regulation of blood glucose levels or insulin (Yamamoto et al., 1987, Yamamoto et al., 1984). Interestingly, mice that had lesions in the SCN displayed disrupted patterns of activity, energy uptake and expenditure. Furthermore, mice with SCN lesions had impaired hepatic insulin sensitivity (Coomans et al., 2013). While the mice with SCN lesions showed a mild phenotype – weight gain (compared to sham mice) but the impaired hepatic insulin sensitivity is the first indication of a metabolic disorder.

While the disruption of SCN manifested in metabolic dysfunction, the intracellular molecular oscillator described in section 1.5.1 is not unique to the central clock but exists in every metabolic tissue across the body such as muscle, adipose tissue, kidney, liver, and pancreas (Eckel-Mahan and Sassone-Corsi, 2013). For example, serum-shocked rat fibroblasts that are immortalized and maintained *ex vivo* express circadian clock genes in a diurnal pattern (Greco et al., 2014). These peripheral clocks can be entrained by signals generated by the central clock function but can also be uncoupled from the SCN to function autonomously (Mohawk et al., 2012, Kornmann et al., 2007). Metabolic disorders resulting from a desynchrony between the central and peripheral clock can result from circadian dysfunction. However, when this was tested using a discordant mouse model, which has a lengthened circadian period in the SCN but not in the peripheral tissues, there was no manifestation of metabolic disorders in the mouse (van der Vinne et al., 2018). Additional metabolic hits like disrupted feeding rhythms or a high-fat diet could potentially induce metabolic syndromes. Another animal model, referred to as the Clock$^{\Delta 19}$ mutant mouse, identified by positional cloning following mutational screening (King et al., 1997, Antoch et al., 1997), developed obesity because of altered feeding patterns and hyperphagia. The Clock$^{\Delta 19}$ mutant mouse had a lengthened period just like the discordant mouse and exhibited a pattern of increased food intake over 24 hours. Hyperlipidemia, hyperglycemia and hypoinsulinemia were observed in the Clock$^{\Delta 19}$ mutant mouse, suggesting a metabolic syndrome phenotype as a result of this circadian disruption (Turek et al., 2005).

Since the discovery of the Clock$^{\Delta 19}$ mutant mouse, several genetic mouse models whereby key genes of the circadian oscillator have been deleted have been developed and characterized to demonstrate the importance of the circadian clock in the maintenance of metabolic homeostasis. A whole-body *Bmal1* knockout mouse (*Bmal1*$^{-/-}$) was first generated by Bunger et al (2000). It displayed a lean phenotype but had impaired glucose homeostasis characterised by glucose intolerance, hyperglycemia and hypoinsulinemia (Kondratov et al., 2006, Shimba et al., 2005). Similarly, The *Per1*-null mouse had a lean phenotype, but had a heightened glucose clearing response, suggesting that *Per*1 contributed to maintaining metabolic homeostasis (Dallmann et al., 2006). Lean *Reverbα*-null mice had high triglyceride levels and an altered lipoprotein metabolism. These studies collectively emphasize the involvement of circadian machinery in regulating metabolism (Raspe et al., 2002). Importantly, these studies have exploited whole-body knockout models, which are not ideal to study metabolic disorders due to the complex nature of metabolic effects involving interactions among multiple organs, making it quite difficult

to associate phenotype to an organ or tissue, and consequently, difficult to tease out the effects of the central and peripheral clocks contributing to each phenotype.

1.5.2.1 ***Pancreatic Clock***

The development of tissue-specific knockout mouse models have helped link phenotype to mechanism. Our overall understanding of the involvement of the peripheral clocks in maintaining energy homeostasis is just beginning to become clear. One common phenotype that arises as a consequence of the whole-body knockout models is impaired glucose homeostasis. Pancreatic islets and their endocrine hormones are at the heart of the regulation of blood glucose levels over 24 hours. In 2010, Marcheva et. al. demonstrated that pancreatic islets possess a cell-autonomous circadian oscillator. Using *Per2:luciferase* (Per2:Luc) knock-in reporter mice, high amplitude rhythmic oscillations of *Per2* were observed in isolated islets synchronized *ex vivo* with forskolin (Marcheva et al., 2010). Since this initial study, several groups have demonstrated robust circadian rhythms in *Per2* and other core clock genes in rodent (Petrenko et al., 2017, Sadacca et al., 2011, Qian et al., 2013, Qian et al., 2015), and cultured human islets (Pulimeno et al., 2013, Petrenko et al., 2020) . To explore the role of the circadian oscillator in islet function and metabolic health, several genetic circadian mutant and transgenic models have been created and characterized. Notably, glucose intolerance and insulin secretion impairments were more severe and developed at a younger age (2-4 months vs 8 months) in the pancreas- and β-cell-specific *Bmal1* knockout models compared with the whole-body *ClockΔ19/Δ19* mutant, indicating that circadian disruption of the β-cell alone can autonomously drive diabetes development, largely via an insulin secretion defect. Additionally, specific ablation of the β-cell circadian clock during adulthood using tamoxifen-inducible CreER models (*Pdx:CreERT* and *Ins2:CreERT*), triggered a similar rapid impairment of GSIS within 2 weeks of tamoxifen injection (Perelis et al., 2015, Lee et al., 2013, Rakshit et al., 2016a), indicating that circadian disruption during embryogenesis/development is not a prerequisite for β-cell dysfunction in these models. Rather, acquired circadian disruption in the adult β-cell can sufficiently drive insulin secretion impairment and diabetes development. In line with rodent circadian disruption models, siRNA knockdown of CLOCK in cultured human islets impaired the overall capacity of islets to secrete insulin in response to a glucose challenge and also disrupted the circadian rhythm of insulin secretion at basal glucose over a 48-hour period (Saini et al., 2016). Moreover, human cadaveric donor islets from T2D patients show substantial signs of circadian dysfunction, including reduced expression of the core clock genes, *Per1 to 3*, *Cry2*, *Rev-erbα*, *Clock*, and *Dbp* in T2D islets (Petrenko et al., 2020, Stamenkovic et al., 2012). Of these genes, PER2 and CRY2 levels showed a negative association with donor HbA1c (ie, poorer glucose control was associated with lower circadian clock gene expression) (Stamenkovic et al., 2012), while PER2, PER3, and CRY showed a positive association with insulin mRNA and protein expression (Stamenkovic et al., 2012). Introduction of *Bmal1:Luc* and *Per2:Luc* reporter constructs into human islet cells revealed significantly reduced circadian amplitude of the core oscillator and compromised

circadian insulin secretion profiles in a synchronized population of mixed islet cells from human T2D donors (Petrenko et al., 2020). Together, these studies demonstrate that, like rodent islets, cultured human islets (both whole islets and dispersed islet cells) display high-amplitude rhythms of the core circadian oscillator when synchronized *ex vivo* and that perturbations in the human islet circadian oscillator impact insulin secretion capacity and dynamics, potentially contributing to islet pathophysiology in T2D development. Importantly, there is a paucity of experiments in this area of circadian human islet research, mainly due to limited donor tissue availability. Clearly, much more research is needed in this area to elucidate the cause-and-effect relationship between circadian disruption and β-cell dysfunction in the pathophysiology of diabetes.

1.5.2.1.1 ***The Islet and β-Cell Circadian Transcriptomes***

Pancreatic islets comprise a heterogenous population of endocrine cell types and the assessment of whole islet clocks includes input from circadian oscillators in all endocrine cell types. Studies using a triple transgenic mouse line that expresses β-cell– (RIP-Cherry) and α cell– (Gcg- Venus) specific fluorescent markers along with the *Per2*:Luc reporter system not only demonstrate that the individual islet cell types express the highly conserved core circadian machinery, but that the circadian properties of the β-cells are unique relative to other cell islet types (Petrenko et al., 2017). Notably, α- and β-cells displayed circadian oscillations with the same circadian period; however, unique circadian properties were observed, including distinct expression patterns of the core clock transcripts (same amplitude and period but 4 hours phase-advanced in the β-cell) as well as different phases of hormone secretion (the glucagon secretion peak lagged 2 hours behind insulin) (Petrenko et al., 2017),(Zhang et al., 2014). In whole isolated islets, ~27% of transcripts show high amplitude oscillatory transcriptional profiles (Perelis et al., 2015); however, in sorted populations of α and β-cells, it was determined that closer to ~60% of transcripts are oscillatory in one or both cell types, likely reflecting different circadian phases in the individual islet cell types that are masked at the whole islet level, but nonetheless demonstrating that β-cells have a high ratio of cycling to non-cycling genes typically seen in metabolic tissues (Zhang et al., 2014). Using healthy male C57BL6 isolated islets synchronized *ex vivo* and sampled for RNA-seq analyses over two circadian cycles, Perelis et. al., (2015) found significant enrichment of genes critically involved in insulin secretion among the cycling islet gene set, including glucose-sensing and secretion coupling factors (eg, *Slc2a2, Gnaq, Creb1, Creb3, Cacna1c*) as well as vesicle maturation, trafficking, and exocytosis (eg, *Stx1a and Vamp8*) (Perelis et al., 2015). Similar results were reported using synchronized human islets from healthy male cadaveric donors where 1800 cycling genes were identified; 481 of which were orthologous to those identified as cycling in mouse, including several similar factors involved in insulin vesicle exocytosis, trafficking, and fusion (Petrenko et al., 2017).

In 2016, a similar transcriptional profiling study, but rather than isolating islets in batch and synchronizing *ex vivo*, they isolated islets from C57BL6 mice every 4 hours over the light/dark cycle and determined the detailed diurnal expression pattern of key transcripts and pathways in relation to the light (inactive)/dark (active) cycle

(Rakshit et al., 2016b). Nineteen distinct time-dependent cycling profiles were identified that showed significant enrichment of important islet genes in a time-of-day-dependent manner. KEGG analysis of the profiles that peaked in the dark or at the onset of the dark phase (a time when food intake is anticipated and insulin demand and secretion capacity are greatest) revealed enrichment of a number of pathways that are critical for insulin secretion, including "protein processing in the endoplasmic reticulum" (eg, *Bip, Hsp40, Hsp70, Grp94, Erolβ, Eif2AK3, Dsk2*); "insulin secretion" (eg, *Slc2a2, Gck, Creb3L1, Pdx1, KcnJ11*); "insulin signaling" (eg, *InsR, Ins1*), "SNARE interactions in vesicular transport" (eg, *Bet1, Snap29, Vamp4*); and "oxidative phosphorylation" (eg, *Atp5c1, Cox4l1, Ndufa2*). Conversely, in the light/inactive phase (or at the end of the dark phase), the most enriched pathways were related to positive regulation of the cell cycle and DNA repair. The antiphase expression of these pathways in the islet suggests a role for the circadian clock in temporally gating these important and diverse biological pathways, which may represent a critical mechanism that allows the β-cell to optimally direct energy and resources for maximal insulin synthesis and secretion in a time-limited manner when food is anticipated, while alternately allowing for defined periods of β-cell rest, repair, and growth, when insulin demand is low. In support of this notion, disruption of the islet/ β-cell circadian oscillator in adult islets has been shown to alter the transcriptional profile of genes/pathways not only essential for insulin secretion, but also cell cycle control and DNA repair. Pancreas-specific *Bmal1* silencing altered the expression of many islet genes (1757); many of which were identified as oscillating in the C57BL6 islet profiling studies (Perelis et al., 2015). KEGG pathway annotation of the altered cycling gene set revealed that highly impacted pathways included vesicle trafficking, tethering, and fusion. Similarly, RNA-seq transcriptional profiling after siRNA knockdown of CLOCK in adult human islets revealed altered expression of transcripts involved in insulin granule formation and secretion (SLC30A8, VAMP3, STX6) as well as altered expression of genes involved in glucose-sensing and metabolism (GNAQ, ATP1A1, ATP5G2, KCNJ11) (Saini et al., 2016), collectively suggesting that the circadian clock machinery not only converges on and transcriptionally regulates pathways involved in insulin exocytosis, but also upstream glucose secretion coupling pathways. Furthermore, β-cell–specific *Bmal1* deletion attenuated the expression of various cell cycle activators (*Bcl2, Brca1, Ccnb2, Cdk6, Cdc20*) while also increasing the expression of a number of cell cycle inhibitors (*Wee1, Cdkn2b, Rbl2, Hus1, Gadd45a*), which was associated with reduced compensatory β-cell proliferation and increased apoptosis when challenged with a high-fat diet (Rakshit et al., 2016a). Collectively, these findings illustrate a potentially critical role for the β-cell circadian oscillator in coordinating cycles of insulin secretion priming (within a time-limited window) followed by periods of insulin secretion suppression that are associated with recovery and growth. As such, circadian disruption, in addition to driving GSIS impairment, may also impact the ability of the β-cell to recover from or respond to stress-induced DNA damage, leading to greater susceptibility to cellular dysfunction and apoptosis. This concept is discussed in more detail in the following sections.

*1.5.2.1.2 **Beyond Circadian Transcriptional Regulation of the ß-Cell***

In addition to transcriptional regulation, many circadian clock output genes are also mediators of posttranscriptional (i.e,. mRNA polyadenylation (Kojima et al., 2012) and m6A methylation (Fustin et al., 2013)) and posttranslational modifications (i.e., phosphorylation, acetylation, sumoylation, methylation, and ubiquitination) (Perelis et al., 2015),(Gallego and Virshup, 2007), adding layers of complexity to circadian regulation and underscoring the importance of looking beyond circadian transcriptional control and evaluating the functional impact of the circadian clock on key regulatory pathways of insulin secretion, in a temporal manner. Several studies have examined the insulin content of whole isolated islets from various circadian-deficient models and none have reported an impact (Perelis et al., 2015, Marcheva et al., 2010, Lee et al., 2013), suggesting that insulin biosynthesis *per se* is not directly impacted by the circadian clock. Rather, circadian-deficient models consistently display impaired GSIS, likely stemming from disruption somewhere in the secretion coupling and/or exocytotic pathways. Potassium chloride (KCl), an insulin secretagogue that directly depolarizes the cell membrane, is often used as a tool to determine where (i.e., upstream in glucose metabolism or downstream of depolarization) a specific defect in the insulin secretory pathway might lie. Notably, application of KCl to *Bmal1*-/- islets has yielded conflicting reports. Marcheva et al., demonstrated impaired KCl-induced insulin secretion in *Bmal1*-/- islets, indicative of defective insulin exocytosis (Marcheva et al., 2010); however, Lee et. al., did not observe such an impairment (Lee et al., 2011), suggesting a primary defect in glucose metabolism caused by genetically induced circadian dysfunction. While these discrepant results remain unclarified, functional assessment of insulin exocytosis in human islet cells with siRNA-mediated CLOCK knockdown have demonstrated aberrant exocytotic events. Using human islets where the secretory granules are labeled with NPY-cherry and individual islet cell types are labeled with cell-type–specific fluorescent markers, Petrenko et al (2020) elegantly demonstrated that the density of plasma membrane-docked granules was reduced by ~34% in β-cells when CLOCK was knocked down using siRNA (Pildes et al., 1969). Additionally, stimulation of exocytosis with K^+ after siRNA-mediated CLOCK knockdown in human islets showed significantly reduced exocytotic events. Nearly identical functional results were observed in islets isolated from *Bmal1*$^{-/-}$ mice (Petrenko et al., 2020) demonstrating that disruption of the islet circadian oscillator functionally impacts insulin exocytosis, in both mouse and human islets. In addition to the functional defects observed at the level of insulin exocytosis, circadian disruption has also been shown to negatively impact oxidative glucose metabolism. Using *Bmal1*$^{-/-}$, Lee et. al., (2011) demonstrated that Bmal1 deficiency abrogates glucose-induced mitochondrial membrane hyperpolarization with a concomitant reduction in the ATP/ADP ratio, without affecting GLUT-2 or glucokinase expression, mitochondrial number, or expression of electron transport chain complex subunits (Lee et al., 2011). While glucose oxidation pathways remained largely intact at the transcriptional level, these findings suggest that *Bmal1* deficiency causes uncoupling of the electron transport chain function from ATP production, which may

be responsible for reduction in glucose-stimulated mitochondrial membrane hyperpolarization, as well as the reduced ATP production and impaired GSIS observed in *Bmal1*$^{-/-}$ islets. Indeed, UCP2, a mitochondrial uncoupling protein that is expressed in β-cells as well as the other endocrine islet cell types, was significantly elevated in *Bmal1*$^{-/-}$ islets (Lee et al., 2011). Furthermore, treatment of *Bmal1*$^{-/-}$ islets with genipin, a pharmacological UCP2 inhibitor, restored glucose-induced ATP production and rescued GSIS deficiency, uncovering an important functional relationship between UCP2, the β-cell circadian oscillator, and control of GSIS (Lee et al., 2011).These studies have been confirmed using a β-cell–specific *Bmal1* knockout mouse, which demonstrates that this effect is not the consequence of systemic *Bmal1* deletion, but rather is an intrinsic β-cell–specific effect (Lee et al., 2013).

1.5.2.1.3 A Role for the Circadian Clock in Postnatal β-Cell Functional Maturation?

While β-cells emerge from endocrine progenitors during early- to mid-embryogenesis, β-cell development continues postnatally. At birth, amino acid infusion, but not glucose infusion, increases plasma insulin levels in newborn infants (Pildes et al., 1969, Grasso et al., 1968), demonstrating a lack of glucose-responsiveness in immature neonatal β-cells, which is also seen in rodent models, despite normal insulin content and ion channel activity (Rozzo et al., 2009, Rorsman et al., 1989, Blum et al., 2012, Aguayo-Mazzucato et al., 2006). While the intrinsic and extrinsic cellular factors and mechanisms that control postnatal β-cell maturation remain incompletely understood, emerging evidence suggests that establishment of global circadian rhythms and the β-cell circadian oscillator may be critical. Using *Per1*:LUC isolated rat islets, Rakshit et. al., recently demonstrated that rhythmic islet circadian oscillations emerge in the early perinatal period (prior to weaning), with robust circadian cycles observed by postnatal day 30, when daily variations in plasma insulin and robust GSIS are also evident (Rakshit et al., 2018). Notably, a similar timing of circadian establishment is seen in the liver (Sladek et al., 2007), which corresponds with the development of circadian feeding rhythms in rodents. Importantly, embryonic deletion of *Bmal1* in the β-cell (β-*Bmal1*$^{-/-}$) impeded β-cell functional maturation in rat islets, defined by a lack of glucose-responsiveness at postnatal day 25 (when control cells showed functional maturity) and downregulation of pathways critical for β-cell function, including GO terms for oxidation-reduction processes, responses to zinc ions, and regulation of glucose metabolic processes (Rakshit et al., 2018). Surprisingly, the lack of β-cell functional maturation in β-*Bmal1*$^{-/-}$ islets was not associated with changes in the expression of known developmental maturation markers (*Ucn3*, *Pdx-1*, and *Mafa*) or genes typically associated with β-cell immaturity (*Ldha*) (Rakshit et al., 2018). Postnatal β-cell maturation is a highly complex process involving transcriptional reprogramming and major metabolic transitions, which was recently shown to involve nutrient-responsive changes in the microRNA landscape of the islet (Jacovetti et al., 2015). Interestingly, microRNAs were also shown to bind to and alter the expression of the core components of the circadian oscillator (Jacovetti et al., 2017), suggesting a contributory role for nutrient-responsive microRNAs in establishing islet circadian rhythms and

functional maturity; however, this remains debatable as it was also shown that failure to wean pups from maternal lipid-rich milk to a high-carbohydrate chow diet did not affect the establishment of islet circadian rhythms (Rakshit et al., 2016a). While studies of circadian ontology and its role in human islets are lacking, these initial preclinical rodent studies suggest that postnatal induction of *Bmal1* and establishment of circadian rhythms contributes to the complexity of postnatal β-cell functional maturation and warrants further evaluation.

Further evidence for the importance of the circadian clock in β-cell functional maturation comes from research in stem cell replacement therapy. Cell replacement therapies hold strong therapeutic potential for people living with diabetes. Islet transplant procedures are limited by donor supply and host immunogenicity issues, which has made autologous stem cell-derived β-cell replacement an attractive option. Unraveling and defining the physiological and molecular mechanisms that drive β-cell maturation is essential for the successful generation of functionally mature β-cells from human pluripotent stem cells for use in such therapies. Recently, Alvarez-Dominguez et al (2020) demonstrated that in vitro circadian entrainment of late-stage (Ins^{+}/Gcg^{-}) stem cell-derived islets promoted enhanced functional maturity using an optimized entrainment protocol that mimics fasting and feeding cycles. The enhanced functional maturity was characterized by robust and rhythmic patterns of GSIS along with stable and persistent oscillatory expression of genes involved in glucose metabolism, insulin synthesis and secretion, and maturity-linked factors (PDX-1, NKX6.1, NEUROD1, IAPP, MAFA). Additionally, enhanced functional maturity was linked to newly opened but stable chromatin changes, where core clock transcription factors were found enriched at critical insulin regulatory genes (eg, CADPS, SYT4, STX2). Interestingly, core clock oscillators (ARNTL, PER1/2, and CRY1/2) were not expressed at detectable levels in un-entrained stem-cell-derived islets, but rather were only induced upon entrainment, suggesting that fasting and feeding cycles are not only important for synchronization of the islet clock, but also for its activation during development.

*1.5.2.1.4 **A Role for the Circadian Clock in β-Cell Proliferation and Adaptation to Stress?***

Regulation of β-cell proliferation is a dynamic and complex process that requires different factors at different developmental stages, leading to varied proliferative capacities throughout the lifespan. In the perinatal period, functionally immature β-cells are highly proliferative; however, the rate of β-cell proliferation rapidly declines in early life such that, in adulthood, functionally mature β-cells are quiescent with very little proliferative capacity (Gunasekaran et al., 2012). It has been postulated that the neonatal wave of β-cell mass expansion is essential for the establishment of sufficient adult β-cell mass; lack of which is thought to increase susceptibility to T2D (Butler et al., 2007). While not yet explored directly, evaluation of β-cell mass and proliferation in embryonic circadian-deficient models suggest that the islet clock does not impact perinatal β-cell proliferation. Notably, circadian mutants and circadian-deficient rodent models are viable and show little impact, if any, on islet architecture and structure. Whole-body $Clock^{\Delta 19/\Delta 19}$ mutants and $Bmal1^{-/-}$ mice have overall normal islet architecture, but generally smaller islets with reduced Ki67+ staining (Marcheva et al., 2010); however,

evaluation of islet structure in β-cell- and pancreas-specific *Bmal1*knockout models reveals no change in β-cell mass or islet size (Lee et al., 2013, Rakshit et al., 2018), suggesting that the formation of smaller islets in the whole-body circadian mutants is likely secondary to other factors associated with whole-body arrhythmia and not specific to the islet oscillator. Additionally, β-cell mass and proliferation were unchanged in the early postnatal period in β-*Bmal1*$^{-/-}$mice compared with controls, suggesting that the islet circadian oscillator likely does not have a contributory role in regulation of postnatal β-cell mass expansion. In the healthy adult, β-cell mass is maintained by a balance of apoptosis and relatively slow rates of β-cell replication in mice, with less clarity of these processes in humans. Although β-cell mass is relatively stable in adulthood, there are conditions where significant β-cell mass expansion occurs, including during pregnancy and in the obese state. Failed adaptive β-cell mass expansion in these states is associated with the development of gestational diabetes and T2D, respectively. Emerging evidence implicates the β-cell circadian clock in the physiological adaptation of the β-cell to diet-induced obesity (Rakshit et al., 2016a). In control animals, high-fat diet consumption stimulated a 50% increase in β-cell mass with a 3-fold increase in β-cell proliferation as expected; however, conditional deletion of *Bmal1* in adult mouse β-cells prevented high-fat diet–induced β-cell mass expansion (characterized by increased apoptosis and reduced proliferation), which was associated with fasting and diurnal hyperglycemia, exacerbated glucose intolerance, and loss of in vivo and in vitro GSIS (Rakshit et al., 2016a). Interestingly, *Bmal1* deletion altered the expression of important cell cycle genes in this model (increased expression of cell cycles inhibitors and reduced expression of cell cycle repressors) and increased apoptosis, suggesting that the circadian clock likely contributes to the regulation of adaptive β-cell mass by shifting the balance between proliferation and apoptosis. Further, this study suggests that maintenance and/or stimulation of circadian rhythms in the β-cell may provide an important strategy to increase β-cell resilience and adaptation capacity to obesity-driven metabolic stress. β-cell loss contributes significantly to the pathophysiology of both T1D and T2D and current research aims to develop strategies to promote β-cell regeneration as a means to overcome β-cell loss and restore metabolic health in diabetes. While other metabolic tissues, including the intestine and liver, have a high regenerative capacity after acute cell loss, β-cell regeneration is comparatively limited and is a slow process (taking weeks to months) (Nir et al., 2007) and our understanding of the regenerative process in the β-cell is incomplete. Using dox-inducible expression of diphtheria toxin A in β-cells (Ins-rtTA/TET-DTA mice) to induce massive β-cell ablation, Petrenko et al (2020) recently demonstrated that β-cell regeneration (ie, proliferation of residual β-cell) is regulated in a circadian manner with peak proliferation (BrdU incorporation, indicative of entering S-phase) occurring during the dark/active phase of the daily cycle (Petrenko et al., 2020). Importantly, arrhythmic *Bmal1*$^{-/-}$ mice were unable to mount a proliferative response to β-cell ablation, leading to elevated hyperglycemia and fatal diabetes (Petrenko et al., 2020). Single cell transcriptional profiling of residual, regenerating β-cells revealed that β-cell ablation triggered a modified transcriptional landscape, which included 1635 transcripts that lost rhythmic expression and

2208 genes that acquired circadian rhythmicity after ablation compared with control β-cells (Petrenko et al., 2020). Transcripts that lost rhythmicity in residual β-cells were related to mitochondrial function, oxidative phosphorylation, and xenobiotic metabolism; whereas the top 3 canonical pathways that were enriched in the genes that gained circadian rhythmicity included genes related to mitosis, cell cycle control of chromosome replication, and estrogen-mediated S-phase re-entry signaling. The circadian clock–mediated transcriptional reprogramming of the regenerating β-cell provides an interesting perspective and suggests that circadian-regulated transcriptional pathways are malleable and adaptive to environmental and/or stress-related signals, further highlighting the importance of developing strategies to promote or augment circadian function, particularly in high-risk individuals.

Chapter 2

General Hypothesis and Specific Aims

Healthy β-cells secrete insulin in a rhythmic manner to maintain glucose homeostasis. However, the molecular and metabolic factors that fine tune rhythmic insulin secretion over 24 hours are not completely understood. Based on the expression of UCP2 in the pancreatic β-cell and its suggested function during prolonged fasting (48-72hours) in suppressing insulin as a protective mechanism against hypoglycemia, we wanted to understand *when* UCP2 is expressed over 24 hours and determine if it contributes to the regulation of diurnal insulin secretion capacity over 24 hours. As such, we hypothesize the following:

1. UCP2 is dynamically expressed in the β-cell as a mechanism to regulate insulin secretion capacity in a time-of-day manner, assigning an important physiological role for UCP2 in the β-cell
2. UCP2 regulates time-of-day- insulin secretion capacity via control of key insulin signaling triggering molecules including ATP and ROS
3. The circadian clock drives the expression of UCP2 on a daily basis, along with other important metabolic regulators in the β-cell

2.1 Specific Aims

To address the above hypotheses, we have 3 distinct and specific aims:

Aim 1: To examine the expression pattern of UCP2 in the β-cell and its relationship to insulin secretion capacity over 24 hours.

Aim 2: To define the mechanistic players via which UCP2 regulates insulin secretion over 24 hours.

Aim 3: To establish a mechanistic role for the pancreatic β-cell clock in regulating diurnal expression of UCP2 and ultimately diurnal patterns of insulin secretion capacity.

Chapter 3

Materials and Methods

3.1 Animal models

In this study, we used the following mouse strains:

1. ***Ucp2* floxed mice (*Ucp2*$^{flx/flx}$)**

This mouse strain was a gift from Dr. Michael Wheeler (University of Toronto, Ontario, Canada), which was described in Robson-Doucette et al., (2011). The two LoxP sites were sequentially cloned by transformation into EL250 cells, which via homologous recombination with mouse *Ucp2* genomic clone, formed the modified *Ucp2* Bacterial Artificial Chromosome (BAC). Briefly, the targeting construct that contained two LoxP sites at the 2nd and 4th intron of *Ucp2* allele was electroporated into mouse embryonic stem (ES) cells. The resulting targeting construct was then electroporated into mouse embryonic stem (ES) cells (W4/129S6, Taconic, NY). Correctly targeted ES clones were identified and injected into blastocysts resulting in several 100% male chimeras. Chimeras were then bred to mice bearing a flp-recombinase transgene (ROSA-Flp: stock number 003946 from The Jackson Lab, Bar Harbor, ME) to facilitate remove the neomycin selection marker (Kong et al., 2010). The resulting *Ucp2*$^{flx/flx}$ offsprings were then used for further studies.

2. *Bmal1* floxed mice (*Bmal1*$^{flx/flx}$)

This mouse strain was purchased from Jackson Laboratory (Bar Harbor, ME; stock no. 007668). Here, an FRT-flanked Neo cassette followed by LoxP sites was introduced upstream and downstream of Exon 8 of the *Bmal1* gene. The resultant targeted construct was electroporated into mice 129S4/SvJae-derived J1 embryonic stem (ES) cells. The genetically modified ES cell was injected into the blastocyst of a pseudo-pregnant mice and the resultant chimeric mice was further bred to Flpe-expressing mice (stock no. 00394) to excise the neo-cassette. The resultant offspring were bred to a congenic C57BL6 mice (non-germline Cre). After 6 generations of successful backcrossing onto a C57BL6 mice, the resulting *Bmal1*$^{flx/flx}$ offspring were used for breeding purposes in our study.

3. *Ins2*-Cre transgenic mice

To achieve conditional knockout of *Ucp2* in pancreatic β-cells, *Ins2*-Cre mice (also known as *RIP*-Cre or Rat insulin promotor-driven Cre) (B6N.Cg-Tg (Ins2-cre)25Mgn/J; Strain #018960) were used. In this line, Cre expression is driven by the *Ins2* promoter. *Ins2*-Cre shows high Cre recombinase activity in pancreatic β-cells and some neurons of the hypothalamus (Wicksteed et al., 2010)

4. *Ins1*-Cre transgenic mice

To achieve conditional knockout *Bmal1* in pancreatic β-cells, we used *Ins1*-Cre (also known as *MIP*-Cre or Mouse insulin promotor-driven Cre) (purchased from Jackson Laboratory; *Ins1*$^{tm1.1(cre)Thor}$/J; Strain #026801) to drive specific deletion in the β-cell. Note that *Ins1*-Cre was chosen in this case to avoid *Ins2*-Cre-mediated deletion in the hypothalamus. *Ins1*-Cre shows high Cre recombinase activity, specifically in insulin-secreting pancreatic β-cells (Thorens et al., 2015).

5. C57BL6 mice

Male C57BL6/6N mice (originally from Charles River Labs) were obtained from the University of Manitoba (Central Animal Care Facility colony).

3.2 Mouse breeding and Establishment of β-cell-specific Knockout Mice

In this study, cre-expressing mice were crossed with floxed mice to generate the following mouse lines and relevant controls:

1. β-cell-specific *Ucp2* knockout mice (*Ucp2*βKO)

To knockout *Ucp2* in the pancreatic β-cells, we used the breeding strategy described in **Figure 3.1.** We first bred $Ucp2^{flx/flx}$ mice with *Ins2*-Cre mice to produce heterozygous *Ins2*-Cre^{+}:$Ucp2^{flx/wt}$. Heterozygous *Ins2*-Cre^{+}:$Ucp2^{flx/wt}$ were then crossed with each other and offspring selected with the following genotypes to generate 3 groups of mice: 1) *Ins2*-Cre^{+}:$Ucp2^{flx/flx}$ (referred to as β-cell-specific *Ucp2* knockout; ***Ucp2*βKO**); 2) *Ins2*-Cre^{-}:$Ucp2^{flx/flx}$ (Cre-negative, *Ucp2* floxed controls); and 3) *Ins2*-Cre^{+}:$Ucp2^{wt/wt}$ (Cre only controls; referred to as ***Ins2*-Cre**). It has previously been established that the *Ucp2* floxed and the *Ins2*-Cre controls have a similar metabolic phenotype (Robson-Doucette et al 2011), so only *RIP*-Cre controls were used in this study.

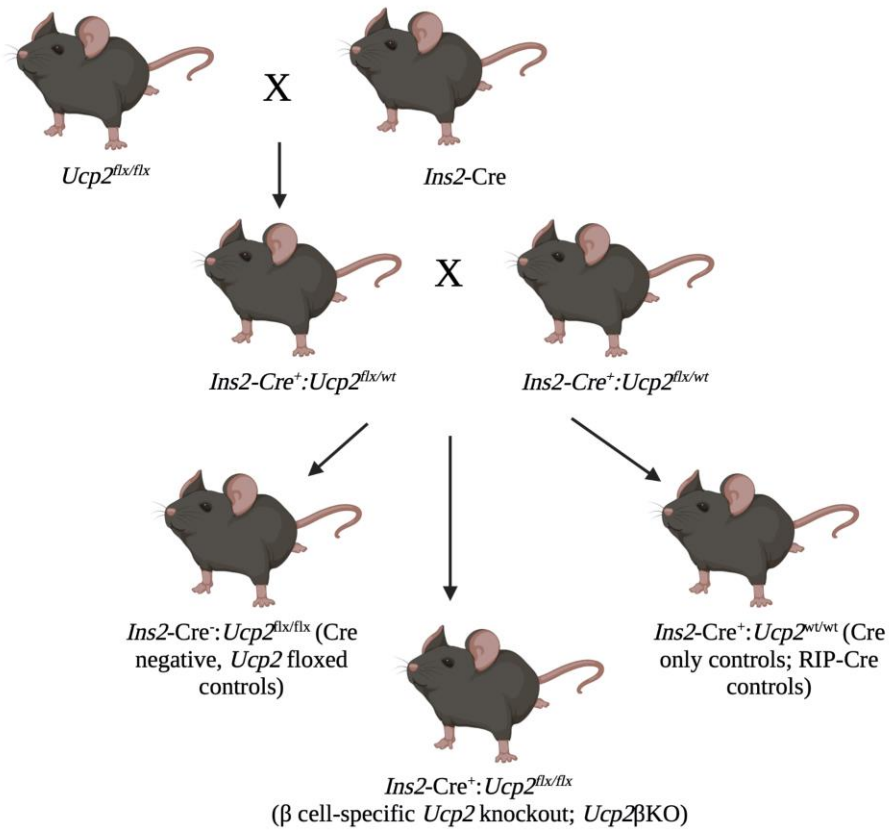


Figure 3.1: Breeding scheme for obtaining β-cell specific *Ucp2* knockout mice (*Ucp2*βKO). *Ucp2*$^{flx/flx}$ were bred with *Ins2*-Cre mice to obtain *Ins2*-Cre^{+}: *Ucp2*$^{flx/wt}$, which when bred with *Ins2*-Cre^{+}: *Ucp2*$^{flx/wt}$ to yield the 3 genotypes used in this study.

2. B-cell-specific *Bmal1* knockout mice (*Bmal1*βKO)

To generate a pancreatic β-cell-specific knockout of *Bmal1*, a core circadian clock gene, we bred *Bmal1*^{flxflx} mice to the *Ins1*-Cre mouse, as outlined in **Figure 3.2,** to generate heterozygous *Ins1*-Cre^{+}:*Bmal1*$^{flx/wt}$. Heterozygous *Ins1*-Cre^{+}:*Bmal1*$^{flx/wt}$ were then crossed with each other and offspring selected with the following genotypes to generate 3 groups of mice: 1) Ins1-Cre^{+}:*Bmal1*$^{flx/flx}$ (**β**-cell-specific *Bmal1* knockout; *Bmal1***β**KO) *Ins1*-Cre^{-}:*Bmal1*$^{flx/flx}$ (Cre negative, *Bmal1* floxed controls) and *Ins1*-Cre^{+}:*Bmal1*$^{wt/wt}$ (*Ins1*-Cre only controls)**.**

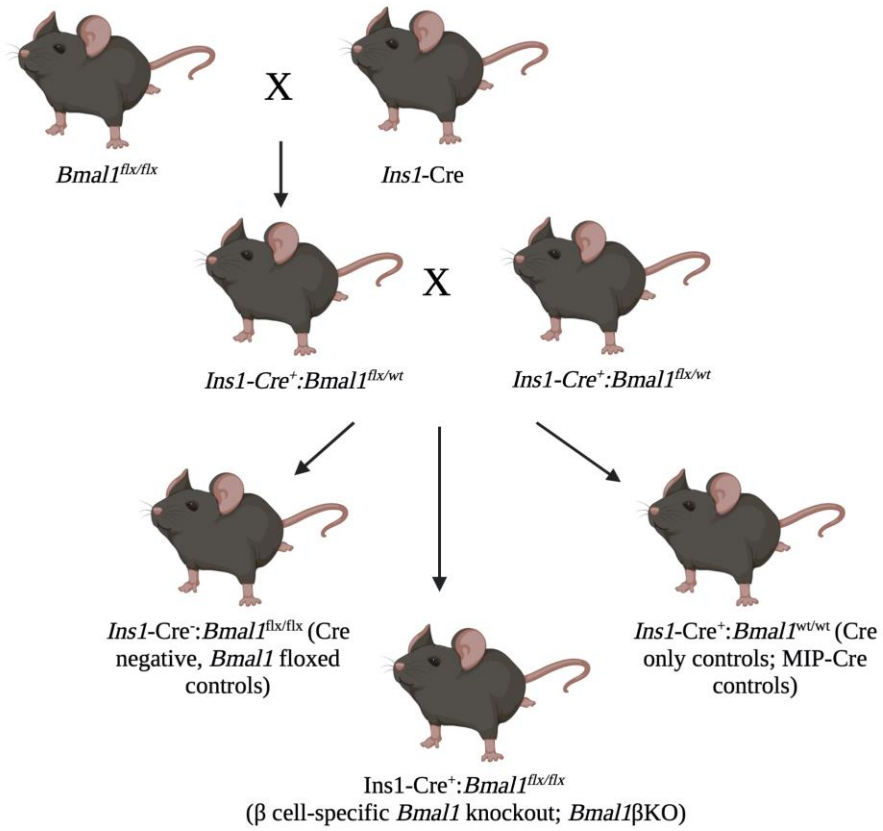


Figure 3.2 : Breeding scheme for obtaining β-cell specific *Bmal1* knockout mice (*Bmal1*βKO). *Bmal1*$^{flx/flx}$ were bred with *Ins1*-Cre mice to obtain *Ins1*-Cre^{+}:*Bmal1*$^{flx/wt}$, which when bred with *Ins1*-Cre^{+}:*Bmal1*$^{flx/wt}$ resulted in *Ins1*-Cre^{-}:*Bmal1*$^{flx/flx}$, *Ins1*-Cre^{+}:*Bmal1*$^{wt/wt\ and}$ I*ns1*-Cre^{+}:*Bmal1*$^{flx/flx}$ (β-cell specific *Bmal1*KO).

3.3 MIN6 cells

MIN6 cells (passage 28-50) were cultured in complete DMEM medium (4500 mg/l glucose and L-glutamine) (Gibco, Thermo Fisher, Waltham, MA, USA) supplemented with 10% fetal bovine serum (Thermo Fisher, Waltham, MA, USA) and 1% penicillin/streptomycin (VWR, Radnor, PA, USA) at 37°C and 5% CO_2.

3.3.1 Entrainment/synchronization of MIN6 cells

MIN6 cells were synchronized using two different methods prior to performing experiments. For the more elaborate 36 hour experiments we used the serum starve/shock protocol was used and for experiments involving two static times as described in chapter 5 and 6 we use Forskolin method.

For *in vitro* experiments outlined in Chapter 4, we used an established serum-starve/shock protocol (Greco et al., 2014, Seshadri et al., 2017). Briefly, 4.5X10^{6} MIN6 cells were plated in each well of a 6-well tissue culture

plate (CS100) (VWR, Radnor, PA, USA) and grown in complete DMEM medium until 60-70% confluency was reached. Cells were washed twice with 1X sterile PBS (1.37M NaCl, 268mM KCl, 81mM Na_2HPO_4 and 147mM KH_2PO_4 at pH:7.4) to remove all traces of FBS. Serum-free media was added to the washed cells and incubated for 12 hours at 37°C in 5% CO_2 incubator. After 12 hours, a bolus of 30% FBS was added to cells for 30 minutes. After 30mins, the serum-free medium was removed and complete DMEM media was placed onto cells. This timepoint was designated constitutes ZT (Zeitgeber) 0. Note zeitgeber refers to time post entrainment, in this case after serum shock. The cells were then sampled for assays described in this thesis for 24-36hrs **[Figure 3.3]**

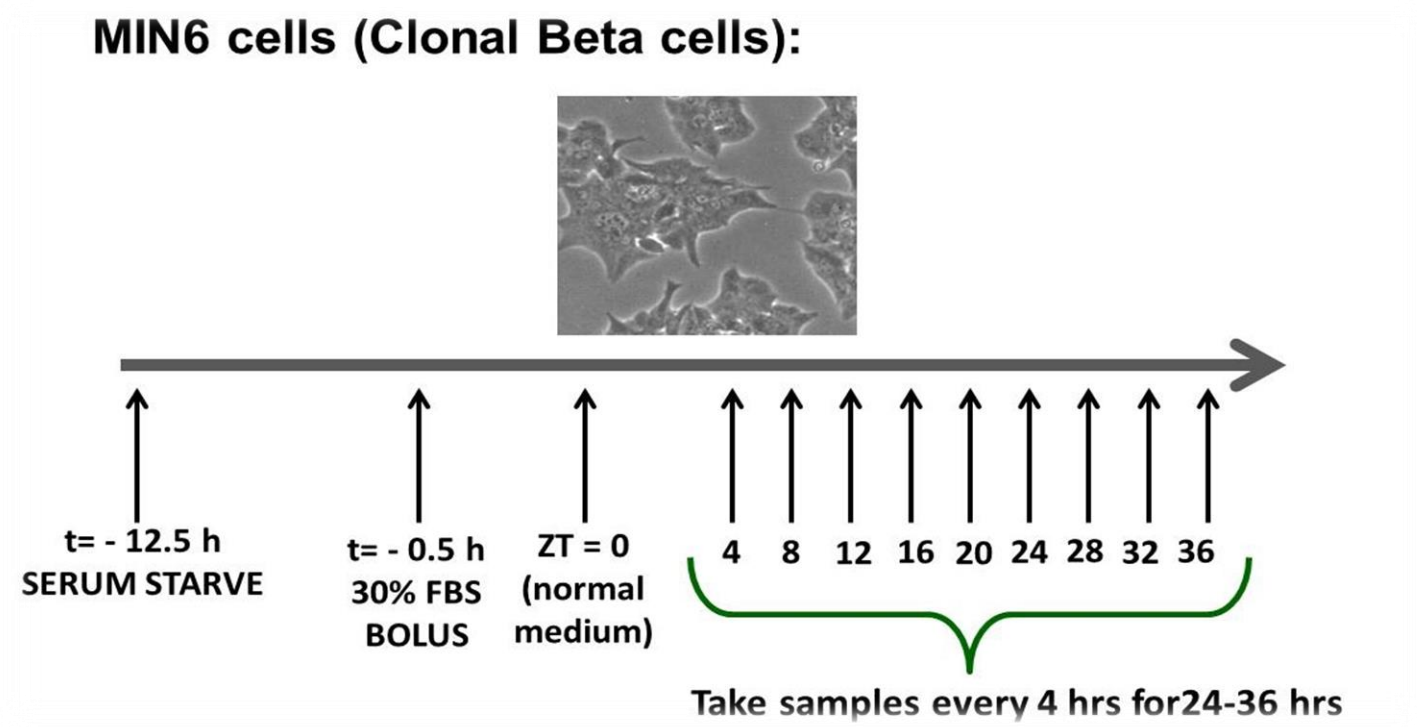


Figure 3.3: In vitro synchronization using serum shock/stave protocol*:* MIN6 cells were synchronized via serum starve (12hrs) followed by serum shock (30%FBS/30 minutes). Samples were collected at 0, 4, 8, 12, 16, 20, 24, 28, 32 and 36 hours for assessment of various parameters.

For *in vitro* experiments outlined in chapters 5 and 6, forskolin was used to entrain the MIN6 cells. $4.5X10^6$ MIN6 cells were plated in each well of a 6-well tissue culture plate (CS100) (VWR, Radnor, PA, USA) and grown in complete DMEM medium until 60-70% confluency was reached. Cells were washed twice with 1X sterile PBS (1.37M NaCl, 268mM KCl, 81mM Na_2HPO_4 and 147mM KH_2PO_4 at pH:7.4) following which serum-free DMEM medium was added. 22.5µM forskolin in dimthylsolufoxide (DMSO) (#F3917-10MG, Sigma, St. Louis, MO) was added to cells. Forskolin has been used in several published studies that have explored the role of the circadian clock in β-cells (Perelis et al., 2015). After 2 hours of incubation with forskolin, the cells were washed and replaced with complete DMEM medium. The addition of complete medium represents ZT0. Samples were collected at specific timepoints for experiments outlined in this thesis **[Figure 3.4].**

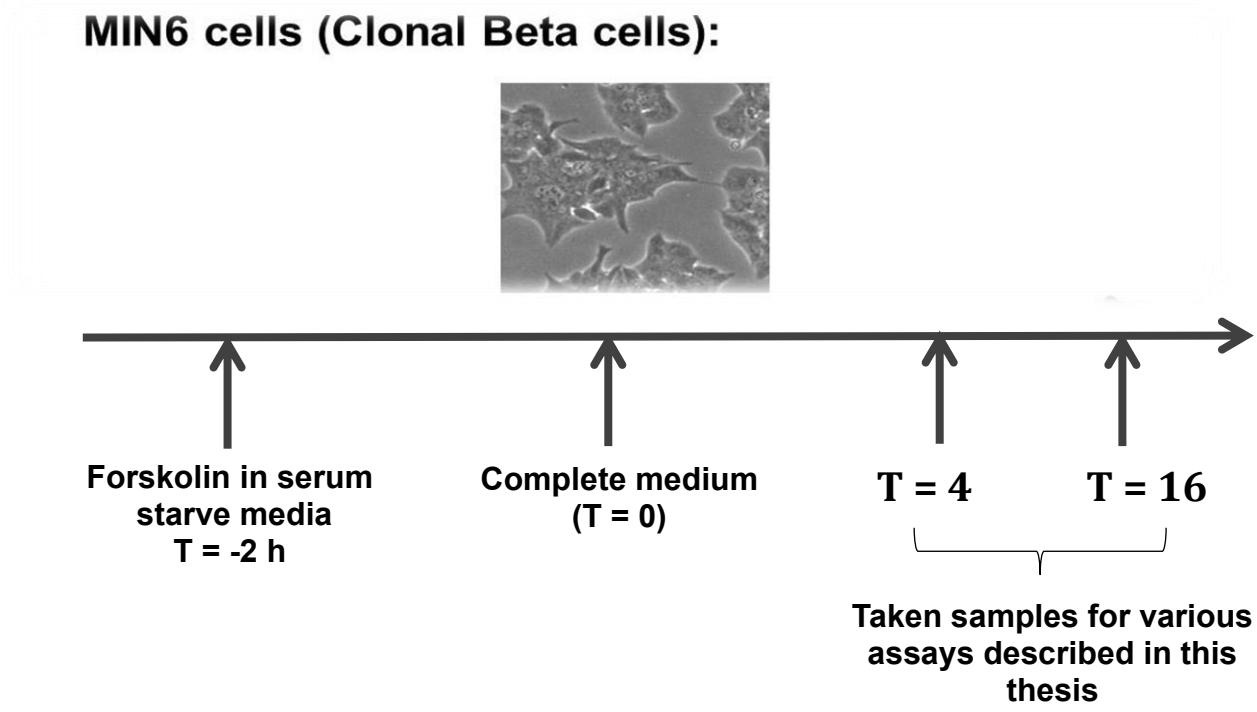


Figure 3.4: *In vitro* synchronization using Forskolin: MIN6 clonal β-cells were synchronized with 22.5μM Forskolin for 2 hrs. Samples taken for various assays at 4- and 16-hours post-synchronization.

3.3.2 siRNA- mediated Bmal1 knockdown in MIN6 cells

MIN6 cells were transfected with siRNA specific for *Bmal1* (Thermo Fischer, Waltham, MA), a core circadian clock protein, to create an *in vitro* model of circadian dysfunction. 100nM of *Bmal1*siRNA and Silencer Select Negative Control and BLOCK-IT (Thermo Fischer, Waltham, MA; fluorescent control) were transfected into cells, maintained overnight in media without antibiotics, using Lipofectamine RNAiMAX Transfection Reagent (Catalogue No. 13778075, Thermo Fischer, Waltham, MA, USA) according to the manufacturer's instructions (Ye et al., 2020). Transfected cells were incubated at 37ºC/5% CO_2 for 8 hours. After the transfection period, cells were washed and the medium changed to complete DMEM (Gibco, Thermo Fisher, Waltham, MA, USA) supplemented with 10% fetal bovine serum (Thermo Fisher, Waltham, MA, USA) and 1% penicillin/streptomycin (VWR, Radnor, PA, USA). The next day, cells were synchronized using the protocol outlined in method section 3.3.1 and used for experimentation as described in chapters 6. Table 3.1 provides a list of transfection reagents and siRNAs used in this study.

Table 3.1: Transfection reagents and siRNAs used in *Bmal1* knockdown studies *in vitro.*

Product Name	Assay ID	Catalogue No.
***Arntl (Bmal1)* Silencer Select Pre-designed siRNA**	S62620	4390771
***Arntl (Bmal1)* Silencer Select Pre-designed siRNA**	S62622	4390771
Silencer Select Negative Control #1 siRNA	-	4390843
BLOCK-iT Alexa Fluor Red Fluorescent Control	-	14750100
Lipofectamine RNAimax	-	13778075

3.4 Animal colony maintenance

All mice used in this study were kept in 12hr:12hr light/dark cycle (lights on at 6:00am/lights off at 6pm). Mice were given 24 hr *ad libitum* access to water and a standard chow diet (Product number: RMH3000 from Federated Co-Op). All studies were done following approval from Institutional Animal Care and Use Committee (University of Manitoba).

3.5 Genotyping

Genotyping of *Ucp2*βKO mice: A standard PCR-based method was used to genotype the mice generated in the "*Ucp2*βKO colony". Briefly, ear punches were obtained from the mice and DNA extraction was performed using the GeneJET gDNA purification kit (Thermofischer, Waltham, MA, USA; Product # K0722), according to the manufacturer's instructions. Briefly, ear punches were lysed using 100µl of lysis buffer containing proteinase K and incubated overnight at 55°C. 1-2µl of DNA extract was added to a PCR reaction mastermix containing 22.5µl of Superblue (Platinum Blue kit; Fischer, Waltham, MA; Catalogue No: 1280015), 0.5µl of 10mM primers (Forward and Reverse; see table 3.4. for sequences) in sterile PCR tubes. Table 3.2 contains the PCR program used to amplify PCR products, which were subsequently run on a 1.5% agarose gel made in 1X TAE buffer (40 mM Tris, 20 mM acetic acid, 1 mM EDTA) at 120V for 30-45 minutes. 6.25µl of SybrSafe (Invitrogen; Waltham, MA; Catalogue No: S33102) was added to visualize the DNA. An amplification size of 380bp was observed for *Ucp2*$^{flx/flx,}$ 270 bp band for *Ucp2*$^{wt/wt}$ and a 250 bp band for Cre^{+}. Appropriate negative

controls (a PCR reaction containing water) and positive controls (a known sample positive for flox and Cre) (PCR reaction without any DNA) were also run(Robson-Doucette et al., 2011).

Table 3.2: PCR reaction setting for genotyping *Ucp2*βKO mice

Temperature	**94°C**	**94°C**	**59°C**	**72°C**	**4°C**
Time	3 min	20sec	30sec	40sec	Infinity
No. of cycles	1	35	35	35	

Genotyping *Bmal1*βKO mice: Ear notches were obtained from mice and placed in 100µl lysis buffer and 0.5-1µl DNA release enzyme for DNA extraction using Plant Phire kit (Product number: F-160L, Thermofischer, Waltham, MA, USA) at 95°C for 5min. 1-2µl of DNA extract was added to a 20µl mastermix containing 10 µl of Phire Plant PCR buffer, 10mM primers (0,5 µl of each of forward and reverse; see table 3.4 for sequences) in PCR tubes and PCR grade water. Table 3.3 contains the PCR program used to amplify PCR products which were run on a 1.5% agarose gel made in 1X TAE buffer (40 mM Tris, 20 mM acetic acid, 1 mM EDTA) at 120V for 30-45 minutes. 6.25µl of SybrSafe (Cat. No. #S33102, Invitrogen, Waltham, MA) was added to visualize the DNA. An amplification size of 431bp was observed for *Bmal1*$^{flx/flx}$, 327bp band for *Bmal1*$^{wt/wt}$ and a 431bp + 327bp for *Bmal1*$^{flx/wt}$. For determining Cre status, a 675 bp band was observed for Cre^{+}. Appropriate negative controls (PCR reaction without any DNA) and positive controls (a known sample positive for flox and Cre) were run.

Table 3.3: PCR reaction settings for genotyping *Bmal1β*KO mice

Temperature	**98°C**	**98°C**	**59°C**	**72°C**	**72**	**4°C**
Time	5 min	5sec	5sec	20sec	1min	Infinity
No. of cycles	1	39	35	35	39	

Table 3.4: List of primers used for genotyping

Primer Name	**Sequence**
Ucp2 $^{flx/flx}$ **Forward Primer**	ACCAGGGCTGTCTCCAAGCAGG
Ucp2 $^{flx/flx}$ **Reverse Primer**	AGAGCTGTTCGAACACCAGGCCA

***Ins2-Cre* Forward Primer**	AAAATTTGCCTGCATTACCG
***Ins2-Cre* Reverse Primer**	ATTCTCCCACCGTCAGTACG
***Bmal1*$^{flx/flx}$ Forward Primer**	ACTGGAAGTAACTTTATCAAACTG
***Bmal1*$^{flx/flx}$ Reverse Primer**	CTGACCAACTTGCTAACAATTA
***Ins1*-Cre Forward Primer**	GTCAAACAGCATCTTTGTGGTC
***Ins1*-Cre Mutant Forward Primer**	GCTGGAAGATGGCGATTAGC
***Ins1*-Cre Common**	GGAAGCAGAATTCCAGATACTTG

3.6 Glucose Tolerance Tests (GTT) and Insulin Tolerance Tests (ITT)

For studies using the Ucp2βKO mice: 12-week-old mice were fasted for 3 hours prior to performing the GTT. A 3-hour fast was chosen because 3 hours is sufficient to return blood glucose to baseline and this shorter fast facilitated performing GTTs at 4-hour intervals across the 24-hour time course (Moro and Magnan, 2021). A 1M glucose stock was made by dissolving 1g glucose into 10ml of sterile water. The glucose stock was filter sterilized using a 0.2-micron filter (Sarstedt; Cat No. 83.1826.001, Germany). Glucose (1g/kg) was administered via an intra-peritoneal injection and blood glucose measured using a glucometer (Contour Next; Mississauga, Ontario, CA) at 0, 10, 20, 30, 60 and 120 mins after glucose injection. GTTs were performed at 6am (lights on), 10am, 2pm, 6pm (lights off), 10pm and 2am.

For studies using the Bmal1βKO mice: 12-week-old mice were fasted for 16 hours prior to performing a GTT. 16-hour fasting is standard practice for performing a GTT in mice (Pereira et al., 2015). Similar to above, a stock glucose solution was made, filter sterilized, and 1g/kg was administered via i.p. injection. Blood glucose measurements were taken at 0, 10, 20, 30, 60 and 120 mins after glucose injection. In this study, GTTs were performed at 10am and 10pm as we found that 10am and 10pm corresponded to the peak and trough times in the circadian cycle. ITTs were performed on 12-week-old mice that were fasted for 4 hours. Insulin (Sigma, Oakville, CA) (3.75UI/kg of body weight) was injected via an i.p. injection following which blood glucose was measured at 0, 15, 30, 45, 60 and 120mins (Dolinsky et al., 2011). ITTs were performed only at 10am as insulin sensitivity was greatly increased at 10pm, which made blood glucose drop too low. In other words, it was not safe for the animals to perform an ITT at 10pm, so this was not done.

3.7 Pancreatic Islet Isolations

Islets were isolated following a collagenase IV (Sigma Oakville, ON, CA) digestion of pancreas via an established protocol (Robson-Doucette et al., 2011). Briefly, mice were anaesthetized by administering sodium pentobarbital (150µl of 0.1% of Sodium Pentobarbital; Stock concentration – 240mg/ml) via an i.p injection and

plane of anesthesia confirmed by toe pinch. The abdominal and thoracic cavities were opened, and cardiac puncture performed to collect blood using a 21-gauge needle, which was later used to quantify plasma insulin levels. To visualize the common bile duct and hepatic artery, the intestine was shifted to the left and the liver was pushed upward towards the diaphragm. The common bile duct was then clamped close to the liver. Next, a small cut was made just above the ampulla of vater (the duct formed by the union of pancreatic and common bile duct) through which the pancreas was perfused with collagenase solution using a 231/2-gauge needle. The pancreas was excised and placed in a 50ml falcon tube containing ~5 mls of RPMI plus 1% pen/strep (without FBS). The tube was placed in a 37ºC water bath for ~13 minutes with gentle shaking to digest the exocrine tissue, leaving the endocrine islets intact. Once completely digested, islets were handpicked into fresh RPMI-1640 media (11.1 mM glucose; Gibco, Thermo Fisher, Waltham, MA, USA), supplemented with 10% FBS (Thermo Fisher, Waltham, MA, USA), 1% Penicillin-Streptomycin (VWR, Radnor, PA, USA) and 1% L-Glutamine (Hyclone - GE Healthcare, Logan, Utah, USA) in a sterile petri dish. This process of picking the islets was repeated 3 times into fresh media. Islets were allowed to rest for 1-2 hours at 37°C in an incubator maintained at 5% CO_2. The islets were used immediately for the described experiments.

3.8 Glucose-stimulated Insulin Secretion (GSIS)

MIN6 cells (passage number 28-50) or 10-15 isolated islets were washed with 1X PBS and incubated in 2.8mM glucose in Krebs-Ringer buffer (KRB;128.8mM NaCl, 4.8mM KCl, 1.2mM KH_2PO_4, 1.2mM $MgSO_4$, 2.5mM $CaCl_2$, 5mM $NaHCO_3$, 10mM HEPES) (also referred to as “low glucose” solution) + 0.1% bovine serum albumin (BSA) at 37°C for an hour. After the hour incubation, the low glucose solution was replaced with fresh low glucose solution and further incubated for 30mins at 37°C. The supernatant was collected and stored in -20°C. Next, cells or islets were incubated in 16.7mM glucose KRB (“high glucose” solution) and incubated at 37°C for 30 minutes. After 30 minutes, the supernatant was again collected and stored at -20°C. For islets, 150µl of acid:alcohol solution (96µl concentrated HCl in 10ml of Absolute Ethanol) was added to the islets and placed at 4°C overnight for DNA extraction. For MIN6 cells, cells were lysed by adding 1ml of water and subjecting the cells to several cycles of freeze and thaw. For all samples, DNA was quantified using a Nanodrop (Thermofischer, Waltham, MA) (Seshadri et al., 2017). To measure insulin in the collected supernatants, samples were thawed, and insulin concentration quantified using a mouse insulin ELISA kit (ALPCO, Salem, USA) normalised to DNA content and expressed as a function of time.

3.9 Immunohistochemistry

Pancreata were dissected from mice and put in 4% paraformaldehyde (PFA) solution and placed on a rotator overnight at 4°C. The 4% PFA solution was removed and the pancreas was processed for 3 days through a series of sucrose solutions with increasing concentrations (10%, 15% and 20%) changed successively with overnight incubations on a rotator at 4°C. Optimal Cutting Temperature (OCT) compound was mixed with equal

proportions of 20% sucrose and allowed to mix on a rotating stand at room temperature. The pancreas in 20% sucrose was cut in half and embedded in OCT within plastic molds while placed on dry ice. Sections of 0.5µm thickness were cut using a cryostat and mounted on charged slides and stored at -20°C until staining. Upon thawing the slides, 100µl of 1X blocking buffer was added to the tissue section (blocking buffer contains 1X PBS, 5% goat serum, 0.2% Triton-X, 0.02% Sodium Azide and 0.1% BSA) was applied to the tissue area and incubated at room temperature for an hour. Slides were stained with primary antibodies specific for BMAL1, insulin or glucagon and incubated overnight at 4 °C (details of antibodies and dilutions used are listed in **Table 3.5**). The next day, the slides were washed 3 times for 10 minutes each with 1X PBS. Next, the slides were stained and incubated at room temperature for 2 hours with appropriate secondary antibody (details of antibodies and dilutions used are listed in **Table 3.5)**. Excess secondary antibody was removed by washing slides with 1x PBS three times for 10 minutes each. Nuclei were stained with 60µl of Vectashield containing DAPI, cover-slipped and sealed with nail polish. The stained slides were imaged on an epifluorescence microscope (Zeiss, Jena, Germany); part of the CHRIM microscopy platform, at 20X magnification (Rakshit et al., 2016a).

Table 3.5: List of primary and secondary antibodies used in Immunofluorescence staining

	Protein	**Host species**	**Dilution**	**Commercial Source**	**Catalogue Number**
Primary Antibody	BMAL1	Rabbit	1:100	Abcam	AB9308
Primary Antibody	INSULIN	goat	1:50	Santa Cruz	C2714
Primary Antibody	GLUCAGON	goat	1:100	Santa Cruz	J1614
Secondary Antibody		Donkey anti- rabbit	1:250	Jackson	711-545-152
Secondary Antibody		Donkey anti- goat	1:125	Jackson	705-585-147

3.10 ATP content quantification

Synchronized MIN6 cells at ZT4 and 16 or 10-15 islets isolated from mice at specific times of the day were first incubated with 1ml of 2.8mM glucose KRB solution for 1 hour. Following which they were incubated in either with 1ml (MIN6 cells) or 150µl (islets) of 2.8 mM glucose or 16.7 mM glucose KRB for 30 mins at 37ºC in 5% CO_2 incubator. The media was aspirated, and the cells/islets were washed two times with sterile PBS. Cells

and islets were lysed with 300µl or 100 µl, respectively, of 0.1 M NaOH/0.5 mM EDTA buffer for 20 min at 60ºC and stored at -80ºC until assayed. An ATP bioluminescent assay kit (Sigma, Oakville, ON, CA) was adapted to a 96-well plate format and the assay performed according to the manufacturer's instructions. Luminescence was detected and quantified using a Fluostar Optima microplate reader (BMG Labtech, Ortenberg, Germany). ATP concentrations were normalized to total mg of DNA as determined using the Nanodrop (Thermofischer, Waltham, MA).

3.11 ROS measurements

Intracellular ROS was measured, using 2',7'- dichlorodohydrofluorescein diacetate (CM-H2-DCFDA; Lifetech, #C6827) and MitoSOX (Life Tech, #M36008) staining of synchronized MIN6 cells treated with either 50µM genipin (DAKO, #078-03021), or anti- and pro-oxidant agents (0.2mM N-acetyl L cysteine and 1mM diethymaleate, respectively; Sigma, Oakville, ON CA). Briefly, synchronized cells were treated with either 5 µM of CM-H2-DCFDA prepared in imaging buffer (130 mM NaCl, 5 mM KCl, 2 mM $CaCl_2$, 1 mM $MgCl_2$, 5 mM $NaHCO_3$, and 10 mM HEPES at pH 7.4) for 30mins (to detect H_2O_2) or 5 µM of Mitosox prepared in DMSO (to detect mitochondrial superoxide). The cells were co-stained with Hoechst 33342 (Thermofischer, Woltham, MA) for 30 mins. Cells were gently washed twice with 1X PBS and imaging buffer was replaced. Fluorescence for CM-H2-DCFDA was detected at 525nm with excitation at 480nm using the Zeiss epiflourescence microscope. Similarly, Mitosox fluorescence was detected at 580nm with excitation at 510nm. Hoechst was detected at 497nm (emission) on excitation at 397nm. All images were captured using the same exposure setting to enable comparison of fluorescent intensity across time. Images were captured using 10X magnification and 5 random fields were imaged per well. In total, two wells were imaged for a single time point. Quantification of fluorescence, including processing such as background correction, was performed using Fiji (ImageJ) software (NIH, USA) (Robson-Doucette et al., 2011).

3.12 Oxygen consumption and extracellular acidification rate using the XF-Analyzer

$4.5X10^4$ MIN6 cells/well were seeded into Seahorse XF-24 cell culture plates (Agilent Technologies, Inc., Santa Clara, CA, USA). Cells were cultured for 24-48 hours in a 5% CO_2 incubator maintained at 37℃ and synchronized using 22.5µm forskolin, as described above in section 3.3.1. One hour before measurement on the XF-24 extracellular flux analyzer, DMEM media was replaced with Seahorse Base Media (0mM glucose supplemented with 4mM of L-Glutamine and placed at 37℃. Stock solutions of glucose (167mM), 2-deoxy-glucose (2-DG;500mM), etomoxir (400µM), oligomycin (10µM), carbonyl cyanide 4-(trifluoromethoxy)phenylhydrazone (FCCP; 20µM), rotenone (10µM) and antimycin A (10µM) were prepared in Seahorse base media and loaded into injection ports A, B, C and D of the XF-24, as per manufacturer's protocol (Martens et al., 2020).

3.12.1 Assessment of glucose oxidation rate

Synchronized MIN6 cells were plated into XF 24-well cell culture plates and cultured to 60-70% confluency, as described above. For the experiments testing the effects of a disrupted circadian clock on glucose oxidation, cells were transfected with *Bmal*1siRNA and a control siRNA prior to synchronization, as described in section 3.3.2. The night before the assay, each well of the XF-24 flux cartridge was filled with 1ml of XF calibrant and placed in a non-CO_2 incubator at 37C. On the day of the assay, cells were washed 2-3 with Seahorse base medium supplemented with 4mM of L-glutamine and 16.7mM glucose, following which cells were incubated in Seahorse base media for 1 hour in CO_2-free incubator at 37℃. Cells were placed in the XF-24 analyzer to measure rate of glucose oxidation, using a user defined program. Briefly, stock solutions of oligomycin, FCCP and rotenone and antimycin A at concentrations stated in in Section 3.12 were injected into drug ports A, B and C, respectively, which are present on the specialized XF Flux cartridge and the loaded cartridge calibrated for 20 mins in the XF-Analyzer before the assay was run. The XF analyser uses specialized microsensors to measure changes in the oxygen consumption rate (OCR) and the extracellular acidification rate (ECAR) in cell media simultaneously. The existing XF-Mito Stress test was modified to the following program. 8 basal measurements were made followed by an injection of oligomycin. Three successive readings were taken followed by an injection of into the media containing the cells. Three more readings were taken and then rotenone/antimycin was injected. Three more reading were taken after this final injection. To normalize the data, cells were washed gently with 1X PBS to remove traces of seahorse media and 150µl RIPA buffer (40mM Tris; 150mM NaCl;1% NP-40; 1% Na Deoxycholic Acid) was used to lyse the cells and protein quantification using Bio-Rad DC (detergent compatible) (VWR; Cat no. #5000111 colorimetric assay was performed against a spectrum of known concentration. Once normalized to protein concentration, several parameters were calculated, namely basal respiration, maximal respiration, proton leak, ATP production and spare reserve capacity using the manufacturer's defined calculations. The formulae used to calculate each parameter are shown in Table 3.6. ECAR traces were obtained.

Table 3.6 Formula used to calculate parameters of OCR

Parameters Calculated	**Formulas used**
Non- mitochondrial Oxygen consumption	Minimum rate after Rotenone injection
Basal respiration	Last measurement before Oligomycin injection- Non-mitochondrial Oxygen consumption.
ATP production	Basal respiration – Proton Leak
Proton Leak	Minimum rate after Oligomycin injection – Non mitochondrial Oxygen consumption

Maximal Respiration	Maximum rate after FFCP injection – Non-mitochondrial Oxygen consumption.
Spare capacity	Maximal respiration – Basal respiration

3.12.3 Assessment of fatty acid oxidation rate

To measure fatty acid oxidation capacity, 1mM palmitate conjugated to 0.17mM BSA (6:1 ratio) was prepared using a protocol defined by Seahorse. For control, BSA (0.17mM) was prepared in Seahorse base media. Palmitate or BSA was added to cells in the Seahorse XF-24 plate, which was then placed in a 5% CO_2 free incubator at 37℃ for 1 hour. For assessment of fatty acid oxidation, oligomycin, FCCP and rotenone/antimycin A stocks were injected into ports A, B and C, respectively. The existing XF-Mito Stress test was modified to the following program: 8 basal measurements followed by an injection of oligomycin. 3 successive readings were taken followed by an injection of FCCP into the media containing the cells. On completion of the 3 more readings, rotenone/antimycin was injected. Three more reading were taken after the final injection. Once normalized to the protein concentration as described above, basal respiration rate, maximal respiration rate, proton leak, ATP production and spare reserve capacity were calculated using the formulae described in Table 3.6.

In a separate set of experiments, we measured OCR in cells in the absence of fatty acids using Etomoxir to inhibit Cpt-1a which is a fatty acid transporter allowing fatty acids to enter the cell. More specifically, stock solutions of Etomoxir (400µM) was injected into PORT O of the plate, along with inhibitors such as Oligomycin, FCCP, Rotenone and Antimycin in Ports A, B and C were applied to cells that were prepped with media containing palmitate (1hr in 5% CO_2 free incubator). Measurements were obtained at 37℃. OCR and ECAR data was normalized to cellular protein concentration quantified using BioRAD DC protein assay. All parameters were calculated using protocols suggested by manufacturer's instructions and formulas summarised in Table 3.6.

Furthermore, to assess the role of Ucp2 in fatty acid oxidation, we applied Genipin (500µM) to inhibit Ucp2 in Port O and measured OCR and ECAR changes in cell media in response to Oligomycin, FCCP, Rotenone and Antimycin. As mentioned above, OCR and ECAR data was normalized using protein concentration quantified using BIO-RAD DC protein assay. On normalization, OCR reading were used to calculate Basal respiration rate, Maximal respiration rate, Proton leak, ATP production and spare capacity using protocols recommended by Agilent technologies and formulas summarised in Table 3.6.

3.12.4 Glycolysis stress test

In order to measure the ability cells to undergo glycolysis, we used to glycolysis stress test. For Glycolysis stress test, We used to 2DG to inhibit glycolysis. Synchronized cells were first washed with 1X PBS three times on the day of the assay. Seahorse base media was prepared by adding 16.7mM glucose and added to cells for 1hour before the assay as described above. Stock solution of Rotenone/Antimycin and 2DG which were prepared

in seahorse base media containing no glucose were injected into Ports O and A. OCR and ECAR values were determined after normalization to protein concentration determined by the Bio-Rad protein assay. Glycolysis, Glycolytic capacity and reserve are calculated from ECAR data and the formulas are described in Table 3.7.

Table 3.7: Parameters calculations for Glycolysis stress test

Parameters	**Formulas**
Glycolysis	Last measurement before Oligomycin
Glycolytic capacities	Last measurement before 2DG injection – Average of measurements before Oligomycin injection
Glycolytic reserve	Glycolytic capacity - Glycolysis

3.13 Gene expression analyses (RT-qPCR)

RNA was isolated from MIN6 cell lysates, and 150-300 islets isolated from mice using an RNA extraction kit from Ambion (Thermofischer, Grand Island, NY, USA). cDNA was reverse transcribed from RNA using a Quantitect Reverse Transcriptase kit (Qiagen, Germantown, MD, USA). 20ng/well of cDNA was used as template in a qPCR reaction containing SYBR green obtained from Quantitect SYBR green PCR kit (Qiagen, Germantown, MD, USA) in a multiplate low-profile 96-well unskirted PCR plate (BioRad, Mississuaga, Ontario, Canada). mRNA was amplified in a Biorad CFX-96 real-time quantitative PCR (RT-qPCR) system using the following program: 95ºC for 15 min, followed by 40 cycles of: 95ºC for 15s, 57ºC for 30s, and 72ºC for 30s. Data was normalized to *Eif2a* mRNA and expressed relative to ZT 0 or ZT4 timepoint from the experiment to calculate 2^{-ddCT} (Livak and Schmittgen, 2001). Table 3.8 lists all the primer sequences used in this project.

Table 3.8: List of general primers

Primer names	**Sequence**
***Ucp2* Forward**	GAGATGTAGGGAAACTCCAGAAC
***Ucp2* Reverse**	GCCTTGTCTTCTGTAGGTCTATG
***Bmal1* Forward**	CAACCCATACACAGAAGCAAAC
***Bmal1* Reverse**	CATCTGCTGCCCTGAGAATTA
***Eif2a* Forward**	CCTGAAGTGTGATCCTGTGTTT
***Eif2a* Reverse**	CCAAATCCAGCCAGCACTAATA
***Per 1* Forward**	CAGTCAGAGCAGCCATACAA
***Per 1* Reverse**	GTCCTGGAGCACACACTTAAT

***Cpt-1a* Forward**	TCGAAACCCAGTGCCTTAAC
***Cpt-1a* Reverse**	AAGCAGCACCCTCACATATC
***Glut-2* Forward**	TGTGCTGCTGGATAAATTCGCCTG
***Glut-2* Reverse**	AACCATGAACCAAGGGATTGGACC
***Ldha* Forward**	CAGACTTGGCTGAGAGCATAA
***Ldha* Reverse**	GATACATGGGACACTGAGGAAG

3.14 Cytosolic lactate quantification

Synchronized MIN6 cells were transfected with FRET-based lactate biosensor [Laconic/pcDNA3.1(-)], a gift from Dr. Joseph Gordon's Lab (University of Manitoba), using the JetPrime Polyplus agent according to manufacturer's protocol (VWR, Radnor, PA). 2µg biosensor was first diluted in 200µl JetPrime dilution buffer, vortexed and mixed at a ratio of 1:1.15 with Jet primer transfection reagent. This mix was incubated for 10mins. 200ul of this mix was added to each well containing 1.8ml of complete media. After a 4hr incubation the cells were washed with 1X PBS and complete media was replaced onto cells. Images were acquired on a Cytation 5 Cell Imaging Multi-Mode Reader (Biotek, Winooski, Vermont) at 48 hours post-transfection. FRET cubes detecting yellow fluorescent probes (YFP) at 527nm and cyanide fluorescent probes (CFP) at 485nm were used. Cytosolic lactate level was calculated as the ratio of bound YFP: CFP/unbound YFP (Martens et al., 2020). Quantification, including processing such as background subtraction, was done on Fiji (ImageJ) software.

3.15 Western Blotting

MIN6 cells synchronized at ZT4 and ZT16 were lysed using 150µl RIPA buffer (40mM Tris, 150mM NaCl, 1% NP-40, 1% Na deoxycholic acid) containing 10µl protease inhibitor cocktail (for 1ml of RIPA buffer prepared) (Sigma, Oakville, ON, CA) and 10µl phosphatase inhibitor cocktail for 1ml of RIPA buffer prepared) (Sigma, Oakville, ON, CA) and centrifuged at 4 ºC at 1000rpm. The supernatant was then stored at -80 ºC until the day of experimentation. Protein concentration from the lysate was estimated using a colorimetric DC assay kit (Bio-Rad, CA) by comparing against a standard curve of known protein concentrations(Hills et al., 2012). Samples were resolved on a 10% SDS page gel prepared using Bio-Rad Fast cast (Bio-Rad, CA) and transferred onto a polyvinylidene fluoride (PVDF) membrane (Fischer, Austria). The membrane was blocked for 1-2 hours in 5% skim milk and then probed with antibody against BMAL1 (Cell signalling, Denver, MA) prepared in 5% BSA at a dilution of 1:1000 and incubated overnight at 4 ºC. The blots were washed 3 times for 15 minutes each with 1X TBST (0.2% tween-20, 50mM tris-HCl and 150mM NaCl, pH7.4) followed by incubation with an anti-rabbit secondary antibody conjugated to HRP (Jackson laboratory; Westgrove, PA, USA) at 1:5000 dilution for 1 hour. The blot was imaged using a Bio-Rad Gel doc (Bio-Rad, CA). Once imaged the membrane was stripped with 0.2N NaOH and the process was repeated with an ACTIN antibody (Santacruz, sc-8432). BMAL1 protein

expression was normalized to ACTIN and expressed relative to ZT4 (4 hours post synchronization) using ImageJ.

3.16 Mitochondrial membrane potential measurements

Synchronized MIN6 cells at ZT4 and ZT16 were incubated with KRB and 25µg/ml of Rhodamine123 (Molecular Probes, Thermofischer, Waltham, MA) dissolved in PBS for 10 minutes at 37ºC/5% CO_2. After washing with KRB solution, a steady state fluorescence was accomplished by adding 2.8mM KRB solution on to plates that are placed on the Zeiss LSM700 Spectral Confocal Microscope, part of the CHRIM microscopy platform, imaging stage. After 2-3 minutes, high glucose (16.7mM) was added to cells, which results in a decrease of fluorescence as result of hyperpolarization. Finally, 5 mmol/L sodium azide (Sigma, Catalogue No. #S-2002) was added to depolarise the cells, causing an increase in fluorescence. Mitochondrial membrane potential ($\Delta\Psi_m$) changes were calculated by quantifying changes after hyperpolarization ($\Delta 1$) and depolarization ($\Delta 2$) was quantified in synchronized MIN6 cells (Diao et al., 2012). For experiments employing the UCP2 inhibitor, Genipin, cells were pre-incubated with 50µM of the drug for an hour before imaging.

3.17 Statistical Analyses

Statistical significance was assessed by two-tailed Student t-test or one- or two-way ANOVA for repeated measures, followed by a Bonferroni post-test comparison using Prism 8 software (GraphPad, San Diego, CA, USA). A value of $P < 0.05$ was considered significant. All data are expressed as the mean $\pm$ SEM.

Chapter 4

Uncoupling protein 2 regulates diurnal rhythms of insulin secretion

This section has been published in the journal of *Molecular Metabolism* titled, **"Uncoupling protein 2 regulates daily rhythms of insulin secretion capacity in MIN6 cells and isolated islets from male mice**" - Nivedita Seshadri, Michael E. Jonasson, Kristin L. Hunt, Bo Xiang, Steven Cooper, Michael B. Wheeler, Vernon W. Dolinsky, and Christine A. Doucette.2017.6(7):760-769

Nivedita Seshadri, Michael E. Jonasson and Steven Cooper performed the GSIS and Ucp2 mRNA expression studies in *in vitro* MIN6 cells. **Bo Xiang** performed the islet perfusions. **Dr. Christine A. Doucette** and **Kristin L Hunt** helped with islet preparations for the experiments outlined in this chapter. **Nivedita Seshadri** did the GSIS experiments and Ucp2 expression outlined in the animal models and compiled the data for each of the experiments. **Dr. Michael Wheeler** provided the Ucp2$^{flx/flx}$ mice. **Dr. Christine A. Doucette** and **Nivedita Seshadri** performed the glucose tolerance tests. This work was supported by research grants awarded to **Dr. Christine A. Doucette** from the National Sciences and Engineering Research Council of Canada (NSERC; Discovery Grant RGPIN- 2015-06551), the Manitoba Medical Services Foundation (8-2014-06), the Children's Hospital Research Institute of Manitoba (2013-13) and the Thorlakson Foundation (University of Manitoba).

4.1 Background and Rationale:

Not surprisingly, numerous gain-of function (Chan et al., 2001, Chan et al., 1999, Hong et al., 2001, Kashemsant and Chan, 2006, Wang et al., 1999, McQuaid et al., 2006) and loss-of-function (Zhang et al., 2001, Joseph et al., 2002, Joseph et al., 2004, Lee et al., 2009, Robson-Doucette et al., 2011, Krauss et al., 2003) studies have been used to interrogate the function of UCP2 in the β-cell and, for the most part, have established a negative relationship between UCP2 and GSIS. For example, whole body (*Ucp2*$^{-/-}$) (Zhang et al., 2001, Joseph et al., 2002) and β-cell-specific *Ucp2* knockout (*Ucp2*-βKO) mice (Robson-Doucette et al., 2011) show augmented GSIS, whereas overexpression of *Ucp2* in clonal β-cell cultures and rat islets impairs GSIS (Chan et al., 1999, McQuaid et al., 2006). Furthermore, *Ucp2* mRNA and protein are markedly upregulated in isolated islets from animal models of type 2 diabetes (T2D) and obesity (Zhang et al., 2001, Joseph et al., 2002, Kassis et al., 2000, Winzell et al., 2003), and treatment of isolated islets *ex vivo* with high glucose and elevated lipid concentrations significantly increases *Ucp2* expression (Joseph et al., 2004, Laybutt et al., 2002, Patane et al., 2002). There is also sufficient evidence that suppression of insulin secretion in humans at risk for T2D is associated with higher expression levels of *Ucp2* (Sasahara et al., 2004, Krempler et al., 2002, Sesti et al., 2003). The negative relationship between Ucp2 expression and GSIS has been dubbed a "surprising whim of nature" (Nedergaard and Cannon, 2003, Sheets et al., 2008) and has provoked us and other research groups to ask an important evolutionary question: Why do β-cells express *Ucp2* if its activity is detrimental to insulin secretion and metabolic health? It is thought that UCP2 must have an important physiological role in the β-cell or it would have been selected against during evolution. Notably, obesity and over-nutrition are relatively 'modern' phenomena; humans evolved in an environment that was prone to prolonged periods of fasting and, in some cases, starvation (O'Rourke R, 2014). The metabolic response to fasting is tightly regulated by insulin such that suppression of insulin during fasting is essential to allow for efficient endogenous glucose production and lipolysis to release metabolic fuels when dietary glucose is not sufficiently available. As such, it has been suggested that the true physiological function of UCP2 is to coordinate insulin secretion capacity with fluctuating nutrient supply, such that upregulation of UCP2 during fasting inhibits insulin secretion to promote fuel mobilization and prevent hypoglycemia (Sheets et al., 2008, Chan and Kashemsant, 2006, Affourtit and Brand, 2008a). Interestingly, *Ucp2* mRNA is upregulated in islets and whole pancreas of starved mice (Bordone et al., 2006), and rats (Greco et al., 2014) and fasted *Ucp2*$^{-/-}$ mice display higher serum insulin levels and blunted lipid metabolic responses (Sheets et al., 2008). Only a few studies have examined the role of UCP2 in the β-cell during fasting, and all have employed either long term (i.e. >24 h) or supra-physiological fasts (i.e. artificially fasting the animals overnight during the normal wake/fed period); however, our diurnal nature dictates that we cycle between acute periods of fasting and feeding on a daily basis, and therefore, UCP2 may play an important physiological role in coordinating insulin secretion with the acute phases of fasting and feeding experienced on a daily basis. The temporal expression of *Ucp2* and its

contribution to GSIS capacity over the course of a daily cycle in a healthy β-cell has not yet been assessed. In this chapter, we hypothesized that *Ucp2* mRNA is dynamically expressed in healthy β-cells over the course of a 24 h daily cycle such that *Ucp2* expression is low in the fed/active phase to promote maximal GSIS capacity and upregulation of *Ucp2* in the fasted/inactive phase suppresses GSIS capacity. To test this, we used synchronized MIN6 clonal β-cells and islets isolated from wild type (WT) and *Ucp2*βKO mouse models to define the daily expression patterns of *Ucp2* mRNA, temporal GSIS capacity and glucose tolerance over 24 hours. Here, we demonstrate that UCP2 plays an important role in the regulation of temporal GSIS capacity, which is vital for the maintenance of glucose tolerance in the inactive/fasted phase of the daily cycle.

4.2 Materials and Methods

Refer to Chapter 3. See Sections 3.13, 3.31, 3.6 and 3.8 specifically.

4.3 Results

4.3.1 *Ucp2* mRNA expression is rhythmic in synchronized MIN6 cells and islets isolated from *Ins2*-Cre mice.

We first set out to determine the dynamics of *Ucp2* mRNA expression over a 24 h period using MIN6 cells. To accomplish this, MIN6 cells were synchronized using an established serum-starve/serum-shock protocol (Greco et al., 2014) and lysates collected every 4 hours over 36 hours for gene expression analyses by RT-PCR. *Ucp2* mRNA transcript levels displayed a dynamic and rhythmic pattern showing approximate 12 h repeating and alternating patterns of low and elevated *Ucp2* mRNA expression **[Figure 4.1A]**. At Zeitgeber time (ZT) 0, 4, and 8, *Ucp2* mRNA expression remained low and unchanged. At ZT 12 and 16, *Ucp2* mRNA levels increased 1.85 ($\pm$0.254; p=0.0102) and 2.318 ($\pm$0.533; p =0.0259) fold, respectively, compared to time 0. Between ZT 24 and ZT 28, *Ucp2* mRNA expression levels returned to baseline and gradually increased over the next 12 hours (up to 36 hours). Notably, beyond ZT 24, a trend towards a subsequent increase in *Ucp2* mRNA was observed up to ZT 36, although not statistically significant by 36 hours, likely due to waning synchronicity of the MIN6 cultures.

Similarly, when *Ucp2* mRNA transcript was measured in islets isolated from *Ins2*-Cre mice at ZT 4 and ZT 16, we observed elevated *Ucp2* mRNA expression at ZT 16 (light and inactive phase) followed by significant reduction at ZT 4 (dark and active phase) in the islets.

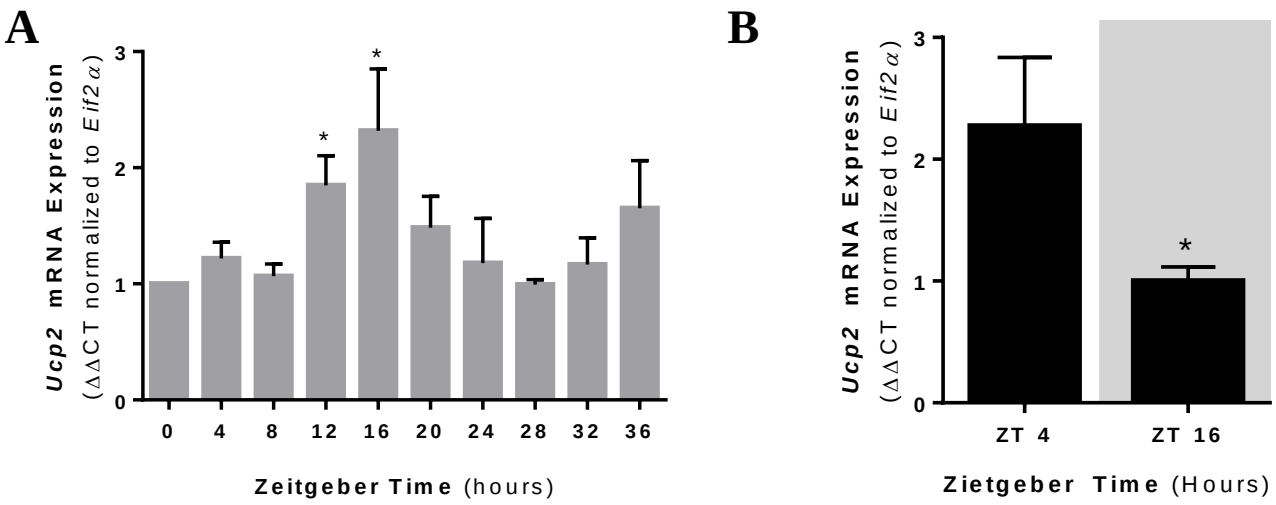


Figure 4.1: *Ucp2* mRNA expression over 24-36 h in synchronized MIN6 cells and islets isolated from C57BL6 mice. [A] *Ucp2* mRNA expression levels at 4 h intervals over 36 h in synchronized MIN6 cells. *Ucp2* mRNA shown is expressed relative to *Eif2a* levels and normalized to mRNA levels at time 0 (immediately after synchronization). Date are Mean ± SEM. N=4-6**.** *p < 0.05. P-value represents after statistical analysis by Two tailed student's t-test. **[B]** Islet *Ucp2* mRNA levels are significantly elevated at ZT 4 (light/inactive phase) compared to ZT 16 (dark/active phase) in *Ins2*-cre control mice. *Ucp2* mRNA shown is expressed relative to *Eif2a* levels and normalized to *Ucp2* mRNA levels ZT 16. Islets were isolated from 3 to 5 mice at each time point. Date are Mean ± SEM.*p < 0.05. P-value represents after statistical analysis by Two tailed student's t-test.

4.3.2 Rhythmic *Ucp2* expression inversely regulates insulin secretion capacity

Next, the temporal capacity of GSIS over 24 hours in synchronized MIN6 cells was established by performing static incubation assays in low (2.8 mM) and high (16.7 mM) glucose concentrations every 4 hours over a 36-hour time course. GSIS capacity varied in a repeatable pattern over 36 hours [**Figure 4.2A**]: From ZT 0 to ZT 12, stimulation with high glucose triggered an average 4.12-fold increase in insulin secretion; whereas during the next 12-hour period (from ZT 16 to ZT 24), GSIS was significantly suppressed, showing only a 2-fold increase when stimulated with high glucose. Beyond 24 hours (ZT 28 to ZT 36), GSIS capacity was again significantly increased, showing an average 3.47-fold increase when stimulated with high glucose. For the most part, the observed rhythmic pattern of GSIS capacity was opposite to the expression level of *Ucp2* mRNA **[Figure 4.1A]**, with the exception of the 12-h time point. At this time, *Ucp2* mRNA increased almost 2-fold, but suppression of GSIS was not yet observed (suppression observed at 16 h). This lag in suppression of GSIS likely represents a lag in the translation of *Ucp2* mRNA into functional protein. Unfortunately, protein levels were not measured due the lack of an available antibody that has sufficient sensitivity and specificity for UCP2.

To demonstrate that the observed rhythmic GSIS was dependent on the observed rhythms in UCP2 activity, we performed GSIS assays at ZT 4 and ZT 16 (time points that correspond to robust and suppressed GSIS, respectively) in the presence of genipin, a well-established pharmacological UCP2 inhibitor (Zhang et al.,

2006, Parton et al., 2007, Allister et al., 2013). Application of genipin prevented the suppression of GSIS in control MIN6 cells at ZT 16 but had no effect on GSIS capacity at ZT4 when *Ucp2* mRNA expression was low **[Figure 4.2G]**, suggesting that UCP2 activity at ZT 16 contributes to the suppression of GSIS at this time point. Together, these data demonstrate that rhythmic GSIS capacity is dependent on inverse rhythms of *Ucp2* expression/UCP2 activity in MIN6 cells.

To determine if rhythmic GSIS capacity is dependent on rhythmic *Ucp2* expression in primary β-cells, we exploited our previously generated and characterized β-cell-specific *Ucp2* knockout mice (*Ins2-Cre:Ucp2*$^{fl/fl}$; commonly referred to as *Ucp2*βKO) (Robson-Doucette et al., 2011). Similar to MIN6 cells, control (*Ins2*-Cre:*Ucp2*$^{wt/wt}$; commonly referred to as *Ins2*-cre) islets isolated at 4 h intervals over 24 h (lights on at 6am. ZT 0; lights off at 6pm. ZT12) displayed a rhythmic capacity for GSIS that was suppressed in the light/inactive phase of the daily cycle (ZT 0, 4, 8), but became more robust in the dark/active phase (ZT 12, 16, 20) **[Figure 4.2B]**. Suppression of GSIS in isolated *Ins2*-Cre islets at ZT 4 was associated with elevated islet *Ucp2* mRNA expression, whereas the more robust GSIS observed at ZT 16 was associated with reduced islet *Ucp2* mRNA **[Figure 4.1B]**. Importantly, daily rhythms of GSIS were lost in islets isolated from *Ucp2*βKO mice, which displayed robust GSIS across the full 24-hour time course **[Figure 4.2D]**. No differences in fasted plasma insulin levels or fasted blood glucose levels were observed over 24 h between the *Ins2*-cre control and the *Ucp2*βKO mice (data not shown). To reduce genotype and strain effects, we also isolated islets from wild type (WT) C57BL6 mice and treated them with and without genipin to manipulate UCP2 activity prior to performing insulin secretion assays. Similar to *Ins2*-Cre islets, C57BL6 islets displayed suppressed GSIS at ZT 4 in the light/inactive phase and robust GSIS capacity at ZT 16 in the dark/active phase **[Figure 4.2F, black bars]**. Pre-treatment of isolated C57BL6 islets with genipin reversed the suppression of GSIS observed at the ZT 4 time point **[Figure 4.2F, striped bars**]. Together, these data suggest that UCP2 plays an important physiological role in controlling the temporal capacity of GSIS such that increased *Ucp2* expression/ UCP2 activity are required for the normal suppression of GSIS in the light/inactive phase of the daily cycle.

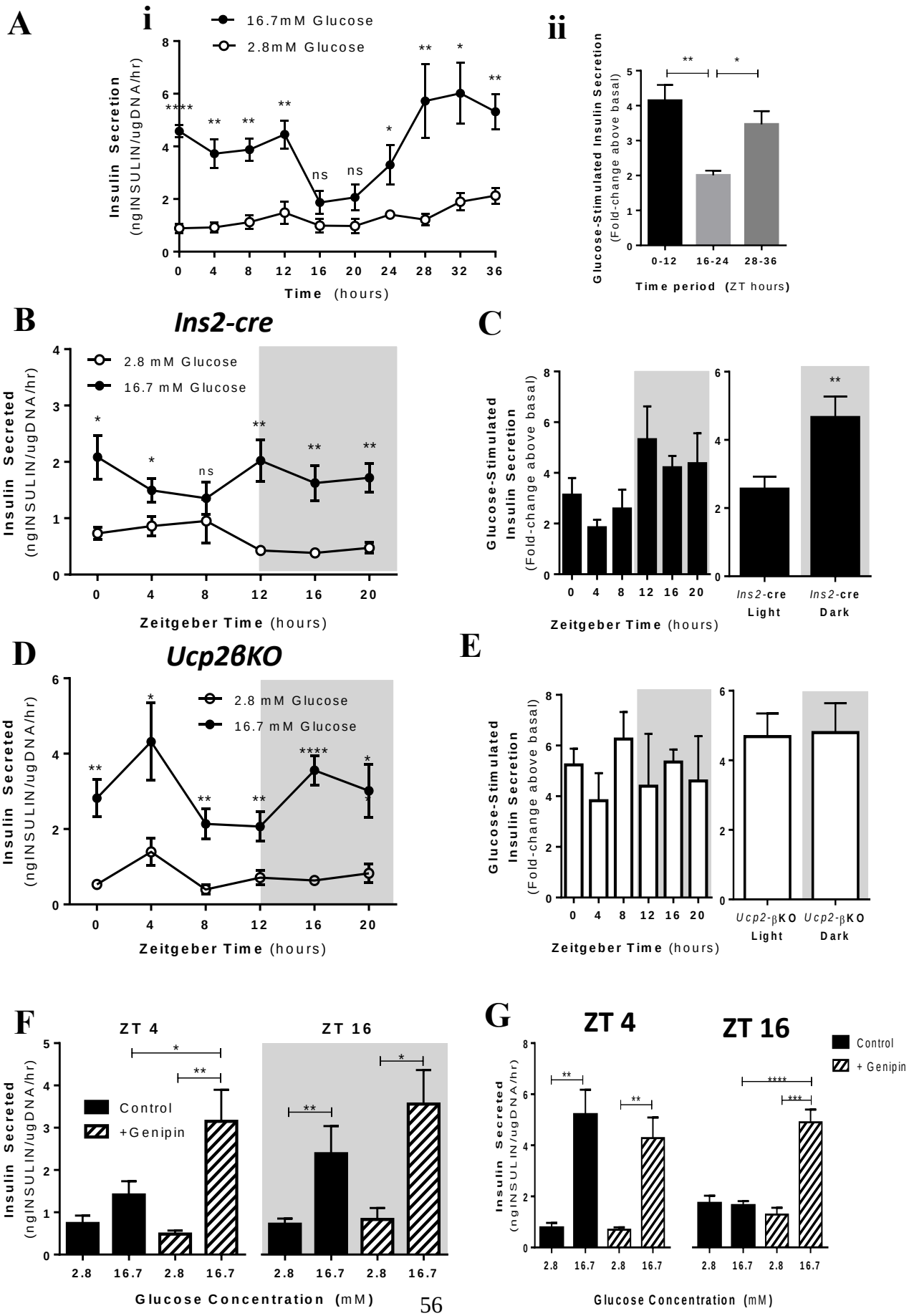

A
i
16.7mM Glucose
2.8mM Glucose
Insulin Secretion (ngINSULIN/ugDNA/hr)
Time (hours)
ns
ii
Glucose-Stimulated Insulin Secretion (Fold-change above basal)
Time period (ZT hours)
0-12
16-24
28-36
B
Ins2-cre
2.8 mM Glucose
16.7 mM Glucose
Insulin Secreted (ngINSULIN/ugDNA/hr)
Zeitgeber Time (hours)
C
Glucose-Stimulated Insulin Secretion (Fold-change above basal)
Ins2-cre Light
Ins2-cre Dark
Zeitgeber Time (hours)
D
Ucp2βKO
2.8 mM Glucose
16.7 mM Glucose
Insulin Secreted (ngINSULIN/ugDNA/hr)
Zeitgeber Time (hours)
E
Glucose-Stimulated Insulin Secretion (Fold-change above basal)
Ucp2-βKO Light
Ucp2-βKO Dark
Zeitgeber Time (hours)
F
ZT 4
ZT 16
Control
+Genipin
Insulin Secreted (ngINSULIN/ugDNA/hr)
Glucose Concentration (mM)
G
ZT 4
ZT 16
Control
+ Genipin
Insulin Secreted (ngINSULIN/ugDNA/hr)
Glucose Concentration (mM)

Figure 4.2: Glucose stimulated insulin secretion capacity of synchronized MIN6 cells and islets isolated from *Ins2*-Cre. [A] [i] GSIS capacity of synchronized MIN6 cells every 4 h over 36 h as measured by static incubation assay. Open circles represent insulin secreted when MIN6 cells are exposed to low (2.8 mM) glucose. Closed circles represent insulin secretion when MIN6 cells are exposed to high glucose (16.7 mM). Date are Mean ± SEM. N=7-8 experiments. P-value represents statistical significance after a One-way ANOVA **[ii]** Average GSIS capacity over segmented 12 h periods. GSIS is presented as the fold-change in insulin secretion above basal (2.8 mM glucose) when stimulated with high (16.7 mM). glucose. **[B]** GSIS capacity assessed every 4 h over 24 h in Ins2-cre (control) isolated islets. Data for insulin secretion capacities at 2.8 mM glucose (open circles) and 16.7 mM glucose (black circles) are shown for each time point. N=4-5 mice per time point. Date are Mean ± SEM. P-value represents statistical significance after a One-way ANOVA **[C]** GSIS capacity assessed every 4 h over 24 h in *Ins2*-cre (control) isolated islets. Data for insulin secretion capacities at 2.8 mM glucose (open circles) and 16.7 mM glucose (black circles) are shown for each time point. N=4-5 mice per time point. Date are Mean ± SEM. P-value represents statistical significance after a One-way ANOVA **[D**] GSIS capacity assessed at 4 h intervals over 24 h in islets isolated from *Ucp2*-βKO mice. Data for insulin secretion capacities at 2.8 mM glucose (open circles) and 16.7 mM glucose (black circles) are shown for each time point. Date are Mean ± SEM . N=4-13 mice per time point. P-value represents statistical significance after a One-way ANOVA **[E]** Left panel: GSIS capacity presented as the fold-change in insulin secretion above basal (2.8 mM glucose) when stimulated with high (16.7 mM) glucose at each time point in islets isolated from *Ins2*-cre mice. Right panel: Average GSIS capacity of isolated islets from *Ins2*-cre mice in the light vs. dark periods. Left panel: GSIS capacity presented as the fold-change in insulin secretion above basal (2.8 mM glucose) when stimulated with high (16.7 mM) glucose at each time point in islets isolated from *Ucp2*-βKO mice. Right panel: Average GSIS capacity of isolated islets from *Ucp2*-βKO mice in the light vs. dark periods. Date are Mean ± SEM. N=5-9 mice per time point. *$p < 0.01$; **$p < 0.01$; ****$p < 0.0001$. P-value represents statistical significance after a One-way ANOVA **[F]** Insulin secretion capacity measured in islets isolated from WT (C57BL6) mice at ZT4 (10 am) and ZT16 (10 pm). Application of Genipin (50 mM, 1 h before assay) shows that inhibition of UCP2 at ZT4 prevents suppression of GSIS at this time point. Daily rhythms of GSIS capacity are dependent on *Ucp2*/UCP2 in isolated islets**.** Date are Mean ± SEM. Two-way ANOVA followed by Bonferroni post-test comparison. **[G]** GSIS capacity at 4 and 16 h post-synchronization in MIN6 cells treated with (hatched bars) and without Genipin (solid black bars), a UCP2 activity inhibitor. Genipin was applied at a final concentration of 50 mM, 1 h before start of GSIS assay and remained present throughout the assay N=5. Date are Mean ± SEM. Two-way ANOVA followed by Bonferroni post-test comparison.

4.3.3 Diurnal *Ucp2* expression is required for maintaining glucose tolerance over 24 hours.

It is well-known that glucose tolerance fluctuates over a 24-hour period such that mild glucose intolerance occurs in the fasting/inactive phase of the daily cycle (Saad et al., 2012, Carroll and Nestel, 1973, Van Cauter et al., 1991, Van Cauter et al., 1989) and our results so far suggest that UCP2 plays an important role in controlling the glucose-stimulated insulin secretion response. To determine if dynamic Ucp2 expression contributes to the overall pattern of glucose tolerance over a 24 h cycle, we performed i.p. glucose tolerance tests (GTTs) every 4 hours over 24 hours in *Ucp2*βKO and *Ins2*-Cre control mice. Note that mice were given ad libitum access to food but were fasted 3 h prior to the GTT to ensure baseline blood glucose levels at the start of the test. *Ins2*-Cre control **[Figure 4.3A - light panels; Figure 4.3B]** and C57BL6 mice (not shown) both displayed normal rhythms of glucose tolerance, which include improved glucose tolerance in the dark/active phase and mild glucose intolerance in the fasted/inactive phase. Interestingly, *Ins2*-Cre control and *Ucp2*βKO mice displayed no

difference in glucose tolerance in the dark/active phase of the daily cycle **[Figure 4.3 A -dark panels; Figure 4.3B]**; however, *Ucp2*βKO mice displayed greater glucose intolerance in the light/inactive phase **[Figure 4.3A - light panels; Figure 4.3B].** Rhythmic *Ucp2* expression, particularly the upregulation of *Ucp2* expression in the light/inactive phase, appears to be required for the regulation of normal cycles of glucose tolerance over a 24 hour period.

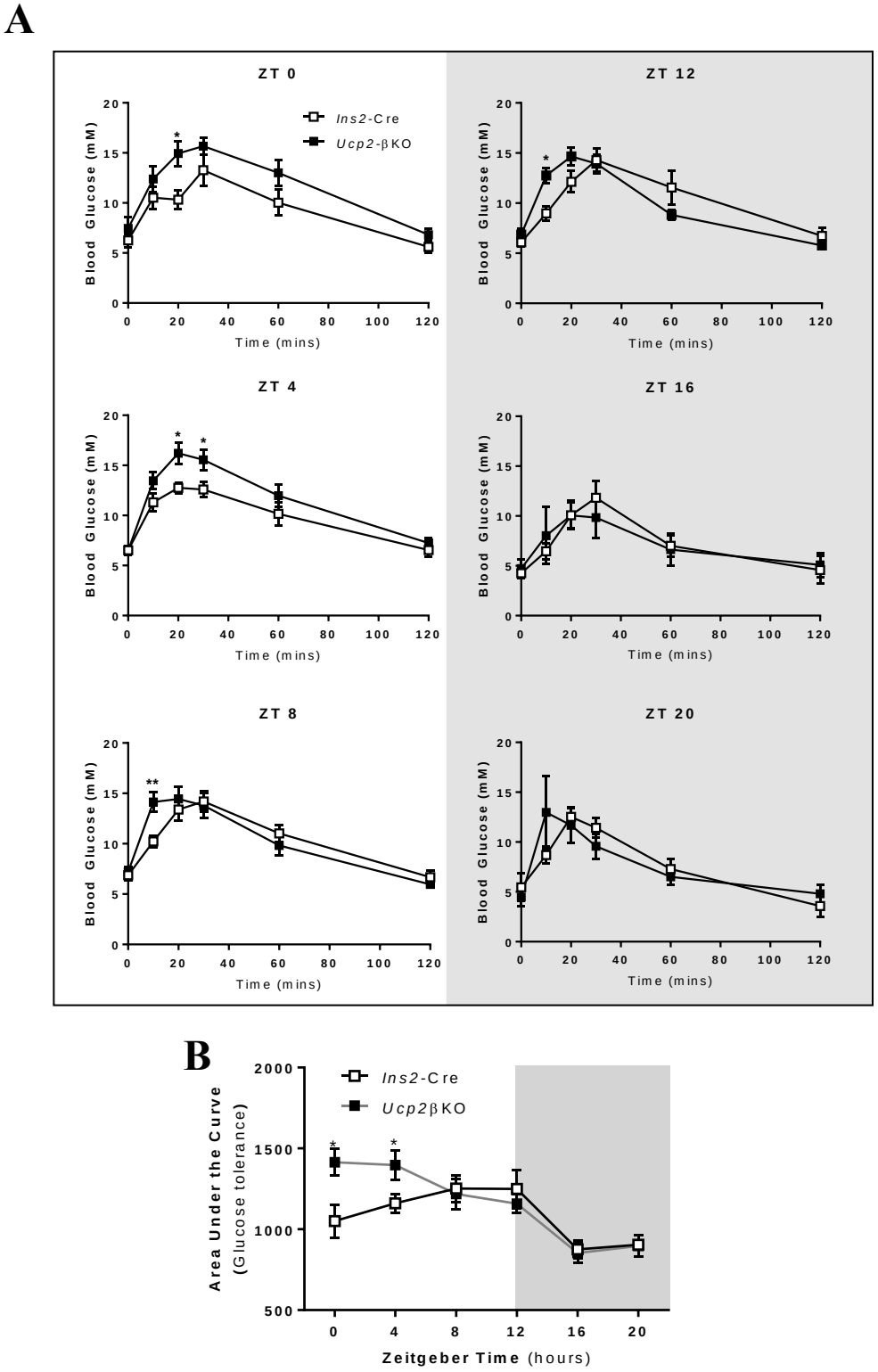


Figure 4.3: UCP2 deficiency impairs glucose tolerance only in the light phase of the daily cycle. [A] Assessment of glucose tolerance by i.p. GTT test was performed at 4 h intervals over 24 h at the following times: i) ZT0 (6 am e lights on), ii) ZT4 (10 am), iii) ZT 8 (2 pm), iv) ZT12 (6 pm e lights off), v) ZT16 (10 pm), and vi) ZT20 (2 am). Open squares are Ins2-cre mice; Closed squares are Ucp2-βKO mice. [B] AUC calculations of each glucose tolerance curve in A. N =18-25 mice per group. *$p < 0.05$; **$p < 0.01$. Date are Mean $\pm$ SEM. P-value represents statistical significance after a One-way ANOVA.

4.4 Discussion

Glucose tolerance in healthy human subjects is greatest in the morning, just before the onset of the feeding phase, whereas glucose tolerance declines significantly in the evening/night, at the onset of the fasted phase (Saad et al., 2012, Carroll and Nestel, 1973, Van Cauter et al., 1991, Van Cauter et al., 1989). While daily fluctuations in peripheral insulin sensitivity likely contribute to this phenomenon, the "capacity" of GSIS varies over 24 hours and contributes significantly to diurnal variations in glucose tolerance (Polonsky et al., 1988a, Polonsky et al., 1988b, Delattre et al., 1999, Picinato et al., 2002). These daily rhythms of GSIS are highly robust and persist in islets isolated from rodent models (Delattre et al., 1999, Picinato et al., 2002), suggesting that an endogenous diurnal metabolic regulator in islets controls the temporal capacity of GSIS and ultimately glucose tolerance; however, the intrinsic metabolic regulators that control daily fluctuations in GSIS capacity and glucose tolerance have not yet been identified. Here, we have demonstrated in synchronized MIN6 cells and isolated islets that *Ucp2* mRNA displays a rhythmic and predictable expression pattern required for the temporal control of GSIS capacity and glucose tolerance over 24 hours, suggesting that UCP2 is an important component of the intrinsic metabolic regulator that controls daily fluctuations of GSIS. However, the rhythms in *Ucp2* mRNA changes did not align with perfectly with changes in insulin secretion capacities. For example, a significant increase in *Ucp2* mRNA expression observed at ZT12 in **[Figure 4.1A]** does not align with suppression in insulin secretion capacities at the same time point **[Figure 4.2A].**

While this study demonstrates that *Ucp2* expression is dynamic in β-cells, it is not currently clear what drives this rhythmic expression. Recent studies have demonstrated that pancreatic islets have remarkably robust endogenous circadian oscillators (Lee et al., 2011, Marcheva et al., 2010, Lee et al., 2013, Sadacca et al., 2011) . Cell autonomous expression of CLOCK/BMAL1 (core transcriptional activator of the circadian machinery) drives 24-hour rhythms of GSIS in isolated wild type islets (Perelis et al., 2015). Interestingly, it has been established that 27% of the β-cell transcriptome displays circadian oscillations (Perelis et al., 2015) and that a number of biological pathways involved in the regulation of insulin secretion and oxidative phosphorylation display enriched expression profiles in the dark/active phase of the daily cycle (Rakshit et al., 2016a). Additionally, the *Ucp2* promoter contains tandem double E-box elements (Medvedev et al., 2002), which are known binding sites for the CLOCK/BMAL1 complex (Perelis et al., 2015); however, chromatin immuno-precipitation (ChIP) of INS1 832/13 cells with anti-BMAL1 antibody and qPCR with primers flanking the putative BMAL1-binding E-Box elements did not show enrichment of *Ucp2* (Lee et al., 2013), suggesting that *Ucp2* may not be a direct transcriptional target of BMAL1. Notably, these studies were performed in an unsynchronized clonal β-cell line and temporal analyses in primary β-cells may yield different results, preventing the exclusion of this possibility. While circadian clock-controlled expression of *Ucp2* is an attractive possibility,

it is also possible that temporal *Ucp2* expression is dictated by daily fluctuations in fasting/feeding rhythms and nutrient availability. Exposure to elevated free fatty acids has been shown to induce upregulation and activation of UCP2 in β-cells (Joseph et al., 2004, Patane et al., 2002, Medvedev et al., 2002, Lameloise et al., 2001), and circulating levels of free fatty acids are significantly increased during fasting. Clearly, further studies are needed to determine what drives the daily cycles of Ucp2 expression in the pancreatic β-cell, but nutritional and circadian cycles are a logical place to start.

At the outset of this study, we hypothesized that rhythmic expression of UCP2 would not only regulate daily cycles of insulin secretion but also daily cycles of glucose tolerance. In a 2011 study (Robson-Doucette et al., 2011), we measured glucose tolerance in *Ins2*-cre and *Ucp2β*KO mice at a single time point (which corresponded with ZT 4 in the current study) and showed impaired glucose tolerance in *Ucp2*βKO mice despite them having significantly elevated GSIS capacity. Furthermore, impaired glucose tolerance observed in light/active phase is not due to differences in insulin sensitivity as demonstrated by a previous study focused on characterization of *Ucp2*βKO animal model. Absence in differences in insulin sensitivity between *Ucp2*βKO and *Ins2*-Cre at ZT 4 also suggests no differences in glucose clearance suggesting of an alternate mechanism for defects in glucose homeostasis. In this earlier study, we further demonstrated that excessive glucagon secretion in *Ucp2*βKO mice, which resulted from aberrant intra-islet reactive oxygen species signaling originating from *Ucp2*-deficient β-cells, was an important contributing factor to glucose intolerance development in these mice. In the current study, we have demonstrated a similar phenomenon where *Ucp2*βKO mice displayed impaired glucose tolerance despite experiencing augmented GSIS capacity, but only in the light phase on the daily cycle. No difference in glucose tolerance was observed in *Ucp2*βKO and *Ins2*-cre in the dark/active phase, a phase when both groups of mice displayed similar GSIS capacities and have low (or no) *Ucp2* expression. These findings suggest that β-cell UCP2 deletion does not chronically impair glucose tolerance but rather selectively contributes to the control of glucose tolerance in the light/inactive phase as the animal enters into an acute period of fasting. Based on our previous studies on the *Ucp2*βKO mouse, it would appear that β-cell UCP2-mediated regulation of glucagon secretion is an important contributor to the control of glucose tolerance and in the light/inactive phase; however, it is not currently clear how rhythmic expression of *Ucp2* in the β-cell affects the 24-hour function of the α cell.

In terms of limitations of this study, we acknowledge that our *Ucp2*βKO mouse was created using the *Ins2* promoter to drive cre recombinase expression. Unfortunately, it has been demonstrated that *Ins2* is also expressed in glucose-sensing regions of the brain (Wicksteed et al., 2010), and we have previously demonstrated minor UCP2 deletion occurs in the hypothalamus of the *Ucp2*βKO mouse (Robson-Doucette et al., 2011). Although the identity, function, and contribution of the *Ins2*-expressing neurons to glucose sensing in the hypothalamus remains unknown, we cannot rule out that UCP2 deletion in the brain may contribute to the results of this study,

particularly the assessment of whole-body glucose tolerance. Notably, we were able to demonstrate that daily rhythms of *Ucp2* expression contribute to daily cycles of GSIS capacity both in islets *ex vivo* as well as in clonal cell lines; models that are removed from central nervous system influence. The use of an *Ins1*-cre model for β-cell specific UCP2 deletion (as *Ins1* is not expressed in the brain (Johnson, 2014) is suggested to validate the glucose tolerance findings in this chapter.

Chapter 5

Identifying the cellular mechanisms underlying UCP2-mediated diurnal insulin secretion capacities

Sections of this chapter has been published in *Molecular Metabolism*, 'Uncoupling protein 2 regulates daily rhythms of insulin secretion capacity in MIN6 cells and isolated islets from male mice". Nivedita Seshadri, Michael E. Jonasson, Kristin L. Hunt, Bo Xiang, Steven Cooper, Michael B. Wheeler, Vernon W. Dolinsky and Christine A. Doucette. Molecular Metabolism. 2017.6(7):760-769

Nivedita Seshadri performed all the experiments outlined in this section of the thesis.

5.1 Introduction

5.1.1 Overall Rationale

In chapter 4, we established that the expression of *Ucp2* in synchronized MIN6 cells and islets isolated from *Ins2*-Cre is dynamic and repetitive, consisting of low, and high alternating patterns over 24hours. The expression pattern of *Ucp2* is inversely proportional to the rhythms of insulin secretion capacity. Furthermore, using *Ucp2*βKO mice and pharmacological inhibition of UCP2 in synchronized MIN6 cells and islets isolated from C57BL6 mice, we were able to demonstrate that insulin secretion capacity over 24 hours is regulated by rhythmic *Ucp2*/UCP2 expression and activity. In this chapter, we will focus on defining the cellular mechanisms by which UCP2 regulates daily capacities of insulin secretion. More specifically, we will examine *Ucp2*-mediated impact on daily cycles of glucose-stimulated ATP production (an important triggering molecule of GSIS), daily cycles of glucose-stimulated ROS production (an important amplifying signal of GSIS), and daily cycles of glucose and fatty acid oxidation capacities.

5.1.2 UCP2-Mediated Regulation of ATP Production in the β-cell.

As stated in section 1.3.1, ATP is a central triggering molecule for GSIS. Given its potential biochemical role as a mitochondrional uncoupler, the discovery of UCP2 led many researchers to explore the impact of UCP2 on ATP production in the β-cell. Initial studies used models of overexpression of the human UCP2 gene in transgenic mice and INS1-E cell lines and showed no impact of UCP2 overexpression on GSIS or the ATP/ADP ratio (Produit-Zengaffinen et al., 2007, Li et al., 2001), while other groups used adenoviral-mediated overexpression of UCP2 in rat islets and showed impairments in GSIS with concomitant decreases in the ATP/ADP ratio (Chan et al., 2001, Sesti et al., 2003). Conversely, islets isolated from whole-body UCP2 knockout mouse models (Zhang et al. 2001; Joseph et al. 2002; Lee et al.2009*)* or inhibition of UCP2 in islets using pharmacological agents like genipin (Zhang et al. 2006) demonstrated that depletion of UCP2 or inhibition of UCP2 activity improved GSIS via increased ATP production. While many studies demonstrate this inverse relationship between UCP2 levels and ATP production (Joseph et al., 2002, Zhang et al., 2001, Wang et al., 2016, Chan et al., 1999), some studies show no impact of UCP2 on ATP (Robson-Doucette et al., 2011, Bouillaud, 2009, Couplan et al., 2002). Importantly, none of these studies have examined the impact of diurnal changes in UCP2 expression on ATP production and the discrepant results in the literature may be the result of time-of-day differences in experimentation. To better understand the mechanism by which diurnal UCP2 expression regulates diurnal GSIS capacity, here, I will explore how diurnal changes in UCP2 expression influence ATP production and ultimately diurnal GSIS patterns.

5.1.3 UCP2-mediated regulation of ROS production in the β-cell

β-cells have inherently low expression levels of antioxidant enzymes (e.g., catalase and glutathione peroxidase; approximately 5% of liver levels) but slightly higher levels of superoxide dismutases (~30% of liver levels; (Tiedge et al., 1997). A relatively higher amount of SOD enzymes could aid in converting the highly reactive superoxides to less reactive hydrogen peroxides, which have been shown to act as secondary messengers in orchestrating important physiological functions in many cell types (Rhee, 2006). Some researchers have postulated that the relatively low level of antioxidants in the β-cell allows for the generation of important ROS signals that, interestingly, have been shown to be amplification signals of GSIS (Maechler et al., 1999, Pi et al., 2007). Numerous studies have demonstrated a regulatory role for UCP2 in the control of mitochondrial-derived ROS production (Echtay et al., 2002, Arsenijevic et al., 2000, Pi and Collins, 2010, Brand and Esteves, 2005) and have labeled UCP2 as an "antioxidant' that plays an important role in protecting β-cell function, integrity and preventing oxidative stress-induced cellular damage (Evans et al., 2003, Droge, 2002). In line with above statement, it is important to note that most studies that have examined the role of UCP2 in ROS regulation have done so in loss-of-function or overexpression models or supraphysiological models where UCP2 is chronically upregulated.(Lee et al., 2009, Robson-Doucette et al., 2011, Negre-Salvayre et al., 1997). More importantly, studies show a plausible impact of UCP2-mediated ROS regulation on insulin secretion capacities when isolated islets are incubated with pro-oxidant and antioxidants; however, whether the rhythms of UCP2/*Ucp2* expression and activity regulate ROS production on a diurnal basis and, in turn, regulate cycles of GSIS capacities over 24 hours remains unknown.

5.1.4 UCP2-Mediated Regulation of Mitochondrial Fuel Oxidation

In 2007, Pecquer et. al., demonstrated that UCP2 contributes to the control of mitochondrial substrate utilization such that mouse embryonic cells isolated from *Ucp2*$^{-/-}$ mouse exhibited a higher responsiveness to glucose, which increased proliferation. Additionally, CHOKI cells (an ovarian cell line) overexpressing *Ucp2* displayed lower dependency on glucose and a lower proliferation rate. As suggested in section 1.4.3, UCP2 also demonstrates a potential functional role as a fatty acid transporter, promoting fatty acid entry into the mitochondria. Therefore, in the absence of *Ucp2*, fatty acid oxidation is reduced and dependency on glucose metabolism is increased; thus, highlighting a potential role of UCP2 in control of metabolic fuel selection (Pecqueur et al., 2008, Parton et al., 2007, Nedergaard and Cannon, 2003). Importantly, fatty acids are potent activators of UCP2-mediated uncoupling activity and expression (Lameloise et al., 2001) as demonstrated by studies in insulinoma cells and rat pancreatic β-cells (Li et al., 2002), suggesting that during fasting, the elevation of fatty acids may promote greater UCP2 activity, resulting in greater fatty acid oxidation and a concomitant suppression in glucose oxidation; however, this has not yet been examined in β-cells over natural 24 hours cycles.

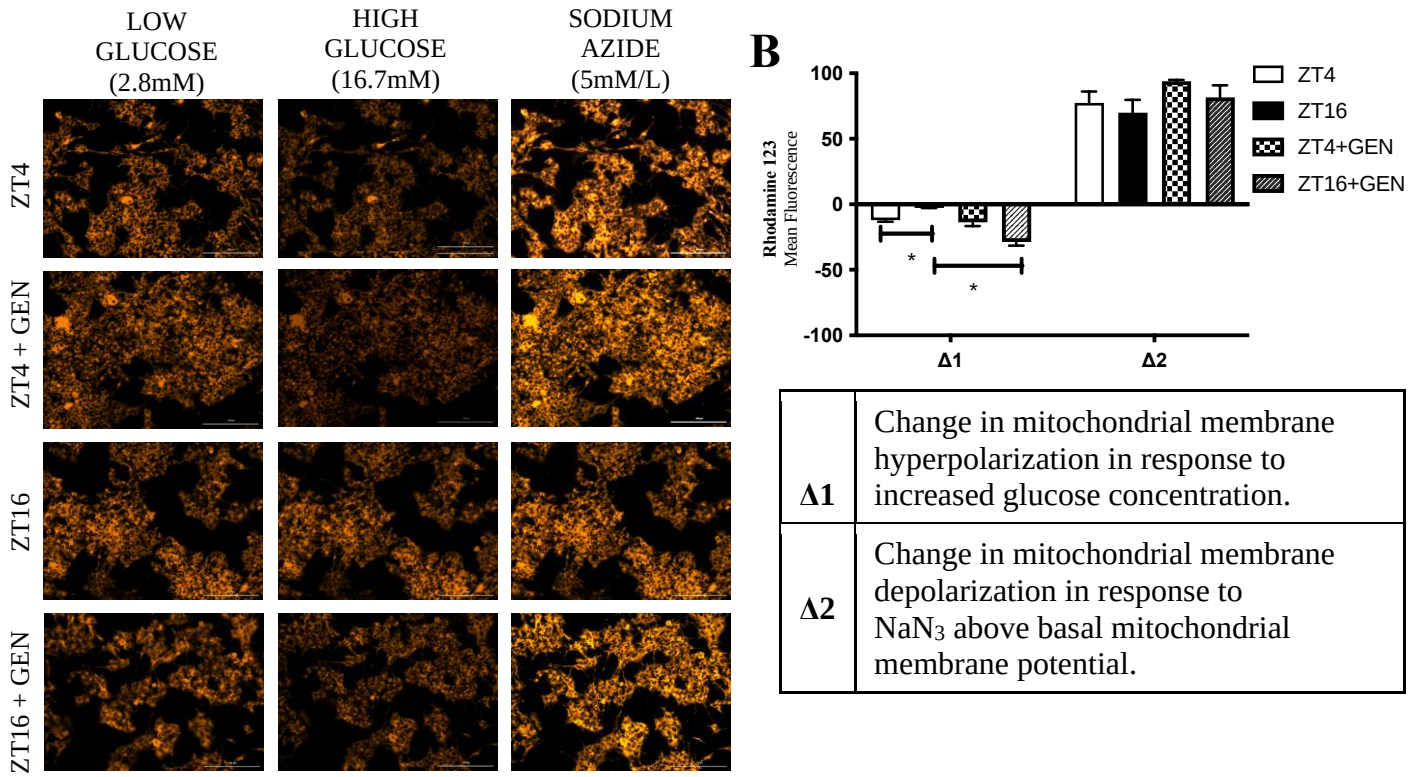
5.2 Materials and methods

Refer to section 3. See specifically sections 3.31, 3.10, 3.11, 3.12, 3.13, 3.16, 3.17 and 3.18.

5.3 Results

5.3.1 Rhythmic *Ucp2* mRNA Expression Translates into Diurnal Changes in UCP2 Activity Over 24hours.

In Chapter 4, we established that *Ucp2* mRNA expression is rhythmic and diurnal over 24 hours; however, changes in mRNA expression do not necessarily translate into changes in activity. Unfortunately, there are no established methods to directly and accurately measure UCP2 activity, so changes in mitochondrial membrane potential ($\Delta\Psi_M$) are commonly assessed as a surrogate measure of mitochondrial coupling (i.e., reduced mitochondrial uncoupling translates to more negative $\Delta\Psi_M$ while greater mitochondrial uncoupling translates in a less negative $\Delta\Psi_M$). Application of a UCP2 inhibitor (genipin) to such experiments allows for the assessment of UCP2-mediated changes in mitochondrial membrane potential (and hence UCP2-mediated uncoupling). Synchronized MIN6 cells at ZT 4 and ZT 16 were stained with Rhodamine 123, a membrane-permeable dye which undergoes quenching upon hyperpolarization (i.e., when the inner mitochondrial membrane potential becomes more negative) and thereby loses fluorescence intensity. At ZT 16, a time point when the endogenous expression of *Ucp2* is high **[Figures 4.1A and B],** we observed a significant reduction in glucose-induced mitochondrial membrane hyperpolarization, (calculated by the change in Rhodamine 123 fluorescence that occurs when glucose is raised from 2.8 mM (low) to 16.7mM (high) glucose) compared to ZT 4 when *Ucp2* mRNA expression is low **[Figures 4.1A and B**]. This suggests that at ZT 4, the mitochondrial membrane is more coupled (i.e., experiences greater hyperpolarization) compared to ZT 16 when *Ucp2* expression is elevated. Importantly, no difference was observed at ZT 16 or ZT 4 when the mitochondrial membrane was completely depolarized using sodium azide (NaN_3). Application of genipin to inhibit UCP2 activity at ZT 16, recovered glucose-induced hyperpolarization to a level similar to ZT 4 **[Figures 5.1A and B]**, when *Ucp2* expression is endogenously low [**Figures 4.1A and B**]. Collectively, these experiments demonstrate there are diurnal changes in mitochondrial coupling that occur between ZT 4 and ZT 16 and that these diurnal changes in mitochondrial coupling are regulated by UCP2 activity. Additionally, these studies suggest that changes in *Ucp2* mRNA expression translation into changes in UCP2-mediated mitochondrial uncoupling activity.



Δ1	Change in mitochondrial membrane hyperpolarization in response to increased glucose concentration.
Δ2	Change in mitochondrial membrane depolarization in response to NaN_3 above basal mitochondrial membrane potential.

Figure 5.1: Assessment of mitochondrial membrane potential at ZT 4 and ZT 16 as a surrogate measure of UCP2 activity. Synchronized MIN6 cells were treated with 50μM genipin for 1 hour prior to incubation with 5mM Rhodamine 123 or vehicle (70% ethanol) for the untreated cells. **[A]** Representative fluorescent images of MIN6 cells at ZT4 and ZT16 pre-treated with genipin or vehicle; and **[B]** Calculated changes in mean ± SEM fluorescence intensity per area for each condition. The Table summarizes the calculation done to quantify changes for Δ1 and Δ2. N = 5. *p < 0.05. Two-way ANOVA followed by multiple comparison.

5.3.2 Rhythmic UCP2 Activity Regulates Diurnal Insulin Secretion Capacity Via Fine-tuning ATP Content in a Time-of-Day Manner

A consequence of increased UCP2 activity is potentially reduced ATP production, which is an important triggering molecular for GSIS. Currently, the contribution of UCP2 in the β-cell to the control of mitochondrial ATP remains controversial. Some groups have demonstrated an effect of β-cell UCP2 manipulation on ATP production (Chan et al., 2001, Zhang et al., 2001, Joseph et al., 2002, Lee et al., 2011) while others show no effect (Robson-Doucette et al., 2011, Van Cauter et al., 1991). Importantly, all prior studies have examined the impact of UCP2 on ATP production in the β-cell either in unsynchronized systems or at single, undocumented (and likely different) times of the day. Given the diurnal expression of *Ucp2*, it is necessary to examine the impact of UCP2 on ATP levels at various times of the day. Here, we measured glucose-stimulated ATP content in both synchronized MIN6 cells **[FIGURE 5.2A]** and islets isolated from C57BL6 mice [**FIGURE 5.2B**] at key time

points, ZT 4 and ZT 16, with and without genipin to determine the impact of UCP2. A significant increase in glucose-stimulated ATP content was observed at ZT 4, which is when maximal GSIS capacity occurs. Conversely, at ZT 16 (when the capacity of GSIS is supressed), a significant reduction in glucose-stimulated ATP content was observed. Application of genipin to inhibit UCP2 activity, had no impact on glucose-induced ATP content at ZT 4, suggesting no available target for genipin at this time point (i.e., endogenously low UCP2 activity), but reversed the reduction in ATP content observed at ZT 16 **[Figure 5.2A]**. Similar results were seen in islets isolated from C57BL6 mice at 10am (light/inactive phase) and 10pm (dark/active phase) **[Figure 5.2B]**. Collectively, these findings demonstrate that UCP2 contributes to the regulation of glucose-induced ATP production in a temporal manner, which is an important regulatory signal for GSIS and may represent an important part of the mechanism that regulates diurnal insulin secretion capacity and glucose tolerance.

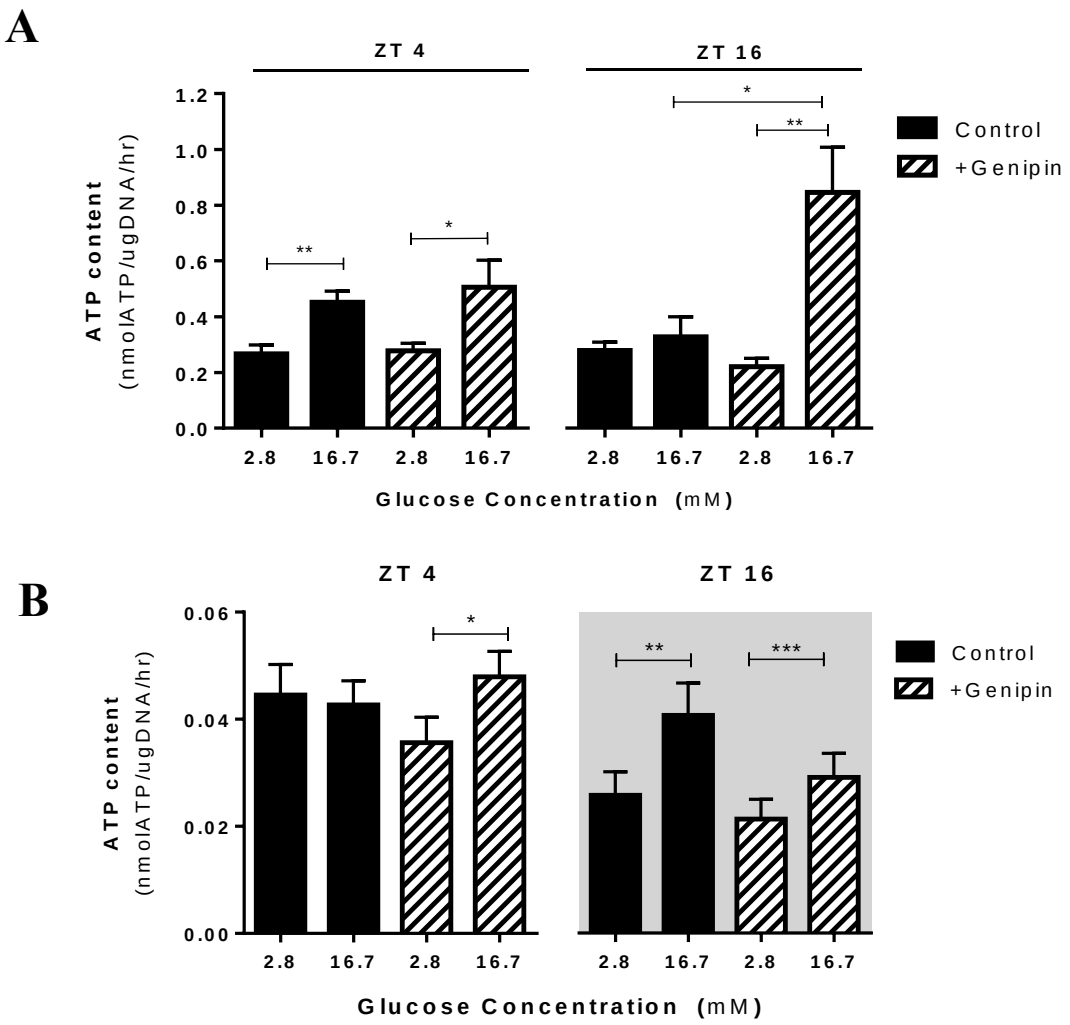


Figure 5.2: Daily Rhythms of UCP2 Activity Control the Temporal Capacity of Glucose-induced ATP Content in MIN6 Cells and Isolated Islets. [**A]** Measurement of ATP content in MIN6 cells after exposure to low (2.8 mM) and high (16.7 mM) glucose concentrations. Glucose-induced ATP content was impaired at

ZT 16 compared to ZT 4. Application of genipin (50µM, 1 h before assay) prevented the impairment of glucose-induced ATP content at ZT 16. Date are Mean ± SEM. N=6-12 . **[B]** Measurement of ATP content in islets isolated from WT C57BL6 mice at ZT 4 (10am) and ZT 16 (10 pm). Application of genipin (50 µM, 1 h before assay) prevented ATP content suppression at ZT 4 but had no impact at ZT 16. N =12-18 mice per time point. *p < 0.05; **p < 0.01; ***p < 0.001. Date are Mean ± SEM. Two-way ANOVA with multiple comparisons.

5.3.3 Rhythmic UCP2 activity regulates dynamic and diurnal changes in ROS production over 24 hours.

Next, we sought to determine whether UCP2 mediates intracellular ROS levels across 24 hours, contributing to the control of diurnal rhythms of GSIS capacity. First, we measured intracellular levels of ROS, specifically H_2O_2 and O_2^-, using cell-permeable fluorescent dyes, CM-H_2-DCFDA and MitoSOX, respectively, in synchronized MIN6 cells at ZT4 and ZT16. Genipin treatment was included to determine how these ROS signals were influenced by UCP2 activity. At ZT 16, both cellular H_2O_2 and O_2^- levels were significantly lower compared to ZT 4 **[Figure 5.3A and B]**, demonstrating that ROS levels are not consistent in the healthy β-cell over 24 hours and that there is diurnal fluctuation. Notably, ROS signals have been implicated as important GSIS-amplifying signals and ROS signals appear to be highest at ZT 4, when GSIS is most robust, which is explored further below. Importantly, application of genipin to inhibit UCP2 had no impact on ROS levels (either H_2O_2 and O_2^-) at ZT 4, but significantly elevated ROS at ZT 16 **[Figure 5.3A and B]**, further demonstrating that diurnal changes in UCP2 activity are required for the regulation of these dynamic ROS signals.

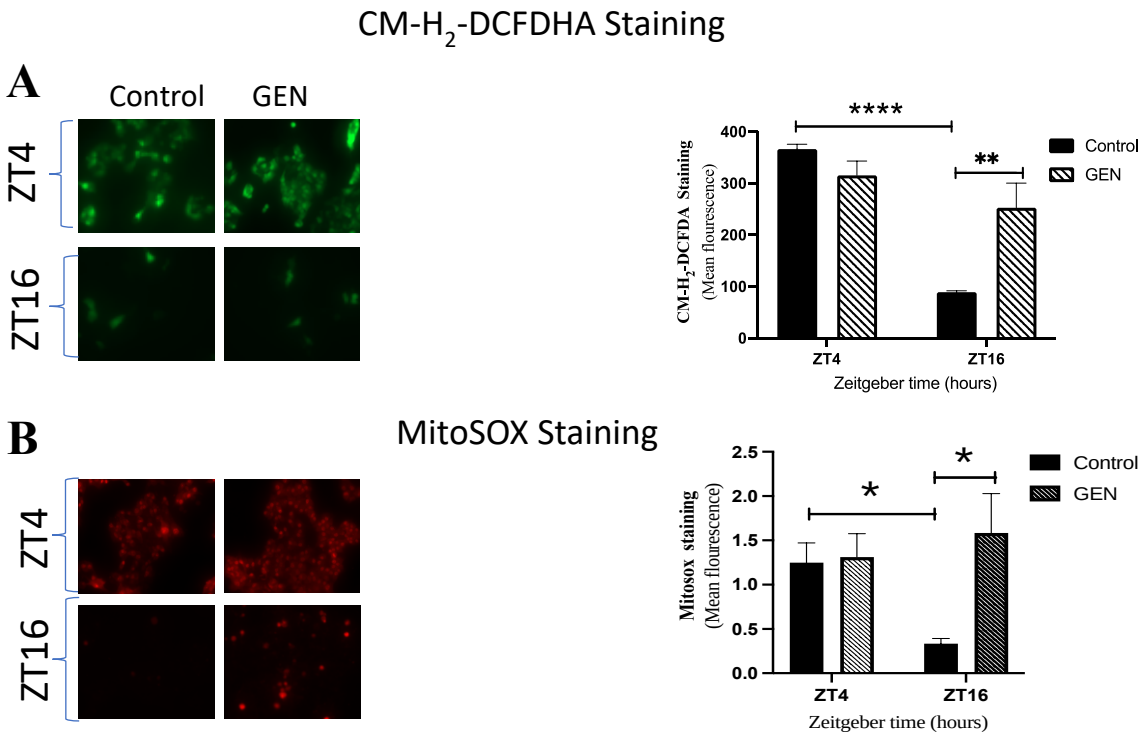


Figure 5.3: Daily Rhythms of UCP2 Activity Control Temporal Changes in ROS production in MIN6 cells. Synchronized MIN6 cells were treated with either vehicle or genipin (GEN) at ZT4 and ZT16 and stained

with **[A]** CM-H_2-DCFDHA and **[B]** Mitosox (ROS indicator) and relative fluorescence was quantified. N= 4. **p < 0.05; **p < 0.01; ****p < 0.0001*. Date are Mean ± SEM Two-way ANOVA with multiple comparisons.

5.3.4 UCP2-mediated Changes in ROS Signals are Essential for Maintenance of Diurnal Patterns of GSIS

In the section above, we demonstrated that UCP2 contributes to the regulation of alternating levels of low and high ROS production over a 24-hour period. To assess if these changes in UCP2-mediated ROS levels were a contributing signal to diurnal GSIS capacity, we measured GSIS at ZT 4 and 16 in synchronized MIN6 cells, but also manipulated these ROS signals using both pro- and antioxidant treatments, diethyl maleate (DEM) and N-acetyl L-cysteine (NAC), respectively. First, we demonstrated that DEM and NAC treatment alone impacted ROS levels in the expected manner. At ZT 4, a timepoint when ROS levels are high, NAC effectively reduced both species of ROS **[Figure 5.4 A and B].** At ZT 16, a timepoint when ROS levels are low, DEM effectively increased both species of ROS **[Figure 5.4 A and B].** Notably, NAC had little impact on ROS levels ZT 16 compared to control (black bars), likely because ROS levels were already relatively low at this time point, collectively demonstrating the effectiveness of these pro-and antioxidant treatments on ROS signals over 24 hours.

To determine how these ROS signals contribute to GSIS capacity, GSIS assays were performed in synchronized MIN6 cells in the presence of NAC or DEM to manipulate these signals. At ZT 4, scavenging ROS with NAC prevented maximal insulin secretion capacity **[FIGURE 5.4C],** suggesting that ROS signaling plays an important role in promoting maximal insulin secretion at this time point. Conversely, application of DEM to increase endogenous ROS levels at ZT 16 elevated the suppressed insulin secretion capacity at ZT 16 **[Figure 5.4D].** These results demonstrate that the variations in ROS signals over 24 hours are required for the temporal control of GSIS capacity. To determine if UCP2 is essential to the regulation of these diurnal ROS signals, cells were pretreated with genipin and GSIS measured at ZT 4 and 16. As expected, genipin restored impaired GSIS at ZT 16, however, the addition of NAC to genipin-treated cells (i.e. scavenging the ROS signal that is generated when UCP2 is inhibited) prevented the recovery of GSIS, emphasizing that UCP2-mediated ROS signals are imperative for the control diurnal GSIS.

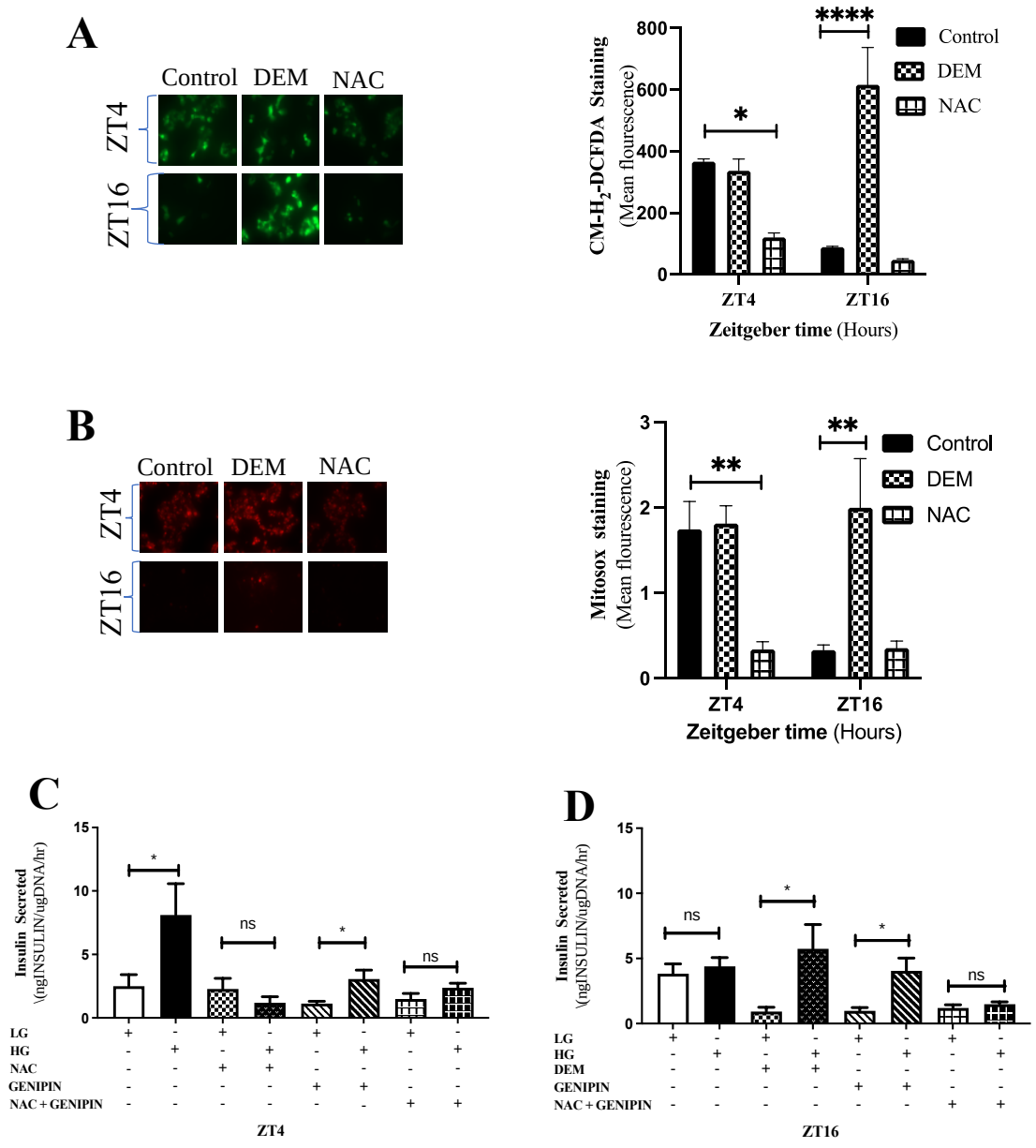


Figure 5.4: Daily Rhythms of UCP2 Activity Control the Temporal Capacity of Insulin Secretion Via Fine-tuning ROS Signals in MIN6 cells. MIN6 synchronized cells were treated with either a pro-oxidant (DEM), antioxidant (NAC) or Genipin (GEN) at ZT4 and ZT16 and stained with [**A]** CM-H2-DCFDHA and [**B]** Mitosox and relative fluorescence was quantified. **[C]** Measurement of insulin secretion capacities in MIN6 cells after exposure to low (2.8 mM) glucose, high (16.7 mM) glucose, NAC and GEN (50µM, 1 h before) at ZT4. Application of NAC suppressed insulin secretion capacities while GEN had no effect. N=4-5.**[D]** Insulin secretion capacities were suppressed at ZT16 compared to ZT4. Application of Genipin (50µM, 1 h before assay) or DEM prevented the impairment of GSIS at ZT 16. Co-treatment of cells with NAC and Genipin suppressed insulin secretion capacities at ZT16. Date are Mean ± SEM. N=4-5. *$p < 0.05$; **$p < 0.01$; ****$p < 0.0001$. Two-way ANOVA followed by multiple comparisons.

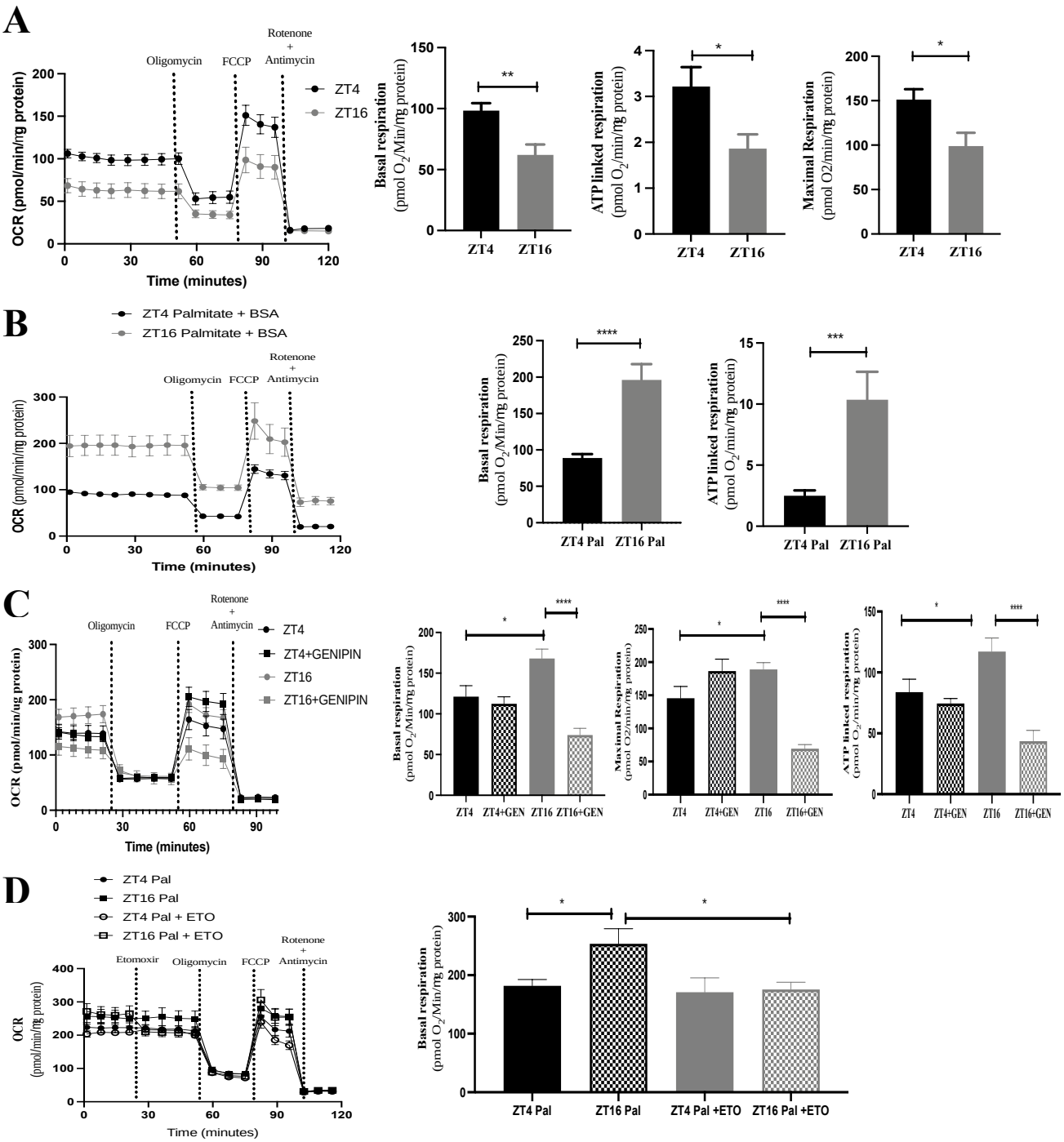
5.3.5 Rhythms of *Ucp2* mRNA expression align with fuel oxidation capacities over 24 hours.

In Section 5.1.3 we discuss in detail the role of UCP2 in fuel oxidation such that elevations in UCP2 expression and activity increase fatty acid oxidation and suppress glucose oxidation. Given the rhythmic expression of *Ucp2* established in chapter 4, we wanted to examine if the reduced *Ucp2* mRNA expression observed at ZT4 **[as shown in figure 4.1A]** was associated with increased glucose oxidation. To address this, we measured both glucose and fatty acid oxidation capacities in synchronized cells MIN6 cells at ZT4 and ZT16 using the Seahorse XF-24 analyzer. AT ZT 4, synchronized MIN6 cells displayed higher rates of basal glucose oxidation compared to ZT16 [**Figure 5.5A**], which aligns with greater GSIS capacity at this time point **[Figure 4.2A**]. Additionally, maximal respiration and ATP-linked respiration were also increased at ZT 4 compared to ZT16 **[Figure 5.5A]**. In support of the cells experiencing increased glucose oxidation at ZT 4, we also observed significantly elevated mRNA expression of *Slc2a2* (GLUT-2 glucose transporter) and *Gck (*glucokinase; the rate limiting step in glycolysis) compared to ZT 16 [**Figure 5.5 F and G**]. Significantly lower expression of *Ldha* mRNA was also found at ZT 4 compared to ZT 16 **[Figure 5.5 I],** an enzyme that is responsible for a bidirectional conversion of pyruvate to lactate (explored further in chapter 6).

Whole cell assessments of Oxygen Consumption Rate (OCR) in the presence of glucose, like those performed in the previous section, give us an indication of how well the complete glucose oxidation pathway (glycolysis, TCA cycle, mitochondrial electron transport chain) is functioning. The Seahorse flux analyzer also measures extracellular acidification rates (ECAR) which gives a more direct measurement of the glycolytic pathway alone. To assess if there are differences in upstream glycolysis at ZT 4 and ZT 16 in our synchronized MIN6 cells, we performed the Seahorse glycolytic stress test, which demonstrated that at ZT 4, glycolytic capacity is significantly elevated **[Figure 5.5E]** compared to ZT 16. This increase in glycolytic capacity is likely the result of elevated expression of glycolytic genes at this time point (i.e. *Gck*) and suggests that multiple pathways inside the glucose oxidation pathways contribute to control of diurnal GSIS capacity, not just UCP2 in the mitochondrial electron transport chain.

Concomitantly, when synchronized MIN6 cells were provided fatty acids as a fuel rather than glucose, we observed higher rates of fatty oxidation at ZT16 (a time-point when *Ucp2* expression is elevated; Fig 4.1) in control cells when compared to ZT4 **[Figure 5.5B],** which also correlated to suppressed insulin secretion (Fig 4.2A). We also observed higher basal and ATP-linked respiration in the presences of fatty acids. In support of an increased fatty acid oxidation capacity at ZT 16 over ZT 4, we also observed 2-fold higher expression of *Cpt-1a* mRNA at ZT 16, which encodes the rate-limiting enzyme in fatty acid β oxidation **[Figure 5.5H]**. Furthermore, when we inhibited CPT-1a using etomoxir and measured rates of fatty acid oxidation, we observed lower basal respiration at ZT 4 when compared to ZT16 control cells (when Cpt-1a was expressed**) [Figure 5.5D].**

To determine if UCP2 directly contributes to the increased fatty acid oxidation observed at ZT 16, we inhibited UCP2 using genipin in the presence of fatty acids in synchronized MIN6 cells and subsequently measured OCR. Under these conditions, we observed lower basal, ATP-linked and maximal rates of oxygen consumption **[Figure 5.5C]**, suggesting that elevated UCP2 activity at ZT 16 is essential for increased fatty acid oxidation at this time of day, which also supports previous postulated roles for UCP2 as a mediator of fatty acid oxidation.



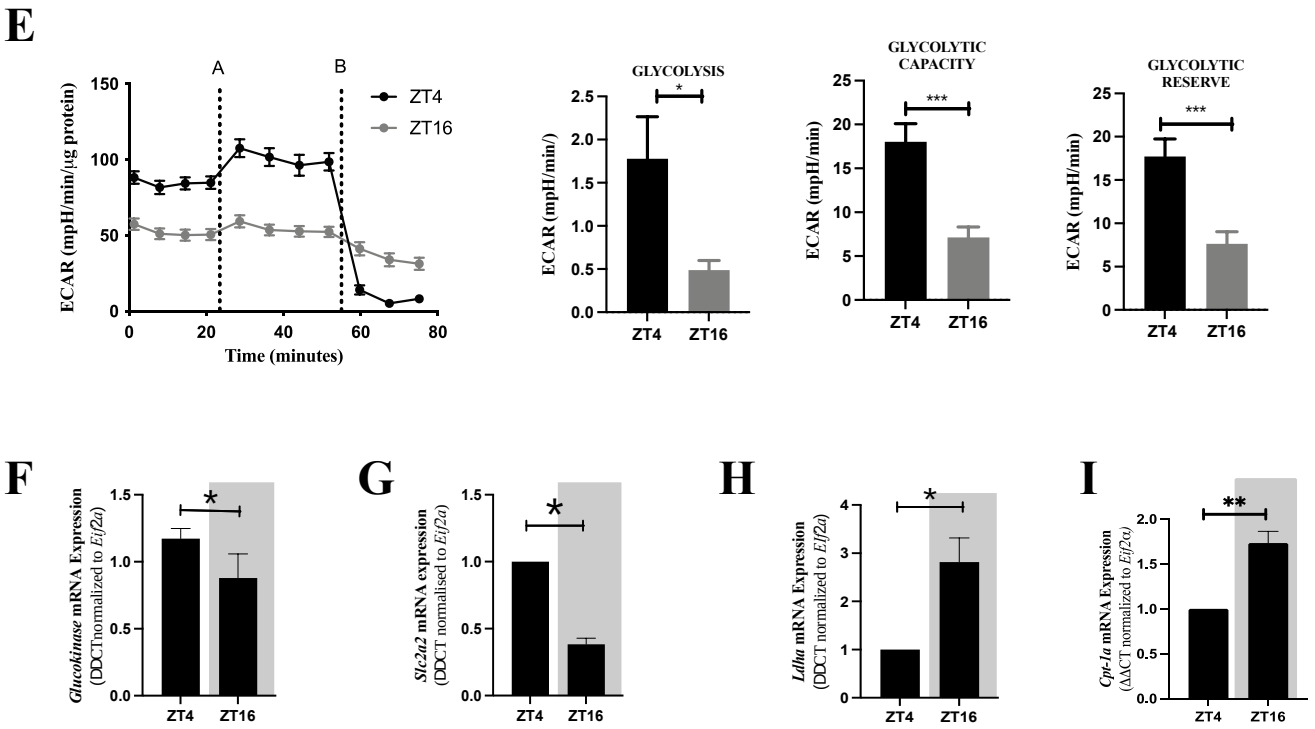


Figure 5.5: Daily rhythms of fuel oxidation capacities is associated temporal capacities in glucose stimulated insulin secretion in MIN6 cells. MIN6 synchronized cells were treated with Oligomycin, FCCP, Rotenone, Antimycin in the presence of **[A]** 16.7mM Glucose and **[B]** 0.25mM Palmitate conjugated to BSA **[C]** 0.25mM Palmitate conjugated to BSA with and without Genipin **[D]** 0.25mM Palmitate conjugated to BSA with and without Etomoxir **[E]** Glycolysis stress test was performed on synchronized MIN-6 cells at ZT4 and ZT16 in the presence of 2-DG. Diurnal mRNA expression of **[F]** *Slc2a2* (Glut2**) [G]** *Glucokinase* **[H]** *Ldha* and **[I]** *Cpt-1a*. Date are Mean ± SEM. N= 4-5. *p < 0.05; **p < 0.001. Two-way ANOVA followed by multiple comparisons.

5.3.6 Rhythmic expression of genes regulating ROS levels in synchronized MIN6 cells.

As mentioned in the introduction, β-cells have low levels of antioxidants. Despite the relatively low levels of expression in β-cells, these genes were upregulated in *Ucp2*βKO mouse models (Robson-Doucette et al., 2011). Based on the rhythms in ROS production and *Ucp2* expression in β-cells over 24 hours, we wanted to measure expression of antioxidants genes such superoxide dismutase (*Sod2*) **[Figure 5.6A]** and glutathione peroxidase (*Gpx-1*) **[FIGURE 5.6B].** We found diurnal expression of *Sod2* and *Gpx-1* over 24 hours such that expression of both these genes were significantly higher at ZT 16 than ZT 4.

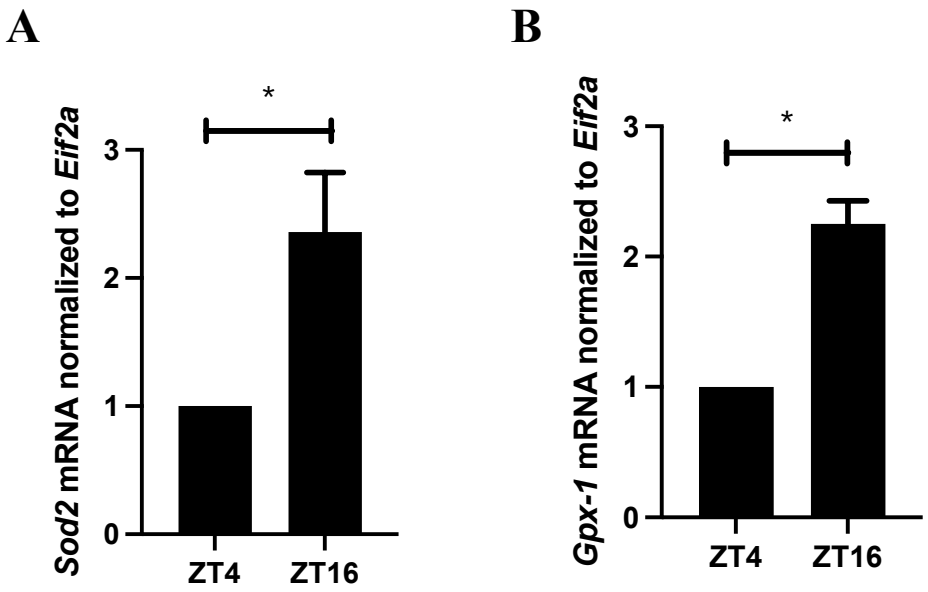


Figure 5.6: Rhythmic expression of genes regulating ROS levels in synchronized MIN6 cells. Diurnal mRNA expression of **[A]** Superoxide Dismutase (*SOD2*) **[B]** Glutathione peroxidase (*Gpx-1*) normalized to both *Eif2a* and ZT4. Date are Mean ± SEM. N= 4-5. *$p < 0.05$; **$p < 0.001$. Student t-test.

5.4 Discussion

Robust diurnal rhythms in insulin secretion exist both *in vivo* and in islets isolated from mouse models and human donors, which contribute to the regulation of diurnal variations in glucose tolerance and glucose homeostasis (Peschke and Peschke, 1998, Delattre et al., 1999, Picinato et al., 2002, Seshadri and Doucette, 2021, Perelis et al., 2015, Petrenko et al., 2017, Saini et al., 2016). The inherent variation in insulin secretion capacity over 24 hours has raised compelling questions about how these rhythms are regulated, warranting further understanding of the underlying molecular and metabolic events that align insulin output to the physiological status of the body. In chapter 4, we identified UCP2 as a part of the endogenous regulator required for diurnal control of insulin secretion and glucose tolerance. In this chapter, we used an *in vitro* model of synchronized MIN6 cells and islets isolated from C57BL6 mice to investigate the role of UCP2 in regulating diurnal rhythms of insulin secretion capacities. To this effect we measured ATP content (an insulin secretion triggering molecule), ROS production (an insulin secretion amplification signal), and glucose vs fatty acid oxidation rates at ZT 4 and ZT 16. The results from this study provide evidence that UCP2 mediates the temporal capacity of ATP and ROS production as well as contributes to the determination of mitochondrial fuel selection, and therefore responsiveness to glucose. Combined, these UCP2-mediated processes/signals ultimately dictate the capacity of insulin secretion in a time-of-day dependant manner.

Firstly, we demonstrated that fluctuations in GSIS capacity are associated with UCP2-mediated fluctuations in ATP production, which helps shed some light on current debatable findings in the literature regarding the role of UCP2 in regulating ATP in the β-cell. Some studies have demonstrated that *Ucp2* knockout augments ATP production (Zhang et al., 2001, Joseph et al., 2004), while others demonstrate no impact on ATP (Robson-Doucette et al., 2011, Bouillaud, 2009). Here, we show that the impact of UCP2 on glucose-induced ATP production is dynamic over a 24 h time course, suggesting that previous discrepancies in the literature may relate to time-of-day differences when performing actual assessments.

The role of ROS in regulating insulin secretion in islets of rat and mouse models at isolated time points has been demonstrated in previous studies (Robson-Doucette et al., 2011, Pi et al., 2007, Newsholme et al., 2019, Ivarsson et al., 2005[Leloup, 2009 #957). To be more specific, the role of H_2O_2 in augmenting insulin secretion has been established (Pi et al., 2009, Pi et al., 2007, Morgan et al., 2009). In our study, we show for the first time that ROS production is dynamic over 24 hours in synchronized MIN6 cells such that higher intracellular H_2O_2 and mitochondrial O_2^- is observed at ZT 4 followed by a reduction of both forms of ROS at ZT 16, and that elevated ROS at ZT 4 contributes to augmented GSIS at this timepoint. Further, we demonstrated that at ZT 16, UCP2 activity is required for the suppression of this ROS signal and ultimately GSIS at this time point. This data provides evidence that UCP2-mediated ROS signals contribute to the control of diurnal rhythms in GSIS. Notably, it has been demonstrated that ROS accumulation induces *Ucp2* mRNA expression (Echtay et al., 2002). Therefore, we cannot conclusively state whether the accumulation of ROS species at earlier time points in the cycle (i.e., ZT 4) contribute to the upregulation of *Ucp2* expression and activity at later time points in the cycle (i.e., ZT 16) or whether independent upregulation of *Ucp2* at ZT 16 is responsible for the reduction in ROS species. While we suggest that upregulated *Ucp2* expression at ZT 16 may quench accumulated ROS produced in the later timepoints of the daily cycle, UCP2 may not be the only antioxidant active and contributing to the regulation of ROS signals at ZT16. Importantly, we also observed increased expression of *Sod2* and *Gpx-1* at ZT 16, which may contribute to the control of ROS signals at ZT 16 and prevent their excessive accumulation leading to oxidative stress. Diurnal rhythms in genes coding for both pro- and antioxidant enzymes, such SOD2 and GPX-1, have been previously reported (Xu et al., 2012) and fits with our findings.

Even though the production of ROS is required for the diurnal regulation of GSIS, we also recognize that unchecked ROS production is harmful to β-cells as evidence of accumulated ROS in islets isolated from both mouse models of T2D (Tanaka et al., 2002, Matsuoka et al., 1997) and human studies (Sakuraba et al., 2002) (Elksnis et al., 2019, Evans et al., 2003). These studies emphasize that chronic and unchecked ROS production in models of glucolipotoxicity and T2D impairs insulin secretion in and possible role of UCP2 in controlling ROS production and ultimately insulin secretion capacities.

In addition to diurnal rhythms in ATP and ROS signals, we also demonstrated that UCP2 contributes to diurnal changes in mitochondrial fuel selection such that at ZT 4, the β-cell favours glucose oxidation over fatty acids, whereas at ZT 16, the opposite occurs and fatty acids become the favoured fuel. These findings fit with previous *in vivo* human studies which have shown increased fatty acid oxidation in healthy human subjects in the evening followed by a significant reduction during early morning period (Barter et al., 1971, Carroll and Nestel, 1973). This increase in fat oxidation during the biological night coincides with increased levels of free fatty acids in plasma. Furthermore, studies in islets have shown that free fatty acids are the main substrate for energy production in a low glucose environment (Lytrivi et al., 2020). In this study, we additionally show rhythms in both glucose and fatty acid transporter expression in synchronized MIN6 cells **[Figure 5.5F and I],** which fits with the diurnal pattern of glucose and fatty acid oxidation, respectively. These changes in transporter expression may be a "priming step" in β-cells to prepare for anticipated fuel changes that occur over daily cycles of fasting and feeding. Notably, prior studies have reported diurnal oscillations in *Cpt-1a* mRNA expression, specifically in β-cells (Petrenko et al., 2017), which fits our study.

Previous studies have demonstrated that fatty acids are potent activators of UCP2 activity (Medvedev et al., 2002). Notably, in a low glucose environment or in a fasted state, CPT-1a is activated and allows for fatty acid entry into the mitochondrion. Upon entry into the mitochondrion, fatty acid-mediated activation of UCP2 could contribute to the reduction of ATP and ROS production, and ultimately suppression of GSIS in the fasted state. Interestingly, our data suggests that fatty acid activation of UCP2 is not necessarily responsible for the suppression of GSIS at ZT 16, but rather, UCP2 is directly contributing to fatty acid oxidation directly, as inhibition of UCP2 with genipin prevented fatty acid oxidation at ZT 16 **[Figure 5.5C]**. Previous studies have reported that UCP2 can function as a fatty acid anion transporter (Berardi and Chou, 2014), which supports our findings and demonstrates a potential role for UCP2 in the regulating daily rhythms of GSIS via regulation of diurnal patterns of mitochondrial fuel oxidation. In addition to association with fatty acid oxidation, elevated *Ucp2* expression associates with higher rates of cellular proliferation, which are diminished when *Ucp2* expression is reduced and glucose oxidation is elevated (Pecqueur et al., 2008)). Our expression data of *Ucp2* shows that *Ucp2* goes through a repetitive and alternating cycle of low and high expression every twelve hours over 24 hours which begs the question: does UCP2 serve as a central regulatory point of pathways related to β-cell proliferation and fuel oxidation rates? Understanding the pathways that regulate these important biological functions will be important for a deepened understanding β-cell physiology in health and disease.

While the studies presented in this chapter provide new insight into the mechanisms via which UCP2 regulates insulin secretion, it also provides a peek into UCP2 physiological functions, other than just control of insulin secretion, such as its potential role in β-cell proliferation (Pecqueur et al., 2008), fuel oxidation, and ROS production over 24 hours.

One limitation of this study that should be considered in the interpretation of these results is the use of only *in vitro* models, as these models do not fully recapitulate primary cell physiology. While further studies are warranted in a more physiologically relevant model (mouse or human islets), translation to humans is important, although metabolic pathways are highly conserved, animal models would be a good starting point to provide rationale for study in precious human tissue. Additionally, sex-specific differences for this part of the study cannot be determined. MIN6 cells were initially generated from male mice (Miyazaki et al., 2021), but over time immortalized cells are known to lose their Y-chromosome (Park et al., 2006), as such, sex-specific difference may be observed and should be examined in primary tissues. Finally, although we have performed these studies at two timepoints (ZT 4 and 16) which were the peak and trough observed in both the *Ucp2* expression as well as insulin secretion capacities studies, we acknowledge that ATP, ROS and fuel oxidation capacities may have different peaks and troughs. That said, the examination of these signals at these time points provides strong evidence for their involvement in the control of insulin secretion at the peak and trough time points; however, more detailed time courses should be performed to fully understand these cycles.

Chapter 6

The Role of the β-cell Circadian Clock in Regulating Diurnal Rhythms of UCP2 and Insulin Secretion Capacity

This section contains unpublished data. Under the guidance of Nivedita Seshadri, **Taylor Morriseau** helped with islet isolation for experiments outlined in this chapter. **Manuel Sebastian** performed the immunofluorescence for validating *Bmal1*βKO in islets. **Diana Prince** performed ATP assays and *Ucp2* expression data in isolated islets. All the other experiments were performed by **Nivedita Seshadri.**

6.1 Background and Rationale

6.1.1 Circadian Regulation of *Ucp2*-Mediated Insulin Secretion

In the previous chapters, we demonstrated that *Ucp2* expression and activity is rhythmic over 24 hours and that the rhythmicity of *Ucp2* is required for the regulation of diurnal regulation of GSIS capacity. Moreover, we showed that UCP2 plays a role in regulating and fine-tuning two key signals that regulate GSIS capacity, namely ROS and ATP. The rhythmic nature of UCP2 expression and subsequent downstream GSIS-regulating signals suggest that the endogenous circadian clock may play a role in driving these rhythms.

The circadian timing system is an endogenous timekeeper that aligns external environmental time of day with biological time within cells and tissues. The primary clock, which is entrained by light signals, coordinates behaviour and whole-body physiology with environmental time and is located in the SCN of the hypothalamus. The peripheral tissues also have endogenous circadian oscillators that play an essential role in the regulation of glucose homeostasis and metabolic health. In 2010, Marcheva et. al., determined that pancreatic islets express the core circadian molecular machinery and that mouse models of circadian disruption (Clock$^{\Delta 19}$ and *Bmal1*$^{-/-}$ mice) develop diabetes secondary to impaired insulin secretion. Since then, several other studies have demonstrated an essential role of the islet and β-cell circadian molecular machinery in the regulation of insulin secretion and metabolic health (Marcheva et al., 2010, Lee et al., 2011, Lee et al., 2013, Perelis et al., 2015, Petrenko and Dibner, 2018, Petrenko et al., 2020a, Petrenko et al., 2017, Petrenko et al., 2020b). These oscillators, observed both in islets isolated from *Per2*::Luciferase knock-in reporter mice and islets synchronized *ex vivo* using forskolin, are extremely robust (Petrenko et al., 2017). In whole isolated islets, ~27% of transcripts, including core circadian transcription factors (*Bmal1, Clock, Cry and period*), show high-amplitude oscillatory transcriptional profiles (Perelis et al., 2015); however, in sorted populations of α and β-cells, it was determined that closer to ~60% of transcripts are oscillatory in one or both cell types, likely reflecting different circadian phases in the individual islet cell types that are masked at the whole islet level, but nonetheless demonstrating that β-cells have a high ratio of cycling to non-cycling genes, typically seen in metabolic tissues (Zhang et al., 2014). Not surprisingly, when the circadian machinery is disrupted in mice and rodents using both genetic knockout models or environmental models of circadian dysfunction such, as in constant light or constant darkness, a loss of first phase insulin secretion is observed. It further resulted in the development of hypoinsulinemia-induced hyperglycemia (Lee et al., 2011, Lee et al., 2013, Rudic et al., 2004, Lamia et al., 2008, Sadacca et al., 2011), characteristic of diabetes.

While several studies have characterized the circadian machinery in islets and β-cells, few studies have examined the *mechanistic* connections between oscillations in the circadian machinery and downstream regulation of insulin secretion. While temporal transcriptomic studies have identified a number of potential pathways (e.g., glucose-sensing and secretion pathways, insulin vesicle exocytosis, trafficking, and fusion, cell

cycle and DNA repair) that are circadian-regulated in the β-cell, few have examined the functional impact of these genetic oscillations on regulation of GSIS. As such, further studies are warranted to understand the functional and mechanistic connections between the β-cell circadian oscillator and rhythmic insulin secretion.

6.1.2 Other Molecular Regulators of Diurnal Rhythms of Insulin Secretion

While this thesis is focussed mainly on the role of UCP2 in the diurnal regulation of GSIS, it is unlikely that UCP2 regulates rhythmic GSIS in isolation. Another important metabolic regulator, which has strong consequences for β-cell function, is lactate dehydrogenase (LDH). Despite the wide expression of lactate dehydrogenase (LDH) in the body, pancreatic β-cells express 8-fold lower levels of LDH compared to islet non-β-cells and 122-fold lower levels than found in the liver (Sekine et al., 1994, Bricker et al., 2012, Liang et al., 1996, Hellman and Taljedal, 1967). Zhao et. al., demonstrated that overexpression of *Ldha* impairs GSIS in MIN6 clonal β-cells (Zhao and Rutter, 1998), which has also been reported in other glucose-responsive cell lines, including βHC9 (Zhao and Rutter, 1998, Ainscow et al., 2000, Ishihara et al., 1999). While the above gain-of-function studies have described a negative impact of LDH on GSIS (Rutter et al., 2015, Ainscow et al., 2000, Zhao and Rutter, 1998), other studies that have demonstrated that LDH plays an important role in maturation and development of β-cells (van Arensbergen et al., 2010, Rorsman et al., 1989, Tan et al., 2002, Jacob et al., 1999, Jermendy et al., 2011, Martens et al., 2005, Jacovetti et al., 2015). In line with the above statement, *Ldha* is found at higher expression levels in immature β-cells, which have not yet acquired glucose-responsiveness. Subsequent functional maturation results in repression of LDH, suggesting a potential role for LDH in regulating overall GSIS capacities in the β-cell. Given the repression of LDH in the functionally mature β-cell as well as the role of LDH in diverting carbon from glucose metabolism away from oxidative phosphorylation and into anaerobic pathways, it has been suggested that LDH expression is 'disallowed' in the β-cell such that its active suppression is required in the glucose-responsive β-cell to promote maximal/optimal capacity to secrete insulin (Schuit et al., 2012). Similar to UCP2, the majority of studies that have examined the impact of LDH on the β-cell function were performed using models of chronic overexpression or deletion and the natural changes in LDH expression that occur over 24 hours and consequently, its impact on diurnal GSIS, has not yet been examined. Given its ability to regulate carbon flux into and out of oxidative phosphorylation, we wondered if LDH might play a role in the diurnal regulation of GSIS capacity and that regulation of LDH by the circadian clock may contribute to 24-hour glucose homeostasis. Here, I ***hypothesize*** that in addition to *Ucp2,* the circadian clock drives daily cycles of *Ldh* expression and that a functional β-cell circadian clock is required for the maintenance of these expression rhythms in the β-cell and ultimately diurnal rhythms in GSIS capacity.

6.2 Material and Methods

Refer to Section 3. For this chapter all subsections of the methods were employed.

6.3 Results

6.3.1 *Bmal1* mRNA Expression is Rhythmic in Synchronized MIN6 Cells and Isolated Islets

To demonstrate that our experimental models displayed appropriate circadian rhythms, we measured the expression of *Bmal1*, a core gene of the molecular circadian oscillator, every 4 hours over a 24-hour period. MIN6 cells were synchronized using an established serum starve/shock protocol (Greco et al., 2014) and cells were collected for qPCR. As expected, *Bmal1* mRNA transcript levels displayed a dynamic and rhythmic expression pattern, showing an approximate 12-hour alternating pattern of high and low expression **[Figure 6.1A].** To align our findings with key time points we have examined in previous chapters, I looked specifically at the expression of *Bmal1* at ZT 4 and ZT 16. At ZT 4, *Bmal1* mRNA expression was highest with levels reaching a mean value of 1.4511-fold higher expression than at ZT 0. At ZT 16, *Bmal1* mRNA levels decreased to 0.63390-fold lower expression than ZT 0. Similarly, when *Bmal1* mRNA transcript was measured in islets isolated from control mice (in this case we used the *Ins1*-Cre as these are controls that are used throughout this study) at 10pm and 10am (note: lights are turned on at 6am and off at 6pm and mice are nocturnal), we observed 2.138-fold higher islet *Bmal1* mRNA expression at 10pm (when mice are in the dark and are active) compared to 10am (light/inactive phase) **[FIGURE 6.1B]**, demonstrating appropriate circadian rhythms exist in both our in vitro and in vivo models.

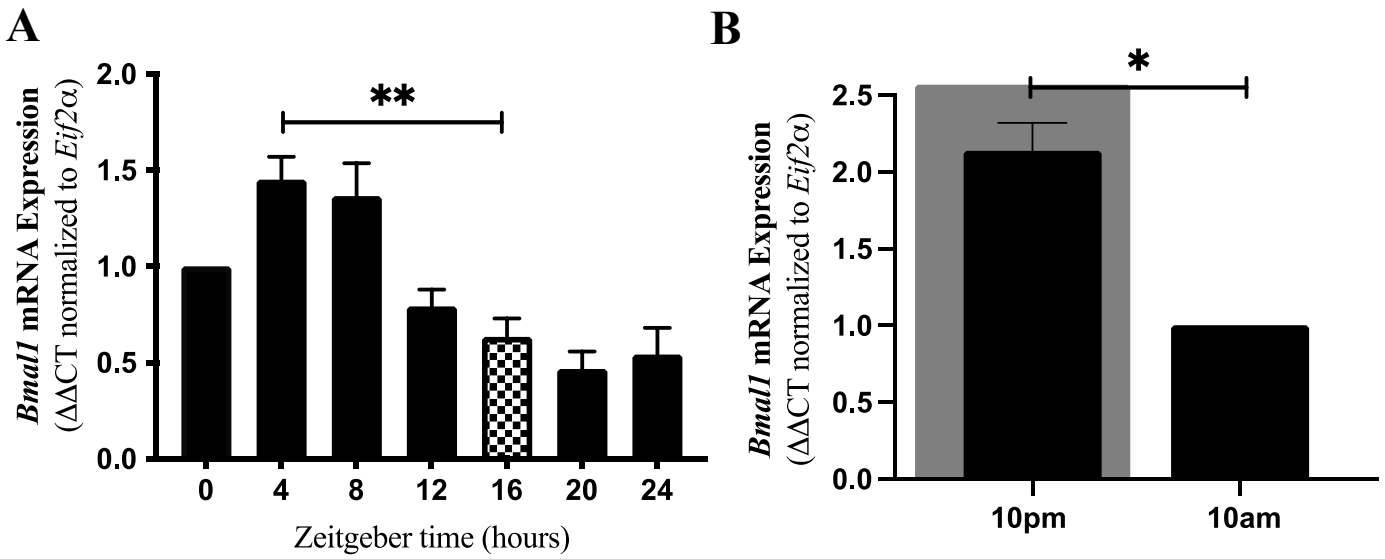


Figure 6.1: Circadian expression pattern of *Bmal1* mRNA in MIN6 cells and isolated islets over 24h. [A] *Bmal1* mRNA expression levels were measured at 4 h intervals over 24 h in synchronized MIN6 cells. *Bmal1* mRNA is expressed relative to *Eif2a* mRNA levels and normalized to mRNA levels at time 0 (immediately after synchronization). N=4-6. **p<0.01**.** P-value represents after statistical analysis by Two tailed student's t-test. **[B]** *Bmal1* expression levels in isolated islets. Islets were isolated from control (*Ins1*-Cre) mice at 10am and 10pm and RNA immediately isolated for qPCR. *Bmal1* mRNA shown is expressed relative to *Eif2a* levels and normalized to *Bmal1* mRNA levels at 10am. Islets were isolated and pooled from 2-3 mice for each N at a particular time point. N=4. *p < 0.05. Date are Mean ± SEM. P value represents statistical analysis by t-test.

6.3.2 Creation and Validation of β-cell-Specific Circadian-Deficient Models

In vitro model: *Bmal1*siRNA in MIN6 cells: We used siRNA specific to *Bmal1* to knockdown *Bmal1* in MIN6 clonal β-cells. We measured *Bmal1* mRNA and protein expression in *Bmal1*siRNA-transfected cells and compared this to MIN6 cells that were transfected with negative control (scramble siRNA) ("control"). Using this method, we consistently achieved 50-70% reduction of Bmal1 both at the transcript and protein levels in our cells transfected with *Bmal1*siRNA compared to control cells **[Figure 6.2A and B].**

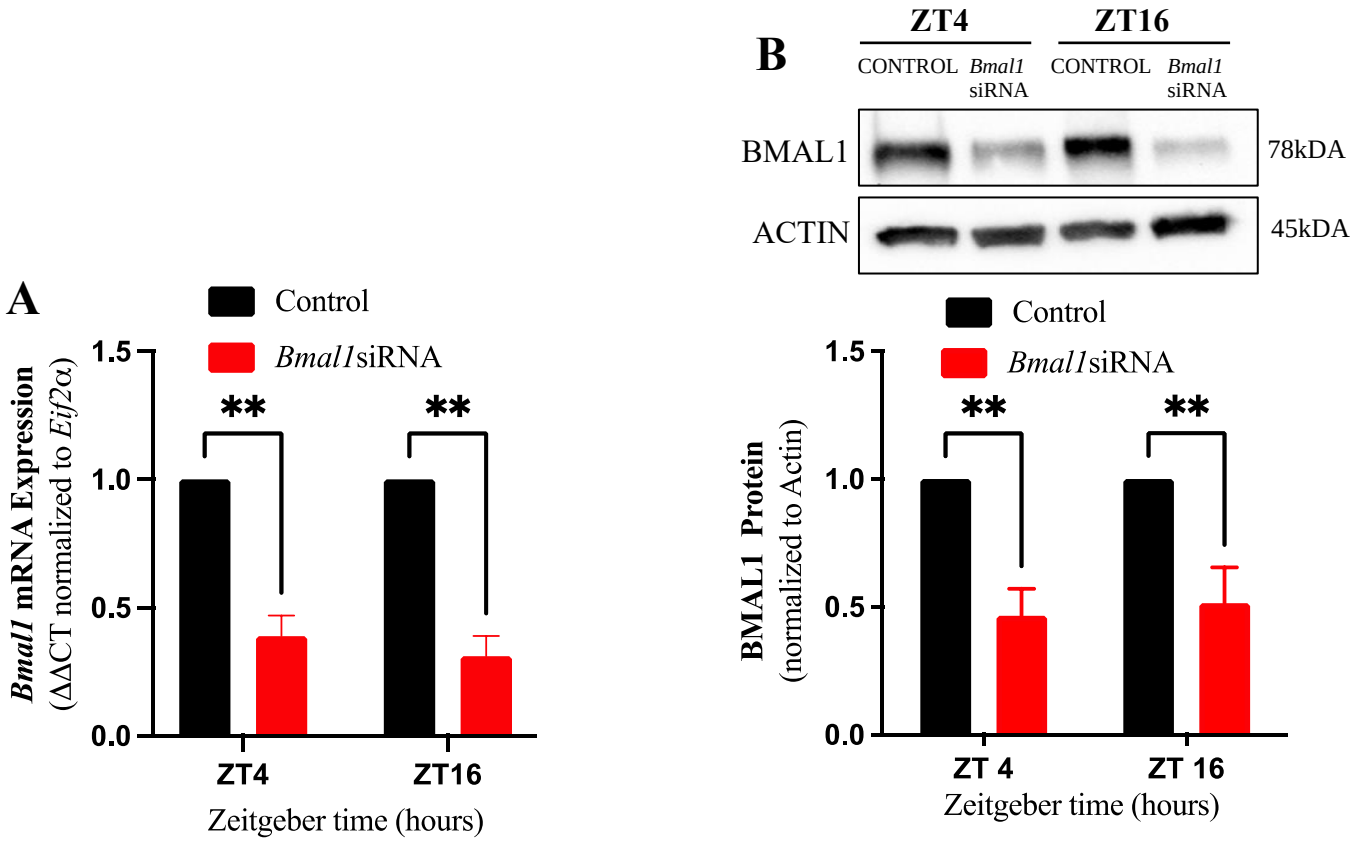


Figure 6.2: Validation of BMAL1 knockdown after siRNA transfection. [A] *Bmal1* mRNA levels in transfected and synchronized MIN6 cells. *Bmal1* mRNA was significantly decreased 50-70% in *Bmal1*-specific siRNA transfected cells compared to cells transfected with scrambled siRNA. **[B]** BMAL1 protein levels in transfected and synchronized MIN6 cells. Top panel shows a representative western blot. Bottom panels should quantification of western blot band intensity. Like mRNA, BMAL1 protein levels were reduced by 60-70% in *Bmal1*siRNA cells compared to control cells. Date are Mean ± SEM. N=5. **p<0.01. Two-way ANOVA with multiple comparisons.

***In vivo* model: Generation of a β-cell specific *Bmal1* knockout mouse (*Bmal1*βKO):** To explore how the β-cell circadian clock impacts rhythms of UCP2 and GSIS, we developed a β-cell-specific *Bmal1* knockout mouse model. This was accomplished by crossing *Ins1*-Cre mice with *Bmal1* floxed mice (both purchased from

Jackson labs). After crossing heterozygous animals for 6 generations (see breeding scheme in Figure 3.2), we validated our *Bmal1*βKO animal model by measuring *Bmal1* mRNA expression in islets isolated from mice of the following genotypes: $Bmal1^{F/F}$ (herein referred to as "*Floxed* controls"), $Bmal1^{WT/WT/Cre}$ ("*Cre* controls") and $Bmal1^{F/F/Cre}$ ("*Bmal1*βKO"). We observed a 70-80% reduction in *Bmal1*mRNA expression in islets isolated from the *Bmal1*βKO compared to *Floxed* controls **[Figure 6.3A]**. Notably, this level of *Bmal1* reduction was expected for whole islets as islets are a heterogenous population of cells and β-cells make up ~70-80% of the cell population. As such, a reduction in *Bmal1* by 70-80% suggests β-cell-specific knockout. To validate our knockout of *Bmal1* more specifically in the β-cell, we also examined BMAL1 protein expression in fixed pancreatic sections *in situ* and co-stained with INSULIN. Using this approach, we observed an overall reduced fluorescent intensity of BMAL1 staining in islets isolated from *Bmal1*βKO mice; however, no co-staining with insulin-positive cells was observed, suggesting effective knockout in the β-cell. Both controls displayed BMAL1 and INSULIN co-staining, suggesting that β-cell expression of BMAL1 is maintained in the β-cell in the controls **[Figure 6.3B].**

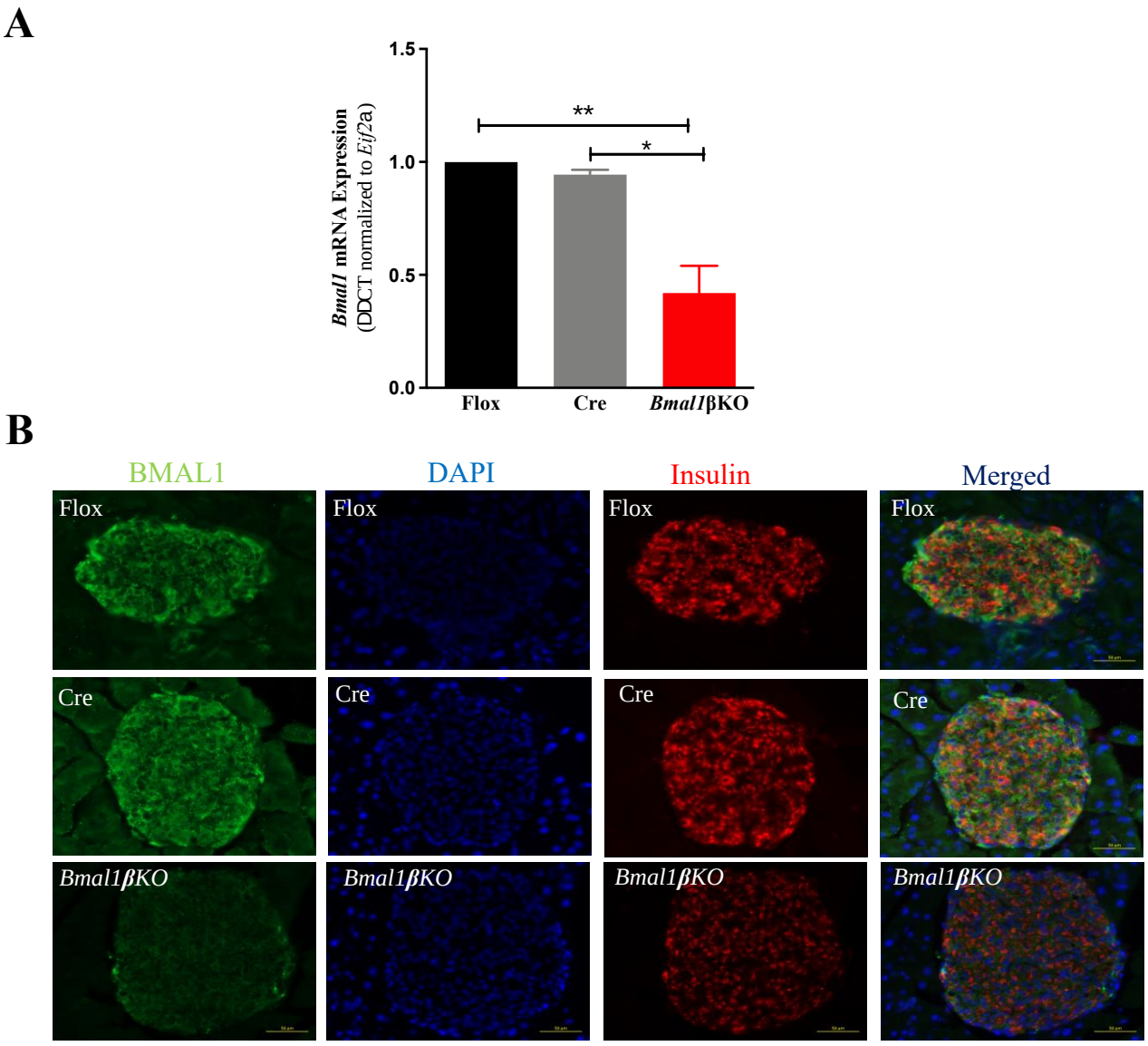


Figure 6.3: Validation of β-cell specific *Bmal1* deletion in islets isolated from *Bmal1*$^{F/F}$ (*Flox* control), *Bmal1*$^{WT/WT/Cre}$ (*Cre* Control) and *Bmal1*$^{F/F/Cre}$ (*Bmal1*βKO). [A] *Bmal1*mRNA expression in islets isolated Floxed control, Cre control and *Bmal1*βKO. Islets pooled from 2-3 mice for each N. Date are Mean ± SEM. N=4. *p<0.05, **p<0.01. Two-way ANOVA with multiple comparisons. **[B]** β-cell-specific immunofluorescence staining of BMAL1 on pancreatic section obtained from Floxed control), Cre Control, and *Bmal1*βKO mice. N=3 per each genotype.

6.3.3 Effects of β-cell-Specific *Bmal1* Deletion on Bodyweight and Fasted Blood Glucose

Previous animal models of β-cell-specific *Bmal1* knockout were founds to display significant fasting hypoinsulinemia and *in vivo* defects in GSIS (Lee et al., 2011). It is well established that the hormone insulin in circulation is known to promote storage of glucose in peripheral tissues. As such, we expected that *Bmal1*βKO mice, which had previously reported to have low insulin, could have potentially lower body weight compared to Floxed and Cre controls. In this study, we observed no differences in total body weights in both male and female mice between *Bmal1*βKO and control mice when measured over 13 weeks. **[Figure 6.4A and B]**.

Additionally, previous studies demonstrate that the *Bmal1*βKO animals develop a diabetes phenotype characterised primarily by fasting hyperglycemia.

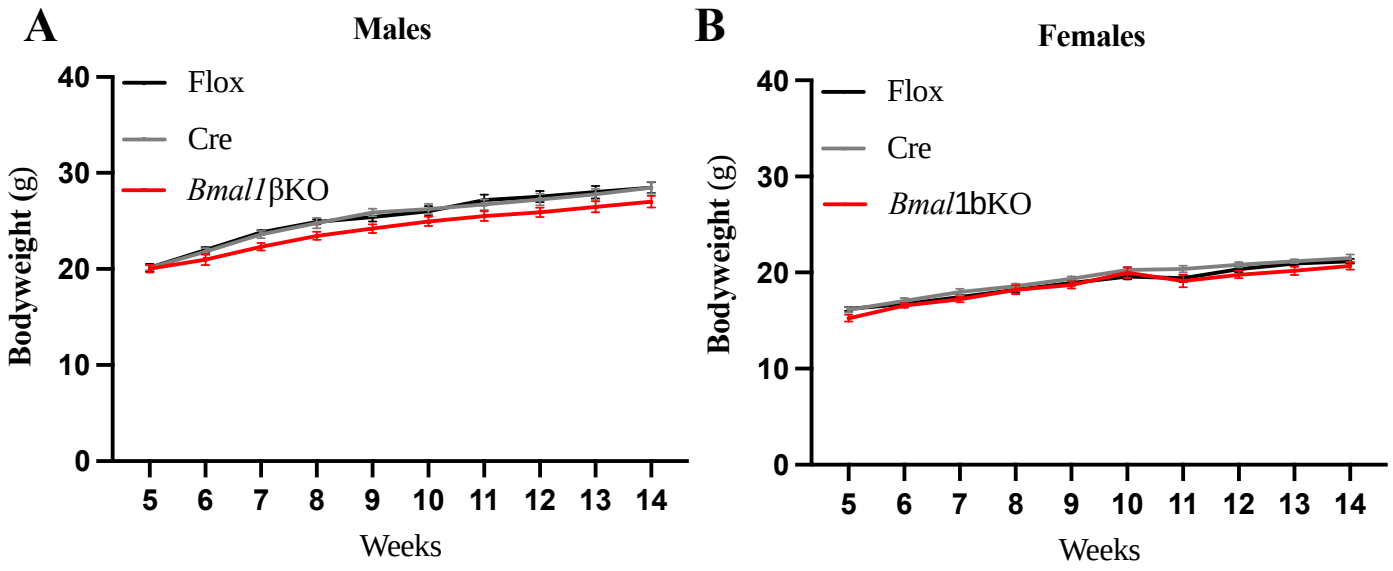


Figure 6.4: Bodyweight measurements (g) obtained from male and female mice over 13 weeks. Bodyweight measurements (g) obtained from **[A]** Male and **[B]** Female mice between 5-14 weeks of age. Date are Mean ± SEM. N=8-10. No statistical difference observed after unpaired non-parametric Mann-Whitney student t-test.

Fasting blood levels were measured in all three groups of mice: Floxed controls, Cre Controls and *Bmal1*BKO over 12 weeks after an overnight fast of about 16 hours in both male and female mice **[Figure 6.5A and B]**. Both male and female *Bmal1*βKO mice had significantly higher fasting blood glucose levels when compared to Floxed and Cre controls. Interestingly, in our model we observed that fasting hyperglycemia is more profound and does not resolve throughout 13 weeks (period of measurement) in the *Bmal1*βKO female mice when compared to flox and Cre female mice: however, blood glucose levels become comparable between genotypes in male mice from week 9 onwards. Fasting hyperglycemia become less profound as they age in *Bmal1*βKO males.

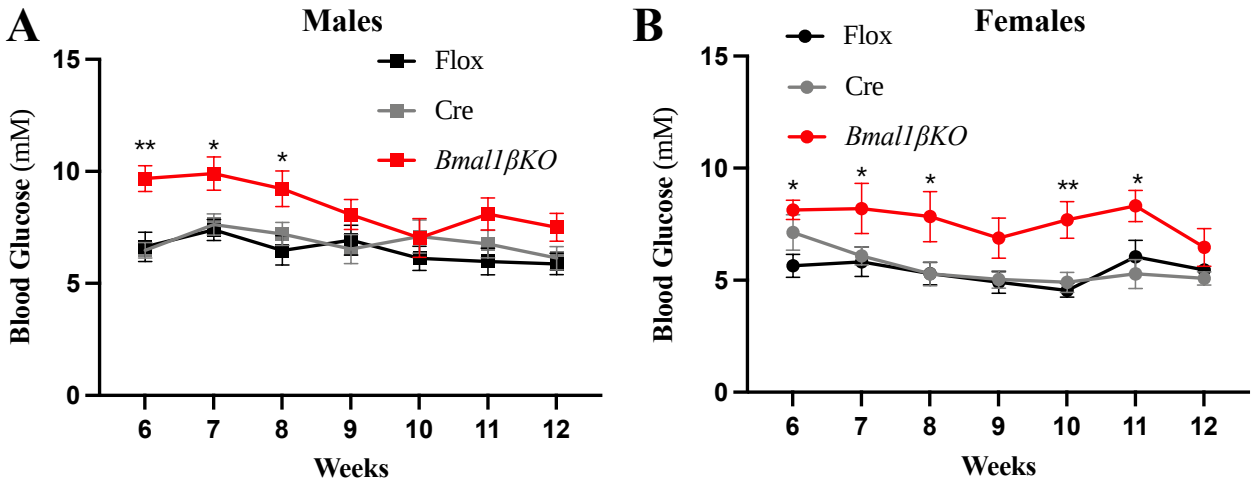


Figure 6.5: Fasted blood glucose measurements done in male and female mice. Fasted blood glucose measurements (mM) done in **[A]** male and **[B]** female mice between week 5-12. Date are Mean ± SEM. N= 8-10 per genotype. **p<0.01; *p<0.05. Statistical significance observed after unpaired non-parametric Mann-Whitney student t-test.

6.3.4 Effect of β-cell-Specific *Bmal1* Deletion on Glucose and Insulin Tolerance

To examine the impact of β-cell-specific *Bmal1* knockout on glucose tolerance at different times of the day, ipGTTs were performed in 12-week-old male and female mice (all 3 groups) at both 10am and 10pm. The above time points were chosen as they lie in the centre of the 12hr:12hr light/dark cycle and avoid the effects of changes in light schedule (note: lights switch ON and OFF at 6am and 6pm respectively). At both 10am and 10pm, *Bmal1*βKO mice exhibited significantly impaired glucose tolerance compared to *Floxed* and *Cre* controls **[Figure 6.6]**.

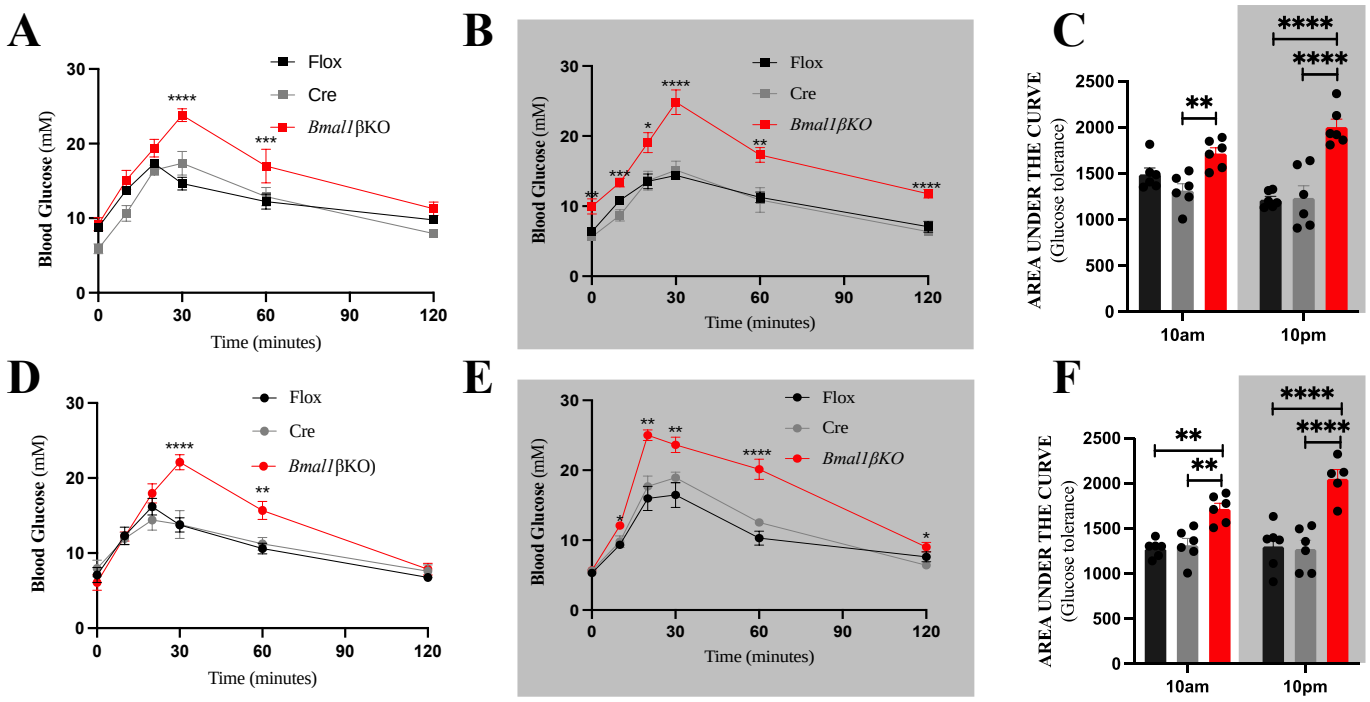


Figure 6.6: *Bmal1* deficiency impairs glucose tolerance over 24 hours. [A] Assessment of glucose tolerance by i.p. GTT test in males at 10am. **[B]** Assessment of glucose tolerance by i.p. GTT test in males at 10pm. **[C]** AUC of GTT in males at both 10am and 10pm **[D]** Assessment of glucose tolerance by i.p. GTT test in females at 10am. **[E]** Assessment of glucose tolerance by i.p. GTT test in females at 10pm. **[F]** AUC of GTT in females at both 10am and 10pm Date are Mean ± SEM. N = 5-6 mice per genotype. ****p < 0.0001; **p < 0.01; *p<0.05 after Two-Way ANOVA with multiple comparisons.

Importantly, impairments in glucose tolerance observed above could be a consequence of impaired uptake of glucose by peripheral tissues (insulin resistance) resulting in high levels of circulating blood glucose rather than an insulin secretory defect at the level of β-cells. To gain a better understanding of the glucose intolerance observed in *Bmal1*βKO male and female mice over 24 hours, we performed an insulin tolerance test (ITTs) on male and female mice in all 3 groups. Notably, *Bmal1*βKO male and female mice displayed no significant differences in insulin tolerance compared to Flox and Cre controls at the same time point **[Figure 6.7A-D]**. Note that ITTs could not be performed in animals at 10pm because control mice were highly insulin sensitive and developed rapid and severe hypoglycemia preventing the completion of ITT protocol. Their blood sugar levels dropped to >1.2mM at 20-30 mins post insulin injections and needed a glucose bolus to prevent from serious health consequences. This finding is in line with previously established circadian rhythms in insulin tolerance such that there is an increase in insulin sensitivity in the active portion of the day when food intake is anticipated (Lee et al., 1992, Pisu et al., 1980). Collectively, our glucose tolerance and insulin tolerance studies suggest that *Bmal1* knockout (driven by *Ins1*-Cre-mediated recombination) causes chronic glucose intolerance without accompanying changes in insulin tolerance, suggesting that *Bmal1* knockout in the β-cell drives a primary insulin

secretion defect, which is supported by previous studies in the literature that characterize knockout of *Bmal1* in the β-cell using the Ins2-Cre system (Lee et al., 2011, Lee et al., 2013, Marcheva et al., 2010).

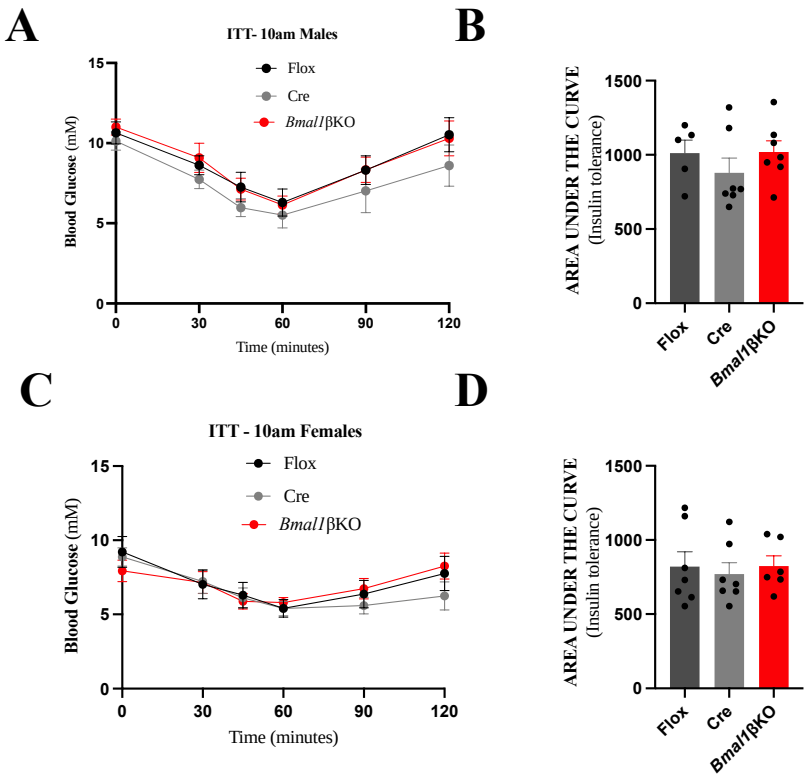


Figure 6.7: *Bmal1* deficiency has no impact on insulin tolerance in male and female mice. [A] Assessment of glucose tolerance by i.p. ITT test at 10am in males. **[B]** AUC of ITT done in males at 10am **[C]** Assessment of glucose tolerance by i.p. ITT test at 10am in females**. [D]** AUC of ITT done in females at 10am. Date are Mean ± SEM. N = 5-6 mice per genotype. No statistical significance observed after Two-Way ANOVA.

6.3.5 ***Bmal1* Deficiency Impairs GSIS in MIN6 cells and isolated islets.**

To determine the impact of Bmal1 deficiency on GSIS, we performed static incubation assays in both synchronized MIN6 cells that were transfected with *Bmal1*siRNA as well as from islets isolated from our *Bmal1*βKO model and respective controls. In the MIN6 cells, the control cells transfected with scrambled siRNA displayed the expected insulin secretion capacities at ZT 4 and ZT 16 (i.e., greater secretion capacity at ZT 4 compared to ZT 16); however, cells transfected with *Bmal1*siRNA showed significantly impaired insulin secretion at ZT4 **[Figure 6.8**]. More specifically, at ZT 4, *Bmal1*siRNA-transfected cells exhibited a GSIS capacity that was only 1.5-fold above basal compared to a 2.5-fold GSIS in control MIN6 cells, suggesting that *Bmal1* is needed to drive increased GSIS capacity at ZT 4. Interestingly, no difference in insulin secretion

capacity at ZT16 was observed between control and *Bmal1*siRNA transfected MIN6 cells **[Figure 6.8].** Notably, at this timepoint, *Bmal1* expression is naturally reduced in control cells (see figure 6.1) and both lines of cells would have low *Bmal1* expression levels. This suggests that suppression of *Bmal1* at ZT 16 is required for suppression of GSIS at this timepoint, although this was not directly tested and would require overexpression studies, which were not performed here.

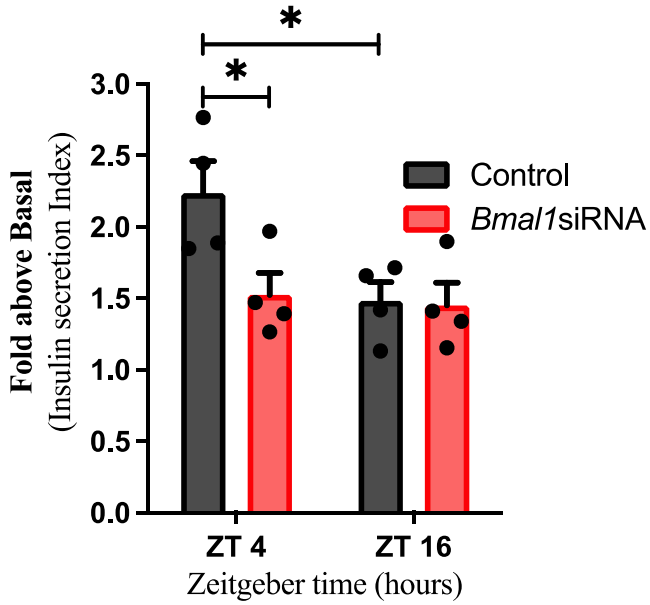


Figure 6.8: *Bmal1* deficiency impairs GSIS in synchronized MIN6 cells. GSIS capacity of synchronized MIN6 cells (control and *Bmal1*siRNA) at ZT 4 and ZT 16 as measured by static incubation assays. Data is represented as the fold-change of insulin stimulated at high glucose (16.7mM) above basal insulin secretion at 2.8mM glucose. The black bars represent the cells transfected with scramble siRNA and is referred to as controls. The red bars represent the *Bmal1* knockdown cells. Date are Mean ± SEM. N=4. *p<0.050. Two-way ANOVA with multiple comparisons.

To examine the impact of β-cell *Bmal1* knockout on insulin secretion in primary islets, islets were isolated from all 3 groups of mice (males and females) at 10am and 10pm. At 10am, when the mice are inactive and the lights are ON, islets isolated from *Bmal1*βKO exhibited normal GSIS capacities compared to islets isolated from control mice **[Figure 6.9A and B – unshaded region].** However, at 10pm when the mice are active and anticipating food intake, islets isolated from *Bmal1*βKO displayed significantly impaired GSIS compared to both groups of control mice **[Figure 6.9A and B shaded region].** Furthermore, a trend towards increased GSIS capacity was observed in islets isolated from control mice at 10pm relative to GSIS capacity at 10am **[Figure 6.9A and B].** This pattern of GSIS is expected based on our previous findings **[Figure 4.2 B];** however, this rhythm is lost in the *Bmal1*βKO mice, suggesting that a functional circadian clock is required to drive rhythmic changes in GSIS. While previous studies using *Bmal1*βKO have demonstrated that *Bmal1* deficiency in the β-cell

impairs GSIS in general, this is the first to show that this impairment occurs at timepoints in the dark phases and that the natural rhythm of GSIS capacity is lost in the *Bmal1*-deficient state.

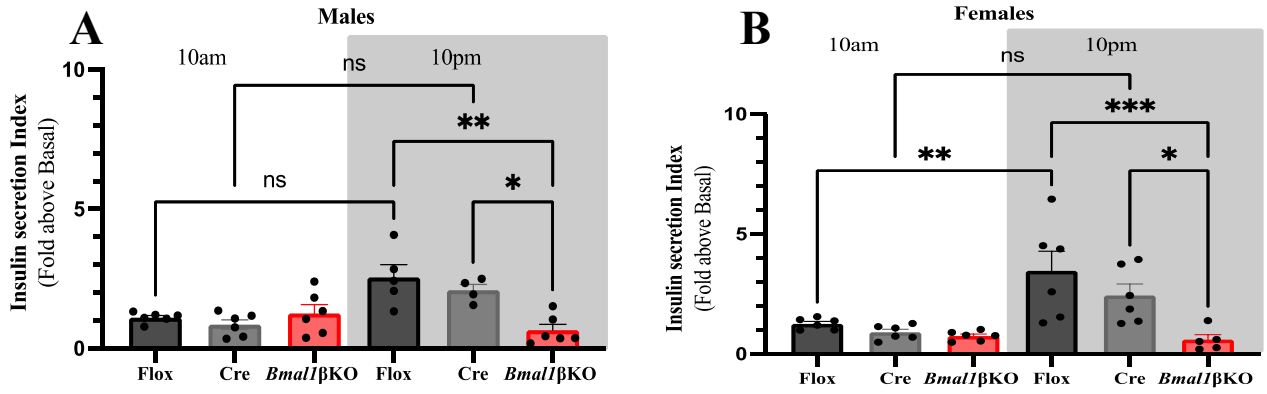


Figure 6.9: *Bmal1* deletion in the β-cell Disrupts Diurnal GSIS Capacity. [A] GSIS capacity represented as fold-change above basal secretion at 2.8mM glucose in islets isolated from 10am and 10pm males **[B]** GSIS capacity represented as fold above basal in islets isolated from 10am and 10pm females, N=4-6 animals per genotype. Date are Mean ± SEM. ****p < 0.0001; **p < 0.01; *p<0.05. Two-way ANOVA with multiple comparisons.

6.3.6 Impaired GSIS in *Bmal1*-Deficient β-cells Is Dependent on Chronic Upregulation of *Ucp2*

In chapter 4, we established that diurnal rhythms in *Ucp2* expression are essential for the establishment of daily rhythms in GSIS capacity and glucose tolerance. Here, we wanted to determine if *Bmal1* deficiency impacted the natural expression pattern of *Ucp2* and if this contributed to impaired rhythms of GSIS. To accomplish this, we examined *Ucp2* mRNA expression levels by qPCR in control and *Bmal1*siRNA MIN6 cells at ZT 4 and 16. While control cells exhibited normal diurnal rhythms in *Ucp2* expression, as established in chapter 4 **[Figure 4.1A and Figure 6.10; low at ZT 4 and high at ZT 16]**, *Bmal1* knockdown disrupted *Ucp2* rhythms such that a 2-fold upregulation of *Ucp2* mRNA was observed at ZT 4 compared to control cells at this timepoint **[Figure 6.10].**

We further measured *Ucp2* mRNA in islets isolated from *Bmal1* deficient mouse model using qPCR and compared it to islets isolated from *Bmal1*F/F (control mice) both at 10am and 10pm. While *Ucp2* expression in islets isolated from *Bmal1*$^{F/F}$ mice exhibited a normal rhythm as observed in Chapter 4.1A with increased *Ucp2* expression at 10am when compared to 10pm. However, the rhythm of *Ucp2* was completely abrogated in islets isolated from *Bmal1* deficient islets **[Figure 6.10B].**

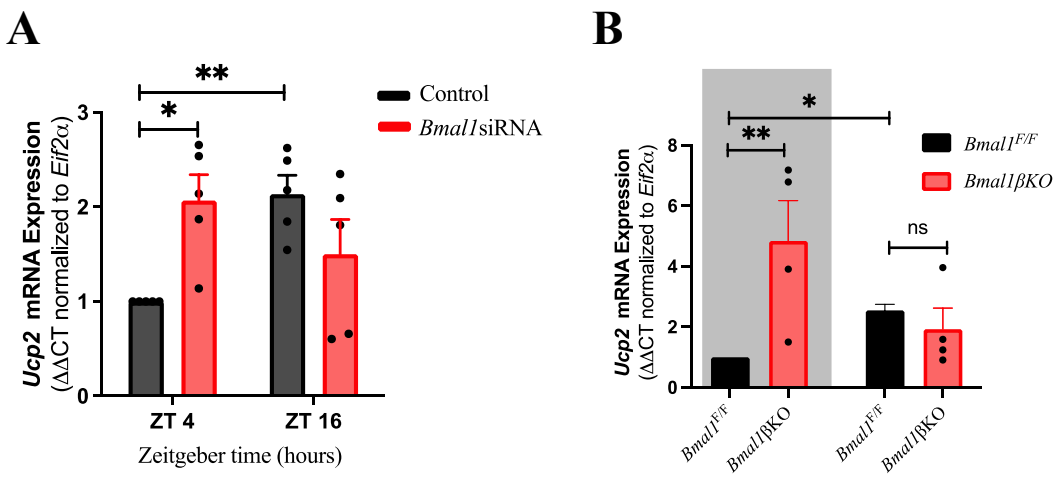


Figure 6.10: *Bmal1* Knockdown Upregulates *Ucp2 mRNA* Expression at ZT4 and 10pm, Disrupting the Diurnal Rhythms of *Ucp2* Expression. [A] *Ucp2* expression was quantified using qPCR in both control and *Bmal1*siRNA transfected cells at ZT 4 and ZT 16. [B] *Ucp2* expression was quantified using qPCR in islets isolated from *Bmal1*F/F and *Bmal1*βKO at 10am and 10pm. The expression is relative to *Eif2a* (housekeeping gene) and normalized to ZT 4 control cells and 10pm control islets. Islets were isolated and pooled from 2-3 mice for each N at a particular time point. Date are Mean ± SEM. N=4.**p < 0.01; *p<0.05 after Two-Way ANOVA with multiple comparisons.

To establish that impaired GSIS at ZT 4 in *Bmal1* knockdown cells is dependent on increased UCP2 activity at this time point, cells were pre-incubated in genipin to inhibit UCP2 activity and then the impact on GSIS at ZT 4 and ZT 16 in both groups of cells was assessed. While inhibition of UCP2 inhibition had no effect on GSIS control cells at ZT 4 (*Ucp2* expression is low in these cells at this time point), genipin significantly ameliorated the defects in GSIS observed *Bmal1*siRNA cells (where *Ucp2* expression is high), bringing GSIS capacity to a level similar to that seen in control MIN6 cells at ZT 4. **[Figure 6.11].** These results suggest that the upregulation of UCP2 at ZT 4 contributes to impaired GSIS in *Bmal1*-deficient β-cells. Notably, this experiment was only performed at the ZT 4 time point because at ZT 16, *Ucp2* mRNA expression is equally high in both groups of cells, and we have previously established that upregulated *Ucp2* at this time point contributes to reduced GSIS at ZT 16 (Seshadri, N et al., 2017).

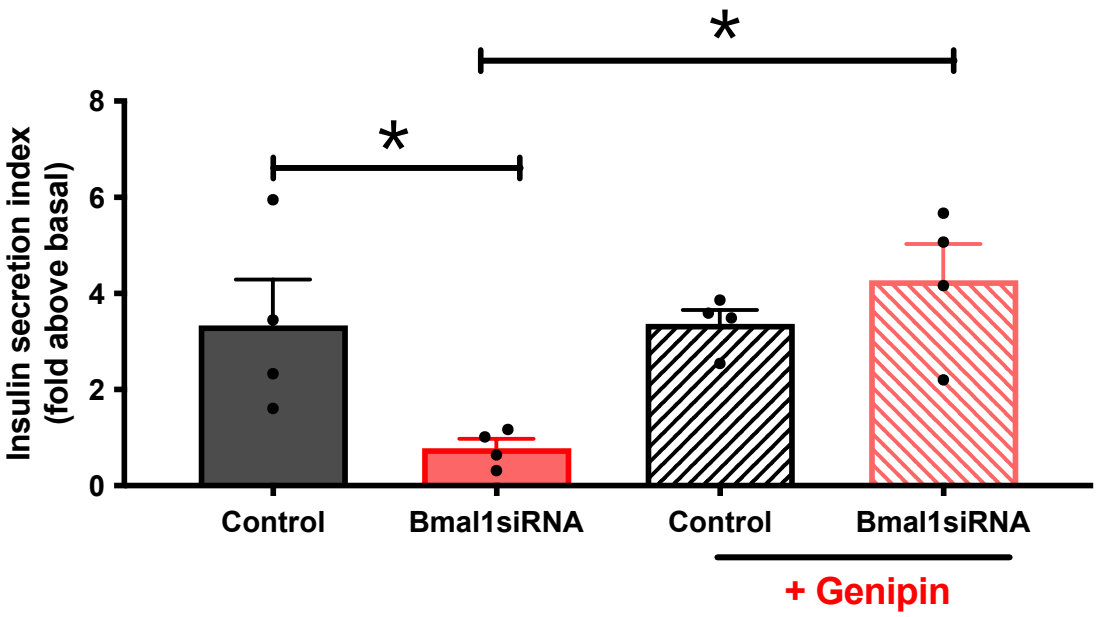


Figure 6.11: Inhibition of UCP2 Activity at ZT4 Recovers Impaired GSIS in *Bmal1*-deficient β Cells. GSIS was measured in controls and *Bmal1*siRNA MIN6 cells at ZT 4 with and without 50μM Genipin (UCP2 inhibitor). Insulin secreted in response to 16.7mM and 2.8mM glucose was assessed and the data expressed as the fold change above basal insulin secretion at 2.8mM glucose. Date are Mean ± SEM. N=4. Two-way ANOVA with multiple comparisons. *P<0.05.

To follow up the MIN6 cells studies in isolated islets, we isolated islets at 10am and 10pm from all 3 groups of mice (both males and females) and preincubated the islets in genipin to inhibit UCP2 before assessing GSIS capacity. As expected, at 10am (light/inactive), islets isolated from *Flox* and *Cre* control mice display reduced GSIS compared to islets isolated at 10pm (dark/active) (compare **Figure 6.12 A/B vs C/D**). While *Bmal1*βKO mice displayed similar GSIS capacity as the controls at 10am **[Figure 6.12A],** *Bmal1*βKO mice showed impaired GSIS at 10pm **[Figure 6.12C]** in both male and female mice. Notably, this impaired GSIS capacity at 10pm is similar to the impaired GSIS capacity observed at ZT 4 in MIN6 cells (Figure 6.8). At 10am, preincubation with genipin restored GSIS in all 3 genotypes **[Figure 6.12A and B],** suggesting that UCP2 activity is equally high in all 3 groups of mice at this timepoint, and it contributes to suppressed GSIS at this timepoint, which we expected based on our studies in chapter 4. However, at 10pm, genipin preincubation of islets isolated only from *Bmal1*βKO showed restored GSIS **[Figure 6.12C and D],** further demonstrating that the impaired GSIS observed in *Bmal1*βKO mice at 10pm is dependent on elevated UCP2 activity.

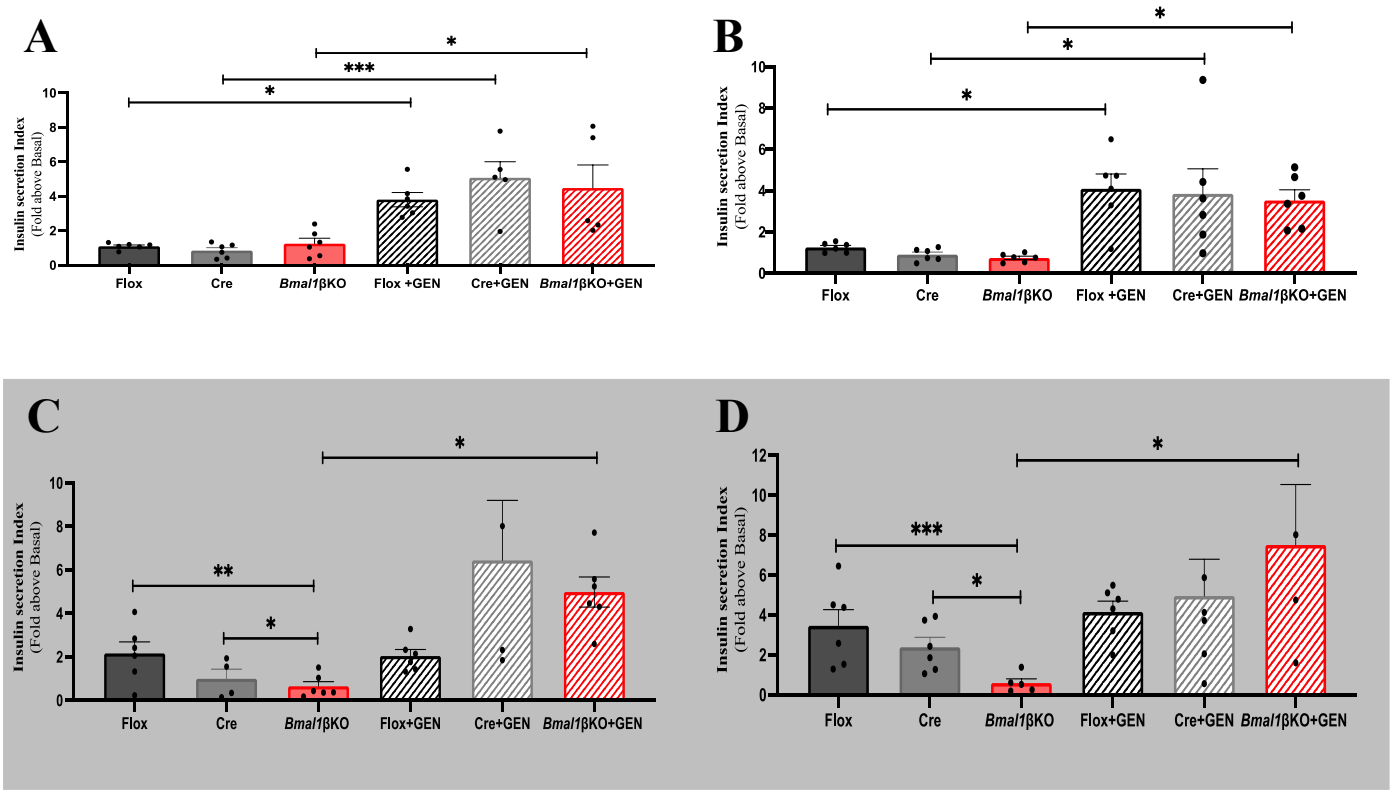


Figure 6.12*:* Genipin Restores Impaired GSIS at 10pm in *Bmal1*-Deficient Islets. GSIS was measured in controls and *Bmal1*βKO islets with and without 50μM Genipin (UCP2 inhibitor) at 10am and 10pm. Insulin secreted in response to 16.7mM and 2.8mM glucose was assessed and the data expressed as the fold change above basal insulin secretion at 2.8mM glucose. GSIS capacity represented as fold-change above basal secretion at 2.8mM glucose in islets isolated from **[A]** 10am males and **[B]** females. GSIS capacity represented as fold above basal in islets isolated from **[C]**10pm males and **[D]** females. Date are Mean ± SEM. N=4-6 animals per genotype. ***p < 0.001; **p < 0.01; *p<0.05. Two-way ANOVA with multiple comparisons.

6.3.7 Glucose-Induced ATP Production is Reduced in β-cell *Bmal1* Deficiency.

In Chapter 4, we elucidated part of the mechanism by which diurnal rhythm of UCP2 activity regulate diurnal GSIS rhythms. We demonstrated that UCP2-mediated regulation of glucose-induced ATP production was an important part of this mechanism. Here, we sought to determine if the upregulation of *Ucp2* that occurs at ZT 4 in MIN6 cells and at 10pm in isolated islets in *Bmal1*-deficient β-cells was also associated with reduced glucose-induced ATP content. A ~1.5-fold reduction in ATP content after glucose-stimulation was observed in *Bmal1*siRNA MIN6 cells relative to control cells at ZT 4 **[Figure 6.13].** Importantly, no difference was observed between *Bmal1*siRNA and control MIN6 cells at ZT 16 **[Figure 6.13]**, again likely because *Ucp2* expression is equally elevated in both conditions at this time point **[Figure 6.10]**, which would uncouple and suppress ATP generation in the presence of glucose.

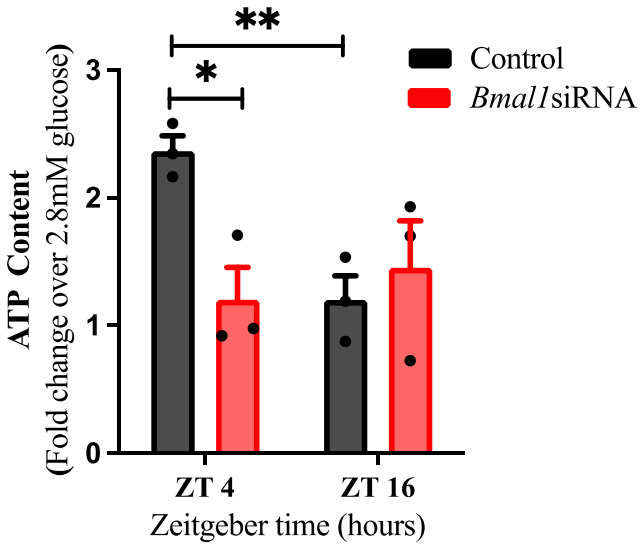


Figure 6.13: *Bmal1* Knockdown in MIN6 Cells Impairs Glucose-Induced ATP accumulation in synchronized MIN6 cells. GSIS capacity of synchronized MIN6 cells at ZT4 and ZT16 as measured by static incubation assay on siRNA mediated knockdown of *Bmal1* is represented as fold change above LG (Low glucose or 2.8mM glucose). The back bars represent the cells transfected with scramble siRNA and is referred to as controls. The red bars represent the *Bmal1* deficient cells. Date are Mean ± SEM. N=4. **p < 0.01; *p<0.05. Two-way ANOVA with multiple comparisons.

Similar to the results in MIN6 cells, assessment of glucose-induced ATP content in islets isolated from all 3 genotypes at 10 am and 10pm revealed an ~1.5-fold reduction in ATP content in islets isolated from *Bmal1*βKO relative to control groups at 10pm **[Figure 6.14B**]. Importantly, no difference was observed between *Bmal1*βKO and control at 10am **[Figure 6.14A],** again likely because UCP2 activity is high in all 3 conditions at this time point **[Figure 6.12A and B]**, which also explains why genipin equally restored glucose-induced ATP content in all 3 groups at this timepoint. Furthermore, at 10pm, genipin restored impaired glucose-induced ATP production in the islets isolated from *Bmal1*βKO mice. Collectively, this data suggests that impairments in insulin secretion observed at 10pm in islets isolated from *Bmal1*βKO was mediated by impairments in glucose-induced ATP production. Furthermore, impairments in insulin secretion capacities mediated by reduced glucose-induced ATP production are regulated UCP2 at 10am. In conclusion, defects in insulin secretion capacities observed in disrupted β-cell clock is a result of impaired ATP production due to defects in *Ucp2* expression. Although the role of UCP2 in regulation of glucose induced ATP production has been previously published by our group (Seshadri et al., 2017), we are the first to show impairments in glucose induced ATP production mediated by disrupted Ucp2 expression in a *Bmal1* β-cell deficient model.

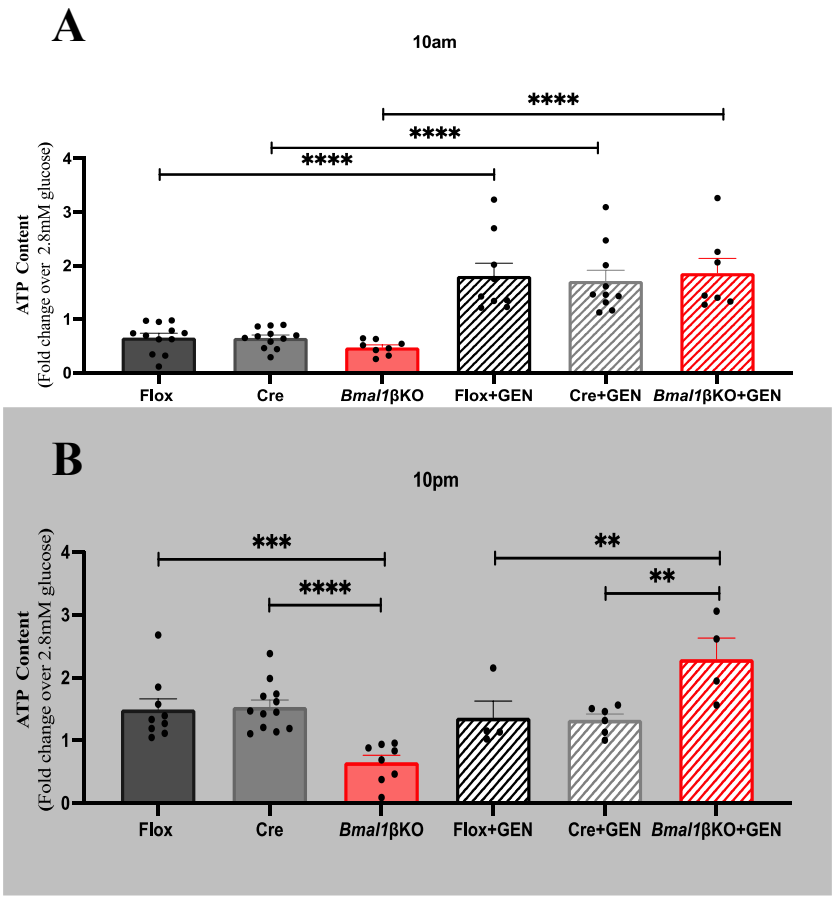


Figure 6.14: *Bmal1βKO* Islets Display Reduced Glucose-Stimulated ATP Accumulation at 10pm that is Rescued by Genipin. Glucose-stimulated ATP production assessed at **[A]** 10am, and **[B]** 10pm in *Flox* (bars in black), *Cre* (bars in tin) and *Bmal1*βKO (red) isolated islets treated with Genipin. N=4-12 animals per genotype. Date are Mean ± SEM. ****p < 0.0001; ***p < 0.001; **p<0.01; *p<0.05. Two-way ANOVA followed by multiple comparisons.

6.3.8 *Bmal1* Deficiency Impairs Rhythms in Glucose Oxidation in MIN6 Cells.

In section 5.5, we demonstrated that β-cells have the capacity to utilize specific fuels (glucose and fatty acid) in a time-of-day-specific manner and that UCP2 plays some role in the selection of this fuel. Here, we compared glucose oxidation rates in control and *Bmal1*siRNA MIN6 cells at ZT 4; the time point where we expect higher rates of glucose oxidation and GSIS in control cells. Knockdown of *Bmal1* significantly reduced basal oxygen consumption, ATP-linked respiration, maximal respiration in the presence of glucose at ZT 4 **[Figure**

6.15 A], suggesting that a functional β-cell circadian oscillator is required for the increase in glucose oxidation observed at ZT 4 and may be important for the regulation of daily cycles of fuel selection.

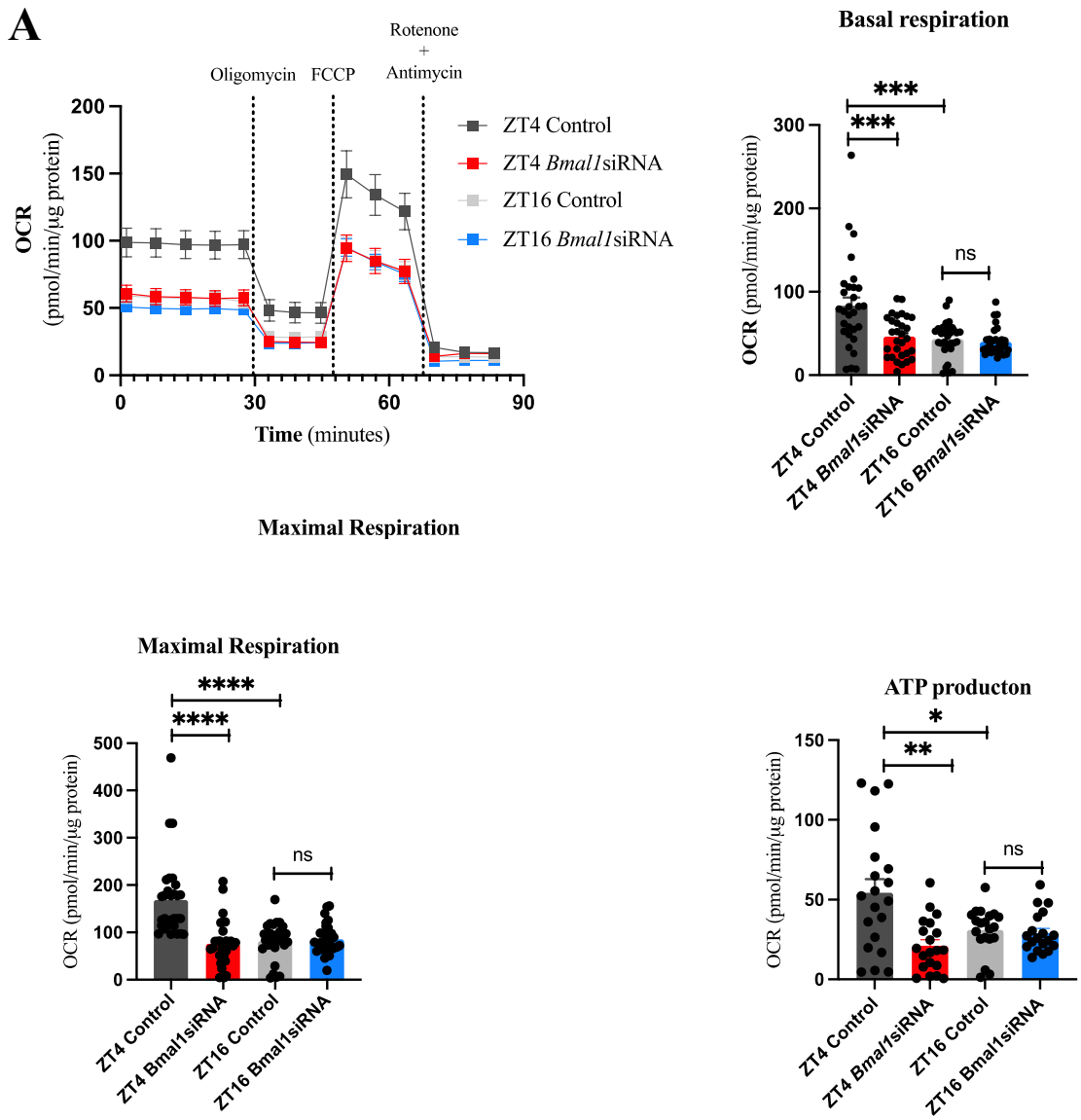


Figure 6.15: *Bmal1* knockdown impairs glucose oxidation at ZT 4 in synchronized MIN6 cells. [A] Oxygen consumption rate (OCR) over time by synchronized MIN6 cells utilizing glucose, normalized to cellular protein (average of all experiments). N=3, [10 wells per group]. Basal respiration, maximal (FCCP uncoupled) respiration and ATP production (oligomycin sensitive**)** were calculated from the OCR trace. ****p < 0.0001; ***p < 0.001; **p<0.01. Date are Mean ± SEM. Two-way ANOVA followed by multiple comparisons.

6.3.9 *Bmal1* Knockdown Impairs Rhythmic Expression of Glucose-Sensing and Metabolism Genes

We and others have shown that key metabolic genes display diurnal patterns of gene **expression [Figures. 5.5F-I)** (Petrenko et al., 2017). In chapter 5, we demonstrated that the pattern of expression of key glucose (*Slc2a2*, *Gck*) and fatty acid oxidation (*Cpt-1a*) genes associate with the pattern of fuel oxidation in the β-cell **[Figure 5.5 E-I].** Furthermore, we observed a decrease in glucose oxidation in the *Bmal1*-deficient cells at ZT 4

compared to control cells. Here, we examined how *Bmal1* deficiency in the β-cell impacts the expression of these important metabolic genes. We measured the expression of *Slc2a2* and *Cpt-1a* in *Bmal1*-deficient MIN6 cells and found impairments in the rhythmic expression patterns of these genes **[Figure 6.16B and C],** such that *Bmal1* knockdown elevated *Cpt-1a* at ZT 4 but suppressed *Slc2a2* at ZT 4. No difference in *Cpt-1a* was observed at ZT 16, whereas *Slc2a2* was massively upregulated at ZT 16. The reduced expression of *Slc2a2* at ZT 4 fits with reduced glucose oxidation observed in **Figure 6.15**. Additionally, we also measured *Ldha* mRNA transcript levels and surprisingly found significant changes in *Ldha* mRNA levels in control MIN6 cells between ZT 4 and ZT 16. Notably, we expected low levels of *Ldha* expression in MIN6 cells at all time points given that is was previously postulated that *Ldha* was "disallowed" in the β-cell (Schuit et al., 2012). Given the surprising nature of this finding examined LDH expression and activity in more detail in Figure 6.17 and 6.18 in section 6.3.10 and 6.3.11. Furthermore, *Bmal1*-deficiency in MIN6 cells upregulated *Ldha* expression at ZT 4, but not at ZT 16; a similar pattern to that observed for *Ucp2* **[Figure 6.10]** and *Cpt-1a* **[Figure 6.16A].** Collectively, these studies suggest that the β-cell circadian clock contributes to the temporal control of not only UCP2 expression, but also key metabolic genes, including *Ldha*, *Slc2a2* and *Cpt-1a*.

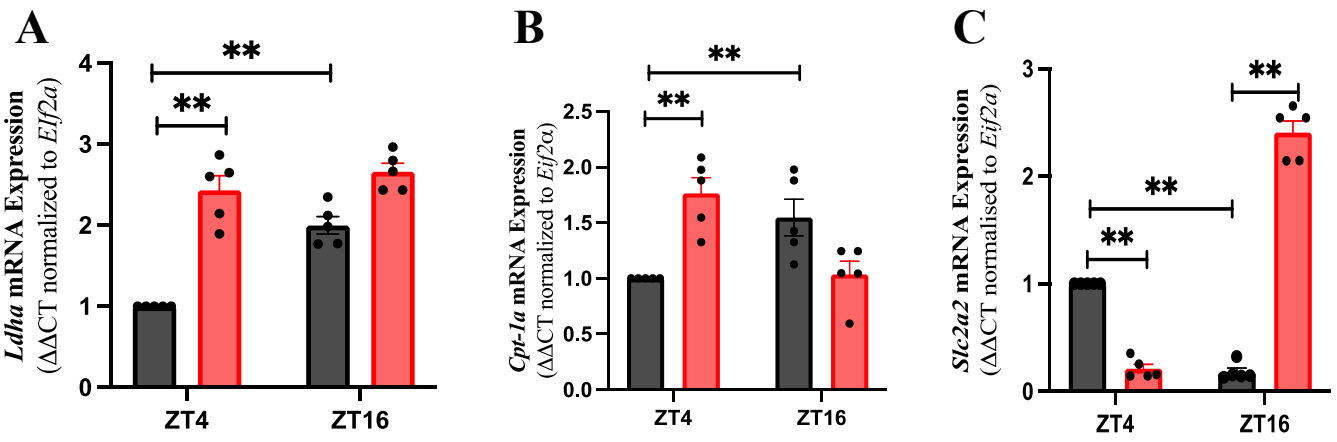


Figure 6.16: *Bmal1* knockdown impairs rhythmic expression of genes known to impact glucose-sensing and metabolism. Expression of genes **[A]** *Ldha,* **[B]** *Cpt-1a,* and **[C]** *Slc2a2* (*Glut2*) mRNA expression in cells transfected with *Bmal1*siRNA (red bars) and control cells (black bars) in synchronized MIN6 cells were measured by qPCR and normalized to *Eif2a* and expression of each gene in cells transfected with scramble siRNA (Control). Date are Mean ± SEM. N=4-5. *P<0.05; **P<0.01. Two-way ANOVA followed by multiple comparisons.

6.3.10 *Ldha* mRNA Expression in Synchronized MIN6 Cells and Isolated Islets.

Among the few genes that we targeted for the above study; we were particularly intrigued with the *Ldha* mRNA expression data. As such, we decided to look closer at the *Ldha* mRNA expression pattern in MIN6 cells and islets. First, assessment of mRNA levels every 4 hours by qPCR in synchronized MIN6 cells revealed a dynamic and rhythmic pattern of *Ldha* expression over a 36-hour time course showing approximate 12 hour

repeating and alternating patterns of low and elevated *Ldha* mRNA expression **[Figure 6.17A]**, similar to that observed for *Ucp2* **[Figure 4.1A].** At ZT 0, 4, and 8, *Ldha* mRNA expression remained low and unchanged. At ZT 12 and 16, *Ldha* mRNA levels increased to 1.8377- (Median= 0.8267; p=0.0361) and 2.09 - (Median = ±1.7444; p<0.0001) fold, respectively, compared to time 0. Between ZT 24 and ZT 28, *Ldha* mRNA expression levels returned to baseline and gradually increased over the next 12 h (up to 36 h).

Similarly, when *Ldha* mRNA transcript was measured in islets isolated from C57BL6 mice during light/inactive phase (10am,2 pm and 6pm) and dark phase (10pm, 2am and 6am), we observed elevated islet *Ldha* mRNA expression in the light/inactive phase followed by significant reduction at dark /active phase **[Figure 6.17B].** Collectively, we demonstrate for the first time that *Ldha* mRNA expression is not chronically suppressed in pancreatic β-cells and islets, but rather is rhythmic over time and may contribute to the fine regulation of the temporal control of GSIS over 24 hours.

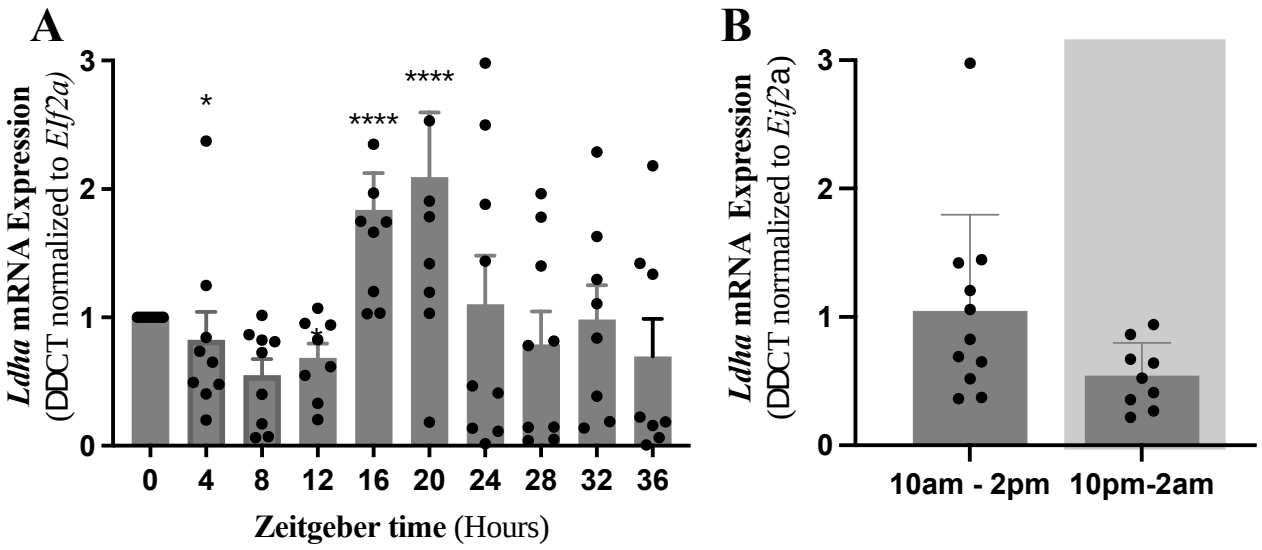


Figure 6.17: *Ldha* mRNA expression levels at 4-hour intervals over 36 hours in synchronized MIN6 cells and islets isolated from C57BL6 mice. [A] *Ldha* mRNA shown is expressed relative to *Eif2a* levels and normalized to mRNA levels at ZT 0 (immediately after synchronization). Date are Mean ± SEM. N=4-8. P-values demonstrate statistical significance after two tailed student's t-test. **[B]** Islet were collected every 4 hours for 24 hours and pooled to examine expression levels from all time points in the light vs dark. *Ldha* mRNA levels are elevated in the light/inactive phase between 10am-2pm compared dark/active phase between 10pm-2am in C57BL/6 mice. *Ldha* mRNA shown is expressed relative to *Eif2a* levels and normalized to *Ldha* mRNA levels at light/inactive phase. Islets were isolated from 3 to 5 mice at each time point. Date are Mean ± SEM.

6.3.11 LDHA Activity is Rhythmic over 24 hours in synchronized MIN6 cells.

To determine the dynamics of LDHA *activity* over a 24 h period in synchronized MIN6 cells, MIN6 cells were transfected with the FRET-based Laconic sensor and synchronized using the serum-starve/serum-shock protocol. Transfected cells were imaged every 4 hours over 24 hours. FRET emission of the Laconic biosensor was increased at ZT16 when compared to ZT4 **[Figure 6.18]**, indicating greater LDH activity at ZT 16 as this increased lactate accumulation corresponds to the previously observed increase in *Ldha* mRNA expression **[Figure 6.17A]**. At ZT 28, FRET emission from the biosensor was reduced, which also correlated with the reduced *Ldha* mRNA expression that was observed at this time point **[Figure 6.17A]**.

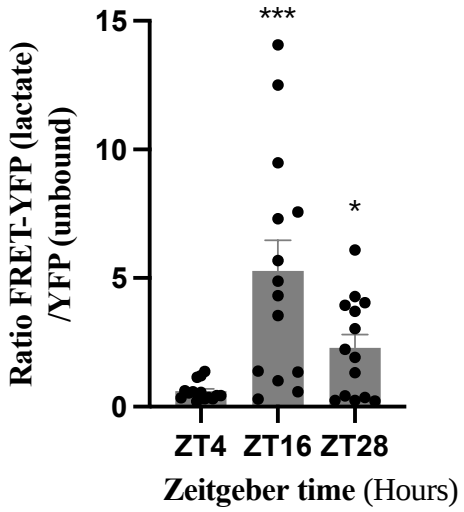


Figure 6.18: LDHA activity is rhythmic over 36 hours in synchronized MIN6 cells. Laconic biosensor was used to indicate cytosolic lactate content over 24 hours. Cells were imaged by FRET-based microscopy. Quantification of FRET emission in 8-10 random field across 3 independent experiments where the FRET YFP (Lactate) signal was divided by the YFP (unbound biosensor). Date are Mean ± SEM. ***p < 0.001. P-value represents statistical significance after a 2 tailed student's t-test

6.4 Discussion

In this chapter, we set out to investigate the role of pancreatic β-cell clock in regulating diurnal patterns of *Ucp2* expression and potentially other important metabolic regulators of the β-cell (i.e., *Ldha)* over 24 hours to better understand what drives these important biological rhythms. To accomplished this, we established two models: 1) an *in vitro* model of circadian dysfunction using siRNA knockdown *Bmal1* in MIN6 cells; and 2) an *in vivo* model of β-cell circadian deficiency (*Bmal1*βKO mouse model) that were used to test if the β-cell circadian clock controlled *Ucp2*/UCP2 expression and activity contributing to the alignment of GSIS rhythms in a time-of-day specific manner.

Our studies have shown that synchronized MIN6 cells express diurnal rhythms of circadian clock genes, including *Bmal1* **[Figure 6.1]**, which aligns with previous studies that show circadian rhythms in fibroblasts

(Greco et al., 2014), further demonstrating the validity of using this model to study circadian cycles in the β-cells. Using this model, we showed that *Bmal1* knockdown reduced glucose-induced ATP content at ZT4, resulting in impaired insulin secretion at a time point when insulin secretion capacity should be robust **[Figure 4.2A].** Furthermore, we observed a significant upregulation *of Ucp2* at ZT 4 in *Bmal1*-deficient cells **[Figure 6.10A and B].** Although, *Ucp2* upregulation has been previously reported in islets isolated from whole *Bmal1*$^{-/-}$ mice, β-cell-specific *Bmal1* knockout mouse and shRNA-mediated *Bmal1* knockdown in INS-1 cells (Lee et al., 2011, Lee et al., 2013), these studies as its main findings focussed on oxidative stress as a consequence of a dysfunctional β-cell clock. These previous studies demonstrated that oxidative stress (increased ROS production) resulted in insulin secretion defects and *Ucp2* upregulation. In other words, *Ucp2* upregulation was reported to be more of a *consequence* of oxidative stress resulting in mitochondrial OXPHOS dysfunction and impairing insulin secretion rather than a driver of rhythmic GSIS. Although in our study, we did not measure ROS production in our *Bmal1* deficient MIN6 models, we did show that a dysfunction β-cell clock results in loss of rhythmic *Ucp2* expression, leading to reductions in ATP content and impaired GSIS. The Lee et al (2013) further demonstrated that a loss of *Bmal1*-mediated control of the antioxidant system via dysfunctional NRF2 expression was the molecular mechanism that drove oxidative stress in β-cell-specific *Bmal1* knockout mouse model. Although we do not focus on NRF2 in our studies, we do show, in chapter 5, that diurnal rhythms in *Ucp2*/UCP2 expression and activity are required for control of GSIS rhythms. Furthermore, loss of rhythmic *Ucp2* expression may also contribute to an uncontrolled ROS generation leading to oxidative stress described in the previous studies (Bouillaud, 2009); however, this was not explored here. Data from our studies could add to the idea that diurnal cycles of ROS production may control UCP2 activity which in turn endogenously regulates insulin secretion capacity in a time-of-day dependent manner. However, the series of events that occurs in models of chrono-disruption whether 1.) circadian deficiency inducing *Ucp2* expression results in impairments ROS production or 2.) circadian deficiency result in uncontrolled ROS production (oxidative stress) which activates *Ucp2* expression.

Additionally, the previous study by Lee et al in 2013, demonstrated direct binding of BMAL1 to E-box elements in the cis-promoter region of Nrf2, an antioxidant response element (ARE) transcription factor that critically regulates antioxidant gene expression potentially regulating ROS signals in a diurnal cycle, which may then be the signal to control UCP2 (Lee et al., 2013). We set out to determine if the circadian clock drives *Ucp2* expression via direct binding of *Bmal1* to E-box elements in the *Ucp2* promoter. To this effect Lee et al (2013) performed chromatin immunoprecipitation (ChIP) assays using INS-1 cells (unsynchronized, at a single time point) (Lee et al., 2013). No enrichment of BMAL1 at the *Ucp2* promoter was observed, suggesting that the circadian oscillator does not directly drive the temporal expression of *Ucp2* but rather, it is likely that secondary signals or other transcription factors that are themselves circadian clock-driven are the driving force behind rhythmic *Ucp2* expression. However, it cannot be discounted that BMAL1-CLOCK complexes have significantly

different chromatin binding properties at different times of the day (Trott and Menet, 2018) and that assessment of CLOCK-BMAL1 binding to the UCP2 promoter should be assessed over a daily time course. It should be noted that we attempted to perform these experiments, but due to technical issues with the antibody, we were not able to complete these studies. However, future endeavours should include examination of the *Ucp2* promoter and determine what binds at this locus in a time-of-day manner (i.e., temporal ChIP-seq). While direct binding of BMAL1 to *Ucp2* is an attractive possibility, as mentioned in chapter 4 discussion, it is also possible that temporal *Ucp2* expression is dictated by daily fluctuations in fasting/feeding rhythms and nutrient availability. Importantly, several regulators of *Ucp2*, including SIRT1, PGC-1α, and SREBP1c, are expressed in a circadian fashion in other metabolic tissues (Asher and Schibler, 2011), but this level of regulation has not been further explored in a β-cell context. The regulation of *Ucp2* via one of the above-mentioned players is yet another possibility to be explored.

In addition to examining the impact of circadian disruption on insulin secretion, we also examined how *Bmal1* deficiency influenced glucose oxidation in synchronized MIN6 cells. We observed significant reduction in basal glucose oxidation rate (as measured by oxygen consumption rate in the presence of glucose), ATP production, and maximal respiration in *Bmal1*-deficient cells at ZT4. To understand if the reduced oxidation rate of glucose was associated with changes in expression in glucose transporter (*Glut2*), we measured *Glut2* expression using qPCR in our *Bmal1*-deficient MIN6 cells and found disruptions in its diurnal expression pattern when compared to control cells at ZT4. Although, we did not measure glucose uptake directly in our cells, we observed diurnal mRNA expression of the gene encoding the main glucose transporter in the β-cell, *Glut2*, which was completely abrogated when the circadian clock was disrupted in the *Bmal1*-deficient state. This finding is in line with previous studies in the literature, which showed diurnal changes in *Glut2* expression in islets isolated from whole body *Bmal1*-deficient mice (Frese et al., 2007). This discrepant finding could be the result of differences in sampling approaches for the two studies (i.e., the Lee et al study only examined *Glut2* expression at a single time point whereas we looked at two time points 12 hours apart), or this discrepant result could be due to differences in the models used (whole body *Bmal1* knockout vs *Bmal1* knockdown in MIN6 cells). In addition to assessment of *Glut 2* levels, we also examined *Cpt1a* and *Ldha* mRNA in *Bmal1*-deficient cells and observed disruption in the expression patterns of both of these genes. More specifically, *Bmal1* deficiency increased the expression of these genes at ZT 4 without affecting gene expression at ZT 16. Importantly, the rhythmic expression of *Ldha* in synchronized MIN6 cells and islets isolated from C57BL6 mice is a novel finding as this gene was reported to be "disallowed" and expressed at constitutively low levels in in mature pancreatic β-cells. This finding suggests that *Ldha* may have a dynamic role in the β-cell and may contribute to diurnal cycles of β-cell metabolism and control of insulin secretion.

In addition to creating an *in vitro* model, we also created and characterized a novel β-cell specific *Bmal1* knockout mouse that utilizes the *Ins1*-Cre promoter to knock *Bmal1* out of the β-cell. While previous studies have created and characterized a β-cell-specific *Bmal1* knockout, these studies used the *Ins2*-Cre or *RIP*-Cre mouse to drive Bmal1 deletion in the β-cell (Rakshit et al., 2016a, Lee et al., 2013). which is complicated by *Ins2*-Cre expression in some of the glucose-sensing regions of the brain (Wicksteed et al., 2010), Although the identity, function, and contribution of the *Ins2*-expressing neurons to glucose sensing in the hypothalamus remains unknown, we cannot rule out that *Bmal1* deletion in the brain may contribute to the results of these previous studies, particularly the assessment of whole-body glucose tolerance. To overcome the limitations of using the *Ins2*-Cre model, we used *Ins1*-Cre to knockout *Bmal1* in the pancreatic β-cell. Like the previous studies that characterized β-cell-specific *Bmal1* knockout mouse, no differences were found in body weight between controls and *Bmal1*βKO. Weekly fasted blood glucose levels were significantly increased in *Bmal1*βKO compared to *Cre* and *Flox* controls.

Unlike previous studies which used only male mice, we performed our studies in both male and female mice to determine if sex-specific differences could be delineated. Interestingly, in our model we observed that fasting hyperglycemia is more profound and does not resolve throughout 13 weeks (period of measurement) in the *Bmal1*βKO female mice: however, blood glucose levels become comparable between genotypes in male mice from week 9 onwards. Fasting hyperglycemia become less profound as they age in *Bmal1*βKO males. Differences in the trends in fasted blood glucose between the genotypes observed in males and females could be attributed to differences in physiology, as we know both differences in sex and age have an impact on circadian alignment (Duffy et al., 2011). All previous studies that have shown differences in fasted blood glucose levels in *Bmal1*βKO have done the studies at 8 weeks. *Bmal1*βKO mice (both male and female) show significantly higher fasted blood glucose levels at 8 weeks showing phenotypes previously observed in *Bmal1*βKO models. We chose to do our assessments at 12 weeks to be able to correlate the phenotype with our *Ucp2*βKO study in chapter 4.

Although, *Bmal1*βKO showed no differences in fasted blood glucose levels at 12 weeks, they were significantly glucose intolerant when compared to both *Cre* and *Flox*. *Bmal1*βKO were glucose intolerant at both 10am and 10pm (male and female mice) compared to *Cre* and *Flox*. We found no differences in insulin tolerance test in *Bmal1*βKO (male and female) at 10am. We were not able to perform ITTs at 10pm as blood glucose levels dropped low to 1-2mM after 30 mins of insulin injections. This finding is in line with previously established circadian rhythms in insulin tolerance such that there is an increase in insulin tolerance in the active portion of the day when food intake is anticipated (Lee et al., 1992, Pisu et al., 1980). Collectively, our glucose tolerance and insulin tolerance studies suggest that *Bmal1* knockout (driven by *Ins1*-Cre-mediated recombination) causes chronic glucose intolerance without accompanying changes in insulin tolerance, suggesting that *Bmal1* knockout in the β-cell drives a primary insulin secretion defect, which is supported by previous studies in the literature that

knock out of *Bmal1* in the β-cell using the *Ins2*-Cre system (Lee et al., 2011, Lee et al., 2013, Marcheva et al., 2010).

In accordance with our study described in chapter 4, we found rhythmic insulin secretion from islets isolated from *Bmal1*$^{F/F}$ at 10am and 10pm. Islets isolated all three genotypes showed no impairments in insulin secretion and ATP content at 10am, which corresponds to the inactive/fasting phase of the day when insulin secretion capacities were supressed **[Figure 6.14].** Impairments in insulin secretion observed in *Bmal1*βKO was mediated by differences in glucose-stimulated ATP production at 10pm. Additionally. in both models defects in insulin secretion and glucose-stimulated ATP production were rescued by inhibition of UCP2 using Genipin, suggesting that BMAL1 deficiency leads to impaired GSIS and ATP via upregulation of *Ucp2* **[Figure 6.10A and B],** which is supported by previous findings (Lee et al., 2011, Lee et al., 2013). We can conclude that both from our *in vitro* model of circadian dysfunction and *ex vivo* islets from pancreatic β-cell clock knockout out mouse model that β-cell clock regulates rhythms in insulin secretion via fine tuning *Ucp2*/UCP2 expression/activity.

It is important to note that the previous studies have shown that *Bmal1* deficiency upregulates UCP2 and suggests that this is a chronic pathological mechanism. A significant strength of our study is the use of two time points, 12 hours apart. This suggests that *Bmal1* deficiency only has pathological consequences for 12 hours of the day, specifically in the active/fed phase of the day when UCP2 suppression is required for maximal GSIS capacity. Together, these studies demonstrate that regulation of rhythmic insulin secretion capacity and ultimately temporal glucose tolerance are dependent on the rhythmic expression and activation of key proteins (UCP2, in this case) that regulate glucose-stimulated ATP production. Inhibiting the upregulation of *Ucp2* in our *in vitro* and *in vivo* model of circadian dysfunction rescued insulin secretion defects highlighting the therapeutic benefits of this molecular target. However, given the novel physiological function of UCP2 described in detail in chapter 4, targeting *Ucp2*/UCP2 as a therapy for T2D or other metabolic diseases must consider the rhythmic nature of its expression and its impact on glucose tolerance over 24 h, specifically during the fasted phase.

While the studies presented in this chapter provide data to support the fact that pancreatic β-cell clock regulated UCP2, we have yet to convincingly demonstrate that BMAL1 directly interacts with UCP2. This piece of information is crucial to directly link BMAL1 to UCP2 at a molecular level. A strength of this study is the attempt to study both female and male mice for this part of the study, but further analysis needs to be performed to confirm sex specific differences bearing in mind that circadian rhythms are different in men and women. Further addition to data interpretation would be to add a few timepoints on 24 hours spectrum which would no doubt provide more value to the study. However, it should be recognized as a strength because previous studies that attempted to study the connection of *Bmal1* and β-cell function have only done so at one single static timepoint.

Chapter 7

Overall Discussion

7.1 Overview

At the outset of the study, we aimed to understand the physiological function of UCP2 in the pancreatic β-cell. Numerous gain-of-function (Chan et al., 1999, Chan et al., 2001, Hong et al., 2001, Kashemsant and Chan, 2006, McQuaid et al., 2006) and loss-of-function (Zhang et al., 2001, Joseph et al., 2004, Joseph et al., 2002, Lee et al., 2009, Robson-Doucette et al., 2011) studies have interrogated the impact of UCP2 on β-cell function and, for the most part, have established a negative relationship between UCP2 and GSIS (Affourtit et al., 2011, Chan and Kashemsant, 2006, Fleury et al., 1997). Additionally, *Ucp2* upregulation has been observed in models of T2D and β-cell dysfunction. While there appears to be a pathological mechanism of increased UCP2 expression, specifically related to β-cell dysfunction in diabetes, these findings were considered to be perplexing and prompted researchers to question what the evolutionary significance of UCP2 was in the β-cell. In 2008, Sheets et. al. postulated that UCP2 plays an important physiological role in starvation. They demonstrated that starved *Ucp2*$^{-/-}$ mice exhibit higher serum insulin levels, blunted peripheral lipolysis and hepatic lipid utilization, along with lower blood sugar compared to wildtype mice. These findings suggested that UCP2 evolved in the β-cell to control insulin secretion during starvation such that UCP2 upregulation suppresses insulin and therefore the peripheral effects of insulin, ultimately accommodating the switch from glucose to fatty acid utilization during starvation. This study highlights the importance of UCP2 expression and UCP2-mediated control of insulin secretion during starvation as a protective mechanism to prevent hypoglycemia during prolonged periods of fasting (Sheets et al., 2008). Ultimately, the results from this study laid the foundation for our hypothesis that UCP2 plays an important physiological role during daily cycles of acute fasting such that UCP2 expression in the β-cell is dynamic and rhythmic, which is necessary for the control of diurnal cycles of insulin secretion capacity and glucose tolerance.

Using synchronized MIN6 clonal β-cells and islets isolated from β-cell-specific *Ucp2* knockout mice, we demonstrated that *Ucp2* expression is rhythmic in the pancreatic β-cell and that daily cycles of GSIS capacity are dependent on the cycle of *Ucp2* expression. Furthermore, we showed that rhythmic *Ucp2* expression also regulates daily cycles of glucose tolerance, such that loss of cycling *Ucp2* expression impaired glucose tolerance, specifically in the fasted or inactive phase of the daily cycle. Surprisingly, impaired glucose tolerance during the fasted/inactive phase in *Ucp2*βKO mouse correlated with enhanced insulin secretion at the same time of day. The enhanced insulin secretion in islets isolated from *Ucp2*βKO mice observed during the light/inactive phase was attributed to intra-islet ROS signalling resulting from increased glucagon secretion, a mechanism previously described in Robson-Doucette et al, 2011 (Robson-Doucette et al., 2011). Additionally, we were able to use mitochondrial membrane potential as a surrogate marker to demonstrate that cycles of *Ucp2* gene expression translate into changes in mitochondrial uncoupling activity by UCP2.

Further experimentation using our model systems (synchronized MIN6 cells and isolated islets) revealed important UCP2-mediated metabolic signals that contribute to the control of daily cycles of GSIS capacity, namely, ATP and ROS. Although the impact of UCP2 on ATP regulation in β-cells was previously debatable in the literature as some research groups demonstrated that *Ucp2* knockout augments ATP production (Zhang et al., 2001, Joseph et al., 2004), while others have demonstrated no impact on ATP (Robson-Doucette et al., 2011, Bouillaud, 2009). In this study, we demonstrate that the impact of UCP2 on glucose-induced ATP production varies in a dynamic and predictable manner over the 24h time course, suggesting that the previous discrepancies that existed in the literature may relate to time-of-day differences in experimentation. The impact of *Ucp2* expression on ROS regulation in β-cells has been extensively studied and well established. Traditionally, it has been shown that acute overexpression of *Ucp2* protects β-cells from oxidative damage (Li et al, 2001), while *Ucp2* knockout increases ROS production (Lee et al., 2009, Robson-Doucette et al., 2011, Negre-Salvayre et al., 1997). Additionally, acute and mild exposure to H_2O_2, a form of ROS, has been shown to augment insulin secretion in *in vitro* models (Rhee, 2006) as well in islets isolated from WT mice, suggesting that ROS signaling can augment insulin secretion (Robson-Doucette et al., 2011). What remained to be determined was how does rhythmic *Ucp2*/UCP2 expression/activity impact ROS signaling in the β-cell and how does this in turn contribute to the control of daily cycles of GSIS capacity? In our study, we showed that ROS levels is increased when insulin secretion are robust and decreased ROS levels are found correlated to reduced insulin secretion. It is plausible that when ROS production is beyond a certain threshold it activates UCP2 leading to the decrease ROS production and ultimately insulin secretion. This is the first study to demonstrate that UCP2 mediates ROS production in a dynamic manner over 24 hours and ultimately regulates insulin secretion in a time-of-day-dependant manner.

In addition to the regulation of mitochondrial ROS and ATP production, UCP2 has been shown to influence the rate of cellular proliferation in mouse embryonic cells and CHOK1 cells which in turn associates with mitochondrial fuel selection; that is, increased UCP2 expression was associated with increased fatty acid oxidation, which supported greater rates of cellular proliferation in CHOK1 cells (Pecquer et al, 2007). While we did not measure rates of proliferation in our study, we did measure fuel oxidation capacities at two timepoints over the 24-hour period and showed that UCP2 expression levels correlated strongly with rates of glucose and fatty acid oxidation such that lower expression levels of UCP2 correlated with increased rates of glucose oxidation while higher UCP2 expression correlated with increased rates of fatty acid oxidation. We further demonstrated that the expression of both glucose and fatty acid transporters are dynamically expressed over 24hours and fit with this pattern of fuel oxidation. Furthermore, using our synchronized MIN6 cell model, we demonstrated that the capacity to oxidise glucose is greater at ZT 4 than ZT 16 and that fatty acid oxidation is greater at ZT 16 than ZT 4, which is in line with the dynamic transporter expression. Importantly, one postulated biochemical function

of UCP2 is that of a fatty acid transporter and may serve as an explanation for the observed increase in fatty acid oxidation when *Ucp2* expression is elevated. The above finding needs to be further explored. Taken together, our results demonstrate that dynamic *Ucp2 e*xpression is not only required to regulate dynamic daily cycles of insulin secretion capacity, but also to regulate daily cycles of mitochondrial fuel selection, disruption of which may significantly impair GSIS and ultimately contribute to diabetes development; however, this remains to be explored.

After examination of the daily cycles of *Ucp2* expression in the β-cell and the possible mechanisms that link rhythmic *Ucp2* to rhythmic GSIS capacities, the next obvious question was to ask: what regulates dynamic cycles of *Ucp2* expression over 24hours? We hypothesized that the β-cell circadian clock drove daily cycles of *Ucp2* expression. The β-cell clock is essential for the proper regulation of insulin secretion over 24 hours (Lee et al., 2011, Lee et al., 2013, Marcheva et al., 2010) and disruption of the β-cell clock results in mitochondrial uncoupling and impairments in GSIS (Lee et al., 2013). In this thesis, we showed in both *in vitro* and *in vivo* model of circadian dysfunction, the loss of circadian cycles in the β-cell impacts *Ucp2* expression and insulin secretion. We have shown that loss of BMAL1 disrupts *Ucp2* expression patterns such that UCP2 expression is chronically upregulated over 24 hours **[Figure 6.10A and B]**. Loss of rhythmic *Ucp2* in this context resulted in a loss of daily cycles of ATP and GSIS. In addition to *Ucp2*, β-cell circadian dysfunction dysregulates other important metabolic players, such as *Cp1-1a and Slc2a2* transporters (fatty acid and glucose), which have been previously reported to have a diurnal rhythm **[Figure 6.16]**. Dysregulation in the expression of the genes encoding fuel transporters may emphasize that defects in insulin secretion in *Bmal1*β KO models could be attributed to fuel sensing defects. An interesting finding in this circadian-deficient model was the observed chronic upregulation *Ldha*. Importantly, we demonstrated in control MIN6 cells and wild type islets that *Ldha* expression and activity displays a diurnal pattern similar to that of *Ucp2*. This was surprising because *Ldha* has been described as a 'disallowed gene' (Schuit et al., 2012) in the β-cell meaning that its expression is suppressed in functionally mature β-cells. Our data suggests that daily fluctuations in *Ldha*/LDHA expression/activity are inversely related to GSIS rhythms. One explanation for the above statement is the plausible shunting of the incoming glucose away from entering TCA cycle for insulin secretion thereby reducing it. However, we do not show any physiological function for *Ldha* in our study beyond its rhythms in expression and activity and our hypothesis for *Ldha* as a regulator of insulin secretion is speculative at this point. An important thing to keep in mind is that the *Ldha* shunt is just one of many metabolic regulatory steps that could be functioning together to regulate physiologically appropriate insulin secretion responses in a time-of-day dependant manner, which is worthy of further exploration.

Taken together, we have sufficiently addressed the three main specific aims of this these that were initially stated in chapter 2. We have, for the first time, demonstrated that *Ucp2* expression/activity is rhythmic in

pancreatic β-cell and regulates insulin secretion capacity dynamically over 24 hours, ultimately regulating glucose tolerance in a time-of-day dependant manner. Secondly, we show that *Ucp2* regulates insulin secretion capacity via its effects on glucose-induced ATP and ROS production. Thirdly, the β-cell clock regulates diurnal cycles of insulin secretion via fine tuning *Ucp2*/UCP2 expression/activity **[Figure 7.1]**. To reiterate, we have shown that pancreatic β-cell clock regulates rhythmic insulin secretion capacities via fine tuning Ucp2 mRNA expression which is in turn modulated by ATP, ROS and fuel metabolism.

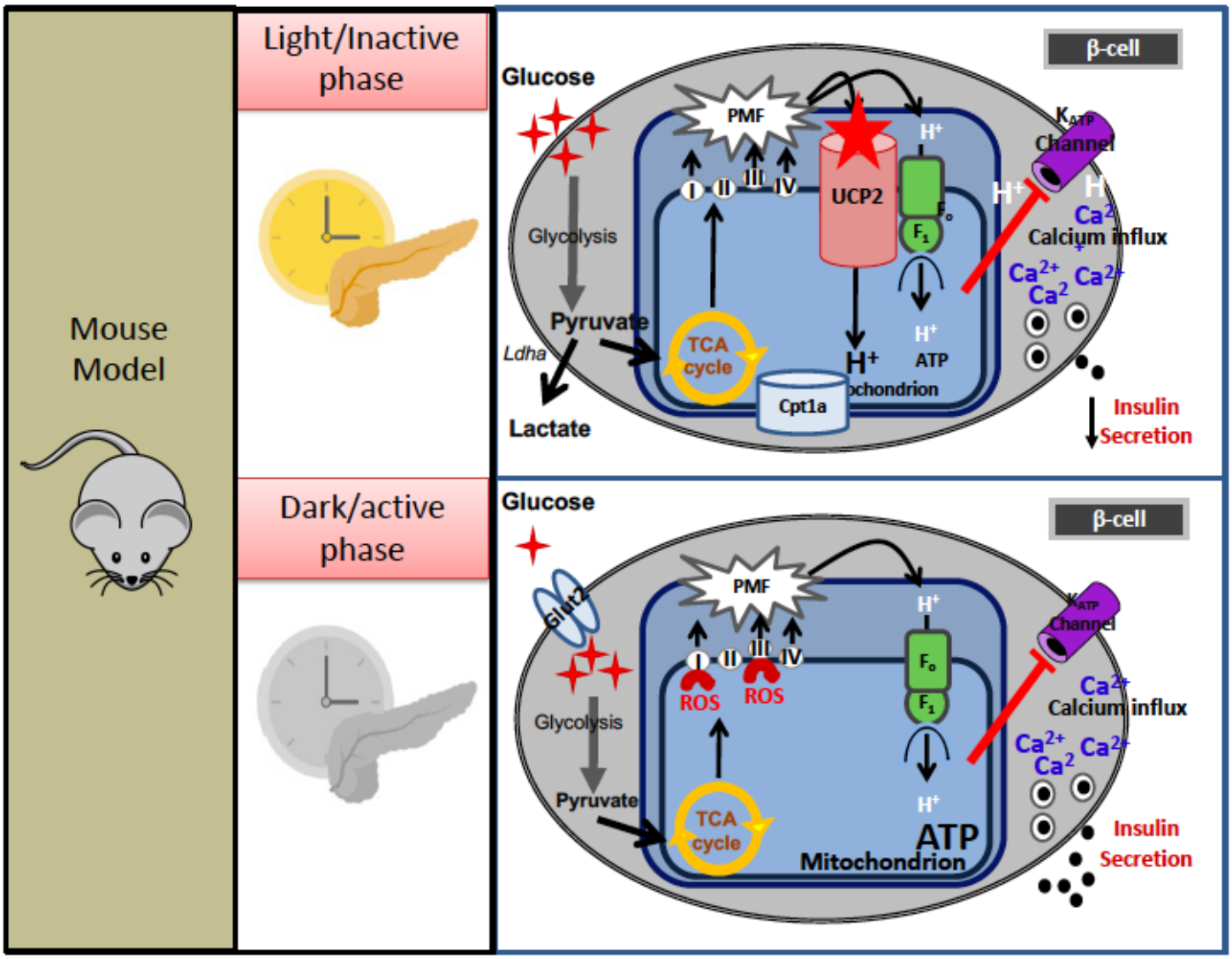


Figure 0.1: Pancreatic β-cell clock regulates insulin secretion via UCP2. Using a combination of *in vitro* and *in vivo* mouse models, we have shown that the pancreatic β-cell clock regulates dynamic cycles of insulin secretion capacities. In the dark/active phase, β-cell display robust insulin secretion capacities. *Glut2* mRNA expression is significantly elevated resulting in increased glucose-sensing leading to increased ROS production (increased glucose oxidation) and ATP production. In the light/inactive phase, β-cell experience suppressed insulin secretion. *Glut2* mRNA expression is reduced, *Ldha* mRNA expression is elevated, potentially shunting the glucose molecule towards anaerobic respiration. Concomitantly, *Ucp2* mRNA expression was elevated

resulting in decreases in ROS production (decreased glucose oxidation) and ATP production. *Cpt-1a* mRNA expression was found to be elevated at this time of day.

7.2 Strengths and Limitations

7.2.1 Strengths

All studies to date that have aimed at understanding the physiological role of UCP2 in the β-cell have been done so in the context of either loss- or gain-of-function models or in supra- or pathophysiological models, including models of diabetes or extreme starvation. There are limitations associated with utilizing chronic genetic or supraphysiological models to study the physiological function of a gene product, especially if the gene has a circadian function in the cell. That is, chronic suppression or overexpression will prevent examination of fluctuations in the gene of interest that naturally occur over 24 hours. Rather than chronically overexpressing or knocking out *Ucp2*, this study measured natural *Ucp2* expression levels in healthy β-cell over 24 hours for the first time. This approach clearly demonstrated that *Ucp2* expression is dynamic over 24 hours, allowing us to define a physiological function for UCP2 in the β-cell as a cell-autonomous regulator of daily cycles of insulin secretion capacity and ultimately time-of-day glucose tolerance. In addition to demonstrating an important physiological function for UCP2 in the β-cell, the research outlined in this PhD thesis emphasizes that time of day can impact gene expression and function, demonstrating the importance of using temporal approaches to study the function of genes; particularly metabolic genes, as it has been shown that a substantial number of metabolic genes are circadian-regulated (Perelis et al., 2015, Petrenko et al., 2020). While interpreting physiological function for a gene with metabolic functions it is imperative to consider the time of day during which the experiments were performed. In our study we studied the expression of *Ucp2* across 10 time points (0, 4, 8, 12, 16, 20, 24, 28, 32 and 36-hours post synchronization) in our *in vitro* model and 6 time points (10am, 2pm, 6pm, 10pm, 2am, 6am) in our *in vivo* model. The use of such an elaborate study design and the results obtained herein indicate that the time of day in which analyses are done can dramatically impact experimental outcomes and interpretation, and time of day should be considered in study design.

Another strength of this study is the use of multiple model systems, including both *in vitro* and *in vivo* genetic manipulations as well as studies that employ pharmacological inhibitors. The use of multiple approaches allows confidence in data interpretation as pharmacological inhibitors can have off-target effects and genetic manipulation can be "leaky". For example, it has been shown that the *Ins2*-Cre model drives recombination and knockout in glucose-sensing neurons in the hypothalamus, as well as in the pancreas (Wicksteed et al., 2010). The use of multiple models, all demonstrating the same phenomena, allows us to be confident that these potential off-target issues do not influence our conclusions and data interpretation.

Furthermore, most *Bmal1*$^{-/-}$ and β-cell specific *Bmal1*KO studies have performed experiments at only a single, static time point and some studies do not specifically state the time of day, making interpretation of these studies challenging. In the *in vivo* experiments outlined in this substantial body of work, we collected islets from *Ucp2*βKO and *Bmal1*βKO mouse at different time points spread across both the active/dark and inactive/light phase of the day, giving more credit to the physiological interpretations. Most interpretations made in the traditional circadian knockout models have been done by comparing the control and knockout mouse lines and often perform experiments only at one static time point (in the fasting phase) (Lee et al., 2011, Lee et al., 2013, Marcheva et al., 2010). In addition to performing experiments at several time points in the day, we were also able to address sex-specific difference in chapter 6 of this thesis. We observed sex-specific differences in fasted blood glucose that remained significant throughout the 6-11 weeks of measurement. Profound differences in fasted blood glucose that were observed in *Bmal1*βKO males at 8 weeks disappeared as the mice aged; however, this difference in fasted blood glucose normalised at 12 weeks in males. Differences in fasted blood glucose levels in males and females could be attributed to differences in physiology, as we know both differences in sex and age have an impact on circadian alignment (Duffy et al., 2011). Older men and women have weaker circadian entrainment and women have a shorter and earlier circadian clock than men (Morin et al., 1977). It is but common knowledge that circadian rhythms are different between men and women (Duffy et al., 2011) and these differences should be accounted for when designing models for scientific questions.

7.2.2 Limitations

In terms of limitations of this study, we acknowledge that the *Ucp2*βKO mouse used in chapter 4 and 5 of this thesis, was created using the *Ins2* promoter to drive cre recombinase expression. It has been demonstrated that *Ins2* is also expressed in glucose-sensing regions of the brain (Wicksteed et al., 2010) and it has been previously demonstrated that minor UCP2 deletion occurs in the hypothalamus of the *Ucp2*βKO mouse (Robson-Doucette et al., 2011). Although the identity, function, and contribution of the *Ins2*-expressing neurons to glucose sensing in the hypothalamus remains unknown, we cannot rule out that UCP2 deletion in the brain may contribute to the results of this study, particularly the assessment of whole-body glucose tolerance. Notably, we were able to demonstrate that daily rhythms of *Ucp2* expression contribute to daily cycles of GSIS capacity both in islets *ex vivo* as well as in clonal cell lines; models that are removed from central nervous system influence. The use of an *Ins*-cre model for β-cell-specific *Ucp2* deletion (as *Ins1* is not expressed in the brain (Johnson, 2014)) is suggested to validate the glucose tolerance findings in this paper.

An additional limitation to these studies is that some of the experiments outlined in chapter 5 that explore the mechanistic role of UCP2 in regulating diurnal cycles of GSIS have only been performed in our *in vitro* MIN6 cell model. Notably, despite their ability to secrete insulin in response to glucose stimuli, *in vitro* clonal β-cell models do not fully recapitulate primary cell physiology. While further studies are warranted in a more

physiologically relevant model (mouse or human islets), we do know most pathways are conserved across species. We have substantial evidence from human islet studies of rhythmic insulin secretion, clock gene expression and impairments in the above in models of T2D. We, however, lack the information on the involvement of *Ucp2*-mediated ATP and ROS regulation in human islets, which needs to be further explored. Although metabolic pathways are highly conserved, animal models would be a good starting point to provide rationale for study in precious human tissue.

Many experiments performed in this thesis have employed the use of Genipin to inhibit UCP2 in both MIN6 cells and islets outlined throughout the thesis. While the use of pharmacological drug inhibitors in general provides more stable and reliable inhibition when compared to the use of siRNAs which are more transient one cannot dismiss the limitation of using pharmacological drugs such as Genipin (drug used in the work outlined in this thesis). Genipin is a naturally occurring crosslinking agent isolated from the extract of *Gardenia jasminoides* (Ellis Fruit). One major limitation of Genipin is cross-linking activity producing adverse and non-specific impacts in the cell via interaction with other protein (Zhang et al., 2006). However, the cross-linking activity of Genipin is not responsible for inhibition of UCP2 but the above limitation cannot be overlooked.

7.3 Impact of COVID-19 pandemic on research and thesis.

This thesis would be incomplete if the impact of the COVID-19 pandemic was not addressed. COVID-19 pandemic has caused detrimental impact on human health both physical and mental primarily. Its impact on the completion of this study cannot be left unmentioned. When the COVID-19 pandemic hit, we were just beginning studies on circadian deficient animal model. We had just begun to characterise the animal model when non-essential research shutdown was put in place. We had to minimise animal colony to a maintenance level for 2-4 months. While the university was extremely gracious to offer a 4-month automatic extension to all doctoral students, I needed 2-3 months to revive the animal colony to yield enough. Additionally, we performed all experiments outlined in study 2 at 10am and 10pm which required that many more animals which takes both time and money to generate. Along with time, we also faced financial burden of culling animals at the time of shut down and investing money at the time of colony regeneration. However, I was able to complete all required experiments by the end of May 2020 and begin writing my thesis. Many follow up experiments had to be cancelled considering this impact of COVID-19.

7.4 Future Directions

The work described in this thesis is focussed on the mechanisms that regulate diurnal insulin secretion, including the role of the circadian clock. While our study demonstrates that knockout of the circadian clock in the β-cell (*Bmal1* knockout) impairs diurnal cycles of *Ucp2* and subsequent GSIS-regulating signals, it is not clear if the circadian machinery directly regulates the expression cycles of *Ucp2* or if this cyclic regulation of *Ucp2*

occurs though an indirect mechanism. We know that BMAL1 regulates its molecular targets by binding to regulatory E-box elements present in the promoter region of target genes. Notably, the *Ucp2* promoter contains tandem double E-box elements (Medvedev et al., 2002); however, chromatin immuno-precipitation (ChIP) of INS1 832/13 cells with anti-BMAL1 antibody and qPCR with primers flanking the putative BMAL1- binding E-Box elements did not show enrichment of UCP2 (Lee et al., 2013), suggesting that UCP2 may not be a direct transcriptional target of BMAL1. Notably, these studies were performed in an unsynchronized clonal β-cell line and temporal analyses in primary β-cells may yield different results, preventing the exclusion of this possibility. While circadian clock-controlled expression of UCP2 is an attractive possibility, it is also possible that temporal *Ucp2* expression is dictated by daily fluctuations in fasting/feeding rhythms and nutrient availability. Exposure to elevated free fatty acids induces upregulation and activation of UCP2 in β-cells (Joseph et al., 2004, Patane et al., 2002, Medvedev et al., 2002, Lameloise et al., 2001) and circulating levels of free fatty acids are significantly increased during fasting. Clearly, further studies are needed to determine what drives the daily cycles of *Ucp2* expression in the pancreatic β-cell, but nutritional and circadian cycles are a logical place to start.

In the experiments outlined in chapter 4 and 5, we have demonstrated that *Ucp2*βKO mice displayed impaired glucose tolerance despite experiencing augmented GSIS capacity, but only in the light phase on the daily cycle. No difference in glucose tolerance was observed in *Ucp2*βKO and *Ins2*-cre in the dark/active phase, a phase when both groups of mice displayed similar GSIS capacities and have low (or no) *Ucp2* expression. These findings suggest that β-cell *Ucp2* deletion does not chronically impair glucose tolerance but rather selectively contributes to the control of glucose tolerance in the light/inactive phase as the animal enters into an acute period of fasting. Based on our previous studies on the *Ucp2*βKO mouse, it would appear that β-cell *Ucp2*-mediated regulation of glucagon secretion is an important contributor to the control of glucose tolerance and in the light/inactive phase. The expression of *Ucp2* in the α cell and its effect on α cell function has been defined (Diao et al., 2008, Allister et al., 2013). Furthermore, glucagon secretion by the α-cell has been demonstrated to be diurnal (Petrenko et al., 2017) disrupted in T2D. However, it is not currently clear how rhythmic expression of *Ucp2* in the β-cell affects the 24-hour function of the α cell. Further experimentation is required to delineate this β-cell-*Ucp2*-α cell axis in the regulation of 24-hour glucose tolerance.

Bmal1 deficiency in β-cell results in oxidative stress and concomitant upregulation of *Ucp2*. While our results demonstrate that the regulation of *Ucp2*-mediated ROS production is diurnal and is an important mediator of diurnal cycles of GSIS, the role of circadian deficiency in UCP2-mediated ROS production over 24hours is not explored in this thesis. Additionally, we also show that *Bmal1* regulates rhythms in *Ucp2* expression/activity. Lee at al (2013) displayed diurnal *Ucp2* rhythms in Wildtype islets while showing an upregulation in Bmal1βKO islets, the paper did the experiments at only one static time point (light phase, when Ucp2 expression is increased

in expression). To further understand whether uncontrolled ROS activated UCP2 or loss of rhythms in *Ucp2* expression resulted in uncontrolled ROS production over 24hours, we require further experiments.

While we have shown that the β-cell circadian clock regulates insulin secretion capacities via *Ucp2*, recent studies have suggested that there are multiple pathways that are affected by the circadian clock. For example, transcriptional profiling of islets from C57BL6 mice every 4 hours over the light/dark cycle determined the detailed diurnal expression pattern of key transcripts and pathways. KEGG analysis of the profiles that peaked in the dark or at the onset of the dark phase (a time when food intake is anticipated and insulin demand and secretion capacity are greatest) revealed enrichment of a number of pathways that are critical for insulin secretion, including protein processing in the endoplasmic reticulum, insulin signaling, SNARE interactions in vesicular transport and oxidative phosphorylation. Conversely, in the light/inactive phase (or at the end of the dark phase), the most enriched pathways were related to positive regulation of the cell cycle and DNA repair. In support of this notion, disruption of the islet/ β-cell circadian oscillator in adult islets has been shown to alter the transcriptional profile of genes/pathways essential for cell cycle control and DNA repair. Furthermore, β-cell–specific *Bmal1* deletion attenuated the expression of various cell cycle activators, while increasing the expression of a number of cell cycle inhibitors, which was associated with reduced compensatory βcell proliferation and increased apoptosis when challenged with a high-fat diet (Rakshit et al., 2016a). Collectively, these findings illustrate a potentially critical role for the β-cell circadian oscillator in coordinating cycles of insulin secretion priming (within a time-limited window) followed by periods of insulin secretion suppression that are associated with recovery and growth. As such, circadian disruption, in addition to driving GSIS impairment, may also impact the ability of the βcell to recover from or respond to stress-induced DNA damage, leading to greater susceptibility to cellular dysfunction and apoptosis. These studies lay the foundation to the idea that the circadian clock potentially controls alternating cycles of proliferation and function. While the above experiments have been done either in islets isolated from wild-type mice which have intact circadian clock over multiple time points or circadian-deficient models at a single static time point, we have established a β-cell-specific *Bmal1*-deficient model in synchronized MIN6 cells which will aid us in making these comparisons within the same study. RNA seq in *Bmal1*siRNA transfected cells can be performed at different time points and compared to cells transfected with scrambled siRNA (Control) cells. Additionally, these studies can be done in islets isolated from *Ins1*-Cre and *Bmal1*βKO at 10am and 10pm. These findings will not only support already existing studies but will provide new insights into βcell circadian clock role and function.

Bibliography

AFFOURTIT, C. & BRAND, M. D. 2008a. On the role of uncoupling protein-2 in pancreatic beta cells. *Biochim Biophys Acta,* 1777**,** 973-9.

AFFOURTIT, C. & BRAND, M. D. 2008b. Uncoupling protein-2 contributes significantly to high mitochondrial proton leak in INS-1E insulinoma cells and attenuates glucose-stimulated insulin secretion. *Biochem J,* 409**,** 199-204.

AFFOURTIT, C., JASTROCH, M. & BRAND, M. D. 2011. Uncoupling protein-2 attenuates glucose-stimulated insulin secretion in INS-1E insulinoma cells by lowering mitochondrial reactive oxygen species. *Free Radic Biol Med,* 50**,** 609-16.

AGUAYO-MAZZUCATO, C., SANCHEZ-SOTO, C., GODINEZ-PUIG, V., GUTIERREZ-OSPINA, G. & HIRIART, M. 2006. Restructuring of pancreatic islets and insulin secretion in a postnatal critical window. *PLoS One,* 1**,** e35.

AGUILAR-BRYAN, L. & BRYAN, J. 1999. Molecular biology of adenosine triphosphate-sensitive potassium channels. *Endocr Rev,* 20**,** 101-35.

AGUILAR-BRYAN, L., NICHOLS, C. G., WECHSLER, S. W., CLEMENT, J. P. T., BOYD, A. E., 3RD, GONZALEZ, G., HERRERA-SOSA, H., NGUY, K., BRYAN, J. & NELSON, D. A. 1995. Cloning of the beta cell high-affinity sulfonylurea receptor: a regulator of insulin secretion. *Science,* 268**,** 423-6.

AINSCOW, E. K., ZHAO, C. & RUTTER, G. A. 2000. Acute overexpression of lactate dehydrogenase-A perturbs beta-cell mitochondrial metabolism and insulin secretion. *Diabetes,* 49**,** 1149-55.

ALLISTER, E. M., ROBSON-DOUCETTE, C. A., PRENTICE, K. J., HARDY, A. B., SULTAN, S., GAISANO, H. Y., KONG, D., GILON, P., HERRERA, P. L., LOWELL, B. B. & WHEELER, M. B. 2013. UCP2 regulates the glucagon response to fasting and starvation. *Diabetes,* 62**,** 1623-33.

AMERICAN DIABETES, A. 2016. 2. Classification and Diagnosis of Diabetes. *Diabetes Care,* 39 Suppl 1**,** S13-22.

ANTCLIFF, J. F., HAIDER, S., PROKS, P., SANSOM, M. S. & ASHCROFT, F. M. 2005. Functional analysis of a structural model of the ATP-binding site of the KATP channel Kir6.2 subunit. *EMBO J,* 24**,** 229-39.

ARNOUX, J. B., DE LONLAY, P., RIBEIRO, M. J., HUSSAIN, K., BLANKENSTEIN, O., MOHNIKE, K., VALAYANNOPOULOS, V., ROBERT, J. J., RAHIER, J., SEMPOUX, C., BELLANNE, C., VERKARRE, V., AIGRAIN, Y., JAUBERT, F., BRUNELLE, F. & NIHOUL-FEKETE, C. 2010. Congenital hyperinsulinism. *Early Hum Dev,* 86**,** 287-94.

ARSENIJEVIC, D., ONUMA, H., PECQUEUR, C., RAIMBAULT, S., MANNING, B. S., MIROUX, B., COUPLAN, E., ALVES-GUERRA, M. C., GOUBERN, M., SURWIT, R., BOUILLAUD, F., RICHARD, D., COLLINS, S. & RICQUIER, D. 2000. Disruption of the uncoupling protein-2 gene in mice reveals a role in immunity and reactive oxygen species production. *Nat Genet,* 26**,** 435-9.

ASAYAMA, K., KOOY, N. W. & BURR, I. M. 1986. Effect of vitamin E deficiency and selenium deficiency on insulin secretory reserve and free radical scavenging systems in islets: decrease of islet manganosuperoxide dismutase. *J Lab Clin Med,* 107**,** 459-64.

ASHCROFT, F. M. & GRIBBLE, F. M. 1999. ATP-sensitive K+ channels and insulin secretion: their role in health and disease. *Diabetologia,* 42**,** 903-19.

ASHCROFT, F. M. & GRIBBLE, F. M. 2000. New windows on the mechanism of action of K(ATP) channel openers. *Trends Pharmacol Sci,* 21**,** 439-45.

ASHCROFT, F. M., HARRISON, D. E. & ASHCROFT, S. J. 1984. Glucose induces closure of single potassium channels in isolated rat pancreatic beta-cells. *Nature,* 312**,** 446-8.

ASHCROFT, S. J., WEERASINGHE, L. C. & RANDLE, P. J. 1973. Interrelationship of islet metabolism, adenosine triphosphate content and insulin release. *Biochem J,* 132**,** 223-31.

ASHER, G. & SCHIBLER, U. 2011. Crosstalk between components of circadian and metabolic cycles in mammals. *Cell Metab,* 13**,** 125-37.

BALSALOBRE, A., BROWN, S. A., MARCACCI, L., TRONCHE, F., KELLENDONK, C., REICHARDT, H. M., SCHUTZ, G. & SCHIBLER, U. 2000. Resetting of circadian time in peripheral tissues by glucocorticoid signaling. *Science,* 289**,** 2344-7.

BARTER, P. J., CARROLL, K. F. & NESTEL, P. J. 1971. Diurnal fluctuations in triglyceride, free fatty acids, and insulin during sucrose consumption and insulin infusion in man. *J Clin Invest,* 50**,** 583-91.

BELEGRI, E., RIJNSBURGER, M., EGGELS, L., UNMEHOPA, U., SCHEPER, W., BOELEN, A. & LA FLEUR, S. E. 2017. Effects of Fat and Sugar, Either Consumed or Infused toward the Brain, on Hypothalamic ER Stress Markers. *Front Neurosci,* 11**,** 270.

BENSELLAM, M., DUVILLIE, B., RYBACHUK, G., LAYBUTT, D. R., MAGNAN, C., GUIOT, Y., POUYSSEGUR, J. & JONAS, J. C. 2012. Glucose-induced O(2) consumption activates hypoxia inducible factors 1 and 2 in rat insulin-secreting pancreatic beta-cells. *PLoS One,* 7**,** e29807.

BERARDI, M. J. & CHOU, J. J. 2014. Fatty acid flippase activity of UCP2 is essential for its proton transport in mitochondria. *Cell Metab,* 20**,** 541-52.

BINDOKAS, V. P., KUZNETSOV, A., SREENAN, S., POLONSKY, K. S., ROE, M. W. & PHILIPSON, L. H. 2003. Visualizing superoxide production in normal and diabetic rat islets of Langerhans. *J Biol Chem,* 278**,** 9796-801.

BLUM, B., HRVATIN, S., SCHUETZ, C., BONAL, C., REZANIA, A. & MELTON, D. A. 2012. Functional beta-cell maturation is marked by an increased glucose threshold and by expression of urocortin 3. *Nat Biotechnol,* 30**,** 261-4.

BORDONE, L., MOTTA, M. C., PICARD, F., ROBINSON, A., JHALA, U. S., APFELD, J., MCDONAGH, T., LEMIEUX, M., MCBURNEY, M., SZILVASI, A., EASLON, E. J., LIN, S. J. & GUARENTE, L. 2006. Sirt1 regulates insulin secretion by repressing UCP2 in pancreatic beta cells. *PLoS Biol,* 4**,** e31.

BOUILLAUD, F. 2009. UCP2, not a physiologically relevant uncoupler but a glucose sparing switch impacting ROS production and glucose sensing. *Biochim Biophys Acta,* 1787**,** 377-83.

BRAND, M. D. 2010. The sites and topology of mitochondrial superoxide production. *Exp Gerontol,* 45**,** 466-72.

BRAND, M. D. & ESTEVES, T. C. 2005. Physiological functions of the mitochondrial uncoupling proteins UCP2 and UCP3. *Cell Metab,* 2**,** 85-93.

BRICKER, D. K., TAYLOR, E. B., SCHELL, J. C., ORSAK, T., BOUTRON, A., CHEN, Y. C., COX, J. E., CARDON, C. M., VAN VRANKEN, J. G., DEPHOURE, N., REDIN, C., BOUDINA, S., GYGI, S. P., BRIVET, M., THUMMEL, C. S. & RUTTER, J. 2012. A mitochondrial pyruvate carrier required for pyruvate uptake in yeast, Drosophila, and humans. *Science,* 337**,** 96-100.

BROOKES, P. S., PARKER, N., BUCKINGHAM, J. A., VIDAL-PUIG, A., HALESTRAP, A. P., GUNTER, T. E., NICHOLLS, D. G., BERNARDI, P., LEMASTERS, J. J. & BRAND, M. D. 2008. UCPs--unlikely calcium porters. *Nat Cell Biol,* 10**,** 1235-7; author reply 1237-40.

BUNGER, M. K., WILSBACHER, L. D., MORAN, S. M., CLENDENIN, C., RADCLIFFE, L. A., HOGENESCH, J. B., SIMON, M. C., TAKAHASHI, J. S. & BRADFIELD, C. A. 2000. Mop3 is an essential component of the master circadian pacemaker in mammals. *Cell,* 103**,** 1009-17.

BUTLER, P. C., MEIER, J. J., BUTLER, A. E. & BHUSHAN, A. 2007. The replication of beta cells in normal physiology, in disease and for therapy. *Nat Clin Pract Endocrinol Metab,* 3**,** 758-68.

CANNON, B. & NEDERGAARD, J. 2004. Brown adipose tissue: function and physiological significance. *Physiol Rev,* 84**,** 277-359.

CARROLL, K. F. & NESTEL, P. J. 1973. Diurnal variation in glucose tolerance and in insulin secretion in man. *Diabetes,* 22**,** 333-48.

CAUMO, A. & LUZI, L. 2004. First-phase insulin secretion: does it exist in real life? Considerations on shape and function. *Am J Physiol Endocrinol Metab,* 287**,** E371-85.

CHAN, C. B., DE LEO, D., JOSEPH, J. W., MCQUAID, T. S., HA, X. F., XU, F., TSUSHIMA, R. G., PENNEFATHER, P. S., SALAPATEK, A. M. & WHEELER, M. B. 2001. Increased uncoupling protein-2 levels in beta-cells are associated with impaired glucose-stimulated insulin secretion: mechanism of action. *Diabetes,* 50**,** 1302-10.

CHAN, C. B. & KASHEMSANT, N. 2006. Regulation of insulin secretion by uncoupling protein. *Biochem Soc Trans,* 34**,** 802-5.

CHAN, C. B., MACDONALD, P. E., SALEH, M. C., JOHNS, D. C., MARBAN, E. & WHEELER, M. B. 1999. Overexpression of uncoupling protein 2 inhibits glucose-stimulated insulin secretion from rat islets. *Diabetes,* 48**,** 1482-6.

CHEN, H., CARLSON, E. C., PELLET, L., MORITZ, J. T. & EPSTEIN, P. N. 2001. Overexpression of metallothionein in pancreatic beta-cells reduces streptozotocin-induced DNA damage and diabetes. *Diabetes,* 50**,** 2040-6.

COOK, D. L. & HALES, C. N. 1984. Intracellular ATP directly blocks K+ channels in pancreatic B-cells. *Nature,* 311**,** 271-3.

COOMANS, C. P., VAN DEN BERG, S. A., LUCASSEN, E. A., HOUBEN, T., PRONK, A. C., VAN DER SPEK, R. D., KALSBEEK, A., BIERMASZ, N. R., WILLEMS VAN DIJK, K., ROMIJN, J. A. & MEIJER, J. H. 2013. The suprachiasmatic nucleus controls circadian energy metabolism and hepatic insulin sensitivity. *Diabetes,* 62**,** 1102-8.

COUPLAN, E., DEL MAR GONZALEZ-BARROSO, M., ALVES-GUERRA, M. C., RICQUIER, D., GOUBERN, M. & BOUILLAUD, F. 2002. No evidence for a basal, retinoic, or superoxide-induced uncoupling activity of the uncoupling protein 2 present in spleen or lung mitochondria. *J Biol Chem,* 277**,** 26268-75.

CROW, J. P. & BECKMAN, J. S. 1995. The role of peroxynitrite in nitric oxide-mediated toxicity. *Curr Top Microbiol Immunol,* 196**,** 57-73.

D'ADAMO, M., PEREGO, L., CARDELLINI, M., MARINI, M. A., FRONTONI, S., ANDREOZZI, F., SCIACQUA, A., LAURO, D., SBRACCIA, P., FEDERICI, M., PAGANELLI, M., PONTIROLI, A. E., LAURO, R., PERTICONE, F., FOLLI, F. & SESTI, G. 2004. The -866A/A genotype in the promoter of the human uncoupling protein 2 gene is associated with insulin resistance and increased risk of type 2 diabetes. *Diabetes,* 53**,** 1905-10.

DALLMANN, R., TOUMA, C., PALME, R., ALBRECHT, U. & STEINLECHNER, S. 2006. Impaired daily glucocorticoid rhythm in Per1 (Brd) mice. *J Comp Physiol A Neuroethol Sens Neural Behav Physiol,* 192**,** 769-75.

DAN DUNN, J., ALVAREZ, L. A., ZHANG, X. & SOLDATI, T. 2015. Reactive oxygen species and mitochondria: A nexus of cellular homeostasis. *Redox Biol,* 6**,** 472-485.

DANIEL, S., NODA, M., STRAUB, S. G. & SHARP, G. W. 1999. Identification of the docked granule pool responsible for the first phase of glucose-stimulated insulin secretion. *Diabetes,* 48**,** 1686-90.

DE STEFANI, D., RIZZUTO, R. & POZZAN, T. 2016. Enjoy the Trip: Calcium in Mitochondria Back and Forth. *Annu Rev Biochem,* 85**,** 161-92.

DELANEY, C. A., TYRBERG, B., BOUWENS, L., VAGHEF, H., HELLMAN, B. & EIZIRIK, D. L. 1996. Sensitivity of human pancreatic islets to peroxynitrite-induced cell dysfunction and death. *FEBS Lett,* 394**,** 300-6.

DELATTRE, E., CIPOLLA-NETO, J. & BOSCHERO, A. C. 1999. Diurnal variations in insulin secretion and K+ permeability in isolated rat islets. *Clin Exp Pharmacol Physiol,* 26**,** 505-10.

DETIMARY, P., GILON, P., NENQUIN, M. & HENQUIN, J. C. 1994. Two sites of glucose control of insulin release with distinct dependence on the energy state in pancreatic B-cells. *Biochem J,* 297 (Pt 3)**,** 455-61.

DIAO, J., ALLISTER, E. M., KOSHKIN, V., LEE, S. C., BHATTACHARJEE, A., TANG, C., GIACCA, A., CHAN, C. B. & WHEELER, M. B. 2008. UCP2 is highly expressed in pancreatic alpha-cells and influences secretion and survival. *Proc Natl Acad Sci U S A,* 105**,** 12057-62.

DIAO, L., MEI, Q., XU, J. M., LIU, X. C., HU, J., JIN, J., YAO, Q. & CHEN, M. L. 2012. Rebamipide suppresses diclofenac-induced intestinal permeability via mitochondrial protection in mice. *World J Gastroenterol,* 18**,** 1059-66.

DIBNER, C., SCHIBLER, U. & ALBRECHT, U. 2010. The mammalian circadian timing system: organization and coordination of central and peripheral clocks. *Annu Rev Physiol,* 72**,** 517-49.

DO, M. T. & YAU, K. W. 2010. Intrinsically photosensitive retinal ganglion cells. *Physiol Rev,* 90**,** 1547-81.
DOLINSKY, V. W., RUEDA-CLAUSEN, C. F., MORTON, J. S., DAVIDGE, S. T. & DYCK, J. R. 2011. Continued postnatal administration of resveratrol prevents diet-induced metabolic syndrome in rat offspring born growth restricted. *Diabetes,* 60**,** 2274-84.
DONG, K., NI, H., WU, M., TANG, Z., HALIM, M. & SHI, D. 2016. ROS-mediated glucose metabolic reprogram induces insulin resistance in type 2 diabetes. *Biochem Biophys Res Commun,* 476**,** 204-211.
DROGE, W. 2002. Free radicals in the physiological control of cell function. *Physiol Rev,* 82**,** 47-95.
DUFFY, J. F., CAIN, S. W., CHANG, A. M., PHILLIPS, A. J., MUNCH, M. Y., GRONFIER, C., WYATT, J. K., DIJK, D. J., WRIGHT, K. P., JR. & CZEISLER, C. A. 2011. Sex difference in the near-24-hour intrinsic period of the human circadian timing system. *Proc Natl Acad Sci U S A,* 108 Suppl 3**,** 15602-8.
DYACHOK, O., IDEVALL-HAGREN, O., SAGETORP, J., TIAN, G., WUTTKE, A., ARRIEUMERLOU, C., AKUSJARVI, G., GYLFE, E. & TENGHOLM, A. 2008. Glucose-induced cyclic AMP oscillations regulate pulsatile insulin secretion. *Cell Metab,* 8**,** 26-37.
ECHTAY, K. S., ESTEVES, T. C., PAKAY, J. L., JEKABSONS, M. B., LAMBERT, A. J., PORTERO-OTIN, M., PAMPLONA, R., VIDAL-PUIG, A. J., WANG, S., ROEBUCK, S. J. & BRAND, M. D. 2003. A signalling role for 4-hydroxy-2-nonenal in regulation of mitochondrial uncoupling. *EMBO J,* 22**,** 4103-10.
ECHTAY, K. S., ROUSSEL, D., ST-PIERRE, J., JEKABSONS, M. B., CADENAS, S., STUART, J. A., HARPER, J. A., ROEBUCK, S. J., MORRISON, A., PICKERING, S., CLAPHAM, J. C. & BRAND, M. D. 2002. Superoxide activates mitochondrial uncoupling proteins. *Nature,* 415**,** 96-9.
ECKEL-MAHAN, K. & SASSONE-CORSI, P. 2013. Metabolism and the circadian clock converge. *Physiol Rev,* 93**,** 107-35.
ELKSNIS, A., MARTINELL, M., ERIKSSON, O. & ESPES, D. 2019. Heterogeneity of Metabolic Defects in Type 2 Diabetes and Its Relation to Reactive Oxygen Species and Alterations in Beta-Cell Mass. *Front Physiol,* 10**,** 107.
ENKVETCHAKUL, D. & NICHOLS, C. G. 2003. Gating mechanism of KATP channels: function fits form. *J Gen Physiol,* 122**,** 471-80.
EVANS, J. L., GOLDFINE, I. D., MADDUX, B. A. & GRODSKY, G. M. 2003. Are oxidative stress-activated signaling pathways mediators of insulin resistance and beta-cell dysfunction? *Diabetes,* 52**,** 1-8.
FEDERATION, I. D. 2019:. IDF Diabetes Atlas. Brussels, Belgium.
FEDORENKO, A., LISHKO, P. V. & KIRICHOK, Y. 2012. Mechanism of fatty-acid-dependent UCP1 uncoupling in brown fat mitochondria. *Cell,* 151**,** 400-13.
FENG, Y., XIONG, Y., QIAO, T., LI, X., JIA, L. & HAN, Y. 2018. Lactate dehydrogenase A: A key player in carcinogenesis and potential target in cancer therapy. *Cancer Med,* 7**,** 6124-6136.
FLEKAC, M., SKRHA, J., HILGERTOVA, J., LACINOVA, Z. & JAROLIMKOVA, M. 2008. Gene polymorphisms of superoxide dismutases and catalase in diabetes mellitus. *BMC Med Genet,* 9**,** 30.
FLEURY, C., NEVEROVA, M., COLLINS, S., RAIMBAULT, S., CHAMPIGNY, O., LEVI-MEYRUEIS, C., BOUILLAUD, F., SELDIN, M. F., SURWIT, R. S., RICQUIER, D. & WARDEN, C. H. 1997. Uncoupling protein-2: a novel gene linked to obesity and hyperinsulinemia. *Nat Genet,* 15**,** 269-72.
FRESE, T., BAZWINSKY, I., MUHLBAUER, E. & PESCHKE, E. 2007. Circadian and age-dependent expression patterns of GLUT2 and glucokinase in the pancreatic beta-cell of diabetic and nondiabetic rats. *Horm Metab Res,* 39**,** 567-74.
FUSTIN, J. M., DOI, M., YAMAGUCHI, Y., HIDA, H., NISHIMURA, S., YOSHIDA, M., ISAGAWA, T., MORIOKA, M. S., KAKEYA, H., MANABE, I. & OKAMURA, H. 2013. RNA-methylation-dependent RNA processing controls the speed of the circadian clock. *Cell,* 155**,** 793-806.
GABLE, D. R., STEPHENS, J. W., COOPER, J. A., MILLER, G. J. & HUMPHRIES, S. E. 2006. Variation in the UCP2-UCP3 gene cluster predicts the development of type 2 diabetes in healthy middle-aged men. *Diabetes,* 55**,** 1504-11.

GALETTI, S., SARRE, A., PERRETEN, H., PRODUIT-ZENGAFFINEN, N., MUZZIN, P. & ASSIMACOPOULOS-JEANNET, F. 2009. Fatty acids do not activate UCP2 in pancreatic beta cells: comparison with UCP1. *Pflugers Arch,* 457**,** 931-40.

GALLEGO, M. & VIRSHUP, D. M. 2007. Post-translational modifications regulate the ticking of the circadian clock. *Nat Rev Mol Cell Biol,* 8**,** 139-48.

GEMBAL, M., GILON, P. & HENQUIN, J. C. 1992. Evidence that glucose can control insulin release independently from its action on ATP-sensitive K+ channels in mouse B cells. *J Clin Invest,* 89**,** 1288-95.

GILON, P. & HENQUIN, J. C. 1992. Influence of membrane potential changes on cytoplasmic Ca2+ concentration in an electrically excitable cell, the insulin-secreting pancreatic B-cell. *J Biol Chem,* 267**,** 20713-20.

GONZALEZ-BARROSO, M. M., GIURGEA, I., BOUILLAUD, F., ANEDDA, A., BELLANNE-CHANTELOT, C., HUBERT, L., DE KEYZER, Y., DE LONLAY, P. & RICQUIER, D. 2008. Mutations in UCP2 in congenital hyperinsulinism reveal a role for regulation of insulin secretion. *PLoS One,* 3**,** e3850.

GRANCHI, C., BERTINI, S., MACCHIA, M. & MINUTOLO, F. 2010. Inhibitors of lactate dehydrogenase isoforms and their therapeutic potentials. *Curr Med Chem,* 17**,** 672-97.

GRANKVIST, K., MARKLUND, S. L. & TALJEDAL, I. B. 1981. CuZn-superoxide dismutase, Mn-superoxide dismutase, catalase and glutathione peroxidase in pancreatic islets and other tissues in the mouse. *Biochem J,* 199**,** 393-8.

GRAPENGIESSER, E., GYLFE, E. & HELLMAN, B. 1990. Sulfonylurea mimics the effect of glucose in inducing large amplitude oscillations of cytoplasmic Ca2+ in pancreatic beta-cells. *Mol Pharmacol,* 37**,** 461-7.

GRASSO, S., MESSINA, A., SAPORITO, N. & REITANO, G. 1968. Serum-insulin response to glucose and aminoacids in the premature infant. *Lancet,* 2**,** 755-6.

GRECO, J. A., OOSTERMAN, J. E. & BELSHAM, D. D. 2014. Differential effects of omega-3 fatty acid docosahexaenoic acid and palmitate on the circadian transcriptional profile of clock genes in immortalized hypothalamic neurons. *Am J Physiol Regul Integr Comp Physiol,* 307**,** R1049-60.

GREELEY, S. A., TUCKER, S. E., NAYLOR, R. N., BELL, G. I. & PHILIPSON, L. H. 2010. Neonatal diabetes mellitus: a model for personalized medicine. *Trends Endocrinol Metab,* 21**,** 464-72.

GUNASEKARAN, U., HUDGENS, C. W., WRIGHT, B. T., MAULIS, M. F. & GANNON, M. 2012. Differential regulation of embryonic and adult beta cell replication. *Cell Cycle,* 11**,** 2431-42.

GURGUL-CONVEY, E., MEHMETI, I., LORTZ, S. & LENZEN, S. 2011. Cytokine toxicity in insulin-producing cells is mediated by nitro-oxidative stress-induced hydroxyl radical formation in mitochondria. *J Mol Med (Berl),* 89**,** 785-98.

HARMON, J. S., BOGDANI, M., PARAZZOLI, S. D., MAK, S. S., OSEID, E. A., BERGHMANS, M., LEBOEUF, R. C. & ROBERTSON, R. P. 2009. beta-Cell-specific overexpression of glutathione peroxidase preserves intranuclear MafA and reverses diabetes in db/db mice. *Endocrinology,* 150**,** 4855-62.

HARMON, J. S., STEIN, R. & ROBERTSON, R. P. 2005. Oxidative stress-mediated, post-translational loss of MafA protein as a contributing mechanism to loss of insulin gene expression in glucotoxic beta cells. *J Biol Chem,* 280**,** 11107-13.

HELLMAN, B. & TALJEDAL, I. B. 1967. Quantitative studies on isolated pancreatic islets of mammals. Activity and heterogeneity of lactate dehydrogenase in obese-hyporglycemic mice. *Endocrinology,* 81**,** 125-31.

HENQUIN, J. C. 2000. Triggering and amplifying pathways of regulation of insulin secretion by glucose. *Diabetes,* 49**,** 1751-60.

HERCHUELZ, A., POCHET, R., PASTIELS, C. & VAN PRAET, A. 1991. Heterogeneous changes in [Ca2+]i induced by glucose, tolbutamide and K+ in single rat pancreatic B cells. *Cell Calcium,* 12**,** 577-86.

HERZIG, S., RAEMY, E., MONTESSUIT, S., VEUTHEY, J. L., ZAMBONI, N., WESTERMANN, B., KUNJI, E. R. & MARTINOU, J. C. 2012. Identification and functional expression of the mitochondrial pyruvate carrier. *Science,* 337**,** 93-6.

HIBINO, H., INANOBE, A., FURUTANI, K., MURAKAMI, S., FINDLAY, I. & KURACHI, Y. 2010. Inwardly rectifying potassium channels: their structure, function, and physiological roles. *Physiol Rev,* 90**,** 291-366.

HILLS, C. E., YOUNIS, M. Y., BENNETT, J., SIAMANTOURAS, E., LIU, K. K. & SQUIRES, P. E. 2012. Calcium-sensing receptor activation increases cell-cell adhesion and beta-cell function. *Cell Physiol Biochem,* 30**,** 575-86.

HIRAO, A., TAHARA, Y., KIMURA, I. & SHIBATA, S. 2009. A balanced diet is necessary for proper entrainment signals of the mouse liver clock. *PLoS One,* 4**,** e6909.

HONG, Y., FINK, B. D., DILLON, J. S. & SIVITZ, W. I. 2001. Effects of adenoviral overexpression of uncoupling protein-2 and -3 on mitochondrial respiration in insulinoma cells. *Endocrinology,* 142**,** 249-56.

HOUSTIS, N., ROSEN, E. D. & LANDER, E. S. 2006. Reactive oxygen species have a causal role in multiple forms of insulin resistance. *Nature,* 440**,** 944-8.

ISHIHARA, H., WANG, H., DREWES, L. R. & WOLLHEIM, C. B. 1999. Overexpression of monocarboxylate transporter and lactate dehydrogenase alters insulin secretory responses to pyruvate and lactate in beta cells. *J Clin Invest,* 104**,** 1621-9.

IVARSSON, R., QUINTENS, R., DEJONGHE, S., TSUKAMOTO, K., IN 'T VELD, P., RENSTROM, E. & SCHUIT, F. C. 2005. Redox control of exocytosis: regulatory role of NADPH, thioredoxin, and glutaredoxin. *Diabetes,* 54**,** 2132-42.

JACOB, S., RUUS, P., HERMANN, R., TRITSCHLER, H. J., MAERKER, E., RENN, W., AUGUSTIN, H. J., DIETZE, G. J. & RETT, K. 1999. Oral administration of RAC-alpha-lipoic acid modulates insulin sensitivity in patients with type-2 diabetes mellitus: a placebo-controlled pilot trial. *Free Radic Biol Med,* 27**,** 309-14.

JACOVETTI, C., MATKOVICH, S. J., RODRIGUEZ-TREJO, A., GUAY, C. & REGAZZI, R. 2015. Postnatal beta-cell maturation is associated with islet-specific microRNA changes induced by nutrient shifts at weaning. *Nat Commun,* 6**,** 8084.

JACOVETTI, C., RODRIGUEZ-TREJO, A., GUAY, C., SOBEL, J., GATTESCO, S., PETRENKO, V., SAINI, C., DIBNER, C. & REGAZZI, R. 2017. MicroRNAs modulate core-clock gene expression in pancreatic islets during early postnatal life in rats. *Diabetologia,* 60**,** 2011-2020.

JERMENDY, A., TOSCHI, E., AYE, T., KOH, A., AGUAYO-MAZZUCATO, C., SHARMA, A., WEIR, G. C., SGROI, D. & BONNER-WEIR, S. 2011. Rat neonatal beta cells lack the specialised metabolic phenotype of mature beta cells. *Diabetologia,* 54**,** 594-604.

JESINKEY, S. R., MADIRAJU, A. K., ALVES, T. C., YARBOROUGH, O. H., CARDONE, R. L., ZHAO, X., PARSAEI, Y., NASIRI, A. R., BUTRICO, G., LIU, X., MOLINA, A. J., ROUNTREE, A. M., NEAL, A. S., WOLF, D. M., STERPKA, J., PHILBRICK, W. M., SWEET, I. R., SHIRIHAI, O. H. & KIBBEY, R. G. 2019. Mitochondrial GTP Links Nutrient Sensing to beta Cell Health, Mitochondrial Morphology, and Insulin Secretion Independent of OxPhos. *Cell Rep,* 28**,** 759-772 e10.

JEZEK, J., DLASKOVA, A., ZELENKA, J., JABUREK, M. & JEZEK, P. 2015. H(2)O(2)-Activated Mitochondrial Phospholipase iPLA(2)gamma Prevents Lipotoxic Oxidative Stress in Synergy with UCP2, Amplifies Signaling via G-Protein-Coupled Receptor GPR40, and Regulates Insulin Secretion in Pancreatic beta-Cells. *Antioxid Redox Signal,* 23**,** 958-72.

JEZEK, P., OLEJAR, T., SMOLKOVA, K., JEZEK, J., DLASKOVA, A., PLECITA-HLAVATA, L., ZELENKA, J., SPACEK, T., ENGSTOVA, H., PAJUELO REGUERA, D. & JABUREK, M. 2014. Antioxidant and regulatory role of mitochondrial uncoupling protein UCP2 in pancreatic beta-cells. *Physiol Res,* 63**,** S73-91.

JOHNSON, J. D. 2014. A practical guide to genetic engineering of pancreatic beta-cells in vivo: getting a grip on RIP and MIP. *Islets,* 6**,** e944439.

JOSEPH, J. W., KOSHKIN, V., SALEH, M. C., SIVITZ, W. I., ZHANG, C. Y., LOWELL, B. B., CHAN, C. B. & WHEELER, M. B. 2004. Free fatty acid-induced beta-cell defects are dependent on uncoupling protein 2 expression. *J Biol Chem,* 279**,** 51049-56.

JOSEPH, J. W., KOSHKIN, V., ZHANG, C. Y., WANG, J., LOWELL, B. B., CHAN, C. B. & WHEELER, M. B. 2002. Uncoupling protein 2 knockout mice have enhanced insulin secretory capacity after a high-fat diet. *Diabetes,* 51**,** 3211-9.

KAPOOR, R. R., FLANAGAN, S. E., JAMES, C., SHIELD, J., ELLARD, S. & HUSSAIN, K. 2009. Hyperinsulinaemic hypoglycaemia. *Arch Dis Child,* 94**,** 450-7.

KASHEMSANT, N. & CHAN, C. B. 2006. Impact of uncoupling protein-2 overexpression on proinsulin processing. *J Mol Endocrinol,* 37**,** 517-26.

KASSIS, N., BERNARD, C., PUSTERLA, A., CASTEILLA, L., PENICAUD, L., RICHARD, D., RICQUIER, D. & KTORZA, A. 2000. Correlation between pancreatic islet uncoupling protein-2 (UCP2) mRNA concentration and insulin status in rats. *Int J Exp Diabetes Res,* 1**,** 185-93.

KHAN, A. A., ALLEMAILEM, K. S., ALHUMAYDHI, F. A., GOWDER, S. J. T. & RAHMANI, A. H. 2020. The Biochemical and Clinical Perspectives of Lactate Dehydrogenase: An Enzyme of Active Metabolism. *Endocr Metab Immune Disord Drug Targets,* 20**,** 855-868.

KIKUMOTO, Y., SUGIYAMA, H., INOUE, T., MORINAGA, H., TAKIUE, K., KITAGAWA, M., FUKUOKA, N., SAEKI, M., MAESHIMA, Y., WANG, D. H., OGINO, K., MASUOKA, N. & MAKINO, H. 2010. Sensitization to alloxan-induced diabetes and pancreatic cell apoptosis in acatalasemic mice. *Biochim Biophys Acta,* 1802**,** 240-6.

KO, C. H. & TAKAHASHI, J. S. 2006. Molecular components of the mammalian circadian clock. *Hum Mol Genet,* 15 Spec No 2**,** R271-7.

KOJIMA, S., SHER-CHEN, E. L. & GREEN, C. B. 2012. Circadian control of mRNA polyadenylation dynamics regulates rhythmic protein expression. *Genes Dev,* 26**,** 2724-36.

KONDRATOV, R. V., SHAMANNA, R. K., KONDRATOVA, A. A., GORBACHEVA, V. Y. & ANTOCH, M. P. 2006. Dual role of the CLOCK/BMAL1 circadian complex in transcriptional regulation. *FASEB J,* 20**,** 530-2.

KONG, D., VONG, L., PARTON, L. E., YE, C., TONG, Q., HU, X., CHOI, B., BRUNING, J. C. & LOWELL, B. B. 2010. Glucose stimulation of hypothalamic MCH neurons involves K(ATP) channels, is modulated by UCP2, and regulates peripheral glucose homeostasis. *Cell Metab,* 12**,** 545-52.

KORNMANN, B., SCHAAD, O., BUJARD, H., TAKAHASHI, J. S. & SCHIBLER, U. 2007. System-driven and oscillator-dependent circadian transcription in mice with a conditionally active liver clock. *PLoS Biol,* 5**,** e34.

KRAUSE, M. S., MCCLENAGHAN, N. H., FLATT, P. R., DE BITTENCOURT, P. I., MURPHY, C. & NEWSHOLME, P. 2011. L-arginine is essential for pancreatic beta-cell functional integrity, metabolism and defense from inflammatory challenge. *J Endocrinol,* 211**,** 87-97.

KRAUSS, S., ZHANG, C. Y., SCORRANO, L., DALGAARD, L. T., ST-PIERRE, J., GREY, S. T. & LOWELL, B. B. 2003. Superoxide-mediated activation of uncoupling protein 2 causes pancreatic beta cell dysfunction. *J Clin Invest,* 112**,** 1831-42.

KREMPLER, F., ESTERBAUER, H., WEITGASSER, R., EBENBICHLER, C., PATSCH, J. R., MILLER, K., XIE, M., LINNEMAYR, V., OBERKOFLER, H. & PATSCH, W. 2002. A functional polymorphism in the promoter of UCP2 enhances obesity risk but reduces type 2 diabetes risk in obese middle-aged humans. *Diabetes,* 51**,** 3331-5.

KUBISCH, H. M., WANG, J., LUCHE, R., CARLSON, E., BRAY, T. M., EPSTEIN, C. J. & PHILLIPS, J. P. 1994. Transgenic copper/zinc superoxide dismutase modulates susceptibility to type I diabetes. *Proc Natl Acad Sci U S A,* 91**,** 9956-9.

LAMELOISE, N., MUZZIN, P., PRENTKI, M. & ASSIMACOPOULOS-JEANNET, F. 2001. Uncoupling protein 2: a possible link between fatty acid excess and impaired glucose-induced insulin secretion? *Diabetes,* 50**,** 803-9.

LAMIA, K. A., STORCH, K. F. & WEITZ, C. J. 2008. Physiological significance of a peripheral tissue circadian clock. *Proc Natl Acad Sci U S A,* 105**,** 15172-7.
LAYBUTT, D. R., SHARMA, A., SGROI, D. C., GAUDET, J., BONNER-WEIR, S. & WEIR, G. C. 2002. Genetic regulation of metabolic pathways in beta-cells disrupted by hyperglycemia. *J Biol Chem,* 277**,** 10912-21.
LEE, A., ADER, M., BRAY, G. A. & BERGMAN, R. N. 1992. Diurnal variation in glucose tolerance. Cyclic suppression of insulin action and insulin secretion in normal-weight, but not obese, subjects. *Diabetes,* 41**,** 750-9.
LEE, F. Y., LI, Y., ZHU, H., YANG, S., LIN, H. Z., TRUSH, M. & DIEHL, A. M. 1999. Tumor necrosis factor increases mitochondrial oxidant production and induces expression of uncoupling protein-2 in the regenerating mice [correction of rat] liver. *Hepatology,* 29**,** 677-87.
LEE, J., KIM, M. S., LI, R., LIU, V. Y., FU, L., MOORE, D. D., MA, K. & YECHOOR, V. K. 2011. Loss of Bmal1 leads to uncoupling and impaired glucose-stimulated insulin secretion in beta-cells. *Islets,* 3**,** 381-8.
LEE, J., MOULIK, M., FANG, Z., SAHA, P., ZOU, F., XU, Y., NELSON, D. L., MA, K., MOORE, D. D. & YECHOOR, V. K. 2013. Bmal1 and beta-cell clock are required for adaptation to circadian disruption, and their loss of function leads to oxidative stress-induced beta-cell failure in mice. *Mol Cell Biol,* 33**,** 2327-38.
LEE, S. C., ROBSON-DOUCETTE, C. A. & WHEELER, M. B. 2009. Uncoupling protein 2 regulates reactive oxygen species formation in islets and influences susceptibility to diabetogenic action of streptozotocin. *J Endocrinol,* 203**,** 33-43.
LEI, X. G. & VATAMANIUK, M. Z. 2011. Two tales of antioxidant enzymes on beta cells and diabetes. *Antioxid Redox Signal,* 14**,** 489-503.
LENZEN, S., DRINKGERN, J. & TIEDGE, M. 1996. Low antioxidant enzyme gene expression in pancreatic islets compared with various other mouse tissues. *Free Radic Biol Med,* 20**,** 463-6.
LEWANDOWSKI, S. L., CARDONE, R. L., FOSTER, H. R., HO, T., POTAPENKO, E., POUDEL, C., VANDEUSEN, H. R., SDAO, S. M., ALVES, T. C., ZHAO, X., CAPOZZI, M. E., DE SOUZA, A. H., JAHAN, I., THOMAS, C. J., NUNEMAKER, C. S., DAVIS, D. B., CAMPBELL, J. E., KIBBEY, R. G. & MERRINS, M. J. 2020. Pyruvate Kinase Controls Signal Strength in the Insulin Secretory Pathway. *Cell Metab,* 32**,** 736-750 e5.
LI, J., JIANG, R., CONG, X. & ZHAO, Y. 2019. UCP2 gene polymorphisms in obesity and diabetes, and the role of UCP2 in cancer. *FEBS Lett,* 593**,** 2525-2534.
LI, L. X., SKORPEN, F., EGEBERG, K., JORGENSEN, I. H. & GRILL, V. 2001. Uncoupling protein-2 participates in cellular defense against oxidative stress in clonal beta-cells. *Biochem Biophys Res Commun,* 282**,** 273-7.
LI, L. X., SKORPEN, F., EGEBERG, K., JORGENSEN, I. H. & GRILL, V. 2002. Induction of uncoupling protein 2 mRNA in beta-cells is stimulated by oxidation of fatty acids but not by nutrient oversupply. *Endocrinology,* 143**,** 1371-7.
LIANG, Y., BAI, G., DOLIBA, N., BUETTGER, C., WANG, L., BERNER, D. K. & MATSCHINSKY, F. M. 1996. Glucose metabolism and insulin release in mouse beta HC9 cells, as model for wild-type pancreatic beta-cells. *Am J Physiol,* 270**,** E846-57.
LIKE, A. A. & ROSSINI, A. A. 1976. Streptozotocin-induced pancreatic insulitis: new model of diabetes mellitus. *Science,* 193**,** 415-7.
LIU, J. S. & HEBROK, M. 2017. All mixed up: defining roles for beta-cell subtypes in mature islets. *Genes Dev,* 31**,** 228-240.
LIVAK, K. J. & SCHMITTGEN, T. D. 2001. Analysis of relative gene expression data using real-time quantitative PCR and the 2(-Delta Delta C(T)) Method. *Methods,* 25**,** 402-8.
LLANOS, P., CONTRERAS-FERRAT, A., BARRIENTOS, G., VALENCIA, M., MEARS, D. & HIDALGO, C. 2015. Glucose-Dependent Insulin Secretion in Pancreatic beta-Cell Islets from Male Rats Requires Ca2+ Release via ROS-Stimulated Ryanodine Receptors. *PLoS One,* 10**,** e0129238.

LOH, K., DENG, H., FUKUSHIMA, A., CAI, X., BOIVIN, B., GALIC, S., BRUCE, C., SHIELDS, B. J., SKIBA, B., OOMS, L. M., STEPTO, N., WU, B., MITCHELL, C. A., TONKS, N. K., WATT, M. J., FEBBRAIO, M. A., CRACK, P. J., ANDRIKOPOULOS, S. & TIGANIS, T. 2009. Reactive oxygen species enhance insulin sensitivity. *Cell Metab,* 10**,** 260-72.

LYTRIVI, M., CASTELL, A. L., POITOUT, V. & CNOP, M. 2020. Recent Insights Into Mechanisms of β-Cell Lipo- and Glucolipotoxicity in Type 2 Diabetes. *Journal of Molecular Biology,* 432**,** 1514-1534.

MADREITER-SOKOLOWSKI, C. T., KLEC, C., PARICHATIKANOND, W., STRYECK, S., GOTTSCHALK, B., PULIDO, S., ROST, R., EROGLU, E., HOFMANN, N. A., BONDARENKO, A. I., MADL, T., WALDECK-WEIERMAIR, M., MALLI, R. & GRAIER, W. F. 2016. PRMT1-mediated methylation of MICU1 determines the UCP2/3 dependency of mitochondrial Ca(2+) uptake in immortalized cells. *Nat Commun,* 7**,** 12897.

MAECHLER, P., JORNOT, L. & WOLLHEIM, C. B. 1999. Hydrogen peroxide alters mitochondrial activation and insulin secretion in pancreatic beta cells. *J Biol Chem,* 274**,** 27905-13.

MAECHLER, P. & WOLLHEIM, C. B. 2001. Mitochondrial function in normal and diabetic beta-cells. *Nature,* 414**,** 807-12.

MALAISSE, W. J., HUTTON, J. C., KAWAZU, S., HERCHUELZ, A., VALVERDE, I. & SENER, A. 1979. The stimulus-secretion coupling of glucose-induced insulin release. XXXV. The links between metabolic and cationic events. *Diabetologia,* 16**,** 331-41.

MALHERBE, C., DE GASPARO, M., DE HERTOGH, R. & HOET, J. J. 1969. Circadian variations of blood sugar and plasma insulin levels in man. *Diabetologia,* 5**,** 397-404.

MAO, W., YU, X. X., ZHONG, A., LI, W., BRUSH, J., SHERWOOD, S. W., ADAMS, S. H. & PAN, G. 1999. UCP4, a novel brain-specific mitochondrial protein that reduces membrane potential in mammalian cells. *FEBS Lett,* 443**,** 326-30.

MARCHEVA, B., RAMSEY, K. M., BUHR, E. D., KOBAYASHI, Y., SU, H., KO, C. H., IVANOVA, G., OMURA, C., MO, S., VITATERNA, M. H., LOPEZ, J. P., PHILIPSON, L. H., BRADFIELD, C. A., CROSBY, S. D., JEBAILEY, L., WANG, X., TAKAHASHI, J. S. & BASS, J. 2010. Disruption of the clock components CLOCK and BMAL1 leads to hypoinsulinaemia and diabetes. *Nature,* 466**,** 627-31.

MARTENS, G. A., CAI, Y., HINKE, S., STANGE, G., VAN DE CASTEELE, M. & PIPELEERS, D. 2005. Glucose suppresses superoxide generation in metabolically responsive pancreatic beta cells. *J Biol Chem,* 280**,** 20389-96.

MARTENS, M. D., FIELD, J. T., SESHADRI, N., DAY, C., CHAPMAN, D., KEIJZER, R., DOUCETTE, C. A., HATCH, G. M., WEST, A. R., IVANCO, T. L. & GORDON, J. W. 2020. Misoprostol attenuates neonatal cardiomyocyte proliferation through Bnip3, perinuclear calcium signaling, and inhibition of glycolysis. *J Mol Cell Cardiol,* 146**,** 19-31.

MATSUOKA, T., KAJIMOTO, Y., WATADA, H., KANETO, H., KISHIMOTO, M., UMAYAHARA, Y., FUJITANI, Y., KAMADA, T., KAWAMORI, R. & YAMASAKI, Y. 1997. Glycation-dependent, reactive oxygen species-mediated suppression of the insulin gene promoter activity in HIT cells. *J Clin Invest,* 99**,** 144-50.

MCCOMMIS, K. S. & BAINES, C. P. 2012. The role of VDAC in cell death: friend or foe? *Biochim Biophys Acta,* 1818**,** 1444-50.

MCQUAID, T. S., SALEH, M. C., JOSEPH, J. W., GYULKHANDANYAN, A., MANNING-FOX, J. E., MACLELLAN, J. D., WHEELER, M. B. & CHAN, C. B. 2006. cAMP-mediated signaling normalizes glucose-stimulated insulin secretion in uncoupling protein-2 overexpressing beta-cells. *J Endocrinol,* 190**,** 669-80.

MEDVEDEV, A. V., ROBIDOUX, J., BAI, X., CAO, W., FLOERING, L. M., DANIEL, K. W. & COLLINS, S. 2002. Regulation of the uncoupling protein-2 gene in INS-1 beta-cells by oleic acid. *J Biol Chem,* 277**,** 42639-44.

MEGLASSON, M. D., NELSON, J., NELSON, D. & ERECINSKA, M. 1989. Bioenergetic response of pancreatic islets to stimulation by fuel molecules. *Metabolism,* 38**,** 1188-95.

MERCER, R. M., CORCORAN, J. P., PORCEL, J. M., RAHMAN, N. M. & PSALLIDAS, I. 2019. Interpreting pleural fluid results. *Clin Med (Lond),* 19**,** 213-217.
MIKI, T., NAGASHIMA, K. & SEINO, S. 1999. The structure and function of the ATP-sensitive K+ channel in insulin-secreting pancreatic beta-cells. *J Mol Endocrinol,* 22**,** 113-23.
MIYAZAKI, S., TASHIRO, F., TSUCHIYA, T., SASAKI, K. & MIYAZAKI, J. I. 2021. Establishment of a long-term stable beta-cell line and its application to analyze the effect of Gcg expression on insulin secretion. *Sci Rep,* 11**,** 477.
MOHAWK, J. A., GREEN, C. B. & TAKAHASHI, J. S. 2012. Central and peripheral circadian clocks in mammals. *Annu Rev Neurosci,* 35**,** 445-62.
MORGAN, D., REBELATO, E., ABDULKADER, F., GRACIANO, M. F., OLIVEIRA-EMILIO, H. R., HIRATA, A. E., ROCHA, M. S., BORDIN, S., CURI, R. & CARPINELLI, A. R. 2009. Association of NAD(P)H oxidase with glucose-induced insulin secretion by pancreatic beta-cells. *Endocrinology,* 150**,** 2197-201.
MORIN, L. P., FITZGERALD, K. M. & ZUCKER, I. 1977. Estradiol shortens the period of hamster circadian rhythms. *Science,* 196**,** 305-7.
MORO, C. & MAGNAN, C. 2021. GTTs and ITTs: aim for shorter fasting times. *Nat Metab,* 3**,** 1133.
MULLARKY, E. & CANTLEY, L. C. 2015. Diverting Glycolysis to Combat Oxidative Stress. *In:* NAKAO, K., MINATO, N. & UEMOTO, S. (eds.) *Innovative Medicine: Basic Research and Development.* Tokyo.
MYSORE, T. B., SHINKEL, T. A., COLLINS, J., SALVARIS, E. J., FISICARO, N., MURRAY-SEGAL, L. J., JOHNSON, L. E., LEPORE, D. A., WALTERS, S. N., STOKES, R., CHANDRA, A. P., O'CONNELL, P. J., D'APICE, A. J. & COWAN, P. J. 2005. Overexpression of glutathione peroxidase with two isoforms of superoxide dismutase protects mouse islets from oxidative injury and improves islet graft function. *Diabetes,* 54**,** 2109-16.
NEDERGAARD, J. & CANNON, B. 2003. The 'novel' 'uncoupling' proteins UCP2 and UCP3: what do they really do? Pros and cons for suggested functions. *Exp Physiol,* 88**,** 65-84.
NEDERGAARD, J., RICQUIER, D. & KOZAK, L. P. 2005. Uncoupling proteins: current status and therapeutic prospects. *EMBO Rep,* 6**,** 917-21.
NEGRE-SALVAYRE, A., HIRTZ, C., CARRERA, G., CAZENAVE, R., TROLY, M., SALVAYRE, R., PENICAUD, L. & CASTEILLA, L. 1997. A role for uncoupling protein-2 as a regulator of mitochondrial hydrogen peroxide generation. *FASEB J,* 11**,** 809-15.
NEWSHOLME, P., KEANE, K. N., CARLESSI, R. & CRUZAT, V. 2019. Oxidative stress pathways in pancreatic beta-cells and insulin-sensitive cells and tissues: importance to cell metabolism, function, and dysfunction. *Am J Physiol Cell Physiol,* 317**,** C420-C433.
NICHOLLS, D. G. & LOCKE, R. M. 1984. Thermogenic mechanisms in brown fat. *Physiol Rev,* 64**,** 1-64.
NIR, T., MELTON, D. A. & DOR, Y. 2007. Recovery from diabetes in mice by beta cell regeneration. *J Clin Invest,* 117**,** 2553-61.
NOMA, A. 1983. ATP-regulated K+ channels in cardiac muscle. *Nature,* 305**,** 147-8.
NOSTER, J., PERSICKE, M., CHAO, T. C., KRONE, L., HEPPNER, B., HENSEL, M. & HANSMEIER, N. 2019. Impact of ROS-Induced Damage of TCA Cycle Enzymes on Metabolism and Virulence of Salmonella enterica serovar Typhimurium. *Front Microbiol,* 10**,** 762.
O'ROURKE R, W. 2014. Metabolic thrift and the genetic basis of human obesity. *Ann Surg,* 259**,** 642-8.
OHTA, M., NELSON, D., NELSON, J., MEGLASSON, M. D. & ERECINSKA, M. 1991. Relationships between energy level and insulin secretion in isolated rat islets of Langerhans. A study at various pH values. *Biochem Pharmacol,* 42**,** 593-8.
PALOU, A., PICO, C., BONET, M. L. & OLIVER, P. 1998. The uncoupling protein, thermogenin. *Int J Biochem Cell Biol,* 30**,** 7-11.
PANTEN, U., SCHWANSTECHER, M. & SCHWANSTECHER, C. 1996. Sulfonylurea receptors and mechanism of sulfonylurea action. *Exp Clin Endocrinol Diabetes,* 104**,** 1-9.

PARK, S. J., JEONG, S. Y. & KIM, H. J. 2006. Y chromosome loss and other genomic alterations in hepatocellular carcinoma cell lines analyzed by CGH and CGH array. *Cancer Genet Cytogenet,* 166**,** 56-64.

PARTON, L. E., YE, C. P., COPPARI, R., ENRIORI, P. J., CHOI, B., ZHANG, C. Y., XU, C., VIANNA, C. R., BALTHASAR, N., LEE, C. E., ELMQUIST, J. K., COWLEY, M. A. & LOWELL, B. B. 2007. Glucose sensing by POMC neurons regulates glucose homeostasis and is impaired in obesity. *Nature,* 449**,** 228-32.

PATANE, G., ANELLO, M., PIRO, S., VIGNERI, R., PURRELLO, F. & RABUAZZO, A. M. 2002. Role of ATP production and uncoupling protein-2 in the insulin secretory defect induced by chronic exposure to high glucose or free fatty acids and effects of peroxisome proliferator-activated receptor-gamma inhibition. *Diabetes,* 51**,** 2749-56.

PATRON, M., RAFFAELLO, A., GRANATIERO, V., TOSATTO, A., MERLI, G., DE STEFANI, D., WRIGHT, L., PALLAFACCHINA, G., TERRIN, A., MAMMUCARI, C. & RIZZUTO, R. 2013. The mitochondrial calcium uniporter (MCU): molecular identity and physiological roles. *J Biol Chem,* 288**,** 10750-8.

PAYEN, V. L., MINA, E., VAN HEE, V. F., PORPORATO, P. E. & SONVEAUX, P. 2020. Monocarboxylate transporters in cancer. *Mol Metab,* 33**,** 48-66.

PECQUEUR, C., BUI, T., GELLY, C., HAUCHARD, J., BARBOT, C., BOUILLAUD, F., RICQUIER, D., MIROUX, B. & THOMPSON, C. B. 2008. Uncoupling protein-2 controls proliferation by promoting fatty acid oxidation and limiting glycolysis-derived pyruvate utilization. *FASEB J,* 22**,** 9-18.

PEREIRA, T. J., FONSECA, M. A., CAMPBELL, K. E., MOYCE, B. L., COLE, L. K., HATCH, G. M., DOUCETTE, C. A., KLEIN, J., ALIANI, M. & DOLINSKY, V. W. 2015. Maternal obesity characterized by gestational diabetes increases the susceptibility of rat offspring to hepatic steatosis via a disrupted liver metabolome. *J Physiol,* 593**,** 3181-97.

PERELIS, M., MARCHEVA, B., RAMSEY, K. M., SCHIPMA, M. J., HUTCHISON, A. L., TAGUCHI, A., PEEK, C. B., HONG, H., HUANG, W., OMURA, C., ALLRED, A. L., BRADFIELD, C. A., DINNER, A. R., BARISH, G. D. & BASS, J. 2015. Pancreatic beta cell enhancers regulate rhythmic transcription of genes controlling insulin secretion. *Science,* 350**,** aac4250.

PESCHKE, E. & PESCHKE, D. 1998. Evidence for a circadian rhythm of insulin release from perifused rat pancreatic islets. *Diabetologia,* 41**,** 1085-92.

PETRENKO, V. & DIBNER, C. 2018. Cell-specific resetting of mouse islet cellular clocks by glucagon, glucagon-like peptide 1 and somatostatin. *Acta Physiol (Oxf),* 222**,** e13021.

PETRENKO, V., GANDASI, N. R., SAGE, D., TENGHOLM, A., BARG, S. & DIBNER, C. 2020a. In pancreatic islets from type 2 diabetes patients, the dampened circadian oscillators lead to reduced insulin and glucagon exocytosis. *Proc Natl Acad Sci U S A,* 117**,** 2484-2495.

PETRENKO, V., SAINI, C., GIOVANNONI, L., GOBET, C., SAGE, D., UNSER, M., HEDDAD MASSON, M., GU, G., BOSCO, D., GACHON, F., PHILIPPE, J. & DIBNER, C. 2017. Pancreatic alpha- and beta-cellular clocks have distinct molecular properties and impact on islet hormone secretion and gene expression. *Genes Dev,* 31**,** 383-398.

PETRENKO, V., STOLOVICH-RAIN, M., VANDEREYCKEN, B., GIOVANNONI, L., STORCH, K. F., DOR, Y., CHERA, S. & DIBNER, C. 2020b. The core clock transcription factor BMAL1 drives circadian beta-cell proliferation during compensatory regeneration of the endocrine pancreas. *Genes Dev,* 34**,** 1650-1665.

PI, J., BAI, Y., DANIEL, K. W., LIU, D., LYGHT, O., EDELSTEIN, D., BROWNLEE, M., CORKEY, B. E. & COLLINS, S. 2009. Persistent oxidative stress due to absence of uncoupling protein 2 associated with impaired pancreatic beta-cell function. *Endocrinology,* 150**,** 3040-8.

PI, J., BAI, Y., ZHANG, Q., WONG, V., FLOERING, L. M., DANIEL, K., REECE, J. M., DEENEY, J. T., ANDERSEN, M. E., CORKEY, B. E. & COLLINS, S. 2007. Reactive oxygen species as a signal in glucose-stimulated insulin secretion. *Diabetes,* 56**,** 1783-91.

PI, J. & COLLINS, S. 2010. Reactive oxygen species and uncoupling protein 2 in pancreatic beta-cell function. *Diabetes Obes Metab,* 12 Suppl 2**,** 141-8.
PICINATO, M. C., HABER, E. P., CARPINELLI, A. R. & CIPOLLA-NETO, J. 2002. Daily rhythm of glucose-induced insulin secretion by isolated islets from intact and pinealectomized rat. *J Pineal Res,* 33**,** 172-7.
PILDES, R. S., HART, R. J., WARRNER, R. & CORNBLATH, M. 1969. Plasma insulin response during oral glucose tolerance tests in newborns of normal and gestational diabetic mothers. *Pediatrics,* 44**,** 76-83.
PISU, E., DIANA, A., LOMBARDI, A., CASSADER, M. & PAGANO, G. 1980. Diurnal variations in insulin secretion and insulin sensitivity in aged subjects. *Acta Diabetol Lat,* 17**,** 153-60.
POLONSKY, K. S., GIVEN, B. D., HIRSCH, L., SHAPIRO, E. T., TILLIL, H., BEEBE, C., GALLOWAY, J. A., FRANK, B. H., KARRISON, T. & VAN CAUTER, E. 1988a. Quantitative study of insulin secretion and clearance in normal and obese subjects. *J Clin Invest,* 81**,** 435-41.
POLONSKY, K. S., GIVEN, B. D. & VAN CAUTER, E. 1988b. Twenty-four-hour profiles and pulsatile patterns of insulin secretion in normal and obese subjects. *J Clin Invest,* 81**,** 442-8.
PROCHAZKA, B., QURESHI, M. A. & MATTY, A. J. 1970. Lactate dehydrogenase activity and isoenzyme patterns in skeletal muscle, fat, exocrine pancreas and isolated pancreatic islets of normal and obese-Hyperglycaemic mice. *Diabetologia,* 6**,** 493-8.
PRODUIT-ZENGAFFINEN, N., DAVIS-LAMELOISE, N., PERRETEN, H., BECARD, D., GJINOVCI, A., KELLER, P. A., WOLLHEIM, C. B., HERRERA, P., MUZZIN, P. & ASSIMACOPOULOS-JEANNET, F. 2007. Increasing uncoupling protein-2 in pancreatic beta cells does not alter glucose-induced insulin secretion but decreases production of reactive oxygen species. *Diabetologia,* 50**,** 84-93.
PULIMENO, P., MANNIC, T., SAGE, D., GIOVANNONI, L., SALMON, P., LEMEILLE, S., GIRY-LATERRIERE, M., UNSER, M., BOSCO, D., BAUER, C., MORF, J., HALBAN, P., PHILIPPE, J. & DIBNER, C. 2013. Autonomous and self-sustained circadian oscillators displayed in human islet cells. *Diabetologia,* 56**,** 497-507.
QIAN, J., BLOCK, G. D., COLWELL, C. S. & MATVEYENKO, A. V. 2013. Consequences of exposure to light at night on the pancreatic islet circadian clock and function in rats. *Diabetes,* 62**,** 3469-78.
QIAN, J., YEH, B., RAKSHIT, K., COLWELL, C. S. & MATVEYENKO, A. V. 2015. Circadian Disruption and Diet-Induced Obesity Synergize to Promote Development of beta-Cell Failure and Diabetes in Male Rats. *Endocrinology,* 156**,** 4426-36.
RAKSHIT, K., HSU, T. W. & MATVEYENKO, A. V. 2016a. Bmal1 is required for beta cell compensatory expansion, survival and metabolic adaptation to diet-induced obesity in mice. *Diabetologia,* 59**,** 734-43.
RAKSHIT, K., QIAN, J., ERNST, J. & MATVEYENKO, A. V. 2016b. Circadian variation of the pancreatic islet transcriptome. *Physiol Genomics,* 48**,** 677-87.
RAKSHIT, K., QIAN, J., GAONKAR, K. S., DHAWAN, S., COLWELL, C. S. & MATVEYENKO, A. V. 2018. Postnatal Ontogenesis of the Islet Circadian Clock Plays a Contributory Role in beta-Cell Maturation Process. *Diabetes,* 67**,** 911-922.
RAMCHANDANI, N., ELLIS, M. K., JAIN, S., BHANDARI, S., ANHALT, H., MACLAREN, N. K. & TEN, S. 2010. Basal insulin requirements on continuous subcutaneous insulin infusion during the first 12 months after diagnosis of type 1 diabetes mellitus. *J Diabetes Sci Technol,* 4**,** 610-4.
RANI, R. & KUMAR, V. 2016. Recent Update on Human Lactate Dehydrogenase Enzyme 5 (hLDH5) Inhibitors: A Promising Approach for Cancer Chemotherapy. *J Med Chem,* 59**,** 487-96.
RASPE, E., DUEZ, H., MANSEN, A., FONTAINE, C., FIEVET, C., FRUCHART, J. C., VENNSTROM, B. & STAELS, B. 2002. Identification of Rev-erbalpha as a physiological repressor of apoC-III gene transcription. *J Lipid Res,* 43**,** 2172-9.
REMEDI, M. S., ROCHELEAU, J. V., TONG, A., PATTON, B. L., MCDANIEL, M. L., PISTON, D. W., KOSTER, J. C. & NICHOLS, C. G. 2006. Hyperinsulinism in mice with heterozygous loss of K(ATP) channels. *Diabetologia,* 49**,** 2368-78.
REPPERT, S. M. & WEAVER, D. R. 2002. Coordination of circadian timing in mammals. *Nature,* 418**,** 935-41.

RHEE, S. G. 2006. Cell signaling. H2O2, a necessary evil for cell signaling. *Science,* 312**,** 1882-3.
RIGAS, A. N., BITTLES, A. H., HADDEN, D. R. & MONTGOMERY, D. A. 1968. Circadian variation of glucose, insulin, and free fatty acids during long-term use of oral hypoglycaemic agents in diabetes mellitus. *Br Med J,* 4**,** 25-8.
ROBBINS, M. J., SHARP, R. A., SLONIM, A. E. & BURR, I. M. 1980. Protection against streptozotocin-induced diabetes by superoxide dismutase. *Diabetologia,* 18**,** 55-8.
ROBSON-DOUCETTE, C. A., SULTAN, S., ALLISTER, E. M., WIKSTROM, J. D., KOSHKIN, V., BHATTACHARJEE, A., PRENTICE, K. J., SEREDA, S. B., SHIRIHAI, O. S. & WHEELER, M. B. 2011b. Beta-cell uncoupling protein 2 regulates reactive oxygen species production, which influences both insulin and glucagon secretion. *Diabetes,* 60**,** 2710-9.
ROMA, L. P. & JONAS, J. C. 2020. Nutrient Metabolism, Subcellular Redox State, and Oxidative Stress in Pancreatic Islets and beta-Cells. *J Mol Biol,* 432**,** 1461-1493.
RORSMAN, P., ARKHAMMAR, P., BOKVIST, K., HELLERSTROM, C., NILSSON, T., WELSH, M., WELSH, N. & BERGGREN, P. O. 1989. Failure of glucose to elicit a normal secretory response in fetal pancreatic beta cells results from glucose insensitivity of the ATP-regulated K+ channels. *Proc Natl Acad Sci U S A,* 86**,** 4505-9.
RORSMAN, P. & ASHCROFT, F. M. 2018. Pancreatic beta-Cell Electrical Activity and Insulin Secretion: Of Mice and Men. *Physiol Rev,* 98**,** 117-214.
ROUSSET, S., EMRE, Y., JOIN-LAMBERT, O., HURTAUD, C., RICQUIER, D. & CASSARD-DOULCIER, A. M. 2006. The uncoupling protein 2 modulates the cytokine balance in innate immunity. *Cytokine,* 35**,** 135-42.
ROZZO, A., MENEGHEL-ROZZO, T., DELAKORDA, S. L., YANG, S. B. & RUPNIK, M. 2009. Exocytosis of insulin: in vivo maturation of mouse endocrine pancreas. *Ann N Y Acad Sci,* 1152**,** 53-62.
RUDIC, R. D., MCNAMARA, P., CURTIS, A. M., BOSTON, R. C., PANDA, S., HOGENESCH, J. B. & FITZGERALD, G. A. 2004. BMAL1 and CLOCK, two essential components of the circadian clock, are involved in glucose homeostasis. *PLoS Biol,* 2**,** e377.
RUTTER, G. A., PULLEN, T. J., HODSON, D. J. & MARTINEZ-SANCHEZ, A. 2015. Pancreatic beta-cell identity, glucose sensing and the control of insulin secretion. *Biochem J,* 466**,** 203-18.
RUZICKA, M., SKOBISOVA, E., DLASKOVA, A., SANTOROVA, J., SMOLKOVA, K., SPACEK, T., ZACKOVA, M., MODRIANSKY, M. & JEZEK, P. 2005. Recruitment of mitochondrial uncoupling protein UCP2 after lipopolysaccharide induction. *Int J Biochem Cell Biol,* 37**,** 809-21.
SAAD, A., DALLA MAN, C., NANDY, D. K., LEVINE, J. A., BHARUCHA, A. E., RIZZA, R. A., BASU, R., CARTER, R. E., COBELLI, C., KUDVA, Y. C. & BASU, A. 2012. Diurnal pattern to insulin secretion and insulin action in healthy individuals. *Diabetes,* 61**,** 2691-700.
SADACCA, L. A., LAMIA, K. A., DELEMOS, A. S., BLUM, B. & WEITZ, C. J. 2011. An intrinsic circadian clock of the pancreas is required for normal insulin release and glucose homeostasis in mice. *Diabetologia,* 54**,** 120-4.
SAINI, C., PETRENKO, V., PULIMENO, P., GIOVANNONI, L., BERNEY, T., HEBROK, M., HOWALD, C., DERMITZAKIS, E. T. & DIBNER, C. 2016. A functional circadian clock is required for proper insulin secretion by human pancreatic islet cells. *Diabetes Obes Metab,* 18**,** 355-65.
SAKURABA, H., MIZUKAMI, H., YAGIHASHI, N., WADA, R., HANYU, C. & YAGIHASHI, S. 2002. Reduced beta-cell mass and expression of oxidative stress-related DNA damage in the islet of Japanese Type II diabetic patients. *Diabetologia,* 45**,** 85-96.
SASAHARA, M., NISHI, M., KAWASHIMA, H., UEDA, K., SAKAGASHIRA, S., FURUTA, H., MATSUMOTO, E., HANABUSA, T., SASAKI, H. & NANJO, K. 2004. Uncoupling protein 2 promoter polymorphism -866G/A affects its expression in beta-cells and modulates clinical profiles of Japanese type 2 diabetic patients. *Diabetes,* 53**,** 482-5.
SATIN, L. S. 1996. New mechanisms for sulfonylurea control of insulin secretion. *Endocrine,* 4**,** 191-8.
SCHIEBER, M. & CHANDEL, N. S. 2014. ROS function in redox signaling and oxidative stress. *Curr Biol,* 24**,** R453-62.

SCHUIT, F., VAN LOMMEL, L., GRANVIK, M., GOYVAERTS, L., DE FAUDEUR, G., SCHRAENEN, A. & LEMAIRE, K. 2012. beta-cell-specific gene repression: a mechanism to protect against inappropriate or maladjusted insulin secretion? *Diabetes,* 61**,** 969-75.

SEHLIN, J. 1978. Interrelationship between chloride fluxes in pancreatic islets and insulin release. *Am J Physiol,* 235**,** E501-8.

SEKINE, N., CIRULLI, V., REGAZZI, R., BROWN, L. J., GINE, E., TAMARIT-RODRIGUEZ, J., GIROTTI, M., MARIE, S., MACDONALD, M. J., WOLLHEIM, C. B. & ET AL. 1994. Low lactate dehydrogenase and high mitochondrial glycerol phosphate dehydrogenase in pancreatic beta-cells. Potential role in nutrient sensing. *J Biol Chem,* 269**,** 4895-902.

SESHADRI, N. & DOUCETTE, C. A. 2021. Circadian Regulation of the Pancreatic Beta Cell. *Endocrinology,* 162.

SESHADRI, N., JONASSON, M. E., HUNT, K. L., XIANG, B., COOPER, S., WHEELER, M. B., DOLINSKY, V. W. & DOUCETTE, C. A. 2017. Uncoupling protein 2 regulates daily rhythms of insulin secretion capacity in MIN6 cells and isolated islets from male mice. *Mol Metab,* 6**,** 760-769.

SESTI, G., CARDELLINI, M., MARINI, M. A., FRONTONI, S., D'ADAMO, M., DEL GUERRA, S., LAURO, D., DE NICOLAIS, P., SBRACCIA, P., DEL PRATO, S., GAMBARDELLA, S., FEDERICI, M., MARCHETTI, P. & LAURO, R. 2003. A common polymorphism in the promoter of UCP2 contributes to the variation in insulin secretion in glucose-tolerant subjects. *Diabetes,* 52**,** 1280-3.

SHEETS, A. R., FULOP, P., DERDAK, Z., KASSAI, A., SABO, E., MARK, N. M., PARAGH, G., WANDS, J. R. & BAFFY, G. 2008. Uncoupling protein-2 modulates the lipid metabolic response to fasting in mice. *Am J Physiol Gastrointest Liver Physiol,* 294**,** G1017-24.

SHIMBA, S., ISHII, N., OHTA, Y., OHNO, T., WATABE, Y., HAYASHI, M., WADA, T., AOYAGI, T. & TEZUKA, M. 2005. Brain and muscle Arnt-like protein-1 (BMAL1), a component of the molecular clock, regulates adipogenesis. *Proc Natl Acad Sci U S A,* 102**,** 12071-6.

SINTUREL, F., PETRENKO, V. & DIBNER, C. 2020. Circadian Clocks Make Metabolism Run. *J Mol Biol,* 432**,** 3680-3699.

SKULACHEV, V. P. 1991. Fatty acid circuit as a physiological mechanism of uncoupling of oxidative phosphorylation. *FEBS Lett,* 294**,** 158-62.

SLADEK, M., JINDRAKOVA, Z., BENDOVA, Z. & SUMOVA, A. 2007. Postnatal ontogenesis of the circadian clock within the rat liver. *Am J Physiol Regul Integr Comp Physiol,* 292**,** R1224-9.

STAMENKOVIC, J. A., OLSSON, A. H., NAGORNY, C. L., MALMGREN, S., DEKKER-NITERT, M., LING, C. & MULDER, H. 2012. Regulation of core clock genes in human islets. *Metabolism,* 61**,** 978-85.

STARK, R., PASQUEL, F., TURCU, A., PONGRATZ, R. L., RODEN, M., CLINE, G. W., SHULMAN, G. I. & KIBBEY, R. G. 2009. Phosphoenolpyruvate cycling via mitochondrial phosphoenolpyruvate carboxykinase links anaplerosis and mitochondrial GTP with insulin secretion. *J Biol Chem,* 284**,** 26578-90.

SURNIYANTORO, H. N. E., SADEWA, A. H. & HASTUTI, P. 2018. Uncoupling Protein 2 (UCP2) as Genetic Risk Factor for Obesity in Indonesia is Different in Gender Stratification. *Kobe J Med Sci,* 64**,** E64-E72.

SURWIT, R. S., WANG, S., PETRO, A. E., SANCHIS, D., RAIMBAULT, S., RICQUIER, D. & COLLINS, S. 1998. Diet-induced changes in uncoupling proteins in obesity-prone and obesity-resistant strains of mice. *Proc Natl Acad Sci U S A,* 95**,** 4061-5.

TAKASU, N., ASAWA, T., KOMIYA, I., NAGASAWA, Y. & YAMADA, T. 1991. Alloxan-induced DNA strand breaks in pancreatic islets. Evidence for H2O2 as an intermediate. *J Biol Chem,* 266**,** 2112-4.

TAN, C., TUCH, B. E., TU, J. & BROWN, S. A. 2002. Role of NADH shuttles in glucose-induced insulin secretion from fetal beta-cells. *Diabetes,* 51**,** 2989-96.

TANAKA, Y., TRAN, P. O., HARMON, J. & ROBERTSON, R. P. 2002. A role for glutathione peroxidase in protecting pancreatic beta cells against oxidative stress in a model of glucose toxicity. *Proc Natl Acad Sci U S A,* 99**,** 12363-8.

TANG, C., KOULAJIAN, K., SCHUIKI, I., ZHANG, L., DESAI, T., IVOVIC, A., WANG, P., ROBSON-DOUCETTE, C., WHEELER, M. B., MINASSIAN, B., VOLCHUK, A. & GIACCA, A. 2012. Glucose-induced beta cell dysfunction in vivo in rats: link between oxidative stress and endoplasmic reticulum stress. *Diabetologia,* 55**,** 1366-79.

THORENS, B., TARUSSIO, D., MAESTRO, M. A., ROVIRA, M., HEIKKILA, E. & FERRER, J. 2015. Ins1(Cre) knock-in mice for beta cell-specific gene recombination. *Diabetologia,* 58**,** 558-65.

THORREZ, L., LAUDADIO, I., VAN DEUN, K., QUINTENS, R., HENDRICKX, N., GRANVIK, M., LEMAIRE, K., SCHRAENEN, A., VAN LOMMEL, L., LEHNERT, S., AGUAYO-MAZZUCATO, C., CHENG-XUE, R., GILON, P., VAN MECHELEN, I., BONNER-WEIR, S., LEMAIGRE, F. & SCHUIT, F. 2011. Tissue-specific disallowance of housekeeping genes: the other face of cell differentiation. *Genome Res,* 21**,** 95-105.

TIEDGE, M., LORTZ, S., DRINKGERN, J. & LENZEN, S. 1997. Relation between antioxidant enzyme gene expression and antioxidative defense status of insulin-producing cells. *Diabetes,* 46**,** 1733-42.

TRENKER, M., MALLI, R., FERTSCHAI, I., LEVAK-FRANK, S. & GRAIER, W. F. 2007. Uncoupling proteins 2 and 3 are fundamental for mitochondrial Ca2+ uniport. *Nat Cell Biol,* 9**,** 445-452.

TROTT, A. J. & MENET, J. S. 2018. Regulation of circadian clock transcriptional output by CLOCK:BMAL1. *PLoS Genet,* 14**,** e1007156.

TUREK, F. W., JOSHU, C., KOHSAKA, A., LIN, E., IVANOVA, G., MCDEARMON, E., LAPOSKY, A., LOSEE-OLSON, S., EASTON, A., JENSEN, D. R., ECKEL, R. H., TAKAHASHI, J. S. & BASS, J. 2005. Obesity and metabolic syndrome in circadian Clock mutant mice. *Science,* 308**,** 1043-5.

TURNER, J. D., GASPERS, L. D., WANG, G. & THOMAS, A. P. 2010. Uncoupling protein-2 modulates myocardial excitation-contraction coupling. *Circ Res,* 106**,** 730-8.

TURRENS, J. F. 2003. Mitochondrial formation of reactive oxygen species. *J Physiol,* 552**,** 335-44.

VAN ARENSBERGEN, J., GARCIA-HURTADO, J., MORAN, I., MAESTRO, M. A., XU, X., VAN DE CASTEELE, M., SKOUDY, A. L., PALASSINI, M., HEIMBERG, H. & FERRER, J. 2010. Derepression of Polycomb targets during pancreatic organogenesis allows insulin-producing beta-cells to adopt a neural gene activity program. *Genome Res,* 20**,** 722-32.

VAN CAUTER, E., BLACKMAN, J. D., ROLAND, D., SPIRE, J. P., REFETOFF, S. & POLONSKY, K. S. 1991. Modulation of glucose regulation and insulin secretion by circadian rhythmicity and sleep. *J Clin Invest,* 88**,** 934-42.

VAN CAUTER, E., DESIR, D., DECOSTER, C., FERY, F. & BALASSE, E. O. 1989. Nocturnal decrease in glucose tolerance during constant glucose infusion. *J Clin Endocrinol Metab,* 69**,** 604-11.

VAN DER VINNE, V., SWOAP, S. J., VAJTAY, T. J. & WEAVER, D. R. 2018. Desynchrony between brain and peripheral clocks caused by CK1delta/epsilon disruption in GABA neurons does not lead to adverse metabolic outcomes. *Proc Natl Acad Sci U S A,* 115**,** E2437-E2446.

VIDAL-PUIG, A., SOLANES, G., GRUJIC, D., FLIER, J. S. & LOWELL, B. B. 1997. UCP3: an uncoupling protein homologue expressed preferentially and abundantly in skeletal muscle and brown adipose tissue. *Biochem Biophys Res Commun,* 235**,** 79-82.

VOGLER, S., PAHNKE, J., ROUSSET, S., RICQUIER, D., MOCH, H., MIROUX, B. & IBRAHIM, S. M. 2006. Uncoupling protein 2 has protective function during experimental autoimmune encephalomyelitis. *Am J Pathol,* 168**,** 1570-5.

WALDECK-WEIERMAIR, M., MALLI, R., NAGHDI, S., TRENKER, M., KAHN, M. J. & GRAIER, W. F. 2010. The contribution of UCP2 and UCP3 to mitochondrial Ca(2+) uptake is differentially determined by the source of supplied Ca(2+). *Cell Calcium,* 47**,** 433-40.

WANG, D., LI, F., CHI, Y. & XIANG, J. 2012. Potential relationship among three antioxidant enzymes in eliminating hydrogen peroxide in penaeid shrimp. *Cell Stress Chaperones,* 17**,** 423-33.

WANG, M. Y., SHIMABUKURO, M., LEE, Y., TRINH, K. Y., CHEN, J. L., NEWGARD, C. B. & UNGER, R. H. 1999. Adenovirus-mediated overexpression of uncoupling protein-2 in pancreatic islets of Zucker diabetic rats increases oxidative activity and improves beta-cell function. *Diabetes,* 48**,** 1020-5.

WANG, Q., WANG, J., HU, M., YANG, Y., GUO, L., XU, J., LEI, C., JIAO, Y. & XU, J. 2016. Uncoupling Protein 2 Increases Susceptibility to Lipopolysaccharide-Induced Acute Lung Injury in Mice. *Mediators Inflamm,* 2016**,** 9154230.

WANG, X., VATAMANIUK, M. Z., RONEKER, C. A., PEPPER, M. P., HU, L. G., SIMMONS, R. A. & LEI, X. G. 2011. Knockouts of SOD1 and GPX1 exert different impacts on murine islet function and pancreatic integrity. *Antioxid Redox Signal,* 14**,** 391-401.

WANG, Y., BRANICKY, R., NOE, A. & HEKIMI, S. 2018. Superoxide dismutases: Dual roles in controlling ROS damage and regulating ROS signaling. *J Cell Biol,* 217**,** 1915-1928.

WICKSTEED, B., BRISSOVA, M., YAN, W., OPLAND, D. M., PLANK, J. L., REINERT, R. B., DICKSON, L. M., TAMARINA, N. A., PHILIPSON, L. H., SHOSTAK, A., BERNAL-MIZRACHI, E., ELGHAZI, L., ROE, M. W., LABOSKY, P. A., MYERS, M. G., JR., GANNON, M., POWERS, A. C. & DEMPSEY, P. J. 2010. Conditional gene targeting in mouse pancreatic ss-Cells: analysis of ectopic Cre transgene expression in the brain. *Diabetes,* 59**,** 3090-8.

WINZELL, M. S., SVENSSON, H., ENERBACK, S., RAVNSKJAER, K., MANDRUP, S., ESSER, V., ARNER, P., ALVES-GUERRA, M. C., MIROUX, B., SUNDLER, F., AHREN, B. & HOLM, C. 2003. Pancreatic beta-cell lipotoxicity induced by overexpression of hormone-sensitive lipase. *Diabetes,* 52**,** 2057-65.

WOLLHEIM, C. B. & MAECHLER, P. 2002. Beta-cell mitochondria and insulin secretion: messenger role of nucleotides and metabolites. *Diabetes,* 51 Suppl 1**,** S37-42.

XIE, L. H., JOHN, S. A., RIBALET, B. & WEISS, J. N. 2008. Phosphatidylinositol-4,5-bisphosphate (PIP2) regulation of strong inward rectifier Kir2.1 channels: multilevel positive cooperativity. *J Physiol,* 586**,** 1833-48.

XU, B., MORITZ, J. T. & EPSTEIN, P. N. 1999. Overexpression of catalase provides partial protection to transgenic mouse beta cells. *Free Radic Biol Med,* 27**,** 830-7.

XU, Y. Q., ZHANG, D., JIN, T., CAI, D. J., WU, Q., LU, Y., LIU, J. & KLAASSEN, C. D. 2012. Diurnal variation of hepatic antioxidant gene expression in mice. *PLoS One,* 7**,** e44237.

YAMAMOTO, H., NAGAI, K. & NAKAGAWA, H. 1984. Bilateral lesions of the SCN abolish lipolytic and hyperphagic responses to 2DG. *Physiol Behav,* 32**,** 1017-20.

YAMAMOTO, H., NAGAI, K. & NAKAGAWA, H. 1987. Role of SCN in daily rhythms of plasma glucose, FFA, insulin and glucagon. *Chronobiol Int,* 4**,** 483-91.

YE, L., WU, H. & XU, W. 2020. Deletion of Bmal1 Impairs Pancreatic beta-Cell Function via Mitochondrial Signaling Pathway. *Biomed Res Int,* 2020**,** 9803024.

YU, X. X., MAO, W., ZHONG, A., SCHOW, P., BRUSH, J., SHERWOOD, S. W., ADAMS, S. H. & PAN, G. 2000. Characterization of novel UCP5/BMCP1 isoforms and differential regulation of UCP4 and UCP5 expression through dietary or temperature manipulation. *FASEB J,* 14**,** 1611-8.

ZHANG, C. Y., BAFFY, G., PERRET, P., KRAUSS, S., PERONI, O., GRUJIC, D., HAGEN, T., VIDAL-PUIG, A. J., BOSS, O., KIM, Y. B., ZHENG, X. X., WHEELER, M. B., SHULMAN, G. I., CHAN, C. B. & LOWELL, B. B. 2001. Uncoupling protein-2 negatively regulates insulin secretion and is a major link between obesity, beta cell dysfunction, and type 2 diabetes. *Cell,* 105**,** 745-55.

ZHANG, C. Y., PARTON, L. E., YE, C. P., KRAUSS, S., SHEN, R., LIN, C. T., PORCO, J. A., JR. & LOWELL, B. B. 2006. Genipin inhibits UCP2-mediated proton leak and acutely reverses obesity- and high glucose-induced beta cell dysfunction in isolated pancreatic islets. *Cell Metab,* 3**,** 417-27.

ZHANG, R., LAHENS, N. F., BALLANCE, H. I., HUGHES, M. E. & HOGENESCH, J. B. 2014. A circadian gene expression atlas in mammals: implications for biology and medicine. *Proc Natl Acad Sci U S A,* 111**,** 16219-24.

ZHAO, C. & RUTTER, G. A. 1998. Overexpression of lactate dehydrogenase A attenuates glucose-induced insulin secretion in stable MIN-6 beta-cell lines. *FEBS Lett,* 430**,** 213-6.

ZOROV, D. B., JUHASZOVA, M. & SOLLOTT, S. J. 2014. Mitochondrial reactive oxygen species (ROS) and ROS-induced ROS release. *Physiol Rev,* 94**,** 909-50.